



DEVELOPMENT OF NOVEL ELECTROCHEMICAL SENSORS BASED ON
NANOMATERIALS AND POLYMERS FOR 8-HYDROXY-2'-DEOXYGUANOSINE, 1-
HYDROXYPYRENE, 5-AMINOSALICYLIC ACID, AND SULFAPYRIDINE DETECTION

JEERAKIT THANGPHATTHANARUNGRUANG

Graduate School Srinakharinwirot University

2022

การพัฒนากระบวนการเรียนรู้ทางเคมีไฟฟ้ารูปแบบใหม่ด้วยวัสดุขนาดนาโนเมตรและพอลิเมอร์สำหรับการ
ตรวจวัดสารเอท-ไฮดรอกซี-ทู-ดีออกซีกัวโนซีน วัน-ไฮดรอกซีไพรีน ไพฟว-อะมิโนซาลิไซลิก แอซิด
และซัลฟาไพรีดีน



ปริญญานิพนธ์นี้เป็นส่วนหนึ่งของการศึกษาตามหลักสูตร
ปรัชญาดุษฎีบัณฑิต สาขาวิชาเคมีประยุกต์
คณะวิทยาศาสตร์ มหาวิทยาลัยศรีนครินทรวิโรฒ
ปีการศึกษา 2565
ลิขสิทธิ์ของมหาวิทยาลัยศรีนครินทรวิโรฒ

DEVELOPMENT OF NOVEL ELECTROCHEMICAL SENSORS BASED ON
NANOMATERIALS AND POLYMERS FOR 8-HYDROXY-2'-DEOXYGUANOSINE, 1-
HYDROXYPYRENE, 5-AMINOSALICYLIC ACID, AND SULFAPYRIDINE DETECTION



JEERAKIT THANGPHATTHANARUNGRUANG

A Dissertation Submitted in Partial Fulfillment of the Requirements
for the Degree of DOCTOR OF PHILOSOPHY
(Applied Chemistry)

Faculty of Science, Srinakharinwirot University

2022

Copyright of Srinakharinwirot University

THE DISSERTATION TITLED

DEVELOPMENT OF NOVEL ELECTROCHEMICAL SENSORS BASED ON NANOMATERIALS AND
POLYMERS FOR 8-HYDROXY-2'-DEOXYGUANOSINE, 1-HYDROXYPYRENE, 5-AMINOSALICYLIC
ACID, AND SULFAPYRIDINE DETECTION

BY

JEERAKIT THANGPHATTHANARUNGRUANG

HAS BEEN APPROVED BY THE GRADUATE SCHOOL IN PARTIAL FULFILLMENT
OF THE REQUIREMENTS FOR THE DOCTOR OF PHILOSOPHY
IN APPLIED CHEMISTRY AT SRINAKHARINWIROT UNIVERSITY

(Assoc. Prof. Dr. Chatchai Ekpanyaskul, MD.)

Dean of Graduate School

ORAL DEFENSE COMMITTEE

..... Major-advisor

(Assoc. Prof. Dr.Weena Siangproh)

..... Co-advisor

(Dr.Chuleekorn Chotsuwan)

..... Chair

(Prof. Dr.Orawon Chailapakul)

..... Committee

(Assoc. Prof. Dr.Apinya Chaivisuthangkura)

..... Committee

(Assoc. Prof. Dr.Kriangsak Songsirote)

Title	DEVELOPMENT OF NOVEL ELECTROCHEMICAL SENSORS BASED ON NANOMATERIALS AND POLYMERS FOR 8-HYDROXY-2'-DEOXYGUANOSINE, 1-HYDROXYPYRENE, 5-AMINOSALICYLIC ACID, AND SULFAPYRIDINE DETECTION
Author	JEERAKIT THANGPHATTHANARUNGRUANG
Degree	DOCTOR OF PHILOSOPHY
Academic Year	2022
Thesis Advisor	Associate Professor Dr. Weena Siangproh
Co Advisor	Dr. Chuleekorn Chotsuwan

This research concentrated on the development of an electrochemical sensor based on nanomaterials, poly(amino acids), or both for the detection of important biomarkers in clinical applications, which could be classified into three sub-projects. In the first sub-project, an electrochemical sensor based on a nanocomposite between poly(L-methionine) and gold nanoparticle-modified screen-printed graphene electrode was developed for the sensitive and selective detection of 8-hydroxy-2'-deoxyguanosine (8-OHdG) in the presence of uric acid at normal levels in urine. A sodium phosphate buffer solution containing sodium chloride and sodium dodecyl sulfate was used as the supporting electrolyte to increase selectivity for 8-OHdG detection. In the second sub-project, a novel detection for 1-hydroxypyrene (1-OHP) used only a single step of electropolymerization of poly(L-glutamic acid)-modified screen-printed graphene was developed. The electrochemical response of 1-OHP on the modified sensor was three times larger than that of the unmodified sensor. For practical applications, it was utilized to determine 1-OHP in six urine samples, without any interference. Lastly, in the third sub-project, the simultaneous detection of 5-aminosalicylic acid (5-ASA) and sulfapyridine (SPD) using poly(L-methionine)-modified screen-printed graphene electrodes were reported for the first time. The detection of 5-ASA and SPD indicated the therapeutic determinant of the action of sulfasalazine, which is widely used for the treatment of rheumatoid arthritis and inflammatory bowel disease. As aforementioned, these developed electrochemical sensors and proposed methodologies could be directly applied to determine specific target analytes in real human serum and urine samples without additional sample preparation. The results obtained provided satisfactory analytical performances with high accuracy, precision, reproducibility, stability, and reliability.

Keyword : Electrochemical sensor, Nanomaterials, Poly(amino acids), Biomarkers

ACKNOWLEDGEMENTS

It is a sincere pleasure to express my deepest gratitude and appreciation to my advisor, Associate Professor Dr. Weena Siangproh, who has the attitude and the substance of a genius: she consistently and effectively conveyed an adventurous spirit in regard to research. She helped, supported, and advised me in experiments and in writing the journal publication and dissertation. Moreover, she believed in me to overcome the difficulties and fears of research to accomplish this task. Thanks for always telling me that I am diligent, persevering, and take responsibility for the research. I will keep this good part for the future of my career. It has been a wonderful pleasure and honor to work with her as my advisor.

I would also like to appreciate my co-advisor, Dr. Chuleekorn Chotsuwan from the National Nanotechnology Center (NANOTEC), for giving me the opportunity to receive the scholarship and to work on my project for 3 years at NANOTEC. She not only gave counsel about the research but also guided and made suggestions about the lifestyle, working with others, and love as well. Without her persistent help, this dissertation would not have come this far. I hope that I will work with her in the future in the position of postdoctoral research fellow.

My heartfelt gratitude goes to Associate Professor Dr. Takeshi Kondo, who invited me to participate in the "SAKURA SCIENCE" (Japan-Asia Youth Exchange Program in Science) at Tokyo University of Science in 2019. I appreciated the good opportunities he gave me for learning about the research as well as Japanese culture during my 3 weeks in Japan. In addition, I would like to thank all of my oral defense committees, Professor Dr. Orawon Chailapakul, Associate Professor Dr. Apinya Chaivisuthangkura, and Associate Professor Dr. Kriangsak Songsrirote for their valuable time and suggestions.

The most important thing is that I am grateful for the funding received from the Thailand Graduate Institute of Science and Technology (TGIST) to conduct research during my Ph.D. study. In addition, I would like to thank NANOTEC and the National Science and Technology Development Agency (NSTDA) for supporting the facilities that enabled my work to be conducted.

Also, I would like to thank all members of the Electroanalytical and Imaging Sensor Research Group (EISRG) who helped and recommended the research to get the best results.

Last but not least, I would like to express my gratitude to my family for their love, encouragement, understanding, and support throughout my studies, research, dissertation writing, and life in general.

JEERAKIT THANGPHATTHANARUNGRUANG



TABLE OF CONTENTS

	Page
ABSTRACT.....	D
ACKNOWLEDGEMENTS	E
TABLE OF CONTENTS	G
List of tables.....	L
List of figures	M
CHAPTER 1 INTRODUCTION.....	1
Background.....	1
Objectives of the research.....	5
Significance of the research.....	5
Scope of the research	5
CHAPTER 2 THEORY.....	7
2.1 Reactive oxygen species and oxidative DNA damage	7
2.2 8-Hydroxy-2'-deoxyguanosine.....	8
2.3 Polycyclic aromatic hydrocarbons	10
2.4 1-Hydroxypyrene	10
2.5 Sulfasalazine.....	11
2.6 5-Aminosalicylic acid and sulfapyridine	12
2.7 Absorption and metabolism of SSZ and its metabolites	12
2.8 Electrochemical method	14
2.8.1 Voltammetry	14
2.8.1.1 Cyclic voltammetry.....	15

2.8.1.2 Square wave voltammetry	17
2.8.2 Electrochemical impedance spectroscopy	18
2.8.3 Electrodes	19
2.8.3.1 Screen-printed electrodes	20
2.8.3.2 Graphene	20
2.8.3.3 Nanomaterials	21
2.8.3.4 Amino acids	22
CHAPTER 3 METHODOLOGY	24
3.1 A new nanocomposite-based screen-printed graphene electrode for sensitive and selective detection of 8-hydroxy-2'-deoxyguanosine	24
3.1.1 Apparatuses, chemicals, and reagents	24
3.1.2 Fabrication of the electrochemical sensor for 8-OHdG detection	25
3.1.3 Electrochemical measurements	28
3.1.4 Application of the proposed electrochemical sensor for the determination of 8-OHdG in real samples.	29
3.2 A novel and easy-to-construct polymeric L-glutamic acid-modified sensor for urinary 1-hydroxypyrene detection: Human biomonitoring of polycyclic aromatic hydrocarbons exposure	29
3.2.1 Chemicals, materials, and apparatuses	30
3.2.2 Fabrication of conductive polymer thin film modified SPGE	31
3.2.3 Electrochemical measurements	32
3.2.4 Sample preparation	33
3.3 Highly efficient polymeric L-methionine-modified sensor: An application for the simultaneous determination of 5-aminosalicylic acid and sulfapyridine	34

3.3.1 Apparatuses, chemicals, reagents, and materials.....	34
3.3.2 Fabrication of poly(L-methionine)-modified SPGE	35
3.3.3 Electrochemical measurements	36
3.3.4 Real-sample preparation.....	37
CHAPTER 4 RESULTS AND DISCUSSION	39
4.1 A new nanocomposite-based screen-printed graphene electrode for sensitive and selective detection of 8-hydroxy-2'-deoxyguanosine	39
4.1.1 Morphological characterization of the modified sensor	39
4.1.2 Electrochemical characterization of the poly(L-Met)/AuNPs-nanocomposite modified SPGE.....	42
4.1.3 Electrochemical behavior of 8-OHdG on poly(L-Met)/AuNPs/SPGE.....	43
4.1.4 Optimization of deposition for AuNPs and L-methionine.....	45
4.1.5 Influence of pH values and scan rates.....	46
4.1.6 Interference study	48
4.1.7 Detection of a mixture of 8-OHdG and UA.....	50
4.1.8. Analytical performance	52
4.1.9. Analytical application in real samples.....	56
4.2 A novel and easy-to-construct polymeric L-glutamic acid-modified sensor for urinary 1-hydroxypyrene detection: Human biomonitoring of polycyclic aromatic hydrocarbons exposure	58
4.2.1 Surface composition and morphology studies.....	58
4.2.2 Electrochemical characterization of the poly(L-GA)/SPGE	60
4.2.3 Effect of different types of supporting electrolytes on the electrochemical detection of 1-OHP at the poly(L-GA)/SPGE.....	63

4.2.4 Effect of pH values and scan rates	64
4.2.5 Optimization of electropolymerization for L-GA.....	66
4.2.6 Electrochemical behavior of 1-OHP on poly(L-GA)/SPGE	66
4.2.7 Analytical performance	67
4.2.8 Interference study	71
4.2.9 Dilution and matrix effect	71
4.2.10 Application in real urine samples	72
4.3 Highly efficient polymeric L-methionine-modified sensor: An application for the simultaneous determination of 5-aminosalicylic acid and sulfapyridine	74
4.3.1 Electrochemical behaviors of 5-ASA and SPD on poly(L-Met)/SPGE	74
4.3.2 Effect of pH values and scan rates	75
4.3.3 Optimization of electropolymerization for L-Met.....	77
4.3.4 Influence of the proportion between MeOH and PBS	78
4.3.5 Analytical performance	79
4.3.6 Selectivity, reproducibility, and stability of the sensor	82
4.3.7 Determination of 5-ASA and SPD in real samples.....	83
CHAPTER 5 CONCLUSIONS.....	85
5.1 A new nanocomposite-based screen-printed graphene electrode for sensitive and selective detection of 8-hydroxy-2'-deoxyguanosine	85
5.2 A novel and easy-to-construct polymeric L-glutamic acid-modified sensor for urinary 1-hydroxypyrene detection: Human biomonitoring of polycyclic aromatic hydrocarbons exposure	85
5.3 Highly efficient polymeric L-methionine-modified sensor: An application for the simultaneous determination of 5-aminosalicylic acid and sulfapyridine	86

REFERENCES	87
Appendix	100
Appendix 1	101
Appendix 2	111
Appendix 3	120
Appendix 4	133
VITA	145



List of tables

	Page
Table 1 Comparison of the analytical performance between this proposed method and previous works for 8-OHdG detection.	55
Table 2 Results obtained from the determination of 8-OHdG in artificial urine, healthy human urine, and human serum samples using poly(L-Met)/AuNPs/SPGE (n = 3).....	57
Table 3 Comparison of the analytical performance between this proposed method and previous works for 1-OHP detection.	70
Table 4 Results obtained from the determination of 1-OHP in healthy volunteer's urine using poly(L-GA)/SPGE (n = 3).....	73
Table 5 Practical applications of poly(L-Met)/SPGE for the simultaneous analysis of 5-ASA and SPD in real urine samples.....	84

List of figures

	Page
Figure 1 Pathway of generation of free radicals and scavenged enzymes in cellular.	8
Figure 2 Pathway of 8-OHdG and its tautomer of 8-oxodG by hydroxyl radicals.	9
Figure 3 Metabolism of pyrene.	11
Figure 4 Bioactivation of sulfasalazine by azo reductase into sulfapyridine and 5-aminosalicylic acid.	12
Figure 5 Absorption and metabolism of sulfasalazine (S) and its metabolites (Sulfapyridine (SP) and 5-aminosalicylic acid (5-ASA)).	13
Figure 6 Potential–time excitation signal in a cyclic voltammetric technique.	16
Figure 7 Typical cyclic voltammogram for a reversible redox process.	17
Figure 8 Excitation waveform of square wave voltammetry.	18
Figure 9 Simple Randles equivalent circuit for an electrochemical cell.	19
Figure 10 Illustration of the fabrication of a new electrochemical sensor for 8-OHdG detection.	27
Figure 11 Cyclic voltammograms for the electrodeposition of AuNPs in 5% hydrochloric acid on SPGE with a scan rate of 150 mV s^{-1} for seven cycles (A) and the electropolymerization of L-methionine in 0.1 M sodium phosphate buffer solution at pH 7.0 on AuNPs/SPGE with a scan rate of 100 mV s^{-1} for ten cycles (B).	28
Figure 12 Illustration of the possible structure of L-methionine film on AuNPs modified SPGE.	28
Figure 13 Cyclic voltammograms for the electropolymerization of 30 mM L-GA in 0.1 M Na-PBS (pH 7.0) at SPGE with a scan rate of 100 mV s^{-1} for 5 cycles.	32
Figure 14 Mechanism of electropolymerization of L-GA on the SPGE surface.	32

Figure 15 Effects of a potential increment (a), an amplitude (b), a frequency (c), and a quiet time (d) for 1-OHP detection in Gly-NaOH (pH 9.4) at the poly(L-GA)/SPGE. Error bars represent the standard deviation of 10 μM 1-OHP detection using SWV for three repetitive measurements ($n = 3$).....	33
Figure 16 Cyclic voltammograms for the 6 mM L-Met electropolymerization on SPGE with a scan rate of 100 mV s^{-1} for 3 cycles.	36
Figure 17 The crucial SWV parameters, including an amplitude (a), a potential increment (b), a frequency (c), and a quiet time (d) for the simultaneous detection of 5-ASA and SPD at the poly(L-Met)/SPGE. Error bars represent the standard deviation of the simultaneous detection of 100 μM 5-ASA and SPD using SWV for three repetitive measurements ($n = 3$).....	37
Figure 18 SEM images of SPGE (a, e), AuNPs/SPGE (b, f), poly(L-Met)/SPGE (c, g), and poly(L-Met)/AuNPs/SPGE (d, h) at magnifications of 10,000 \times (a, b, c, d) and 50,000 \times (e, f, g, h). EDS mapping (i). Composition of poly(L-Met)/AuNPs/SPGE (j). Cyclic voltammograms of 5 mM $[\text{Fe}(\text{CN})_6]^{3-/4-}$ in 0.1 M KCl with a scan rate of 30 mV s^{-1} (k) and EIS Nyquist plots of 5 mM $[\text{Fe}(\text{CN})_6]^{3-/4-}$ in 0.1 M KCl (l) at the unmodified and modified SPGE.	41
Figure 19 Cyclic voltammograms (A) and a chart of the current intensity (B) of 100 μM 8-OHdG in 0.1 M Na-PBS (pH 7.0) at different sensors.....	45
Figure 20 Effects of concentration of standard gold solution (A) and L-methionine solution (D), number of cycles for gold (B) and L-methionine deposition (E), and scan rate for gold (C) and L-methionine deposition (F) on SPGE.	46
Figure 21 Cyclic voltammograms of 10 μM 8-OHdG at the poly(L-Met)/AuNPs/SPGE using various pH values (A) and the plot of E_{pa} vs. pH values (B). Cyclic voltammograms of 10 μM 8-OHdG in 0.1 M Na-PBS (pH 7.0) at the poly(L-Met)/AuNPs/SPGE with different scan rates (C) and the plot of I_{pa} vs. scan rate (D).	48

Figure 22 Effect of interferences toward 8-OHdG detection. The error bars represent the standard deviation of three repetitive measurements.....	49
Figure 23 Square wave voltammograms of 10 μM 8-OHdG and 10 μM uric acid (A) and 10 μM 8-OHdG in presence 20 μM uric acid at the poly(L-Met)/AuNPs/SPGE (B).	50
Figure 24 Square wave voltammograms of 10 μM 8-OHdG in various concentrations of NaCl in 0.1 M Na-PBS (pH 7) at the poly(L-Met)/AuNPs/SPGE.	50
Figure 25 Square wave voltammograms of 10 μM 8-OHdG and 400 μM UA in 0.05 M SDS containing 0.1 M NaCl in 0.1 M Na-PBS (pH 7.0) (A), the effect of the SDS concentration (B), and a chart of the current intensity of 8-OHdG and UA detection (C).	52
Figure 26 Square wave voltammograms showing the electrochemical oxidation of 8-OHdG in 0.05 M SDS containing 0.1 M NaCl in 0.1 M Na-PBS (pH 7.0) at various concentrations on poly(L-Met)/AuNPs/SPGE (A). The calibration curve between the anodic peak current and the concentration of 8-OHdG (B). A chart of the current intensity of reproducibility studies at three concentrations (C).....	54
Figure 27 SEM images of SPGE (a) and poly(L-GA)/SPGE (b) at a magnification of 10,000 \times . EDS mapping for the composition of poly(L-GA)/SPGE (c). XPS data of a bare SPGE (d) and the composite polymer fabricated on SPGE demonstrates the core level spectra for C 1s (e), O 1s (f), and N 1s (g).	59
Figure 28 Cyclic voltammograms of 5 mM $[\text{Fe}(\text{CN})_6]^{3-/4-}$ and $[\text{Ru}(\text{NH}_3)_6]^{3+}$ in 0.1 M KCl with a scan rate of 100 mV s^{-1} at the SPGE and poly(L-GA)/SPGE (a). EIS Nyquist plots of 5 mM $[\text{Fe}(\text{CN})_6]^{3-/4-}$ in 0.1 M KCl with the potential range of 0–0.1 V at the SPGE and poly(L-GA)/SPGE (b).	62
Figure 29 Square wave voltammograms of 1-OHP detection using Na-PBS (a), $\text{Na}_2\text{HPO}_4\text{-NaOH}$ (b), and Gly-NaOH (c) as the supporting electrolyte. Square wave voltammograms for a comparison of each supporting electrolyte type in 1-OHP detection (d).	64

Figure 30 Square wave voltammograms of 10 μM 1-OHP detection at different pH values (a) and the plot of E_{pa} vs. pH values (b). Cyclic voltammograms of 50 μM 1-OHP detection in Gly-NaOH (pH 9.4) at various scan rates (c) and the plot of I_{pa} vs. scan rate (d). Error bars represent the standard deviation of 1-OHP detection at different pH values and scan rates for three repetitive measurements ($n = 3$).....	65
Figure 31 Effects of concentration of glutamic acid (a), number of scans (b), and scan rate for electropolymerization (c) on SPGE. Error bars represent the standard deviation of 10 μM 1-OHP detection using SWV for three repetitive measurements ($n = 3$).....	66
Figure 32 Square wave voltammograms of 10 μM 1-OHP in Gly-NaOH (pH 9.4) at the unmodified and modified SPGE.....	67
Figure 33 The calibration curve between the anodic peak current and the concentration of 1-OHP in the range of 1–1000 nM (a) and corresponding square wave voltammograms of 1-OHP (inset). A comparison of the plotting graphs between a solvent calibration curve and a matrix-matched calibration curve (b). Error bars represent the standard deviation of 1-OHP detection at different concentrations for three repetitive measurements ($n = 3$).....	69
Figure 34 Effect of some interfering substances on the detection of 300 nM 1-OHP at the poly(L-GA)/SPGE by SWV under optimal conditions ($n = 3$).	71
Figure 35 Cyclic voltammograms of individual 5-ASA (a) and SPD (b) detections; cyclic (c) and square wave voltammograms (d) of the simultaneous detection of 5-ASA and SPD in a mixture of MeOH and 0.1 M PBS (pH 5.6) in a proportion of 20:80% v/v on SPGE and poly(L-Met)/SPGE.....	75
Figure 36 The plot of I_{pa} vs. pH values (a). and E_{pa} vs. pH values (b) for 5-ASA and SPD. Cyclic voltammograms of the simultaneous detection of 100 μM 5-ASA and SPD in MeOH:PBS (20:80% v/v) at various scan rates (c) and the plot of I_{pa} vs. the square root of the scan rate (d). Error bars represent the standard deviation of the simultaneous detection of 5-ASA and SPD at various pH values and scan rates for three repetitive measurements ($n = 3$).....	77

Figure 37 Influence of electropolymerization procedure, including concentration of L-methionine (a), number of scans (b), and scan rate (c). Error bars represent the standard deviation of the simultaneous detection of 5-ASA and SPD using SWV for three repetitive measurements (n = 3).....	78
Figure 38 Square wave voltammograms (a) and a chart of the peak current (b) of the simultaneous detection of 5-ASA and SPD in a mixture of MeOH and PBS at different proportions.....	79
Figure 39 Square wave voltammograms for the simultaneous detection of 5-ASA and SPD (a) and the linear dynamic ranges between the peak current and concentration of 5-ASA and SPD (b). Square wave voltammograms (c) and the plotting graph (d) for the 5-ASA detection in the presence of 10 μ M SPD. Square wave voltammograms (e) and the plotting graph (f) for the SPD detection in the presence of 10 μ M 5-ASA.	81
Figure 40 Influence of some interferences on the simultaneous detection of 5-ASA and SPD at the poly(L-Met)/SPGE.	83

CHAPTER 1

INTRODUCTION

Background

In the past decades, based on environmental change and technological advancement, the world population has suffered from environmental pollutants and unsafe diet consumptions, leading to a high possibility of facing various illnesses. These impacts directly lead to a total loss of life and property around the world. For developing countries, these problems are more serious because of the rapid population growth and the inadequacy of modern medical technology to maintain health quickly and comprehensively. Therefore, the development of science technology in parallel with medicinal treatment is very important to obtain a new technology or an alternative method for use worldwide. The ultimate goal of the development is not only to obtain a fast, convenient, inexpensive, effective, accurate, and precise method to apply for diagnosis and follow-up treatment efficiency but also to receive equipment that can be used with minimal restrictions. Hence, the development of new analytical methods and prototypes for portability with the mentioned requirements for the determination of biomarkers, which are used as indicators in clinical applications, is the main objective of this research.

In our body, reactive oxygen species (ROSs) play an important role in physiology and pathology. They are widely used as intracellular signaling molecules, demonstrating an imbalance between free radicals and antioxidants in the body's cells, leading to a situation known as oxidative stress (Chang et al., 2013) (Manavalan et al., 2018). 8-hydroxy-2'-deoxyguanosine (8-OHdG) is known as a specific marker for oxidative stress and is a major product of guanine oxidation in the process of reactive oxygen species attacking the eighth carbon atom of guanine (Shang et al., 2018). Normally, the 8-OHdG biomolecule can be found in several biological samples, e.g., urine, saliva, blood or serum, and tissue (G.V. Martins, Marques, Fortunato, & Sales, 2016), and its corresponding concentration is further correlated with various diseases, such as cancers, aging, diabetes, and neurological disorders (Zhao et al., 2019). Therefore, the

development of an effective approach for 8-OHdG detection is of great importance for disease risk assessment and early diagnosis.

Polycyclic aromatic hydrocarbons (PAHs) are harmful environmental and dietary contaminants (Serrano et al., 2017) that are formed by the incomplete combustion or pyrolysis of organic substances. In our daily life, we are exposed to PAHs all the time through many routes, for example, inhalation, ingestion, and skin contact. The toxicity of PAHs can harm or destroy proteins and DNA within cells. 1-Hydroxypyrene (1-OHP) is a well-studied target for PAH metabolites, which can indicate the evaluation of human PAH exposure. Hence, the invention of a simple, sensitive, and selective approach to monitor the amounts of 1-OHP is meaningful and of considerable significance.

Sulfasalazine (SSZ) has been widely used as a therapy for rheumatoid arthritis (Plosker & Croom, 2005). Furthermore, it has also been employed for the treatment of inflammatory bowel diseases (Wolf & Lashner, 2002). Based on the SSZ structure, it is composed by 5-aminosalicylic acid (5-ASA) and sulfapyridine (SPD) with an azo bond. Nevertheless, in the metabolism process, an azo bond of the SSZ structure can be cleaved by an intracellular azo reductase, releasing 5-ASA and SPD into the colon. Hence, 5-ASA and SPD are the important active components for predicting or monitoring disease treatment. Therefore, the sensitive and selective assay for the simultaneous detection of 5-ASA and SPD in biological fluids is very important for assessing the therapeutic determinant for the action of SSZ.

In recent decades, chromatographic and spectroscopic methods have been reported for determining 8-OHdG, 1-OHP, 5-ASA, and SPD. Although these methods provided high sensitivity and selectivity, unfortunately, there were still some limitations, such as sophisticated instrumentation, expensiveness, the complicated pretreatment steps, long analysis time, the requirement for a large solvent or sample volume, and special-trained operators. Moreover, these methods were not able to achieve portability and were not suitable for routine, on-site, and real-time analysis. To overcome these inherent problems, the method for the determination of these analytes that provides a rapid, simple, and sensitive assay is still required.

Currently, electroanalytical methods have emerged as an alternative method for the detection of biomarkers in biological samples due to their simplicity, high sensitivity and accuracy, fast analysis time, low cost, portability, and compact set-up. Furthermore, electrochemical devices have a small portable size in comparison to a conventional instrument as well as require a small volume of sample for analysis. These benefits can reduce the pain and the fear for patients who must be treated in each case. In the past few years, the design of electrochemical sensors has been progressed to enhance the analytical performance in terms of sensitivity, selectivity, and reliability as well as to provide ease of fabrication and lower costs. Thus, disposable sensors have attracted attention for the use in a variety of applications, such as clinical laboratories, food and beverage testing, the pharmaceutical industry, and environmental analysis. Nowadays, to produce a disposable sensor, the screen-printing technique is a famous technology that can be used for the fabrication of a variety of sensors as well as reduce the size of devices instead of using commercial large-scale electrodes. In addition, the benefits of using the screen-printing technique also come from its economic substrate, diversity, low cost, and particularly the possibility of mass production (Charoenkitamorn, Chaiyo, Chailapakul, & Siangproh, 2018). Screen-printed electrodes (SPEs) are a kind of disposable electrochemical sensor based on screen-printing technology. It has been extensively proposed in the field of electrochemical analysis. In comparison to conventional electrodes, SPEs offer many advantages, such as simplicity, small size, disposable device, portability, inexpensiveness, and the requirement of a small volume of sample (M. Li, Li, Li, & Long, 2012) (Thangphatthanarungruang, Ngamaroonchote, Laocharoensuk, Chotsuwan, & Siangproh, 2018). In addition, these sensors can be fabricated with various types of ink on different substrates depending on the applications. The selection of ink and substrate is important for the sensitivity and selectivity obtained from the analytical procedure. Among the commercial inks, graphene is a well-known carbon material that has received high attention. It consists of two-dimensional structures with sp^2 bonded carbon atoms in a hexagonal configuration (D. Kim, Lee, & Piao, 2017). It has many distinct properties, such as high electrical conductivity, superior electron transportation,

high mechanical and chemical stability, large surface area, and good biocompatibility (Kuila et al., 2011) (Thangphatthanarungruang et al., 2020). From these advantages, a screen-printed graphene electrode (SPGE) furnishes a suitable sensing platform for a highly sensitive electrochemical sensor.

To increase sensitivity and selectivity for electrochemical detection, a strategy can be implemented by using a variety of modifiers. Gold nanoparticles (AuNPs) are one of the most widely employed as metal nanoparticles for the modification of the electrode surface to modify the original properties of sensors. Their special physicochemical characteristics, such as good stability, large surface area, high conductivity, excellent electrocatalytic capability, and good biocompatibility (He et al., 2014). Furthermore, AuNPs can react excellently with organo-sulfur compounds at the electrode surface to form S-Au through covalent bonding, resulting in enhancing the stability of self-assembled monolayers (SAMs) (Łuczak, 2009) (Benvidi, Dehghani-Firouzabadi, Mazloun-Ardakani, Mirjalili, & Zare, 2015).

In recent years, poly(amino acids) modified electrode have been attracted great attention for the determination of several important biological and clinical species because of their simplicity, rapidity, and convenience for the fabrication. It can be used for the modification on the electrode surface by electropolymerization because of its containing $-NH_2$ and $-COOH$ groups. From the benefits of screen-printing technology and modifiers, in this research, simple, sensitive, and selective methods for monitoring 8-OHdG, 1-OHP, 5-ASA, and SPD were proposed by using gold nanoparticles, poly(amino acids), or both modified screen-printed graphene electrode. The electrochemical techniques, such as cyclic voltammetry and square wave voltammetry, were selected for the investigations to receive the high performance of sensor preparation and analytical methods for detection. Finally, these proposed methods could be used as an alternative approach to monitor 8-OHdG, 1-OHP, 5-ASA, and SPD in biological fluid samples. These findings are useful for medical personnel who can use the obtained results as a guideline for evaluating or diagnosing the risk of diseases in biological samples.

Objectives of the research

The aim of the research consisted of two main goals listed below:

1. To develop novel electrochemical methods based on nanomaterials and/or amino acid polymers for determining the levels of 8-OHdG, 1-OHP, 5-ASA, and SPD.
2. To apply the proposed methods for the determination of 8-OHdG, 1-OHP, 5-ASA, and SPD in clinical applications.

Significance of the research

1. These developed electrochemical methods can be used as an alternative model to monitor the amounts of 8-OHdG, 1-OHP, 5-ASA, and SPD for interpreting or diagnosing the risk of diseases.
2. These developed electrochemical methods exhibit good performances with high sensitivity and selectivity for 8-OHdG, 1-OHP, 5-ASA, and SPD detection.
3. The proposed methods can be applied for the quantitative analysis of 8-OHdG, 1-OHP, 5-ASA, and SPD in clinical applications.

Scope of the research

Electrochemical methods for the determination of 8-OHdG, 1-OHP, 5-ASA, and SPD using gold nanoparticles, poly(amino acids), or both modified screen-printed graphene electrodes were developed. The performance of SPGE with and without modification steps toward the electrochemical behaviors of the target analytes will be first studied. To improve the sensitivity of detection, all experimental conditions, including concentration of modifiers, number of scans, scan rate for modification procedure, type and composition of supporting electrolyte, and pH values, were systematically investigated. Furthermore, the electrochemical parameters related to square wave voltammetry were also studied, such as potential increment, amplitude, frequency, and quiet time. For the analytical performance of these methods, various concentrations of the analytes were examined to identify the linear relationship against the peak current. Limits of detection (LOD) and quantitation (LOQ) were calculated as sequences. Owing to the effect of other compounds in real samples on the detection, various interference effects were verified using a tolerance limit ratio, which sets the signal to be less than or higher than 5% of the relative error when compared to the response obtained from the standard

concentration of the analytes. Afterward, these developed methods were applied for the determination of 8-OHdG, 1-OHP, 5-ASA, and SPD in biological fluid samples, e.g., artificial urine, human urine, and human serum.



CHAPTER 2

THEORY

This chapter begins by providing information and significance for all selected analytes, followed by the principles of electrochemical methods, electrode materials, and modifiers used in this dissertation.

2.1 Reactive oxygen species and oxidative DNA damage

Reactive oxygen species (ROS) are a type of unstable molecule that contain oxygen radicals including superoxide (O_2^-), hydrogen peroxide (H_2O_2), hydroxyl radical (OH^\bullet), singlet oxygen ($^1\text{O}_2$), peroxy radical (LOO^\bullet), alkoxy radical (LO^\bullet), lipid hydroperoxide (LOOH), peroxynitrite (ONOO^-), hypochlorous acid (HOCl), and ozone (O_3) (R. Li, Jia, & Trush, 2016). ROS can easily and highly react with other molecules in a cell. The significant sources of free radicals have two sources: (i) inside the body, which come from a physiological metabolism as well as a breathing and exercise and (ii) outside the body, which is from stress, infection, and pollution. Under excessive oxidative stress conditions, ROS can be produced by living cells of aerobic organisms and activation of human inflammatory cells. Moreover, cellular biological structures, including proteins, lipids and membranes, sugars, and DNA, can be harmed by excessive ROS. ROS are also involved with oxidative stress and carcinogenesis since replication of damaged DNA. Therefore, they can lead to proliferation, anti-apoptosis, aggressiveness, and metastasis (Wirasorn, Klarod, Hongprabhas, & Boonsiri, 2014) (Cooke, Olinski, & Lof, 2008). Damage of DNA bases can be excised and replaced by DNA repaired genes. The products of oxidative DNA damage are transported through the bloodstream and excreted into the urine (Park et al., 1992). Among previous mentioned, hydroxyl radical is one of the most important oxygen radical causing damage to DNA due to its high reactivity (Cadet et al., 1999). Furthermore, hydroxyl radical can be produced by several mechanisms, particularly by the Fenton reaction of hydrogen peroxide and metal ions (Henle & Linn, 1997) (Valavanidis, Vlachogianni, & Fiotakis, 2009) as shown in Figure 1.

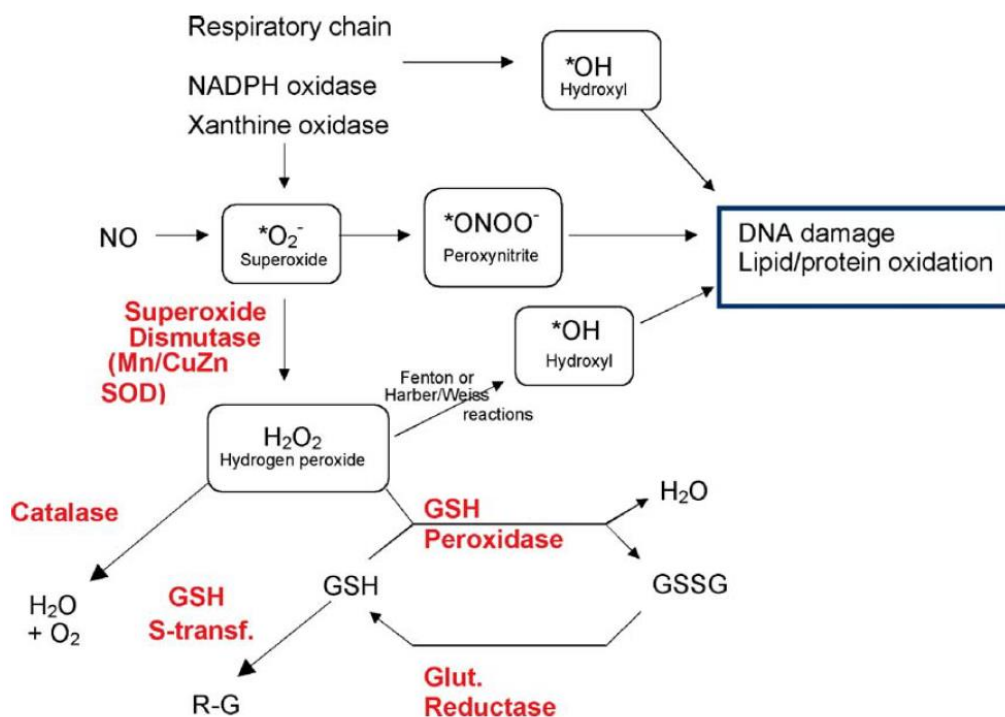


Figure 1 Pathway of generation of free radicals and scavenged enzymes in cellular.

From: Mahmoudi, M.; Mercer, J.; & Bennett, M. (2006). DNA damage and repair in atherosclerosis. p. 259-268.

2.2 8-Hydroxy-2'-deoxyguanosine

8-Hydroxy-2'-deoxyguanosine (8-OHdG) is one of the most widely studied target for oxidized metabolites and is used as a specific marker for oxidative stress. In 1984, Kasai et al. reported on the formation of 8-OHdG by oxygen radicals (Kasai, Hayami, Yamaizumi, Saito, & Nishimura, 1984). The formation of 8-OHdG is caused by interaction of hydroxyl radicals at eighth carbon atom of the guanine DNA base as shown in Figure 2. The 8-OHdG can be easily converted to other isomer forms of the oxidized product of 8-oxo-7,8-dihydro-2'-deoxyguanosine (8-oxodG). These two structures are called keto-enol tautomer (Valavanidis et al., 2009). Normally, the 8-OHdG can be found in several biological samples, such as urine, saliva, blood or serum, and tissue (G.V. Martins et al., 2016). The measurement of 8-OHdG in urine is the most popular for disease risk assessment because it is very stable in urine (Lars Barregard et al., 2013), noninvasive,

and its excretion is reasonable to reflect oxidative damage to DNA (Zanolin et al., 2015) (Graille et al., 2020). The level of 8-OHdG in body fluids is typically correlated with various diseases, e.g., cancers, aging, diabetes, and neurological disorders (Q. Zhang et al., 2018) (Zhao et al., 2019). Note that the normal levels of 8-OHdG in healthy humans have been reported to be below 100 nM (Jia, Liu, & Wang, 2015).

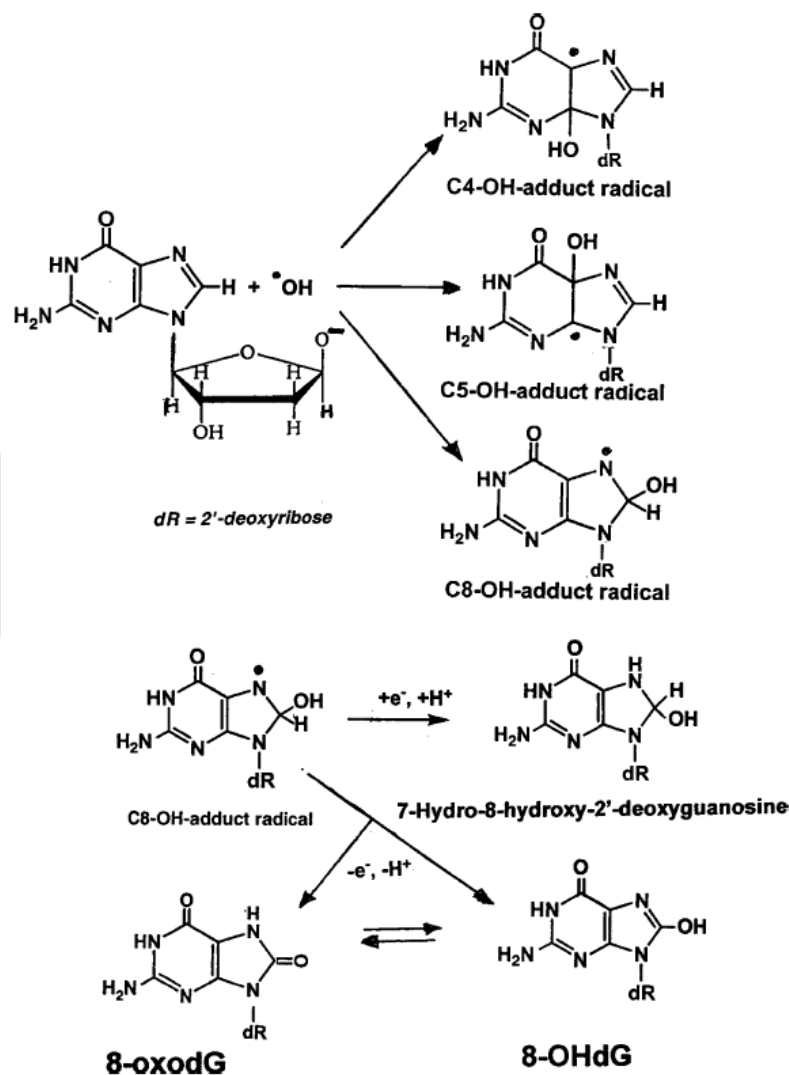


Figure 2 Pathway of 8-OHdG and its tautomer of 8-oxodG by hydroxyl radicals.

From: Valavanidis, A.; Vlachogianni, T.; & Fiotakis, C. (2009). 8-hydroxy-2'-deoxyguanosine (8-OHdG): A critical biomarker of oxidative stress and carcinogenesis. p. 120-139.

2.3 Polycyclic aromatic hydrocarbons

Polycyclic aromatic hydrocarbons (PAHs) are a class of organic chemical compounds that contain two or more fused benzene rings arranged in their structure (K.-H. Kim, Jahan, Kabir, & Brown, 2013). PAHs are harmful environmental and dietary contaminants (Serrano et al., 2017) that are typically formed during the incomplete combustion or pyrolysis of organic substances. The combustion of engines or various fuels in industrial plants, including coal and crude oil processing, petroleum refineries, gasoline stations, tire and rubber industries, and vehicle traffic, is the primary source of PAHs (Omidi, Khadem, Dehghani, Seyedsomeah, & Shahtaheri, 2020). Moreover, they can be found in cooking processes, such as barbecuing, grilling, and deep-frying at high temperature (Chen & Chen, 2001; Essumang, Dodoo, & Adjei, 2013). In our daily life, we are exposed to PAHs all the time through many routes, for example, inhalation, ingestion, and skin contact, which may come from dust, smoke from cars, cigarettes, or forest fires, the substances of asphalt making roads, and eating grilled food. However, there has been considerable concern about the toxicity of PAHs because they can damage or destroy proteins and DNA within a cell, leading to carcinogenic, teratogenic, and mutagenic effects (H. Zhang et al., 2016), developing malformations, cardiovascular disease, deterioration of pulmonary function, obesity, and neurodevelopmental issues (Pang, Huang, Li, Feng, & Shen, 2019).

2.4 1-Hydroxypyrene

1-Hydroxypyrene (1-OHP) is a metabolite of pyrene, which commonly occurs and is abundant in most PAH mixtures as seen in Figure 3 (Jeng & Pan, 2015). 1-OHP is a well-studied target for PAH metabolites. Furthermore, 1-OHP is a useful biomarker and a trustworthy indicator to evaluate human PAH exposure in a variety of investigations, notably in environmental and occupational health. Generally, 1-OHP can be detected in urine because pyrene is absorbed through the gastrointestinal system, lungs, and/or skin and then converted to 1-OHP, which is eliminated in urine (Jeng & Pan, 2015). According to the American Conference of Governmental Industrial Hygienists, the biological monitoring benchmark for urinary 1-OHP is $1.0 \mu\text{g L}^{-1}$. (Omidi et al., 2020).

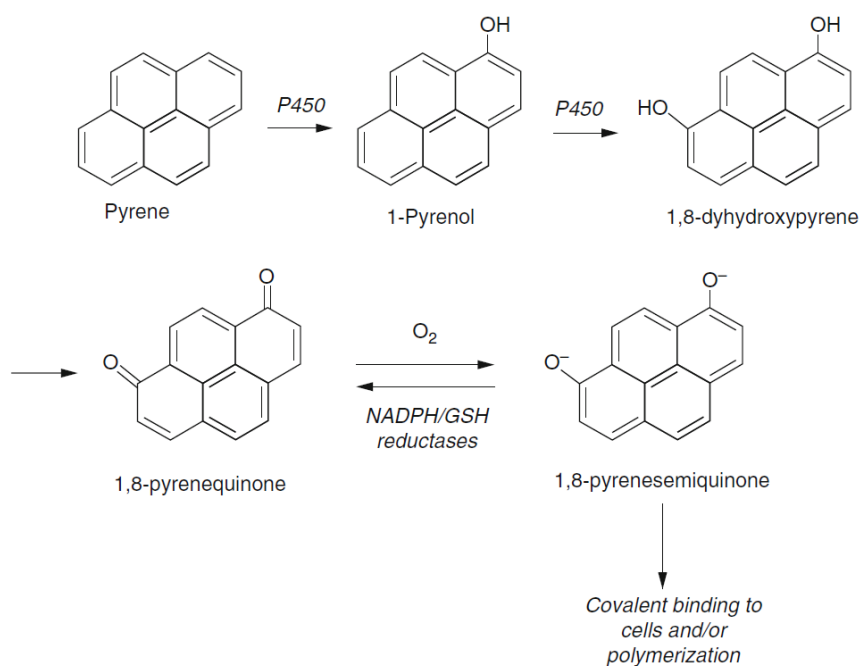


Figure 3 Metabolism of pyrene.

From: Jeng, H.A.; Pan, C.-H. (2015). 1-Hydroxypyrene as a Biomarker for Environmental Health. p. 597.

2.5 Sulfasalazine

Sulfasalazine (SSZ) or salazosulfapyridine is used in many countries for the treatment of rheumatoid arthritis (RA). Moreover, SSZ is also widely employed in the short and long-term treatment of inflammatory bowel disease (IBD) (Klotz, 1985), which is classified into two disease: (i) ulcerative colitis (UC) and (ii) Crohn's disease (CD). The chemical structure of SSZ is combined between 5-aminosalicylic acid and sulfapyridine by an azo bond. When patients take the SSZ drug, it will be delivered to a specific site in the colon. The azo bond is broken down by the enzyme azo reductase, which is produced by colonic bacteria, leading to the generation of 5-aminosalicylic acid and sulfapyridine as shown in Figure 4 (Choudhary, Goykar, Kalyane, Sreeharsha, & Tekade, 2020). For dosing information, the recommended dose for adults is 2 g daily for RA and 3 to 4 g daily for UC (France, 2022). In this research, we focused on the simultaneous determination of

its metabolites (5-aminosalicylic acid and sulfapyridine) in biological fluids, which are described the details of two metabolites in the next section.

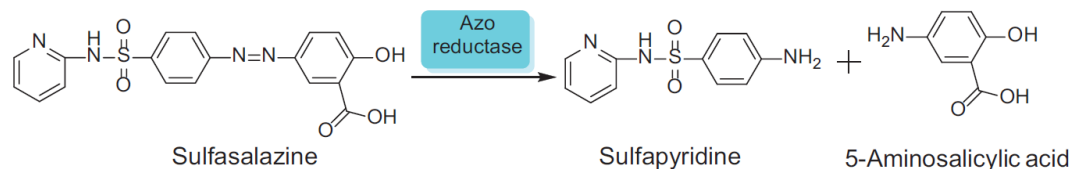


Figure 4 Bioactivation of sulfasalazine by azo reductase into sulfapyridine and 5-aminosalicylic acid.

From: Choudhary, D.; Goykar, H.; Kalyane, D.; Sreeharsha, N.; Tekade, R.K. (2020). Prodrug design for improving the biopharmaceutical properties of therapeutic drugs. p. 186.

2.6 5-Aminosalicylic acid and sulfapyridine

5-Aminosalicylic acid (5-ASA), also known as mesalazine or mesalamine, is a synthetic drug from the family of nonsteroidal anti-inflammatory drugs (NSAIDs) (Beiranvand, 2021). 5-ASA is a major component of the SSZ drug, which has anti-inflammatory activity. Sulfapyridine (SPD) is one of the components of SSZ, which has antibiotic activity (Klotz, 1985). Therefore, these two components play an important role in the therapeutic determinant for the action of SSZ.

2.7 Absorption and metabolism of SSZ and its metabolites

As we all know, the chemical structure of SSZ consists of two components, 5-ASA and SPD, connected by an azo bond. After oral administration of SSZ in patients, approximately 10-30% of SSZ is absorbed from the gastrointestinal tract. The unchanged SSZ can be found in blood and serum after oral ingestion but cannot be demonstratively detected because of its low bioavailability level (Klotz, 1985; Plosker & Croom, 2005). Less than 10% of the total absorbed SSZ is eliminated unchanged in the urine. For the non-absorbed portion of SSZ, it reaches the small intestine and colon. In the colon, an azo bond of the SSZ structure is cleaved by an intracellular azo reductase of the colonic bacteria, releasing 5-ASA and SPD. SPD is almost completely absorbed (>90%) from the

colon and excreted in the urine as the free sulfonamide or as its metabolites (the acetyl and glucuronide derivatives) (Peppercorn, 1984). In contrast, only a small portion of 5-ASA is absorbed (20-30%) from the colon and excreted in the urine as the acetylated derivative (Arvind & Farthing, 1988). The remaining 5-ASA is eliminated in the faeces. The absorption and metabolism of SSZ and its metabolites can be described in Figure 5 (Arvind & Farthing, 1988).

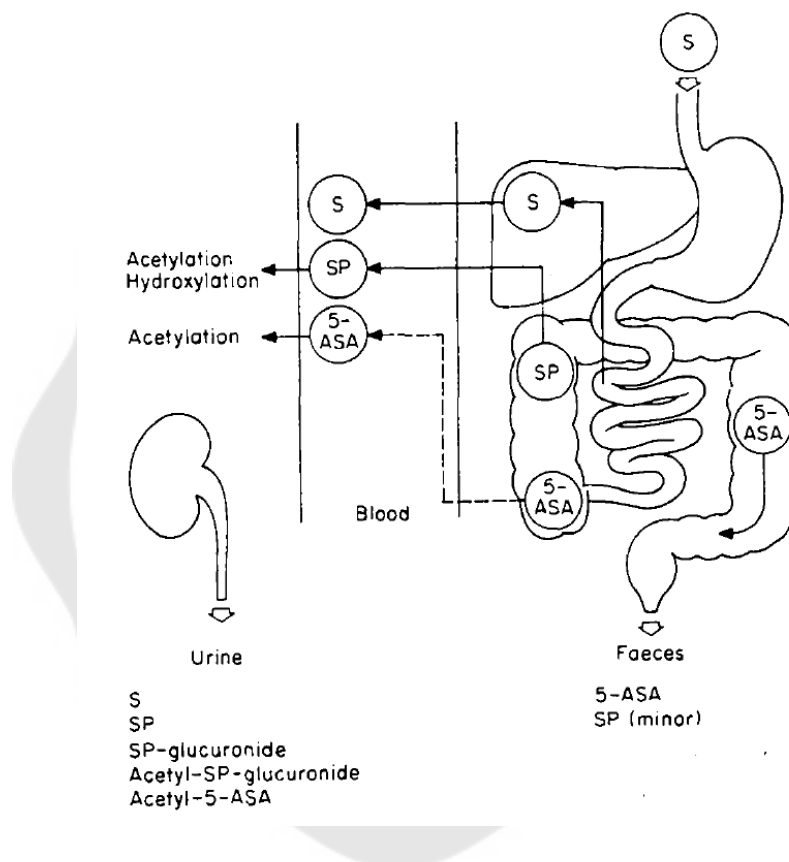


Figure 5 Absorption and metabolism of sulfasalazine (S) and its metabolites (Sulfapyridine (SP) and 5-aminosalicylic acid (5-ASA)).

From: Arvind, A.S.; Farthing, M.J.G. (1988). Review: new aminosalicic acid derivatives for the treatment of inflammatory bowel disease. p. 283.

Previously, chromatographic and spectroscopic methods were reported for determining 8-OHdG, 1-OHP, 5-ASA, and SPD. However, there were still some limitations, such as sophisticated and expensive instrumentation, the complicated pretreatment

steps, the need for complicated sample preparation, long analysis time, the use of unstable and high-cost enzymes, the requirement for a large solvent or sample volume, and special-trained operators. Moreover, these methods were not able to achieve portability and were not suitable for routine, on-site, and real-time analysis. To overcome these inherent problems, the development of new methods that provide rapid, simple, and sensitive assays is still required.

2.8 Electrochemical method

Electrochemistry is the branch of analytical chemistry that studies the movement of charges (charge transfer) across the junction between the surface of electrode and the solution based on the interrelation of electrical and chemical effects. A main part of this field deals with the study of chemical changes caused by the passage of an electric potential or current and the production of electrical energy by chemical reactions (Bard & Faulkner, 2001). As mentioned for the principles of electrochemistry, it can be applied to study many chemical reactions, such as electrophoresis, corrosion, as well as the mechanism and kinetic of organic and inorganic synthesis reactions, and the use of electrochemical principles to quantitatively determine analytes is important. The measured electrical values, such as current, charge, potential, conductance, or resistance, are directly proportional to the amounts of analytes. There are different techniques that can provide their own specific signal, which is used for the quantitation of analytes. Generally, the electrochemical measurement has two main groups, including potentiometry and voltammetry. In this research, voltammetric techniques have been chosen as an electrochemical method to study the electrochemical behaviors and to determine the amounts of analytes.

2.8.1 Voltammetry

Voltammetry is classified as electrolysis; therefore, the chemical changes occur by applying electrical energy from an external source into the system. Voltammetry is the collective name for a group of electrochemical methods which measure the current (i) at various potentials (E) given into the system under polarized experimental conditions on the working electrode. The resulting plotted graph between current versus applied potential is called a voltammogram. An electrochemical cell in voltammetric techniques

uses a three-electrode system, including a working electrode, a counter electrode, and a reference electrode. Among these three electrodes, the working electrode plays the most important role in an electrochemical cell because the analytes will be reacted at the electrode surface, causing the flow of current that can be measured as the quantity of analytes. The reference electrode is the second important electrode which has an exactly constant potential and does not vary owing to the type and composition of that electrode. It is used to compare the potential applied to the working electrode for the measurement. For the auxiliary or counter electrode, it is used for the completion of the electrode system. In this research, voltammetric techniques used for the preparation of modified electrodes, investigation of the electrochemical behaviors, and the determination of 8-OHdG, 1-OHP, 5-ASA, and SPD are cyclic voltammetry and square wave voltammetry.

2.8.1.1 Cyclic voltammetry

Cyclic voltammetry (CV) is one of voltammetric techniques that is the most widely used for acquiring qualitative information about the electrochemical behavior of an analyte. Moreover, CV can also provide information about the electrochemical reactions, such as the thermodynamics of redox processes, the kinetics of heterogeneous electron transfer reactions, and coupled chemical reactions or adsorption processes (J. Wang, 2006).

In measurement process, the equipment required to perform CV consists of a potentiostat connected to a three-electrode system (working, reference, and counter electrode) immersed in the supporting electrolyte solution. When the potential is applied linearly to the working electrode in both positive and negative direction, as a triangular potential waveform as shown in Figure 6, the oxidation and/or reduction reactions will be occurred. During the potential sweep, the potentiostat measures the current of reactions that occurred at the electrode surface resulting from applying the potential to the system. The current obtained is proportional to the concentration of the analyte. From the results, the current–potential plot is called a cyclic voltammogram.

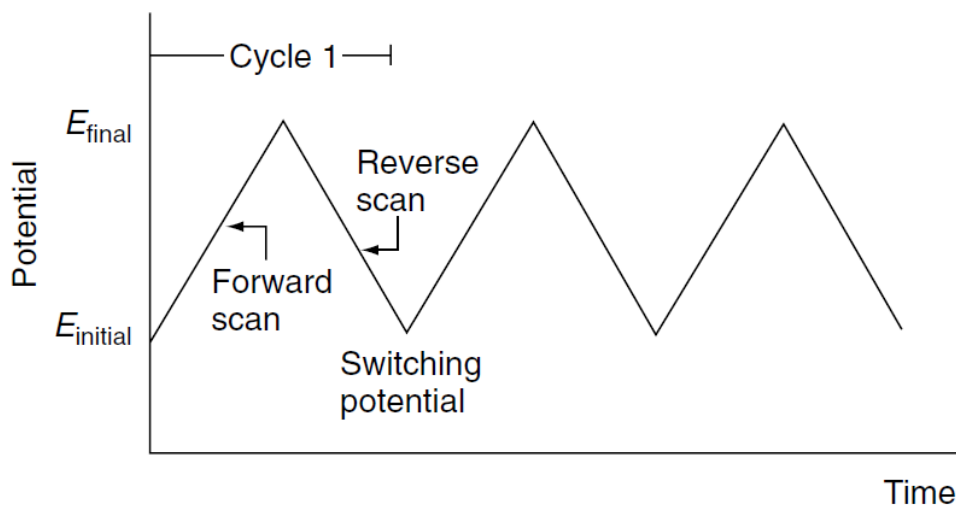


Figure 6 Potential–time excitation signal in a cyclic voltammetric technique.

From: Wang, J. (2006). Analytical Electrochemistry. p. 30.

The response of a reversible redox reaction in a single potential cycle was shown in Figure 7. When the potential is applied in a positive direction (forward scan), the electroactive species at the working electrode will lose an electron, leading to an oxidation reaction. The measured current signal will be anodic peak current (i_{pa}) that provides the oxidation peak at the anodic peak potential (E_{pa}). Then, in reverse scan, the electroactive species at the working electrode will be filled with an electron, leading to a reduction reaction. The measured current signal will be cathodic peak current (i_{pc}) that provides the reduction peak at the cathodic peak potential (E_{pc}).

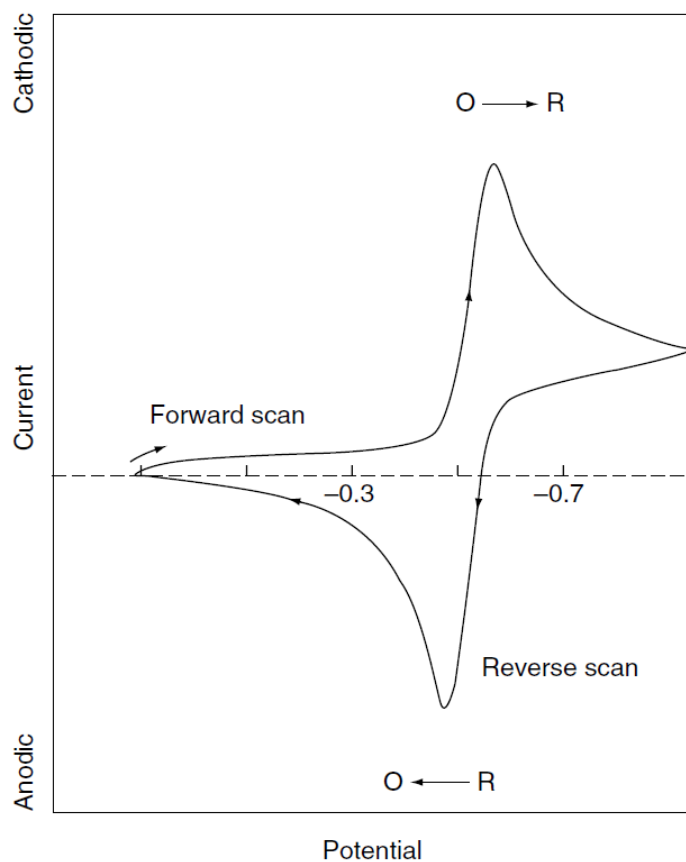


Figure 7 Typical cyclic voltammogram for a reversible redox process.

From: Wang, J. (2006). Analytical Electrochemistry. p. 30.

2.8.1.2 Square wave voltammetry

Square wave voltammetry (SWV) is an effective electrochemical technique that is frequently used for the quantitative determination of organic and inorganic compounds, especially in trace and ultra-trace analysis. This technique can also combine the operation of anodic stripping voltammetry which is called square wave anodic stripping voltammetry (SWASV). The potential waveform against time of SWV was presented in Figure 8. The excitation signal of the waveform consists of symmetric square wave pulses (forward and reverse pulses) which are superimposed on a staircase (E_s) potential. The current signal is measured at the end of a forward pulse (point 1) and the end of a reverse pulse (point 2). A difference current is obtained by calculating forward

and reverse currents (i_1 - $(-i_2)$). Then, the difference current is plotted versus the potential staircase, resulting in the shape of a square wave voltammogram. Hence, this technique has excellent sensitivity because the net current obtained is larger than either the forward or reverse currents. The peak height in a square wave voltammogram will be directly proportional to the concentration of electroactive species.

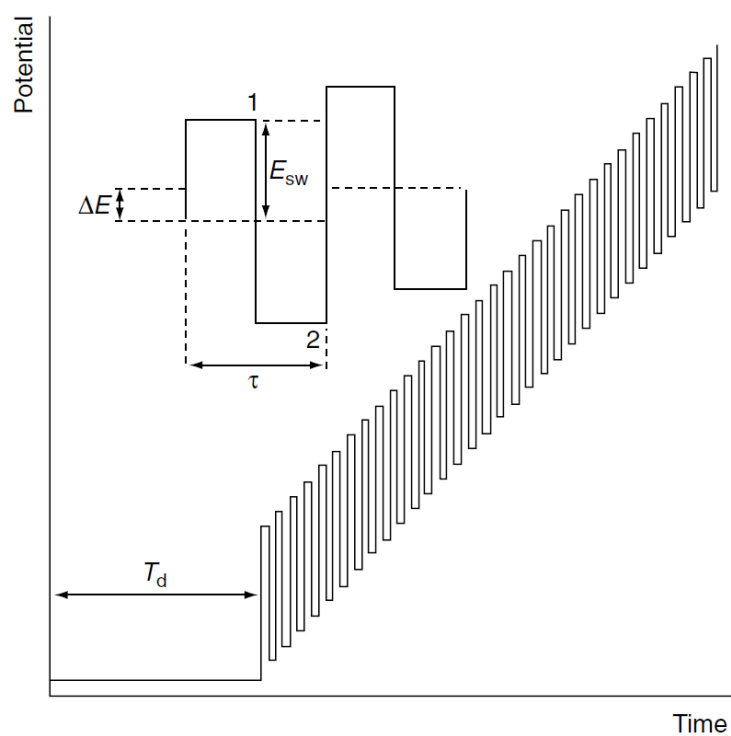


Figure 8 Excitation waveform of square wave voltammetry.

From: Wang, J. (2006). Analytical Electrochemistry. p. 81.

2.8.2 Electrochemical impedance spectroscopy

Electrochemical impedance spectroscopy (EIS) is a valuable and powerful method for investigating the impedance changes of the interface properties after modification of the electrode surface (Katz & Willner, 2003) due to its ability to interpret physical and electronic properties of electrochemical systems, such as the rate constants of electron transfer, charge transfer resistance, and capacitance. In theory, impedance is measured using the same units as resistance, which is often the force that opposes

electrical current in a circuit. For EIS experiment, a fixed sinusoidal voltage is applied to a potentiostat connected to a three-electrode system under the solution study. As exhibited in Figure 9, the impedance components are plotted against one another in Nyquist plots. The impedance result will be the semicircle diameter, which arises from the solution resistance (R_s), the charge transfer resistance (R_{ct}), double layer charging at the electrode surface (C_{dl}), and the Warburg Element (Z_w).

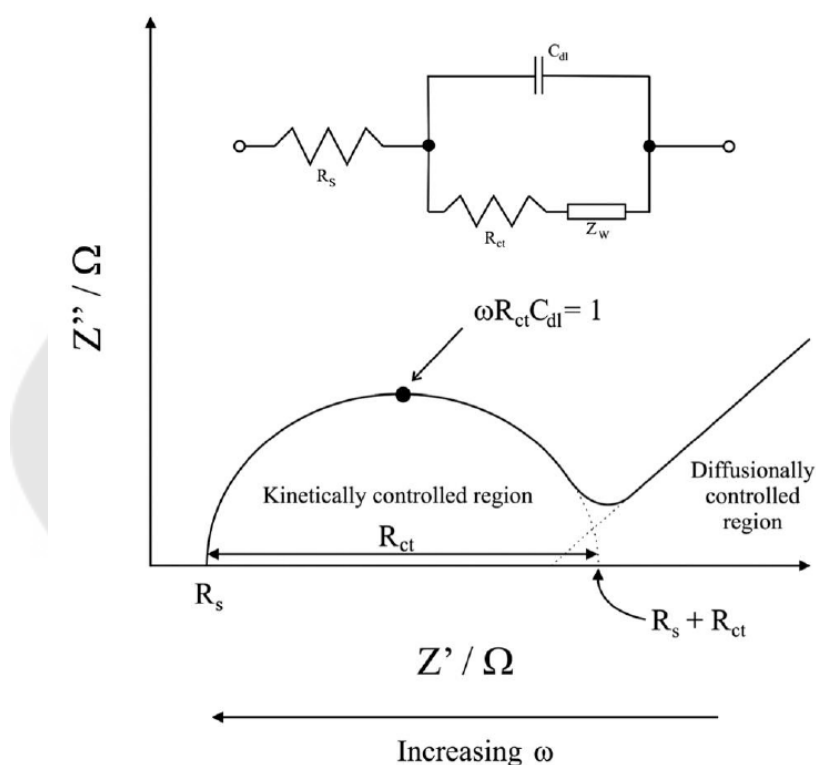


Figure 9 Simple Randles equivalent circuit for an electrochemical cell.

From: Randviir, E.P.; Banks, C.E. (2013). Electrochemical impedance spectroscopy: an overview of bioanalytical applications.

2.8.3 Electrodes

Typically, voltammetric measurements are carried out in the three-electrode system, comprising working, reference, and counter electrode, which have different roles in the current measurement. These electrodes serve as conductors that are immersed in

an electrolyte solution and connected to the electrochemical analyzer. The electrolytes are typically liquid solutions containing ionic species in water or non-aqueous solvent. In addition, the electrolyte solution or the solvent must be of an adequately low resistance to obtain high sensitivity in detection (Nantaphol, 2016).

2.8.3.1 Screen-printed electrodes

Nowadays, screen-printed electrodes (SPEs) are a novel type of electrode employing the development of electrochemical sensing platforms. It is easy and rapid to fabricate by using the screen-printing method. As compared to conventional systems, the screen-printed method can be used as an alternative platform for the fabrication of disposable sensors because of its economic substrate, low cost, rapid response, simplicity, capability of mass production, and suitability of routine, on-site, and real-time analysis (Charoenkitamorn et al., 2018). The SPEs can be fabricated from various types of ink on different substrates, which are important to obtain the high sensitivity and selectivity from the developed analytical detection. Normally, inks for screening are chosen as conducting materials, e.g., carbon, graphene, or graphene oxide, which are screened onto substrates (paper, plastic, or ceramic). The major advantages of SPEs are simplicity, small size, disposable device, portability, as well as inexpensiveness and the requirement of a small volume of sample or solvent. Therefore, the SPEs are extensively used for chemical and biological detection.

2.8.3.2 Graphene

Graphene is a well-known carbon material that consists of two-dimensional structures with sp^2 bonded carbon atoms in a hexagonal configuration (D. Kim et al., 2017). It has been extensively used to study and apply for many purposes because of its high electrical conductivity, superior electron transportation, and particularly outstanding surface area. Moreover, graphene is also used for several applications, such as sensors (Smith et al., 2015), mechanical reinforcement (Samori, Kinloch, Feng, & Palermo, 2015), energy storage (Bonaccorso et al., 2015) (Zhu et al., 2011), and energy capture (Tan et al., 2012). From these advantages, graphene ink is chosen as a conducting material for the screen-printed method, which is so-called a screen-printed graphene electrode (SPGE). Therefore, this research focused on the

development of electrochemical sensors for 8-OHdG, 1-OHP, 5-ASA, and SPD detection using SPGE.

2.8.3.3 Nanomaterials

Owing to the continuous and rapidly increasing advancements in the fields of nanoscience and nanotechnology, the development of electrochemical sensors for enhancing the electrical signals and improving the sensitivity and selectivity of detection is very important to obtain a new electrochemical sensor for widespread use. Nanomaterials (NMs) have a length scale of size in the range of 1–100 nm. Each material has different properties depending on the size. As compared to normal materials, NMs have distinct properties, e.g., large surface area, high reactivity and catalytic activity, excellent electrical conductivity, and providing for the use of much less material (Kurbanoglu, Ozkan, & Merkoci, 2017). Hence, several NMs, e.g., carbon nanomaterials, magnetic nanoparticles, metallic nanoparticles, nanowires, nanocomposites, and quantum dots, have been widely employed as electrochemical transducers or labels in enzymatic sensors, DNA sensors, immunosensors (Merkoçi, 2013), and carriers or tracers (Liu, Zhang, Wang, & Wang, 2014). Recently, NMs emerged as an attractive choice for modifying the electrode surface due to their high sensitivity, a wide potential range, and the ability to transform the surface of the electrode (Shah, Akhtar, Aftab, Shah, & Kraatz, 2017).

Metal nanoparticles are submicron-scale entities made from pure metals, e.g., Au, Ag, Pt, Cu, Zn, Fe, Ti, Ce, and TI (Piñón-Segundo, Mendoza-Muñoz, & Quintanar-Guerrero, 2013). They have been widely used as a sensing material to modify electrodes due to their unique electric and catalytic properties. In addition, modification of the electrode surface with metal nanoparticles can increase surface area, improve diffusion, and promote electron transfer for many electrochemical reactions as well. Among various metal nanoparticles, gold nanoparticles (AuNPs) are one of the most widely employed as metal nanoparticles for modifying the electrode surface. AuNPs are colloidal particles that have a particle size in the range of 1–100 nm. They have many advantages, including physical and chemical properties, such as good stability, large specific surface area, high

surface free energy and conductivity, excellent electrocatalytic capability, and good biocompatibility (He et al., 2014) (Yuting Wang et al., 2014). Furthermore, AuNPs can also react excellently with organo-sulfur compounds at the electrode surface to form S–Au through covalent bonding, resulting in enhancing the stability of self-assembled monolayers (SAMs) (Łuczak, 2009) (Benvidi et al., 2015). Therefore, in this research, gold nanoparticles are chosen as metal nanoparticles to modify the electrode surface, enhancing the sensitivity and stability of the screen-printed graphene electrode for 8-OHdG detection.

2.8.3.4 Amino acids

Amino acids are organic compounds containing a basic amino group ($-NH_2$), an acidic carboxyl group ($-COOH$), and an organic R group (or side chain) that is linked to the same carbon atom as the specificity of the individual amino acid. Amino acids play a crucial role in the building blocks of peptides and proteins, metabolic pathways, gene expression, and cell signal transduction regulation. The polymers of amino acids are formed a single amino acid repeating the unit of the polymer formed via polymerization process between $-NH_2$ and $-COOH$ groups which is called poly(amino acids).

In recent years, poly(amino acids) modified electrode have been attracted great attention for the determination of various important biological and clinical species because of their simplicity, rapidity, and conveniences of fabrication. The $-NH_2$ and $-COOH$ groups of amino acids play a key role in the electropolymerization procedure for the modification of the electrode surface (Cheemalapati, Devadas, & Chen, 2014). Remarkably, the use of poly(amino acids) as a surface modifying agent has several advantages, such as facilitating the sensitivity and selectivity towards the target analytes, promoting the rate of electron transfer, decreasing electrode surface fouling, providing reproducibility of the electrode response, and improving the electrode surface area by forming homogenous films (Gomes, Leite, Ferraz, Mourao, & Malagutti, 2019; Thangphatthanarunguang, Chotsuwan, & Siangproh, 2023). From the excellent properties of amino acids, it has been greatly used for electrochemical sensor

applications. L-Methionine (L-Met) is an essential amino acid that plays an important role in many plants and proteins, including the proteins in foods (e.g., meat, fish, and dairy products), and cell functions of the body (Schnekenburger & Diederich, 2015). L-Met is one of the sulfur-containing proteinogenic amino acids; its derivative S-adenosyl methionine serves as a methyl donor. Additionally, it can be used as a modifier for the modification of the electrode surface by electropolymerization process because of its containing $-NH_2$ and $-COOH$ groups and via SAM with gold nanoparticles to provide high stability of the electrode. Furthermore, L-Glutamic acid (L-GA) is one of the amino acids that can be easily synthesized via electropolymerization as well. Owing to the above-mentioned benefits of gold nanoparticles and poly(amino acids), several researchers have used them for modifying the electrode surface to increase the electroactive surface area and enhance the electrocatalytic performance of the electrode. Thus, this research focused on the development of electrochemical sensors by using AuNPs, L-Met, and L-GA modified SPGE for the determination of 8-OHdG, 1-OHP, 5-ASA, and SPD.

CHAPTER 3

METHODOLOGY

This chapter is divided into three sub-projects. Sub-project I (section 3.1) reported on a new nanocomposite-based screen-printed graphene electrode for sensitive and selective detection of 8-hydroxy-2'-deoxyguanosine. Sub-project II (section 3.2) described a novel and easy-to-construct polymeric L-glutamic acid-modified sensor for urinary 1-hydroxypyrene detection: Human biomonitoring of polycyclic aromatic hydrocarbons exposure. Sub-project III (section 3.3) revealed a highly efficient polymeric L-methionine-modified sensor: An application for the simultaneous determination of 5-aminosalicylic acid and sulfapyridine. Each sub-project consisted of apparatuses, chemicals, reagents, materials, fabrication and measurement methods, and sample preparations.

3.1 A new nanocomposite-based screen-printed graphene electrode for sensitive and selective detection of 8-hydroxy-2'-deoxyguanosine

The contents of this sub-project are based on the original research article, which is shown in appendix 1.

3.1.1 Apparatuses, chemicals, and reagents

Electrochemical measurement was carried out using a model CHI660D electrochemical analyzer (CH Instrument, USA). All experiments were performed using a three-electrode system, including poly(L-methionine) and gold nanoparticles-modified screen-printed graphene working electrode, a graphene ink counter electrode, and a silver/silver chloride ink reference electrode, all were screen-printed onto the same transparent sheet. The screen-printed template blocks were generated by Chaiyaboon Co. Ltd. (Bangkok, Thailand).

Field emission scanning electron microscope and energy dispersive x-ray spectroscopy (FESEM-EDS) was performed with an electron microscope at 5 kV (JSM-7610F, JEOL, United Kingdom, England).

8-Hydroxy-2'-deoxyguanosine (8-OHdG) was acquired from Fujifilm Wako Pure Chemical Corporation (Osaka, Japan). Standard gold solution 1000 ppm (Product

number: 08269, CAS: 7647-01-0), methionine, sodium dodecyl sulfate, uric acid, dopamine, ascorbic acid, bovine serum albumin, and citric acid were purchased from Sigma-Aldrich. Glucose, sodium chloride, potassium chloride, calcium chloride, magnesium chloride, methanol, sodium hydroxide, sodium dihydrogen orthophosphate ($\text{NaH}_2\text{PO}_4 \cdot 2\text{H}_2\text{O}$), di-sodium hydrogen orthophosphate ($\text{Na}_2\text{HPO}_4 \cdot 2\text{H}_2\text{O}$), and hydrochloric acid were obtained from Ajax Finechem Pty., Ltd. (New South Wales, Australia). Copper sulphate was received from Asia Pacific Specialty Chemicals Ltd. (New South Wales, Australia). Zinc sulphate was purchased from Merck (Darmstadt, Germany). Artificial urine was acquired from Carolina Biological Supply Company (Burlington, USA). Acetone was obtained from CaHC Co., Ltd. (Bangkok, Thailand). Graphene ink was received from Serve Science Co., Ltd. (Bangkok, Thailand). Silver/silver chloride (Ag/AgCl) ink was purchased from Sun chemical Ltd. (Slough, United Kingdom). All chemicals and reagents used in this work were of analytical grade and were used without any purification.

The stock standard solution of 8-OHdG was prepared in Milli-Q water and stored in the dark at 2-8°C. The working solutions of 8-OHdG were prepared by dilution of the 1 mM solution of 8-OHdG with supporting electrolyte and mixed using a vortex mixer. Sodium phosphate buffer solution (Na-PBS) was prepared by mixing two stock solutions of NaH_2PO_4 and Na_2HPO_4 following the standard recipes. To obtain other pH values, 0.1 M Na-PBS was adjusted to the desired value by using 0.1 M hydrochloric acid or 0.1 M sodium hydroxide. All solutions were prepared in Milli-Q water from a Millipore water purification system ($R \geq 18.2 \text{ M}\Omega \text{ cm}$).

Human urine samples were collected from healthy human volunteers in our laboratory and immediately refrigerated at 4°C. We informed all volunteers about what would happen to the human subjects in a trial. Human serum samples were taken from healthy patient and used without purification process.

3.1.2 Fabrication of the electrochemical sensor for 8-OHdG detection

The electrode pattern was designed by using Adobe Illustrator CS6. Screen-printed electrode (SPGE) was fabricated using an in-house screen-printing method on the

transparent sheet substrate. For fabrication steps of SPGE, graphene ink was first screened onto the transparent sheet as the first layer to obtain the working and counter electrode. Then, this screen-printed electrode was baked at 60°C for 30 min to clear up the solvent from the electrode surface. The last step was the screening of Ag/AgCl ink as the reference electrode and conductive pads. Afterward, this screen-printed electrode was baked again at 60°C for 30 min. Finally, the obtained screen-printed graphene electrode was kept in a dry place and ready to use for an experiment.

The sequential “layer-by-layer” film was fabricated on SPGE via cyclic voltammetry (CV). Initially, AuNPs-modified SPGE was prepared by dropping 50 μL of 1000 ppm standard gold solution in 5% hydrochloric acid onto the three-electrode surface of SPGE. Then, electrodeposition of gold atoms was performed in the potential range from -0.4 V to +1.4 V with a scan rate of 150 mV s^{-1} for seven cycles. Subsequently, the electrode was rinsed with deionized water and air-dried. To prepare poly(L-Met)/AuNPs-modified SPGE, electropolymerization of L-methionine on the AuNPs/SPGE was performed by dropping 50 μL of 2 mM L-methionine solution in 0.1 M sodium phosphate buffer solution at pH 7.0 onto the surface of AuNPs/SPGE and applying 10 cyclic voltammetric scans in the potential range from -0.6 V to +2.0 V with a scan rate of 100 mV s^{-1} . Afterward, this electrode was then rinsed thoroughly with deionized water and air-dried once again. Finally, the poly(L-Met)/AuNPs-modified SPGE was obtained and stored in a dry place for analytical measurements. The preparation process of the fabricated electrochemical sensor for 8-OHdG detection is summarized in Figure 10. To validate the performance of the proposed sensor, different sensors were also prepared using the same protocol without AuNPs and poly(L-Met).

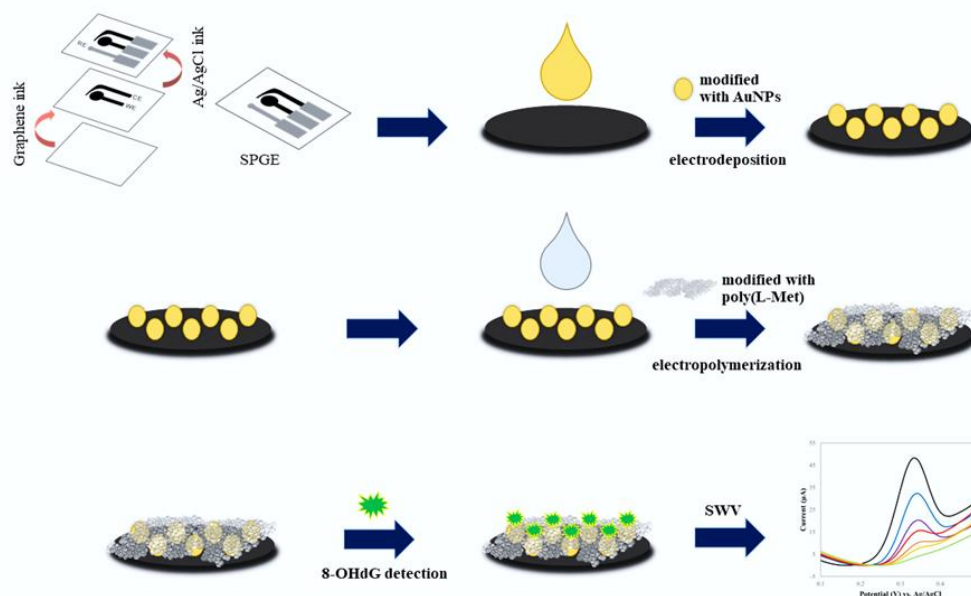


Figure 10 Illustration of the fabrication of a new electrochemical sensor for 8-OHdG detection.

CV was used as an efficient technique for the deposition of AuNPs and the polymeric thin-film layer of L-methionine on the surface of SPGE. The fabrication of layer-by-layer film on SPGE involves two steps: (1) electrodeposition of AuNPs on SPGE and (2) electropolymerization of L-methionine on AuNPs/SPGE. CV curves obtained from the electrodeposition of AuNPs at SPGE are presented in Figure 11A. As can be seen from the figure, the resulting CV from AuNPs-modified SPGE appeared two peaks corresponding to the oxidation and reduction process of gold. Afterward, the poly(L-Met) on AuNPs/SPGE was prepared by placing L-methionine monomer, followed by electropolymerization. As presented in Figure 11B, the oxidation peaks of L-methionine were observed around +1.7 V. For the first three cycles, the anodic peak currents gradually increased, indicating the formation and growth of the polymeric film on the electrode surface as seen previously (P. S. Ganesh & Swamy, 2015). After the fourth cycle, the increasing anodic peak current tended to be constant, suggesting that the poly(L-Met) film had increasingly grown and reached a saturation level (J. Li & Zhang, 2012).

A possible model illustrating the AuNPs electrodeposition and the electropolymerization onto the electrode surface is proposed in Figure 12.

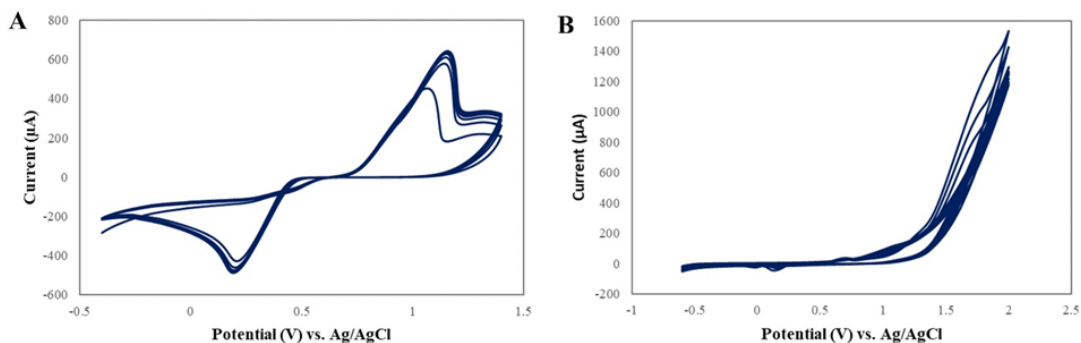


Figure 11 Cyclic voltammograms for the electrodeposition of AuNPs in 5% hydrochloric acid on SPGE with a scan rate of 150 mV s^{-1} for seven cycles (A) and the electropolymerization of L-methionine in 0.1 M sodium phosphate buffer solution at pH 7.0 on AuNPs/SPGE with a scan rate of 100 mV s^{-1} for ten cycles (B).

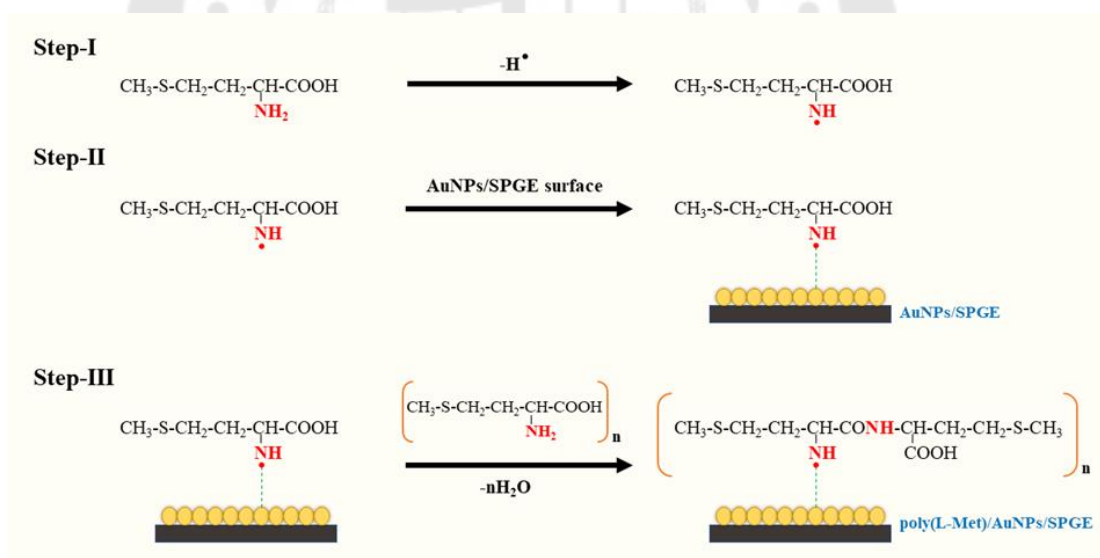


Figure 12 Illustration of the possible structure of L-methionine film on AuNPs modified SPGE.

3.1.3 Electrochemical measurements

For the measurement process in this work, a $50 \mu\text{L}$ aliquot of the standard or sample solution was dropped, covering the three-electrode area. CV was employed for

the preliminary investigation of the electrochemical 8-OHdG behavior. The parameters were set in the potential range from 0.0 V to +0.3 V with a fixed scan rate of 100 mV s^{-1} . Contrarily, square wave voltammetry (SWV) was used for optimization and quantitative determination due to the benefits provided by the technique in terms of sensitivity. The affected SWV parameters were conducted in the potential range from +0.1 V to +0.5 V with a potential increment of 0.015 V, an amplitude of 0.05 V, and a frequency of 30 Hz. These SWV parameters were the optimal values that are ready to use. All experiments were conducted in triplicate at room temperature.

Electrochemical impedance spectroscopy (EIS) was performed using an Autolab electrochemical system with a potentiostat PGSTAT 204 (Utrecht, Netherlands). EIS measurements were performed in 5 mM $\text{K}_3[\text{Fe}(\text{CN})_6]$ containing 0.1 M KCl with a potential of 0.1 V, a frequency range from 0.1 Hz to 100 kHz, and an amplitude of 0.1 V.

3.1.4 Application of the proposed electrochemical sensor for the determination of 8-OHdG in real samples.

To demonstrate efficiency of the modified SPGE and developed electrochemical method, poly(L-Met)/AuNPs-modified SPGE was applied for the determination of 8-OHdG in artificial urine, healthy human urine, and human serum samples using a standard addition method. For the sample preparation, artificial urine, healthy human urine, and human serum were diluted with supporting electrolyte. Then, different concentrations of standard solutions of 8-OHdG with appropriate to calibration curve were spiked into samples. Afterward, the electrochemical analysis of 8-OHdG was conducted via SWV under the optimized conditions as followed by the section 3.1.3. Finally, recoveries and precision were subsequently evaluated and compared to spiked values.

3.2 A novel and easy-to-construct polymeric L-glutamic acid-modified sensor for urinary 1-hydroxypyrene detection: Human biomonitoring of polycyclic aromatic hydrocarbons exposure

The contents of this sub-project are based on the original research article, which is shown in appendix 2.

3.2.1 Chemicals, materials, and apparatuses

1-OHP was acquired from AccuStandard (New Haven, CT, USA). L-GA, uric acid, ascorbic acid, citric acid, bovine serum albumin, creatinine, urea, ammonium persulfate, potassium ferricyanide ($K_3[Fe(CN)_6]$), and hexaammineruthenium(III) chloride ($[Ru(NH_3)_6]Cl_3$) were supplied from Sigma-Aldrich (St. Louis, MO, USA). Glucose, sodium chloride, potassium chloride, calcium chloride, magnesium chloride, sodium hydroxide, methanol, sodium dihydrogen orthophosphate, and di-sodium hydrogen orthophosphate were purchased from Ajax Finechem Pty., Ltd. (New South Wales, Australia). Glycine was obtained from Amresco Inc. (Solon, OH, USA). Acetone was received from CaHC Co., Ltd. (Bangkok, Thailand). Graphene ink was acquired from Serve Science Co., Ltd. (Product code: SSG-1760A, Bangkok, Thailand). Silver/silver chloride (Ag/AgCl) ink was purchased from Sun Chemical Ltd. (Product code: C2130809D5, Slough, UK). All chemicals and reagents used were of analytical grade and were used without any purification.

The stock standard solution of 1-OHP was prepared in methanol and stored in the dark at 2°C–8°C. The 1-OHP working solutions were prepared by dilution with supporting electrolyte and mixing with a vortex mixer. Sodium phosphate buffer solution (Na-PBS), di-sodium hydrogen phosphate-sodium hydroxide buffer solution (Na_2HPO_4 -NaOH), and glycine-sodium hydroxide buffer solution (Gly-NaOH) were prepared by following the standard recipes. All solutions were prepared in Milli-Q water from a Millipore water purification system ($R \geq 18.2 \text{ M}\Omega \text{ cm}$).

Voltammetric measurements, comprising cyclic voltammetry (CV) and square wave voltammetry (SWV), were performed using a model CHI660D electrochemical analyzer (CH Instrument, Austin, TX, USA). Electrochemical impedance spectroscopy (EIS) experiments were conducted using PalmSens4 (Houten, The Netherlands). A field emission scanning electron microscope and energy-dispersive X-ray spectroscopy (FESEM-EDS) were conducted with an electron microscope at 5 kV (JSM-7610F; JEOL, England, UK). X-ray photoelectron spectroscopy (XPS) measurements were executed using the Kratos Axis Ultra DLD X-ray Photoelectron Spectrometer.

3.2.2 Fabrication of conductive polymer thin film modified SPGE

The electrode pattern of SPGE was designed using Adobe Illustrator CS6, and the screen-printed template blocks were generated by Chaiyaboon Co., Ltd. (Bangkok, Thailand). An in-house screen-printing method was manually applied to the fabricated SPGE, composed of a working electrode, a counter electrode, and a reference electrode, on the transparent sheet substrate. For the fabrication steps of SPGE, the working and counter electrodes were first screened onto the transparent sheet using graphene ink. Then, this SPE was baked at 60°C for 30 min to evaporate the solvent from the ink. Subsequently, the reference electrode and conductive pad were screened onto the same transparent sheet using Ag/AgCl ink. Afterward, the completed SPE was baked again for solvent drying. Finally, before use, the obtained SPGE was kept in a ziplock bag in a dark and dry location and ready to be used for an experiment.

The conductive polymer thin film layer modified SPGE was prepared by electropolymerization of L-GA via CV. The procedure of SPGE modification was performed by dropping 100 μL of 30 mM L-GA solution in 0.1 M Na-PBS (pH 7.0) onto the surface of SPGE and scanning the potential range from -0.8 V to +1.7 V for 5 cycles at a scan rate of 100 mV s^{-1} . Then, the sensor was carefully cleaned with deionized water before being air-dried. Cyclic voltammograms for the electropolymerization of L-GA at SPGE are depicted in Figure 13. A probable model demonstrating the electropolymerization of poly(L-GA) on the SPGE surface is presented in Figure 14.

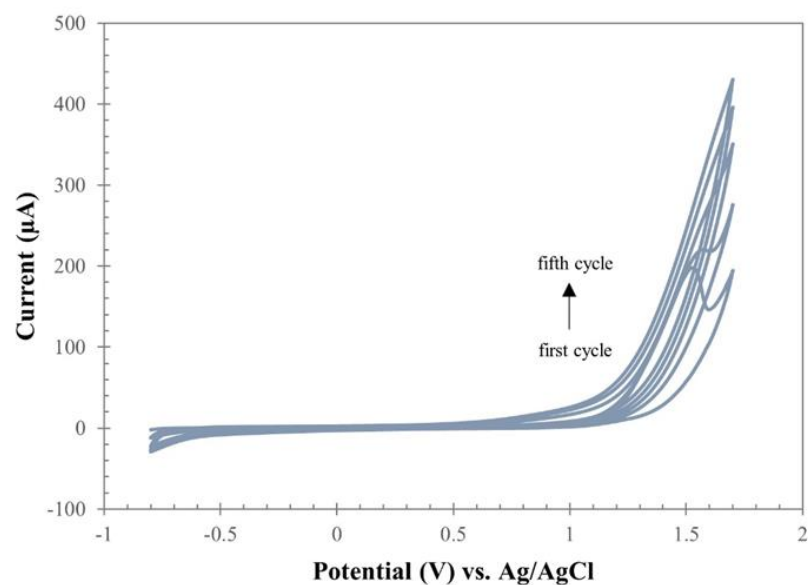


Figure 13 Cyclic voltammograms for the electropolymerization of 30 mM L-GA in 0.1 M Na-PBS (pH 7.0) at SPGE with a scan rate of 100 mV s^{-1} for 5 cycles.

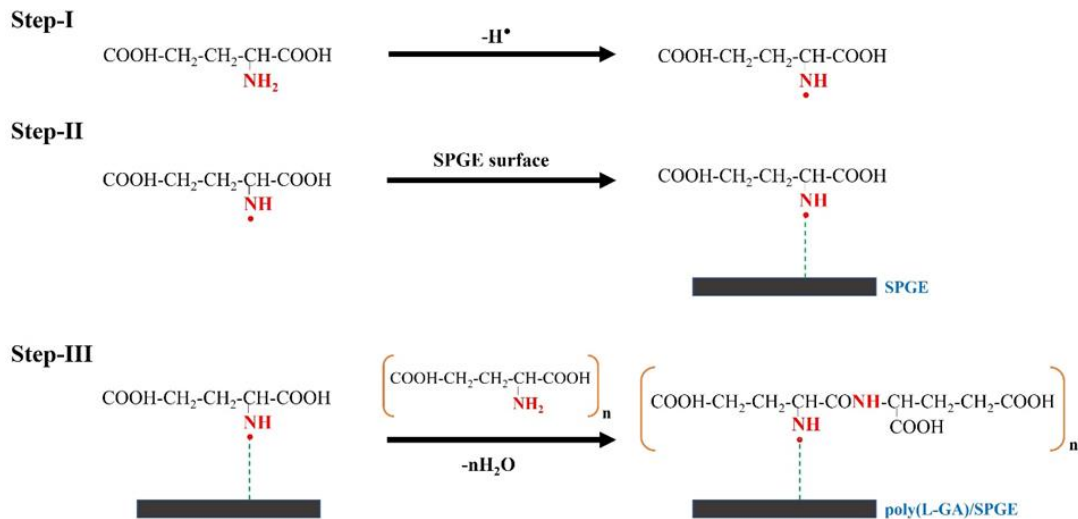


Figure 14 Mechanism of electropolymerization of L-GA on the SPGE surface.

3.2.3 Electrochemical measurements

100 μL of 1-OHP standard solution was dropped onto the three-electrode system of poly(L-GA)/SPGE. CV was employed for characterization of the electrochemical properties of 1-OHP in the potential range from -0.6 V to +0.8 V at a scan rate of 100

mV s^{-1} . SWV was used for optimization and quantitative determination of 1-OHP with scanning the potential range from -0.4 V to $+0.3 \text{ V}$. The optimal SWV parameters were a potential increment of 0.008 V , an amplitude of 0.1 V , a frequency of 40 Hz , and a quiet time of 180 s (Figure 15).

EIS experiments were conducted in $5 \text{ mM K}_3[\text{Fe}(\text{CN})_6]$ in 0.1 M KCl with potential ranges ranging from 0.0 V to 0.1 V , frequency ranges ranging from 0.01 Hz to 50 kHz , and an amplitude of 0.1 V .

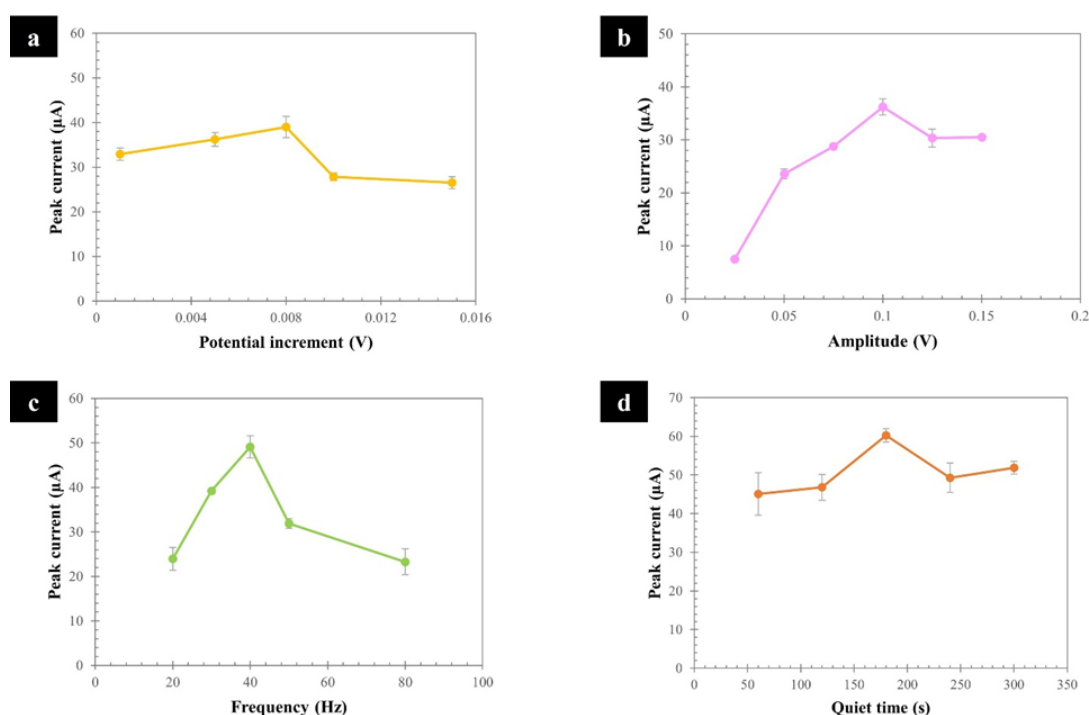


Figure 15 Effects of a potential increment (a), an amplitude (b), a frequency (c), and a quiet time (d) for 1-OHP detection in Gly-NaOH (pH 9.4) at the poly(L-GA)/SPGE. Error bars represent the standard deviation of $10 \mu\text{M}$ 1-OHP detection using SWV for three repetitive measurements ($n = 3$).

3.2.4 Sample preparation

Human urine samples were collected from healthy human volunteers in our laboratory and immediately refrigerated at 4°C . All human urine samples were well received by the trial's volunteers. To demonstrate the efficiency of the modified SPGE and the developed electrochemical method, the poly(L-GA) modified SPGE was applied for

the determination of 1-OHP in healthy human urine samples using a standard addition method. For the sample preparation, healthy human urine samples were diluted with a supporting electrolyte. Then, the standard solutions of 1-OHP (10 and 500 nM) were spiked into the samples. Afterward, the electrochemical analysis of 1-OHP was conducted via SWV under the optimized conditions as followed by Section 3.2.3. Finally, accuracy and precision were subsequently evaluated and compared to spiked values.

3.3 Highly efficient polymeric L-methionine-modified sensor: An application for the simultaneous determination of 5-aminosalicylic acid and sulfapyridine

The contents of this sub-project are in the process of writing the original research article.

3.3.1 Apparatuses, chemicals, reagents, and materials

Voltammetric measurements were conducted using a model CHI660D electrochemical analyzer (CH Instrument, Austin, TX, USA). All experiments were conducted using a three-electrode system, comprising a working, counter, and reference electrode, which screened on the same PVC substrate.

SPD was acquired from Tokyo Chemical Industry Co., Ltd. (Tokyo, Japan). 5-ASA was purchased from Glenthams Life Sciences (Corsham, UK). L-Met, uric acid, ascorbic acid, citric acid, bovine serum albumin, creatinine, urea, and ammonium persulfate were obtained from Sigma-Aldrich (St. Louis, MO, USA). Glucose, sodium chloride, potassium chloride, magnesium chloride, sodium hydroxide, methanol, sodium dihydrogen orthophosphate ($\text{NaH}_2\text{PO}_4 \cdot 2\text{H}_2\text{O}$), and di-sodium hydrogen orthophosphate ($\text{Na}_2\text{HPO}_4 \cdot 2\text{H}_2\text{O}$) were purchased from Ajax Finechem Pty., Ltd. (New South Wales, Australia). Calcium chloride and zinc sulphate were supplied by Carlo Erba Reagents (Val de Reuil, France). Acetone was acquired from CaHC Co., Ltd. (Bangkok, Thailand). Graphene ink was received from Serve Science Co., Ltd. (Product code: SSG-1760A, Bangkok, Thailand). Silver/silver chloride (Ag/AgCl) ink was obtained from Sun Chemical Ltd. (Product code: C2130809D5, Slough, UK).

The stock standard solution of SPD was prepared in methanol, and 5-ASA was arranged in Milli-Q water, then stored in the dark at 2°C–8°C. The SPD and 5-ASA working solutions were prepared in a mixture of the supporting electrolyte containing methanol

(MeOH) and 0.1 M phosphate buffer solution. A 0.1 M phosphate buffer solution (PBS) was prepared by mixing two stock solutions of NaH_2PO_4 and Na_2HPO_4 following the standard recipes. All aqueous solutions were arranged in Milli-Q water from a Millipore water purification system ($R \geq 18.2 \text{ M}\Omega \text{ cm}$ at 25°C).

3.3.2 Fabrication of poly(L-methionine)-modified SPGE

The pattern and manufacturing procedures of SPGE were fabricated on a PVC substrate using an in-house screen-printing technique according to the previous description (Thangphatthanarungruang et al., 2023). Briefly, graphene ink was first screened to obtain a working and counter electrode. Next, this SPE was baked at 60°C for 30 min. Afterward, Ag/AgCl ink was screened on the same SPE to receive a reference electrode and conductive pad. Subsequently, the completed SPGE was baked again. Finally, the SPGE obtained was ready to be used for electrochemical measurements.

Cyclic voltammetry (CV) was employed for the preparation of the polymeric thin film layer modified SPGE by electropolymerization procedure. Initially, the solution of 6 mM L-Met in 0.1 M PBS (pH 7.0) was dropped onto the SPGE surface. Then, electropolymerization of L-Met on the SPGE was carried out in the potential range from -0.6 V to +2.0 V for 3 cycles with a scan rate of 100 mV s^{-1} . Next, this sensor was rinsed thoroughly with deionized water and air-dried. Cyclic voltammograms for the L-Met electropolymerization on SPGE are described in Figure 16.

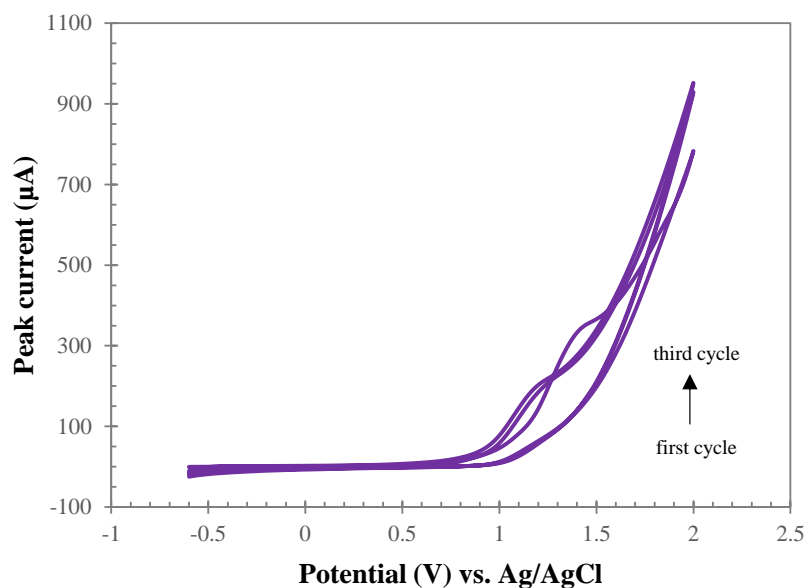


Figure 16 Cyclic voltammograms for the 6 mM L-Met electropolymerization on SPGE with a scan rate of 100 mV s^{-1} for 3 cycles.

3.3.3 Electrochemical measurements

All measurement processes were carried out by dropping $100 \mu\text{L}$ of standard or sample solution onto the three-electrode surface of poly(L-Met)/SPGE. For voltammetric measurements, CV was used for the investigation of the electrochemical behaviors of 5-ASA and SPD in the potential range from -0.2 V to $+0.9 \text{ V}$ with a scan rate of 100 mV s^{-1} . Furthermore, square wave voltammetry (SWV) was chosen for optimization of electrochemical conditions and quantitative determination of 5-ASA and SPD. The affected SWV parameters were successfully accomplished by scanning the potential range from -0.25 V to $+0.90 \text{ V}$ with an amplitude of 0.05 V , a potential increment of 0.025 V , a frequency of 30 Hz , and a quiet time of 60 s (Figure 17).

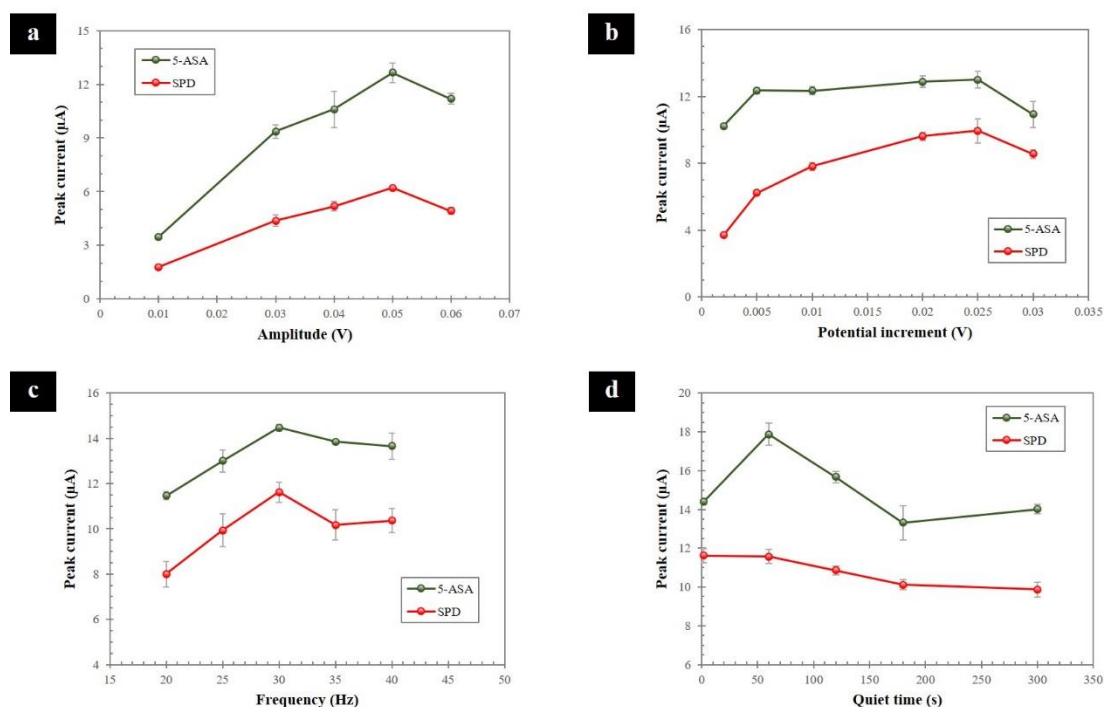


Figure 17 The crucial SWV parameters, including an amplitude (a), a potential increment (b), a frequency (c), and a quiet time (d) for the simultaneous detection of 5-ASA and SPD at the poly(L-Met)/SPGE. Error bars represent the standard deviation of the simultaneous detection of 100 μM 5-ASA and SPD using SWV for three repetitive measurements ($n = 3$).

3.3.4 Real-sample preparation

The poly(L-Met)/SPGE sample applications were investigated using various real human urine samples. All human urine samples were well received by the trial's volunteers in our laboratory. To verify the capability of the proposed sensor and developed method, the poly(L-Met)/SPGE was utilized to simultaneously determine 5-ASA and SPD in real urine samples using a standard addition method. For the sample preparation, first, real urine samples were diluted with a mixture of the supporting electrolyte containing MeOH and 0.1 M PBS (pH 5.6) in a proportion of 5:95% v/v. Next, the standard solutions of 5-ASA and SPD (10 and 30 μM) were spiked into the samples. Then, the simultaneous determination of 5-ASA and SPD was performed via SWV under the optimized conditions as followed by Section 3.3.3. Finally, the evaluations of accuracy and precision were

subsequently approved by analyzing the collected and prepared samples on the same day (Intra-day's study) and three different days (Inter-day's study).



CHAPTER 4

RESULTS AND DISCUSSION

This chapter is divided into three sub-projects according to the methodology. Sub-project I (section 4.1) reported on a new nanocomposite-based screen-printed graphene electrode for sensitive and selective detection of 8-hydroxy-2'-deoxyguanosine. Sub-project II (section 4.2) described a novel and easy-to-construct polymeric L-glutamic acid-modified sensor for urinary 1-hydroxypyrene detection: Human biomonitoring of polycyclic aromatic hydrocarbons exposure. Sub-project III (section 4.3) revealed a highly efficient polymeric L-methionine-modified sensor: An application for the simultaneous determination of 5-aminosalicylic acid and sulfapyridine.

4.1 A new nanocomposite-based screen-printed graphene electrode for sensitive and selective detection of 8-hydroxy-2'-deoxyguanosine

The contents of this sub-project are based on the original research article, which is shown in appendix 1.

4.1.1 Morphological characterization of the modified sensor

Surface morphologies of the unmodified and modified SPGE were characterized via scanning electron microscopy (SEM). Figure 18 shows the SEM images of four different sensors at magnifications of 10,000 \times (a, b, c, and d) and 50,000 \times (e, f, g, and h). The unmodified SPGE (panels a and e) exhibits a rough, porous, and crumpled surface of graphene sheets. The spherical shape and size of AuNPs and their homogeneous distribution throughout the graphene sheets were observed on the SPGE surface (panels b and f) after electrodeposition of AuNPs on SPGE. Panels c and g, which exposes the surface of poly(L-Met)/SPGE following the electropolymerization sequence, shows that the surface of SPGE is covered by the polymeric thin-film layer of L-methionine caused by the formation of multiple uniformly aligned valleys of L-methionine. This morphological feature could improve the active surface area of the modified electrode (Pattan Siddappa Ganesh, Swamy, & Harisha, 2017). Similarly, panels d and h display the surface morphology of poly(L-Met)/AuNPs-modified SPGE. It confirms that a homogeneous layer

of graphene sheet is covered with well-dispersed L-methionine and AuNPs on the electrode surface.

Moreover, the surface composition was verified via energy-dispersive X-ray spectroscopy (EDS) (panels i and j). The EDS image and spectrum of the poly (L-Met)/AuNPs-modified SPGE showed the presence of C, N, O, S, and Au atoms related to AuNPs, and the methionine molecular structure modified the electrode surface and the existence of graphene in the ink composition.



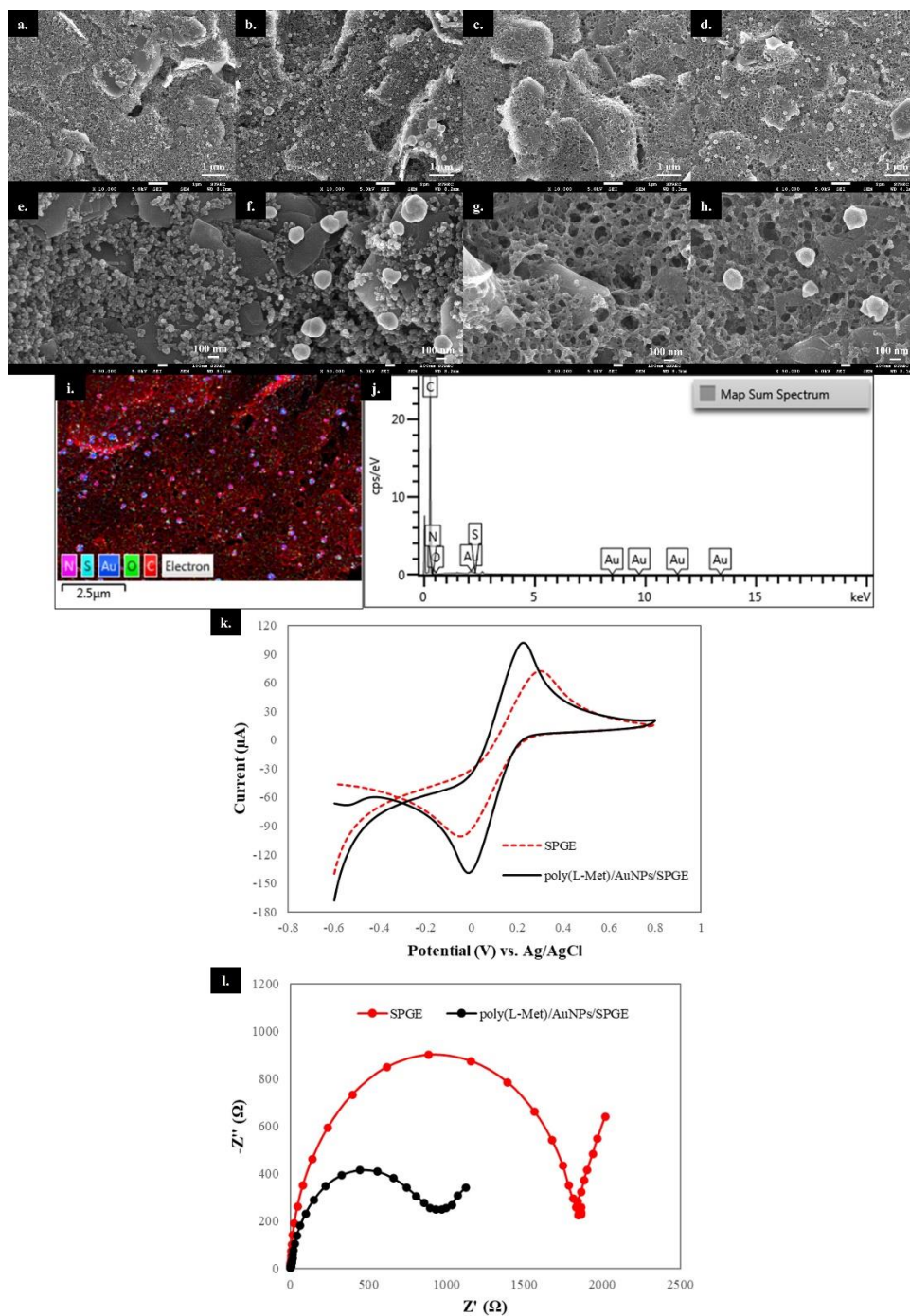


Figure 18 SEM images of SPGE (a, e), AuNPs/SPGE (b, f), poly(L-Met)/SPGE (c, g), and poly(L-Met)/AuNPs/SPGE (d, h) at magnifications of 10,000× (a, b, c, d) and 50,000× (e, f, g, h). EDS mapping (i). Composition of poly(L-Met)/AuNPs/SPGE (j). Cyclic voltammograms of 5 mM $[\text{Fe}(\text{CN})_6]^{3-/4-}$ in 0.1 M KCl with a scan rate of 30 mV s⁻¹ (k) and

EIS Nyquist plots of 5 mM $[\text{Fe}(\text{CN})_6]^{3-/4-}$ in 0.1 M KCl (I) at the unmodified and modified SPGE.

4.1.2 Electrochemical characterization of the poly(L-Met)/AuNPs-nanocomposite modified SPGE

To investigate the electrochemical behavior of the proposed sensor, the unmodified and modified SPGE were characterized via CV and EIS in 5 mM $[\text{Fe}(\text{CN})_6]^{3-/4-}$ in 0.1 M KCl. Figure 18 in panel k presents a reversible redox peak corresponding to $[\text{Fe}(\text{CN})_6]^{3-/4-}$ at the unmodified and modified SPGE. At poly(L-Met)/AuNPs/SPGE, the peak potential separation (ΔE_p) decreased from +0.35 V to +0.23 V, whereas the current response increased compared with SPGE. We strongly believe that this phenomenon is a result of the synergetic effect of conductive graphene sheets, AuNPs, and a modified polymeric thin-film layer. Furthermore, the electroactive surface areas of sensors were increased from 0.096 cm² to 0.132 cm² for SPGE and poly(L-Met)/AuNPs/SPGE.

EIS is a valuable and powerful method for investigating the impedance changes of the interface properties after modification of the electrode surface (Katz & Willner, 2003). The EIS properties of the unmodified and modified SPGE were studied in the presence of a redox couple $[\text{Fe}(\text{CN})_6]^{3-/4-}$. The semicircle diameter obtained from EIS refers to the charge transfer resistance (R_{ct}) at the electrode surface (Ojani, Raouf, Maleki, & Safshekan, 2014). Figure 18 in panel l illustrates Nyquist plots of 5 mM $[\text{Fe}(\text{CN})_6]^{3-/4-}$ containing 0.1 M KCl at SPGE and poly(L-Met)/AuNPs/SPGE. As evidenced, the diameter of the semicircle region of poly(L-Met)/AuNPs/SPGE was smaller than that of SPGE, which corresponds to the R_{ct} values (1,846.4 Ω and 932.3 Ω for SPGE and poly(L-Met)/AuNPs/SPGE). These findings indicated that the composite film of poly(L-Met) and AuNPs was successfully modified on SPGE. Additionally, the electron-transfer apparent rate constant (k_{app}) of each sensor was calculated using the following equation (Gugoasa et al., 2021):

$$k_{app} = RT/n^2F^2AR_{ct}C$$

where R denotes the universal gas constant (8.31447 J K⁻¹ mol⁻¹); T , the absolute temperature (298 K); n , the number of electrons transferred during the redox reaction; F ,

Faraday's constant ($96,485 \text{ C mol}^{-1}$); A , the surface area of the electrode (cm^2); R_{ct} , the charge transfer resistance in Ω ; and C , the concentration of $[\text{Fe}(\text{CN})_6]^{3-/4-}$ (mol cm^{-3}). The k_{app} values were found to be $3.003 \times 10^{-4} \text{ cm s}^{-1}$ and $4.325 \times 10^{-4} \text{ cm s}^{-1}$ for SPGE and poly(L-Met)/AuNPs/SPGE, respectively. The low R_{ct} and high k_{app} values of the modified electrode emphasized the formation of poly(L-Met)/AuNPs on SPGE that could provide excellent catalytic properties, leading to the enhancement of the electron-transfer process of redox $[\text{Fe}(\text{CN})_6]^{3-/4-}$. In addition, the amount of incorporated L-methionine monomer to form the polymeric thin film was an approximate estimation by the total surface coverage of the electrode, which is calculated using the following equation (Pushpanjali, Manjunatha, & Srinivas, 2020; Razmi & Harasi, 2008):

$$\Gamma = Q/nFA$$

where Γ (mol cm^{-2}) denotes the surface coverage of the electrode; Q , the electric charge obtained via the integration of the oxidation peak in C ; n , the number of electrons involved; F , Faraday's constant ($96,485 \text{ C mol}^{-1}$); and A , the surface area of modified electrode in cm^2 . By substituting the respective data in the equation, the Γ value of poly(L-Met)/AuNPs film adhering to the surface of SPGE was calculated to be $4.071 \times 10^{-8} \text{ mol cm}^{-2}$. Therefore, poly(L-Met)/AuNPs/SPGE exhibited a superb property to be a good sensor on applications for the detection of target electroactive species.

4.1.3 Electrochemical behavior of 8-OHdG on poly(L-Met)/AuNPs/SPGE

To accomplish the utilization of the proposed sensor for 8-OHdG determination in clinical applications, the electrochemical behavior of 8-OHdG in 0.1 M Na-PBS (pH 7.0) at the unmodified and modified SPGE was investigated via CV. Figure 19 displays cyclic voltammograms and a chart of the current intensity of 100 μM 8-OHdG compared between the use of unmodified SPGE and use of modified SPGE. On a bare SPGE (red dash line), a poor anodic peak current ($I_{pa} = 5.79 \mu\text{A}$) was observed around +0.15 V vs Ag/AgCl. The oxidation peak potential of 8-OHdG slightly shifted to the negative direction, and the anodic peak current of 8-OHdG still negligibly increased after the modification of AuNPs on SPGE (green line). This result may be concerned with the property of AuNPs, which could improve the electron-transfer kinetics of 8-OHdG at the electrode interface.

Once poly(L-Met) was modified on SPGE (blue line), the anodic peak current of 8-OHdG considerably increased to 14.20 μA , which was 2.5 times higher than that obtained from bare SPGE. This suggested that the polymeric film of L-methionine could enhance the electrocatalytic capability of 8-OHdG oxidation. In addition, the anodic peak current of 8-OHdG dramatically increased in poly(L-Met)/AuNPs/SPGE (black line). The increased electrochemical signal of 8-OHdG was almost four times larger than that of the bare SPGE, resulting from the synergistic coupling effect between poly(L-Met) and AuNPs on SPGE. This combination provided a high specific surface area, enhanced electrical conductivity, and promoted electrochemical activity toward 8-OHdG detection. These results clearly indicated that poly(L-Met)/AuNPs/SPGE was an excellent electrochemical sensor for 8-OHdG detection.

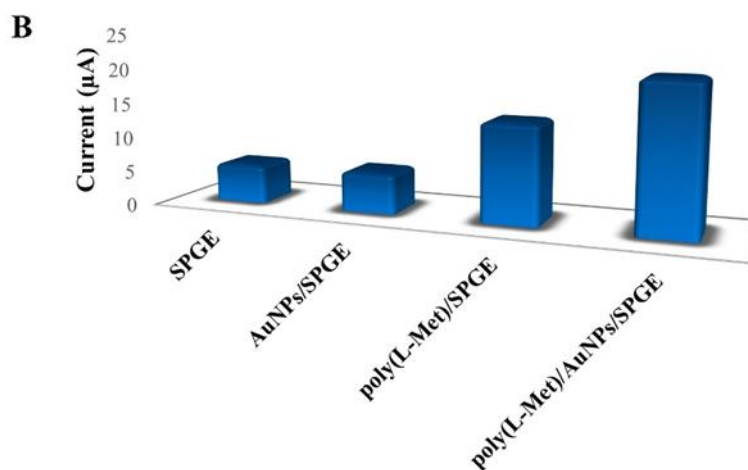
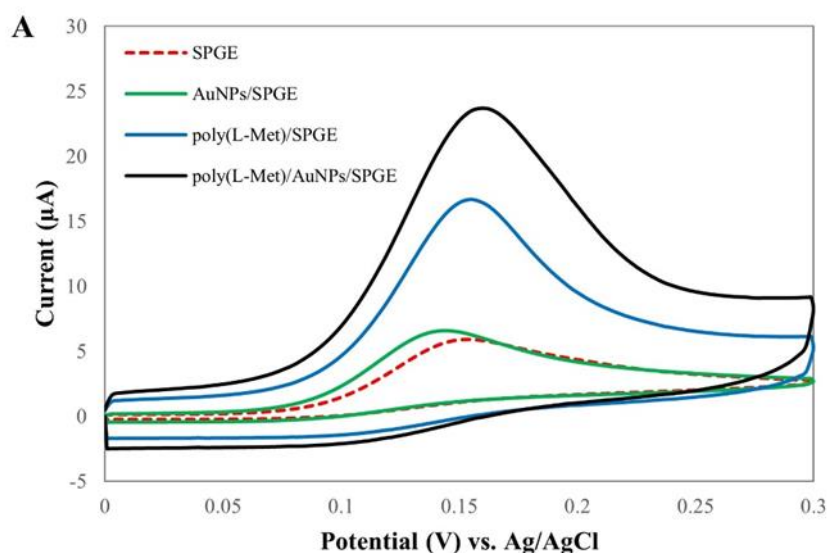


Figure 19 Cyclic voltammograms (A) and a chart of the current intensity (B) of 100 μM 8-OHdG in 0.1 M Na-PBS (pH 7.0) at different sensors.

4.1.4 Optimization of deposition for AuNPs and L-methionine

To achieve optimal conditions for 8-OHdG detection, the main parameters dealing with the formation of film on the electrode surface were investigated. The studied parameters included the concentration of standard gold and L-methionine solutions, the number of cycles for gold and L-methionine deposition, and the scan rate for gold and L-methionine deposition. These parameters are involved in the control of the AuNPs amount and film thickness on the electrode surface, which could directly affect the transferred electrons at the electrode interface. From the results in Figure 20, the optimal values are the concentration of standard gold solution of 1,000 ppm, the number of cycles at 7 cycles, the scan rate of 150 mV s^{-1} , the concentration of L-methionine solution of 2 mM, the number of cycles at 10 cycles, and the scan rate of 100 mV s^{-1} .

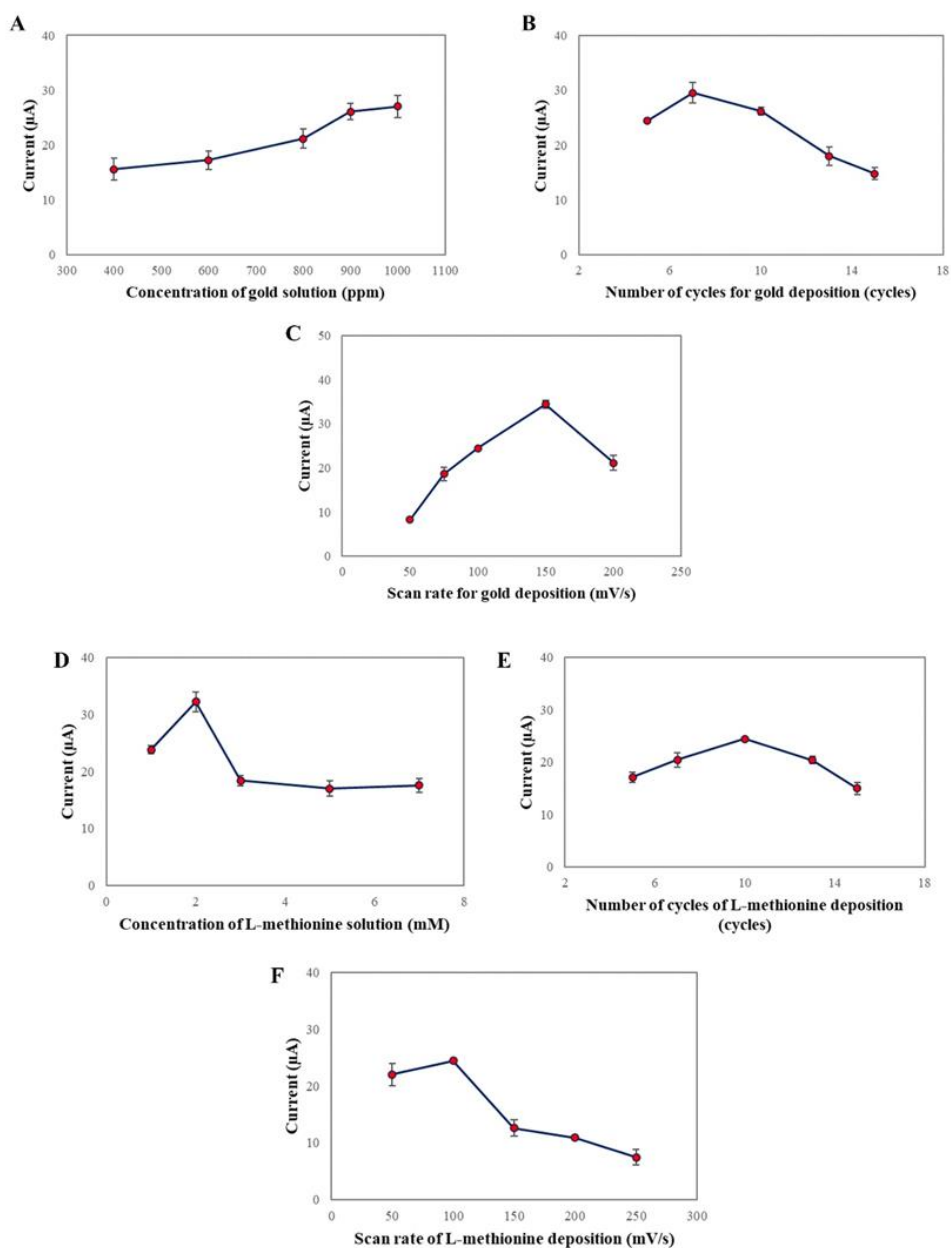


Figure 20 Effects of concentration of standard gold solution (A) and L-methionine solution (D), number of cycles for gold (B) and L-methionine deposition (E), and scan rate for gold (C) and L-methionine deposition (F) on SPGE.

4.1.5 Influence of pH values and scan rates

Adjustment of the pH values of supporting electrolyte significantly affects the oxidative behavior and peak appearance of 8-OHdG. Besides, it can provide information on the number of electrons and protons involved in the electrochemical process of

8-OHdG that occurred at the developed sensor. As shown in Figure 21A, pH 7.0 was selected as the optimal for further experiments as it provided the highest current at a low oxidative potential. Also, as exhibited in Figure 21B, the slope of $-0.0562 \text{ V pH}^{-1}$ was close to the Nernstian theoretical value of -0.059 V pH^{-1} (Guo, Liu, Liu, Wu, & Lu, 2016). Therefore, the number of protons and electrons in the electrochemical process of 8-OHdG was equal.

To clarify whether the mass transfer process of the analyte at the electrode surface is adsorption or diffusion controlled, the effect of the scan rate on the electrooxidation of 8-OHdG was studied by CV (Figure 21C). From the linear regression equation between the anodic peak current (I_{pa}) and the scan rate (ν) in Figure 21D, it demonstrated that the mass transfer process at the electrode surface was controlled by adsorption-limited. In addition, a linear relationship between the log of current and the log of scan rate was plotted to confirm the result. From the linear regression equation, $y = -0.741 + 0.8121 \log \nu$ ($R^2 = 0.9929$), the slope value was close to 1, which is supposed to be surface adsorption (David K. Gosser, 1993).

To calculate the number of electrons (n), the linear regression equation between the anodic peak potential (E_{pa}) and the logarithm of scan rate ($\ln \nu$) and Laviron's equation was used and found that the number of electrons (n) was calculated to be 2. Therefore, it could be concluded that the electrochemical mechanism of 8-OHdG on poly (L-Met)/AuNPs/SPGE involved two electrons and two protons, which is in agreement with previous reports (Guo et al., 2016; Kumar, Rosy, & Goyal, 2017; Shang et al., 2018).

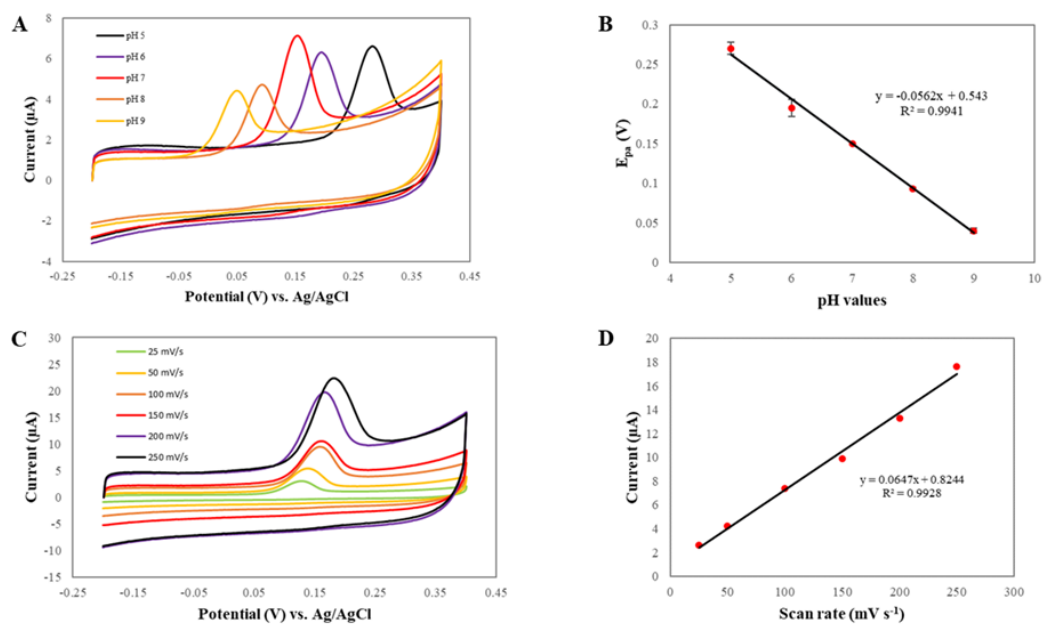


Figure 21 Cyclic voltammograms of 10 μM 8-OHdG at the poly(L-Met)/AuNPs/SPGE using various pH values (A) and the plot of E_{pa} vs. pH values (B). Cyclic voltammograms of 10 μM 8-OHdG in 0.1 M Na-PBS (pH 7.0) at the poly(L-Met)/AuNPs/SPGE with different scan rates (C) and the plot of I_{pa} vs. scan rate (D).

4.1.6 Interference study

To estimate the selectivity of the newly proposed electrochemical platform, the effects of interference, comprising uric acid (UA), dopamine (DA), ascorbic acid (AA), citric acid (CA), bovine serum albumin (BSA), and glucose (Glu), which commonly coexist with 8-OHdG in biological fluids, were examined. In addition, the effects of some ions, including Na^+ , K^+ , Ca^{2+} , Mg^{2+} , Cu^{2+} , and Zn^{2+} , on 8-OHdG detection were investigated. Figure 22 describes the current response of 10 μM 8-OHdG in the presence of 20 μM UA, 40 μM DA, 100 μM AA, 100 μM CA, 500 μM BSA, 500 μM Glu, 1 mM Na^+ , 1 mM K^+ , 1 mM Ca^{2+} , 1 mM Mg^{2+} , 1 mM Cu^{2+} , and 1 mM Zn^{2+} . From the results, it was found that there was no significant change in the current signal of 8-OHdG in the presence of interference.

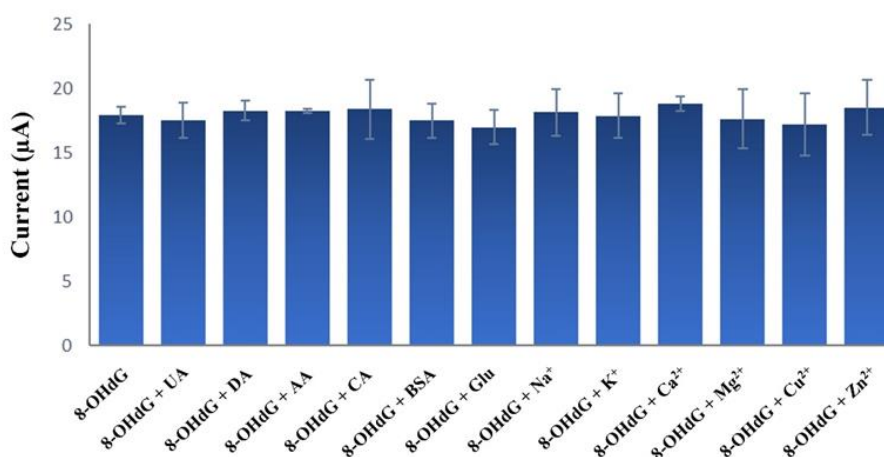


Figure 22 Effect of interferences toward 8-OHdG detection. The error bars represent the standard deviation of three repetitive measurements.

However, the major limitation for the analysis of 8-OHdG in biological fluids, especially in urine, is the effect exerted by UA. Figure 23 reveals the square wave voltammograms of 8-OHdG and UA detected by a developed sensor. As can be seen from Figure 23A, an individual study of standard solution, UA and 8-OHdG appeared at +0.04 and +0.13 V, respectively. Surprisingly, when 20 μM UA was added to 10 μM 8-OHdG, a small shoulder peak appeared near the oxidation peak potential of 8-OHdG (Figure 23B). Nonetheless, the physiological normal level of UA in human urine is 400 μM (Khan, Liu, Tang, & Liu, 2018). Therefore, the concentration of UA at 400 μM absolutely interfered with the detection of 8-OHdG. The effect of chloride content in urine samples is also important. In a normal person's urine, the average concentration of chloride ions is 0.1 M (Siangproh, Teshima, Sakai, Kato, & Chailapakul, 2009). Figure 24 presents the square wave voltammograms of 8-OHdG containing various concentrations of NaCl in 0.1 M Na-PBS (pH 7.0). It demonstrated that there are no significant changes in the current signal of 8-OHdG. Nevertheless, the oxidation peak potentials of 8-OHdG shifted to the positive direction with increasing concentrations of chloride ions. This phenomenon could be concluded that the saturated solution of chloride affected the mass-transfer process at the electrode surface toward 8-OHdG detection. Hence, the determination of 8-OHdG

containing the co-existence of UA and chloride ions in biological samples is a crucial concern that must be resolved.

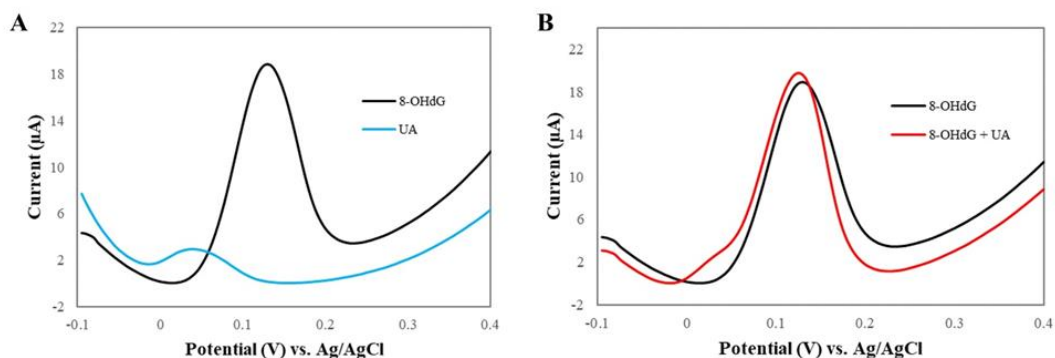


Figure 23 Square wave voltammograms of 10 μM 8-OHdG and 10 μM uric acid (A) and 10 μM 8-OHdG in presence 20 μM uric acid at the poly(L-Met)/AuNPs/SPGE (B).

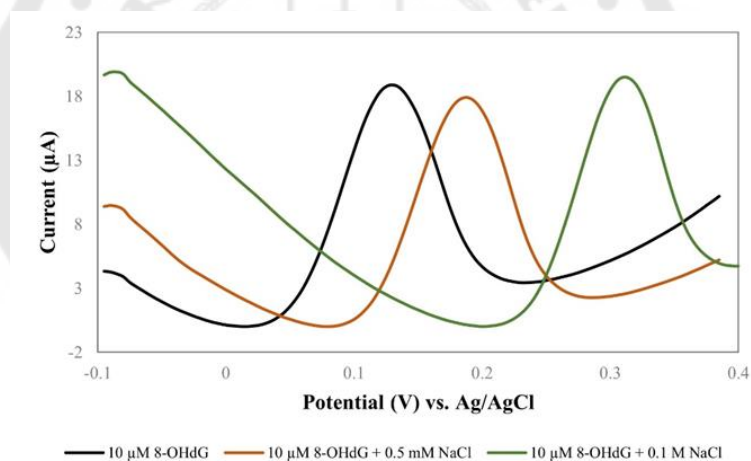


Figure 24 Square wave voltammograms of 10 μM 8-OHdG in various concentrations of NaCl in 0.1 M Na-PBS (pH 7) at the poly(L-Met)/AuNPs/SPGE.

4.1.7 Detection of a mixture of 8-OHdG and UA

To resolve the aforementioned problem, we aimed to use sodium dodecyl sulfate (SDS) containing 0.1 M NaCl in 0.1 M Na-PBS (pH 7.0) as the supporting electrolyte for 8-OHdG detection in the presence of UA at a high level. As evidenced in Figure 25A, the oxidation peak potentials of individual 400 μM UA and 10 μM 8-OHdG were noticed at +0.23 V (blue line) and +0.32 V (black line). To confirm the expected result, a mixture of

400 μM UA and 10 μM 8-OHdG was added to the supporting electrolyte. As observed in the red line, the oxidation peaks of these compounds clearly separated at different peak potentials because SDS is an anionic surfactant that can block the diffusion rate of UA to the electrode surface, causing a difference in the rate of mass transfer from 8-OHdG. These results indicated that the use of saturated chloride in Na-PBS containing SDS as the supporting electrolyte greatly enhanced the selectivity of the proposed method and improved the possibility of 8-OHdG determination in real biological fluid samples.

From the preliminary test, we strongly believe that the SDS concentration may affect the separation. Therefore, the effect of the SDS concentration was systematically studied for a mixture of 10 μM 8-OHdG and 400 μM UA. As evidenced in Figure 25B and 25C, 0.05 M of SDS could obviously separate the oxidation peaks of 8-OHdG and UA and provide the highest current of 8-OHdG while strongly suppressing the response of UA. In addition, the resolution value between the oxidation peak potentials of 8-OHdG and UA was remarkably close to one. Thus, 0.05 M of the SDS concentration was selected as the suitable concentration for the preparation of the supporting electrolyte to detect 8-OHdG in real samples.

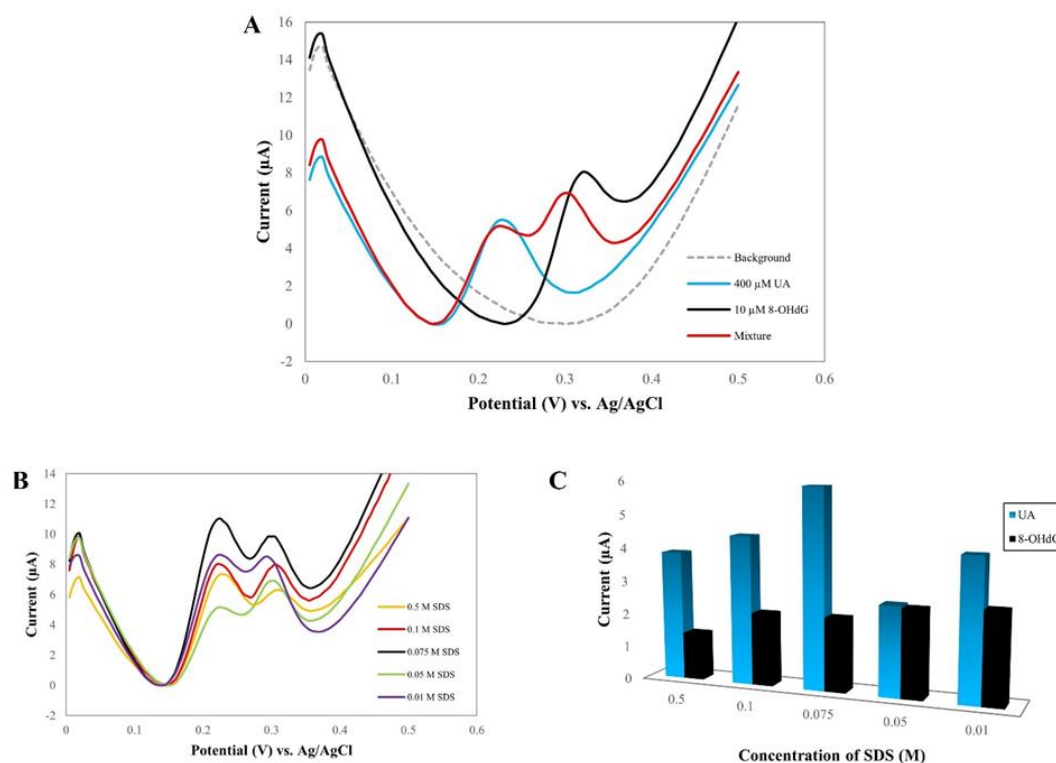


Figure 25 Square wave voltammograms of 10 μM 8-OHdG and 400 μM UA in 0.05 M SDS containing 0.1 M NaCl in 0.1 M Na-PBS (pH 7.0) (A), the effect of the SDS concentration (B), and a chart of the current intensity of 8-OHdG and UA detection (C).

4.1.8. Analytical performance

To verify the analytical performance of the proposed method, the detection of 8-OHdG in various concentrations at poly(L-Met)/AuNPs/SPGE was evaluated via SWV. Under optimum conditions, the square wave voltammograms of the electrochemical oxidation of 8-OHdG at various concentrations are presented in Figure 26A, and the linear regression equation obtained from the calibration curve is demonstrated in Figure 26B. The limit of detection ($\text{LOD} = 3\text{SD}/\text{Slope}$) and limit of quantification ($\text{LOQ} = 10\text{SD}/\text{Slope}$) were found to be 92 and 306 nM, respectively. In addition, a comparison of the analytical performance between this proposed method and previous methods for 8-OHdG detection is summarized in Table 1. Although the analytical performance of some previous works offered a lower limit of detection compared with our method, there was no report on selectivity, particularly UA and chloride ions, at normal levels in humans, which affected

the determination of 8-OHdG in real samples. Furthermore, we first proposed the use of poly(L-Met)/AuNPs/SPGE as a sensor for 8-OHdG detection without enzymatic catalysts to reduce the interference of UA in biological fluid samples. Our developed methodology not only provided high selectivity in the detection but also had sufficiently high potential for use in the determination of 8-OHdG in biological fluid samples.

The precision of the analytical performance by examining the relative standard deviation (RSD) for seven repetitive measurements of 8-OHdG solution was investigated. For the measurement, three concentrations (1, 10, and 50 μM) concerning the probable range in interesting samples were assessed for the reproducibility of the proposed sensor. As presented in Figure 26C, the RSD values were lower than 18%, which could be acceptable by AOAC guidelines (Latimer, 2016). For stability test, poly(L-Met)/AuNPs/SPGE was stored at 4°C for 20 days, and the anodic peak current of 10 μM 8-OHdG still remained at 80.32%, suggesting that this proposed sensor could be favorably employed for 8-OHdG analysis with excellent reproducibility and good stability.

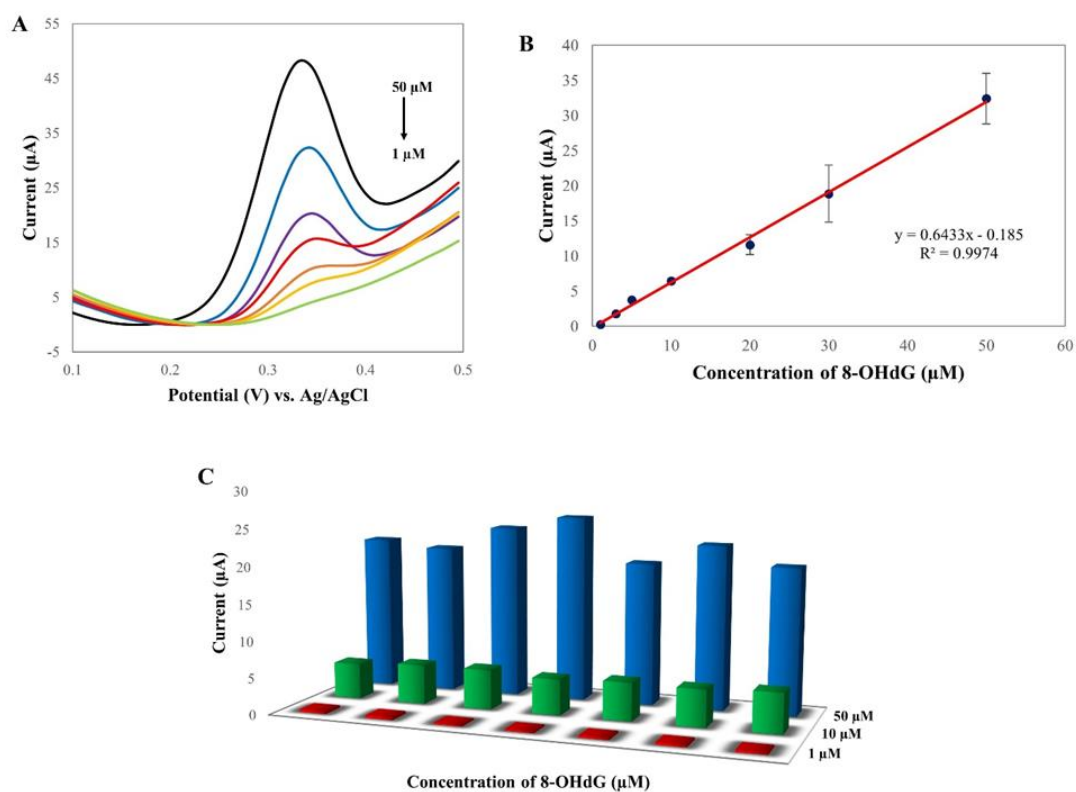


Figure 26 Square wave voltammograms showing the electrochemical oxidation of 8-OHdG in 0.05 M SDS containing 0.1 M NaCl in 0.1 M Na-PBS (pH 7.0) at various concentrations on poly(L-Met)/AuNPs/SPGE (A). The calibration curve between the anodic peak current and the concentration of 8-OHdG (B). A chart of the current intensity of reproducibility studies at three concentrations (C).

Table 1 Comparison of the analytical performance between this proposed method and previous works for 8-OHdG detection.

Electrodes	LOD (nM)	Linear range (nM)	References
P3MT/GCE	100	700-70000	(T. H. Li, Jia, Wang, & Liu, 2007)
CNTs-PEI/GCE	100	500-30000	(Gutiérrez, Gutiérrez, García, Galicia, & Rivas, 2011)
PICA/CHI/GCE	0.106	0.35-35305	(Pan et al., 2015)
PEDOT/CCP	50.84	176.5-3530.5	(G. V. Martins, Tavares, Fortunato, & Sales, 2017)
ZnO@rGO/GCE	1.25	5-5000	(Hao, Wu, Wan, & Tang, 2018)
rGO-AuNPs/poly(L-Arg)/GCE	1	1-10000	(Khan et al., 2018)
GO-COOH/MWCNTs- COOH/PEI/AuNPs/GCE	7.06	14-14120	(Yi et al., 2019)
HKUST-1/GNs/GCE	2.5	10-1000	(Cao, Wu, Tang, & Wan, 2019)
Graphene/SPE	90	300-100000	(Varodi et al., 2019)
Ag-TiO ₂ -rGO/SPE	10	50-2500	(Dhulkefi, Atacan, Bas, & Ozmen, 2020)
poly(L-Met)/AuNPs/SPGE	92	1000-50000	This work

Abbreviation

P3MT: poly(3-methylthiophene); GCE: glassy carbon electrode; CNTs: carbon nanotubes; PEI: polyethylenimine; PICA: poly(indole-5-carboxylic acid); CHI: chitosan; PEDOT: poly(3,4-ethylenedioxythiophene); CCP: carbon-ink coated paper; rGO: reduced graphene oxide; ZnO: zinc oxide; AuNPs: gold nanoparticles; poly(L-Arg): poly(L-Arginine); GO-COOH: carboxyl-functionalized graphene oxide; MWCNTs-COOH: carboxyl-functionalized multi-walled carbon nanotubes; HKUST-1: ultrasmall Cu-based metal organic frame; GNs: graphite nanosheets; SPE: screen-printed electrode; TiO₂: titanium dioxide; poly(L-Met): poly(L-methionine); SPGE: screen-printed graphene electrode.

4.1.9. Analytical application in real samples

To evaluate the applicability of this proposed method, quantitative determination of 8-OHdG was executed in artificial urine, healthy human urine, and human serum samples. For accuracy and precision, the percentages of recovery and RSD were estimated by spiking a known standard solution of 8-OHdG, and a standard addition method was used to prevent the matrix effect (Thangphatthanarunguang, Lomae, Chailapakul, Chaiyo, & Siangproh, 2021). As shown in Table 2, the recovery and RDS values were found in the range of 90.19%–109.73% and 0.51%–14.36%, which could be acceptable by the AOAC guidelines (Latimer, 2016). These results indicated that this approach was acceptable and reliable for the determination of 8-OHdG in real samples. Thereby, poly(L-Met)/AuNPs/SPGE exhibited good accuracy and precision and could be used as an alternative choice for quantitative analysis of 8-OHdG in biological fluid samples.

Table 2 Results obtained from the determination of 8-OHdG in artificial urine, healthy human urine, and human serum samples using poly(L-Met)/AuNPs/SPGE (n = 3).

Samples	Added (μM)	Found (μM)	Recovery (%)	RSD (%)
Artificial urine 1	5	4.79	95.73	3.85
	10	10.76	107.60	3.55
	50	49.08	98.16	9.29
Artificial urine 2	5	5.03	100.60	8.53
	10	9.53	95.27	3.11
	50	45.53	91.05	1.68
Artificial urine 3	5	4.51	90.19	14.36
	10	10.88	108.83	12.76
	50	46.67	93.33	6.40
Human urine 1	5	5.45	109.01	5.93
	10	10.61	106.12	7.01
	50	53.72	107.45	8.24
Human urine 2	5	4.76	95.16	3.80
	10	10.20	101.98	11.73
	50	51.05	102.10	0.51
Human urine 3	5	5.43	108.66	0.81
	10	10.22	102.20	7.00
	50	51.36	102.72	7.24
Human serum 1	5	4.83	96.50	2.30
	10	10.06	100.56	4.74
	50	48.09	96.17	8.99
Human serum 2	5	4.95	99.07	8.81
	10	10.97	109.73	0.59
	50	47.90	95.81	6.19
Human serum 3	5	5.43	108.59	6.36
	10	10.36	103.64	12.59
	50	50.07	100.15	2.20

4.2 A novel and easy-to-construct polymeric L-glutamic acid-modified sensor for urinary 1-hydroxypyrene detection: Human biomonitoring of polycyclic aromatic hydrocarbons exposure

The contents of this sub-project are based on the original research article, which is shown in appendix 2.

4.2.1 Surface composition and morphology studies

Surface morphologies of each sensor (SPGE and poly(L-GA)/SPGE) were investigated by scanning electron microscopy (SEM). Figure 27a and b show SEM images of SPGE and poly(L-GA)/SPGE at a magnification of 10,000 \times . The surface of the unmodified SPGE (Figure 27a) was rugged, crumpled, and wrinkled. After the surface modification of L-GA onto SPGE via an electropolymerization procedure (Figure 27b), its surface exhibited a smooth surface, which was covered by the formation of the poly(L-GA) on the SPGE surface. In addition, the surface composition of poly(L-GA) on the SPGE was approved via energy-dispersive X-ray spectroscopy (EDS). As displayed in Figure 27c, the EDS mapping spectrum of poly(L-GA)/SPGE revealed the presence of C, N, and O atoms, relating to the structure of the glutamic acid molecular modified the electrode surface of SPGE.

To approve the deposition of the poly(L-GA) on SPGE, the surface composition was also characterized using X-ray photoelectron spectroscopy (XPS). XPS data of a bare SPGE (Figure 27d) presents the C 1s core spectra; (C–C) appeared at 284.5 eV and (C=C) at 286.2 eV, corresponding to the presence of two carbon functionalities in the graphene structure. Figure 27e describes the XPS core level spectra for C 1s, indicating the existence of four peaks at 284.8, 285.7, 286.6, and 288.7 eV, corresponding to the (C–C), (C–O), (C–N), and (C=O) carbon bonding, respectively. We believed that these peaks occurred as a result of the structure of the polymerized L-GA monomer. Figure 27f shows the O 1s XPS data and shows the existence of two different oxygen functionalities within the structure of the polymeric thin film; (O–C) appeared at 531.1 eV and (O=C) at 532.7 eV, which was attributed to the carboxylic groups of the L-GA structure. Additionally, the N 1s core spectra in Figure 27g demonstrates a well-defined couple peak obtained at 399.7 and 400.8 eV, corresponding to the (N–C) and (⁺N–C) amine groups in

the L-GA structure. These findings obviously confirmed that the poly(L-GA) was successfully deposited on the SPGE surface.

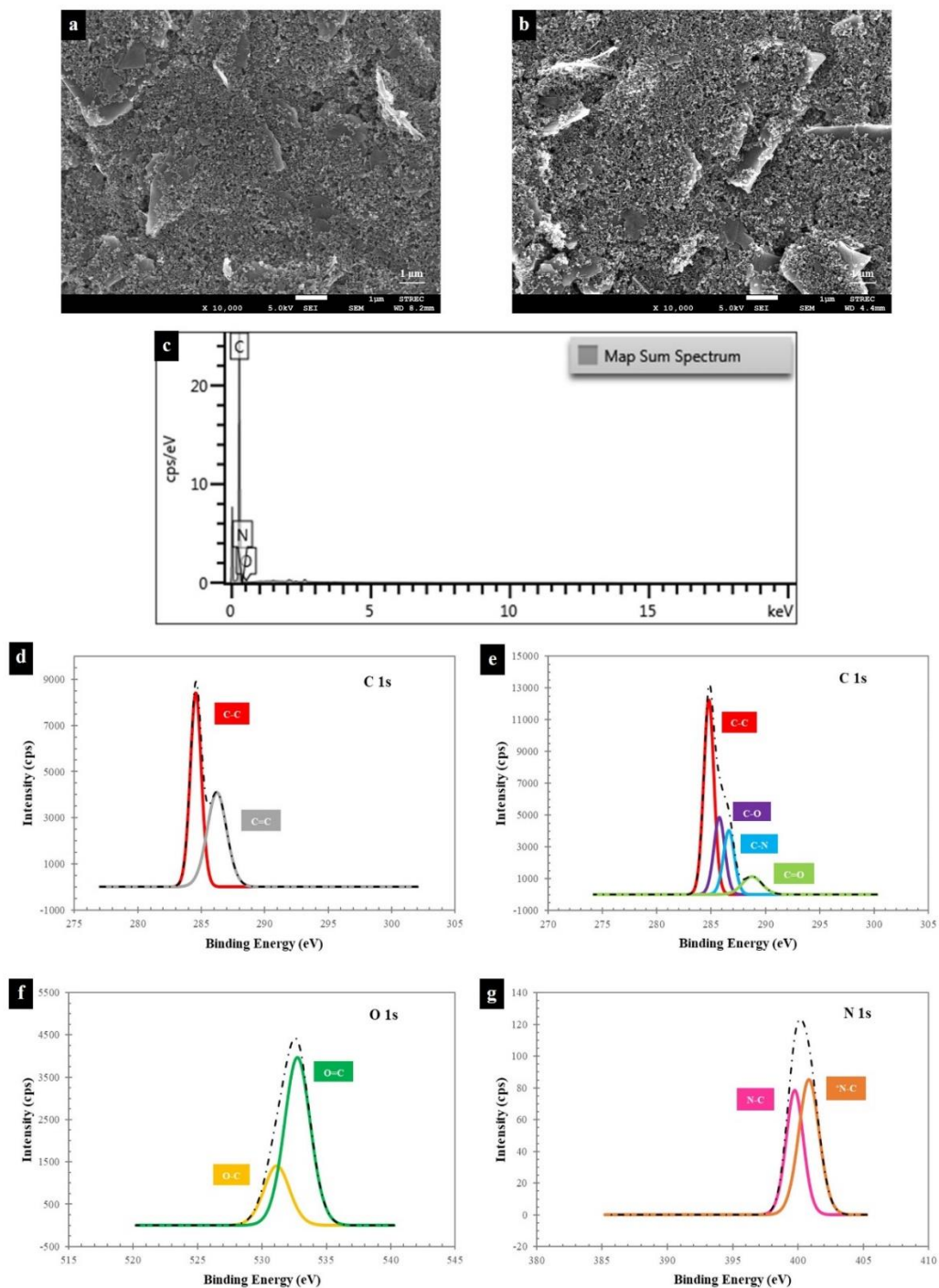


Figure 27 SEM images of SPGE (a) and poly(L-GA)/SPGE (b) at a magnification of 10,000 \times . EDS mapping for the composition of poly(L-GA)/SPGE (c). XPS data of a bare

SPGE (d) and the composite polymer fabricated on SPGE demonstrates the core level spectra for C 1s (e), O 1s (f), and N 1s (g).

4.2.2 Electrochemical characterization of the poly(L-GA)/SPGE

$K_3[Fe(CN)_6]$ and $[Ru(NH_3)_6]Cl_3$ were selected as anionic and cationic redox probes to study the electrochemical behavior on poly(L-GA)/SPGE surface using CV. Figure 28a shows CV voltammograms of two redox probes in 0.1 M KCl with a scan rate of 100 mV s^{-1} at the unmodified and modified SPGE. Certainly, the current signal of 5 mM $[Fe(CN)_6]^{3-/4-}$ was greater than that of 5 mM $[Ru(NH_3)_6]^{3+}$. When 5 mM $[Fe(CN)_6]^{3-/4-}$ detection at the SPGE and poly(L-GA)/SPGE was compared (red dashed line and blue line), the peak potential separation (ΔE_p) at the poly(L-GA)/SPGE was reduced to +0.27 V, but the current signal was increased. This means that it is caused by the electrostatic interaction of the anionic redox probe and the positive charge of amine groups on poly(L-GA)/SPGE surface. Therefore, the poly(L-GA) thin film could enhance the electron-transfer process of $[Fe(CN)_6]^{3-/4-}$, an anionic redox probe. Moreover, the electroactive surface area values of SPGE and poly(L-GA)/SPGE were estimated using the Randles–Sevcik equation as follows:

$$I_p = (2.69 \times 10^5) n^{3/2} A D_0^{1/2} \nu^{1/2} C_0^*$$

where I_p denotes the peak current; n denotes the number of electrons; A denotes the electroactive surface area; D_0 denotes the diffusion coefficient of redox probe species; ν denotes the scan rate (0.1 V s^{-1}); and C_0^* denotes the concentration of redox probe species ($5.0 \times 10^{-6} \text{ mol cm}^{-3}$). Based on known parameters for the $[Fe(CN)_6]^{3-/4-}$ ($n = 1$ and $D_0 = 7.6 \times 10^{-6} \text{ cm}^2 \text{ s}^{-1}$) (Punjiya, Moon, Matharu, Nejad, & Sonkusale, 2018) and the $[Ru(NH_3)_6]^{3+}$ ($n = 1$ and $D_0 = 8.43 \times 10^{-6} \text{ cm}^2 \text{ s}^{-1}$) (Yijun Wang, Limon-Petersen, & Compton, 2011), the electroactive surface area values of SPGE and poly(L-GA)/SPGE were calculated to be 0.120 and 0.150 cm^2 for $[Fe(CN)_6]^{3-/4-}$ and 0.115 and 0.113 cm^2 for $[Ru(NH_3)_6]^{3+}$.

Subsequently, $[Fe(CN)_6]^{3-/4-}$ was selected as an anionic electroactive species to study the electron-transfer process to get a better understanding. As exhibited in Figure 28b, the semicircle diameter of $[Fe(CN)_6]^{3-/4-}$ at the poly(L-GA)/SPGE was smaller than that

of SPGE, corresponding to the R_{ct} values (1.171 and 5.462 k Ω for poly(L-GA)/SPGE and SPGE, respectively). In addition, the electron-transfer apparent rate constant (k_{app}) was estimated using the equation as below (Gugoasa et al., 2021; Thangphatthananarungruang, Chotsuwan, Jampasa, & Siangproh, 2022):

$$k_{app} = RT/n^2F^2AR_{ct}C$$

where R denotes the universal gas constant (8.31447 J K⁻¹ mol⁻¹); T denotes the absolute temperature (298 K); n denotes the number of electrons transferred during the redox reaction; F denotes the Faraday's constant (96,485 C mol⁻¹); A denotes the surface area of the electrode (cm²); R_{ct} denotes the charge transfer resistance with the potential range of 0–0.1 V in Ω ; and C denotes the concentration of [Fe(CN)₆]^{3-/4-} (5.0×10^{-6} mol cm⁻³). The k_{app} values were calculated to be 8.121×10^{-5} and 3.031×10^{-4} cm s⁻¹ for SPGE and poly(L-GA)/SPGE, respectively. The increased k_{app} value in the modified SPGE demonstrated that the modified poly(L-GA) on SPGE improved the electron-transfer process of redox [Fe(CN)₆]^{3-/4-}. The total surface coverage (Γ) of the poly(L-GA)/SPGE was also estimated using the following equation:

$$\Gamma = Q/nFA$$

where Γ (mol cm⁻²) denotes the surface coverage of the electrode; Q , the electric charge obtained via the integration of the oxidation peak in C; n , the number of electrons involved; F , Faraday's constant (96,485 C mol⁻¹); and A , the surface area of modified electrode in cm². It was found to be 16.62 nmol cm⁻². As a result of the electrochemical characterization study, it suggested that poly(L-GA) modified SPGE could be employed as an excellent sensor for the target electroactive species detection.

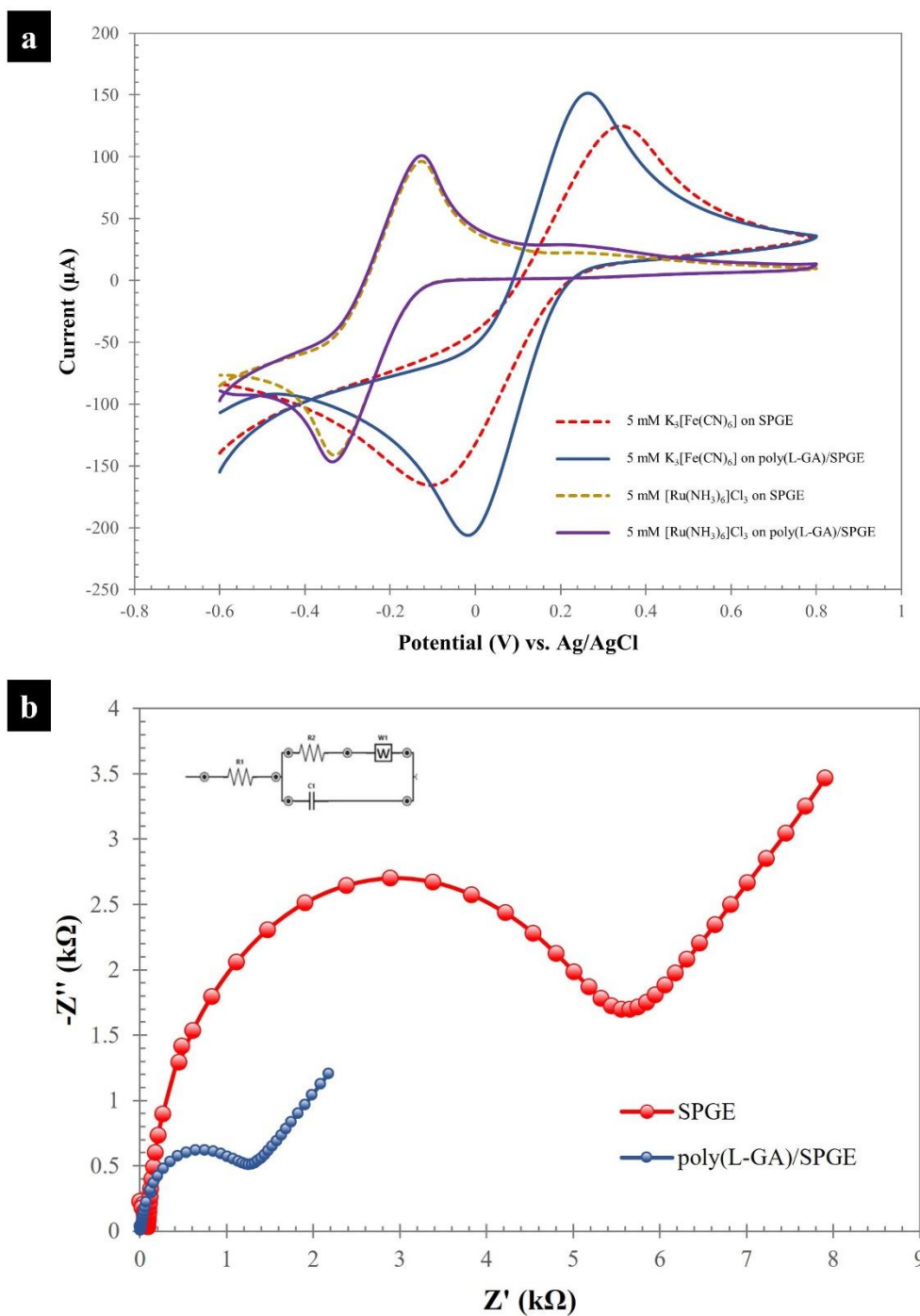


Figure 28 Cyclic voltammograms of 5 mM $[\text{Fe}(\text{CN})_6]^{3-/4-}$ and $[\text{Ru}(\text{NH}_3)_6]^{3+}$ in 0.1 M KCl with a scan rate of 100 mV s^{-1} at the SPGE and poly(L-GA)/SPGE (a). EIS Nyquist plots of 5 mM $[\text{Fe}(\text{CN})_6]^{3-/4-}$ in 0.1 M KCl with the potential range of 0–0.1 V at the SPGE and poly(L-GA)/SPGE (b).

4.2.3 Effect of different types of supporting electrolytes on the electrochemical detection of 1-OHP at the poly(L-GA)/SPGE

To acquire the high sensitivity in the detection and the correctness, suitability, and reliability of the supporting electrolyte type, the influence of the supporting electrolyte type toward 1-OHP electrochemical detection on poly(L-GA)/SPGE was initially studied. For preliminary studies, 0.1 M Na-PBS at three pH values (5.6, 7.4, and 10.25) was used as the supporting electrolyte for investigating 1-OHP electrochemical behavior via SWV. From the results in Figure 29a, when pH values were increased, the electrochemical signal of 1-OHP obviously increased. Nevertheless, at $\text{pH} \geq 10.25$, it was influenced by the effect of ionic strength due to the suitable and dependable pH range for Na-PBS of 5.0–8.0. Therefore, Na-PBS at high pH levels was ineffective to be used as the supporting electrolyte for 1-OHP detection. Subsequently, 0.05 M $\text{Na}_2\text{HPO}_4\text{-NaOH}$ (pH 10.5, 11.0, and 12.0) was chosen as the supporting electrolyte for the study owing to its pH range of 10.5–12.0. Figure 29b shows that the highest current signal of 1-OHP was achieved at a low pH value (pH 10.5). However, to achieve the high sensitivity in detection, we found that in addition to these buffer solutions, Gly-NaOH buffer solution could be used as the supporting electrolyte due to its pH range of 8.5–10.5. Therefore, 0.05 M Gly-NaOH buffer solution at three pH values (8.4, 9.4, and 10.5) was immediately conducted. As observed in Figure 29c, the highest current signal of 1-OHP was obtained at pH 9.4. Interestingly, square wave voltammograms (Figure 29d) of 1-OHP detection using each supporting electrolyte type were compared. It was found that Gly-NaOH buffer solution not only gave the best electrochemical response for 1-OHP detection but also offered the oxidation peak potential of 1-OHP close to 0, resulting in improved selectivity of the proposed approach because most interferences can be easily oxidized at the positive potential. These findings suggested that Gly-NaOH played an important role in the electrooxidation of 1-OHP using the developed sensor. Thus, Gly-NaOH buffer solution was selected as an appropriate supporting electrolyte for this work.

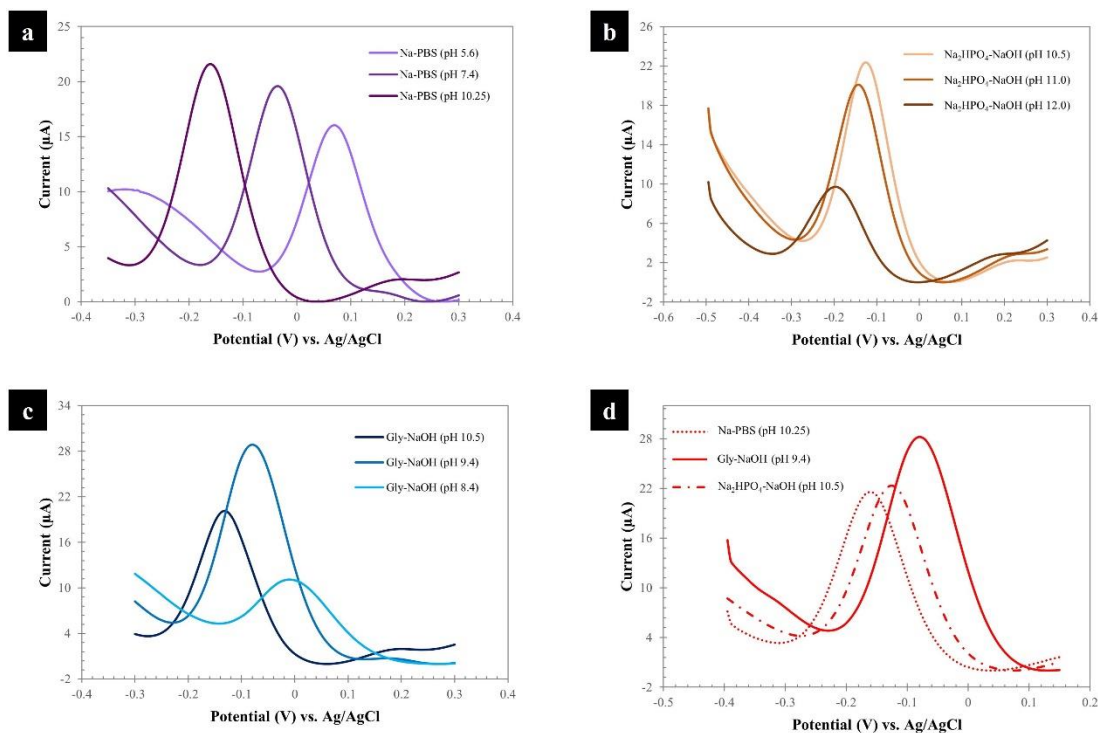


Figure 29 Square wave voltammograms of 1-OHP detection using Na-PBS (a), Na₂HPO₄-NaOH (b), and Gly-NaOH (c) as the supporting electrolyte. Square wave voltammograms for a comparison of each supporting electrolyte type in 1-OHP detection (d).

4.2.4 Effect of pH values and scan rates

The study of different pH values on the oxidative behavior of 1-OHP in Gly-NaOH buffer solution was performed in the pH range of 8.4–10.5 using SWV. As depicted in Figure 30a, the anodic peak currents of 1-OHP gradually increased with increasing pH values. However, at pH values >9.4, anodic peak currents were reduced. We believed that a pH value of 9.4 was sufficient to completely convert 1-OHP to the deprotonated form, which was easily oxidized at the electrode surface of poly(L-GA)/SPGE and electrostatically entirely interacted with the amine groups on the polymer backbone (pK_a value of 1-OHP = 7.44 (Yang et al., 2009)). Therefore, pH 9.4 was selected for further experiments. Also, as seen in the equation (Figure 30b), the slope value of $-0.0527 \text{ V pH}^{-1}$ was close to the Nernstian theoretical value of -0.059 V pH^{-1} , demonstrating

two-protons-transfer coupled with two-electrons-transfer reaction as previously reported (Pang, Zhang, et al., 2019; Shen, Cui, Pang, & Qian, 2012a, 2012b).

The effect of scan rates on 1-OHP electrochemical oxidation on the poly (L-GA)/SPGE was studied in the range of 25–250 mV s^{-1} via CV (Figure 30c). A linear dependence (Figure 30d) was gained between the current response of 1-OHP (I_{pa}) and the scan rate (ν), indicating the adsorption-controlled process at the electrode surface. Furthermore, an adsorption or diffusion controlled electrochemical process can be predicted from the slope of 1.0 or 0.5 by plotting $\log I_{pa}$ and $\log \nu$ (Azizi, Ghasemi, & Amiripour, 2016; David K. Gosser, 1993). From the linear regression equation, $\log I_{pa} = -1.057 + 0.8306 \log \nu$ ($R^2 = 0.9732$), it was found that the slope value was close to 1.0, confirming the adsorption-controlled process.

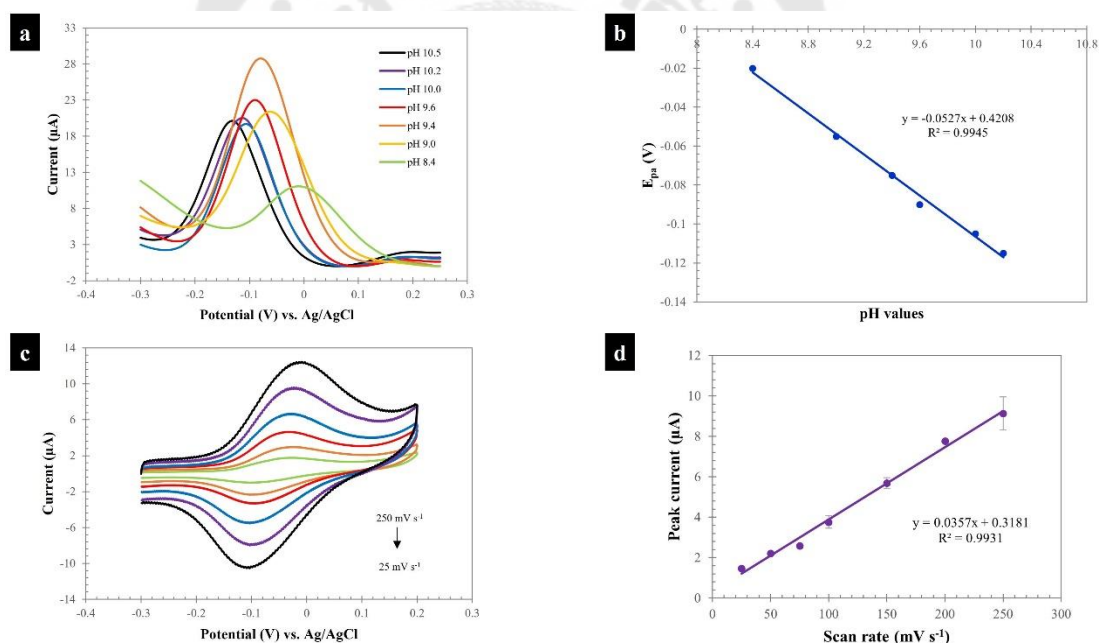


Figure 30 Square wave voltammograms of 10 μM 1-OHP detection at different pH values (a) and the plot of E_{pa} vs. pH values (b). Cyclic voltammograms of 50 μM 1-OHP detection in Gly-NaOH (pH 9.4) at various scan rates (c) and the plot of I_{pa} vs. scan rate (d). Error bars represent the standard deviation of 1-OHP detection at different pH values and scan rates for three repetitive measurements ($n = 3$).

4.2.5 Optimization of electropolymerization for L-GA

To attain high sensitivity for 1-OHP detection, various parameters of the electropolymerization procedure were estimated. The formation of the film thickness on the electrode surface directly affects the electrochemical response of the target analyte. In the current study, the concentration of L-GA solution, the number of scans for electropolymerization, and the scan rate for electropolymerization were investigated to gain the optimal conditions for the fabrication of the polymeric sensor. As seen in Figure 31, the optimal values for electropolymerization were the concentration of L-GA solution of 30 mM, the number of scans at 5 cycles, and the scan rate of 100 mV s^{-1} .

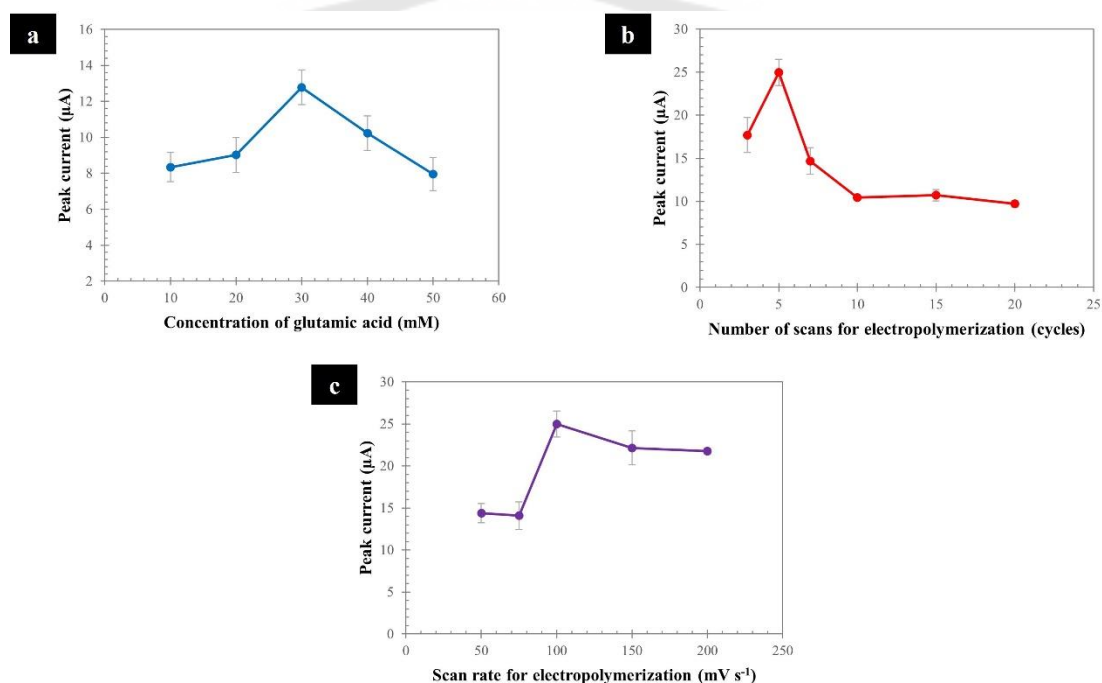


Figure 31 Effects of concentration of glutamic acid (a), number of scans (b), and scan rate for electropolymerization (c) on SPGE. Error bars represent the standard deviation of 10 μM 1-OHP detection using SWV for three repetitive measurements ($n = 3$).

4.2.6 Electrochemical behavior of 1-OHP on poly(L-GA)/SPGE

The electrochemical behavior of 1-OHP in Gly-NaOH (pH 9.4) on SPGE and poly(L-GA)/SPGE was subsequently studied by SWV. Figure 32 shows the performance for the detection of 10 μM 1-OHP in Gly-NaOH (pH 9.4) on SPGE and poly(L-GA)/SPGE.

The anodic peak current of 1-OHP ($i_{pa} = 9.27 \mu\text{A}$) was obtained at around -0.08 V on SPGE (red line). However, when the background signal of Gly-NaOH (pH 9.4) (red dashed line) at the unmodified SPGE was thoroughly magnified, the ghost peak appeared at around -0.10 V . We believed that this phenomenon might be caused by impurities from the graphene ink, which could not determine the 1-OHP at very low concentrations. Therefore, to resolve this issue, we aimed to use L-GA for the surface modification of SPGE. The ghost peak of the background current of Gly-NaOH (pH 9.4) did not occur after the surface modification (blue dashed line). Remarkably, the enlarged current signal of 1-OHP on poly(L-GA)/SPGE (blue line) was three times larger than that of the SPGE. These results suggested that the modified poly(L-GA) on SPGE revealed the electrocatalytic property of 1-OHP oxidation. Therefore, poly(L-GA)/SPGE could be employed as an excellent electrochemical sensor for 1-OHP analysis.

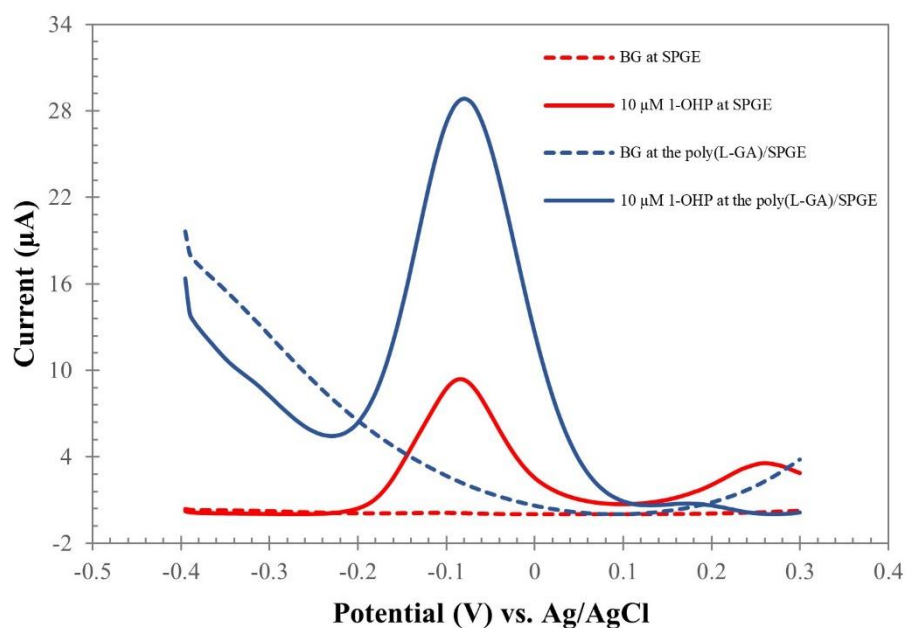


Figure 32 Square wave voltammograms of $10 \mu\text{M}$ 1-OHP in Gly-NaOH (pH 9.4) at the unmodified and modified SPGE.

4.2.7 Analytical performance

Under optimal conditions, the analytical performance of this methodology was verified by detecting 1-OHP in different concentration via SWV. The anodic peak currents

increased with increasing concentrations of 1-OHP (Figure 33a, inset). The linear dynamic range (LDR) was relative in the range of 1–1000 nM (Figure 33a). The limits of detection (LOD) and quantification (LOQ) were evaluated to be 0.95 (3SD/Slope) and 3.16 (10SD/Slope) nM, respectively. Furthermore, the analytical performance of this work was compared with that of previous works, as revealed in Table 3. Although this proposed method did not provide the lowest detection limit, however, the developed sensor had several advantages over the mentioned methods, such as the ease and rapidity of fabrication, the need for only one modifier for a single step of surface modification, and cost-effectiveness. This proposed sensor could also be applied for 1-OHP analysis in real samples. Moreover, the supporting electrolyte used in this work was within the suitable and dependable range of pH. Therefore, this assay had the perfect ability to be an alternative choice for the detection of 1-OHP in real-world applications.

In terms of reproducibility, three concentrations (10, 500, and 1000 nM) concerning the probable range in interesting samples were assessed. The relative standard deviation (RSD) values were <32%, which was accepted by the AOAC recommendation (Latimer, 2016). For the stability study of poly(L-GA)/SPGE, the current signal of 10 μ M 1-OHP remained at 98.55% for 21 days, indicating that this newly developed sensor provided good stability for 1-OHP detection.

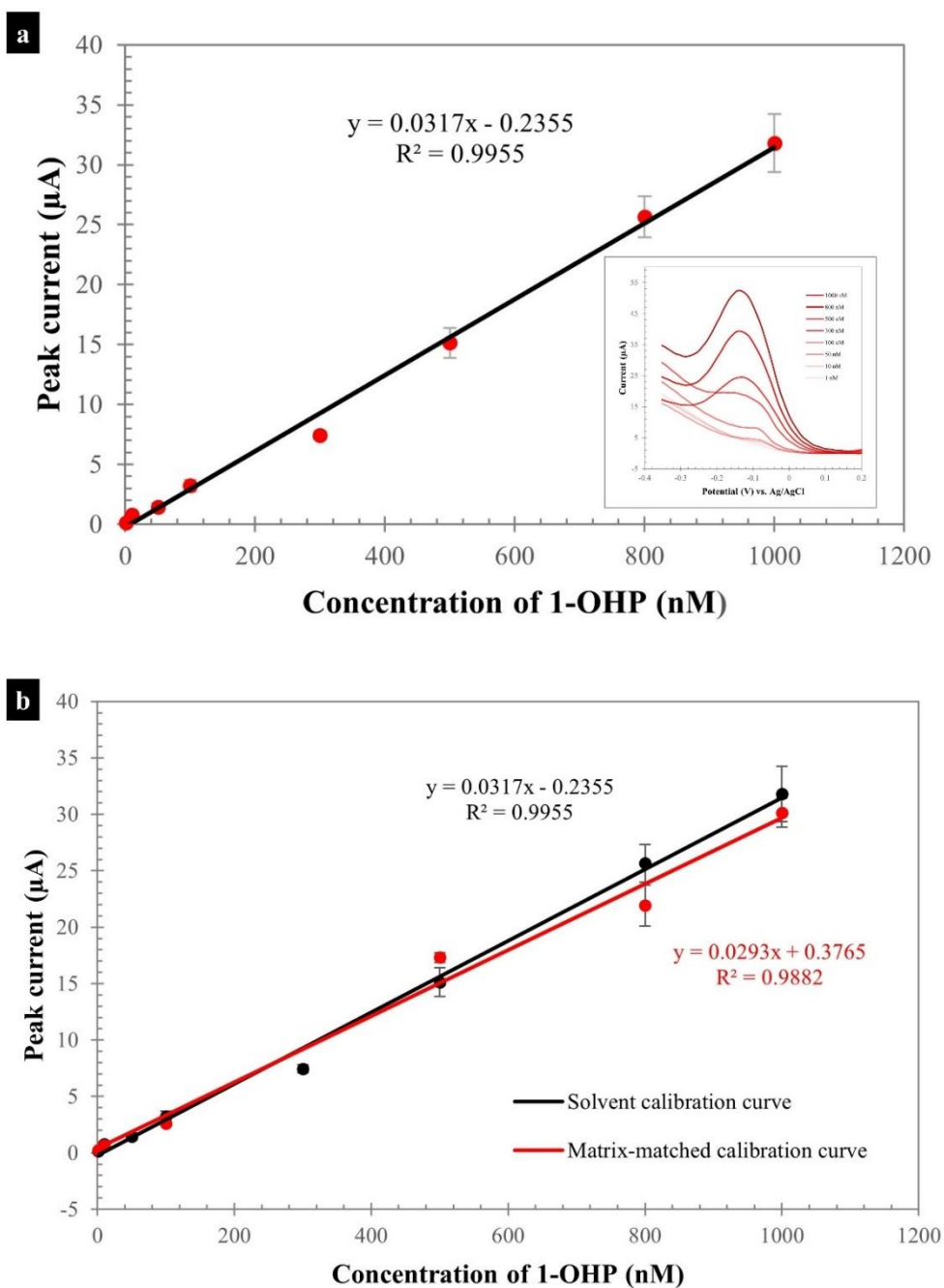


Figure 33 The calibration curve between the anodic peak current and the concentration of 1-OHP in the range of 1–1000 nM (a) and corresponding square wave voltammograms of 1-OHP (inset). A comparison of the plotting graphs between a solvent calibration curve and a matrix-matched calibration curve (b). Error bars represent the standard deviation of 1-OHP detection at different concentrations for three repetitive measurements ($n = 3$).

Table 3 Comparison of the analytical performance between this proposed method and previous works for 1-OHP detection.

Electrodes	Electrolyte	LOD (nM)	Linear range (nM)	References
MIP/SPCE	MeOH-NaOH-NaCl	182	2500-125000	(Kirsch, Honeychurch, Hart, & Whitcombe, 2005)
MWCNTs/GCE	PBS (pH 7.0)	0.1	6-800	(Wu, 2011)
P3MT/GCE	PBS (pH 2.0)	165	500-20000	(Shen et al., 2012b)
GON/OA-POSS/GCE	PBS (pH 2.0)	40	100-12550	(Shen et al., 2012a)
BDDFE	MeOH-BR buffer (pH 5.0)	100	100-10000	(Yosypchuk, Berek, & Vyskočil, 2012)
GR-MN202/GCE	BR buffer (pH 3.0)	1.72	5-12000	(Gao, Tang, Hu, Zhu, & Yang, 2015)
GR/GCE	PBS (pH 2.0)	0.84	5-300	(Pang, Zhang, et al., 2019)
ZIP-8/IL/nano-CPE	PBS (pH 9.0)	10	50-20000	(Y. Li et al., 2020)
Au@ZIF-67/CNFPE	-	0.1	0.5-10000	(Y. Li et al., 2021)
PAMAM/Cr-MOF/rGO/GCE	PBS (pH 2.0)	75	100-6000	(Cui et al., 2021)
poly(L-GA)/SPGE	Gly-NaOH (pH 9.4)	0.95	1-1000	This work

Abbreviation

MIP: molecularly imprinted polymer; SPCE: screen-printed carbon electrode; GCE: glassy carbon electrode; MWCNTs: multi-walled carbon nanotubes; P3MT: poly (3-methylthiophene); GON: graphene oxide nanoribbon; OA-POSS: octa (3-aminopropyl)octasilsesquioxane octahydrochloride; BDDFE: boron-doped diamond film electrode; GR: graphene; MN202: resin MN202; ZIP: zeolitic imidazolate frameworks; IL: ionic liquid; nano-CPE: nano-carbon paste electrode; CNFPE: carbon nanofiber paste electrode; PAMAM: polyamidoamine; Cr-MOF: chromium-centered metal-organic framework; rGO: reduced graphene oxide; poly(L-GA): poly(L-Glutamic acid); SPGE: screen-printed graphene electrode.

4.2.8 Interference study

The effect of interferences, such as uric acid (UA), ascorbic acid (AA), citric acid (CA), glucose (Glu), bovine serum albumin (BSA), urea, and creatinine, along with the effect of some ions, comprising Na^+ , K^+ , Mg^{2+} , Ca^{2+} , and NH_4^+ , which might affect 1-OHP detection, was investigated. Figure 34 describes the percentage of the current signal of 300 nM 1-OHP detection in the presence of 3 μM UA, 9 μM AA, 1500 nM CA, 300 nM Glu, 300 nM BSA, 3 μM urea, 300 nM creatinine, 30 μM Na^+ , 30 μM K^+ , 30 μM Mg^{2+} , 30 μM Ca^{2+} , and 30 μM NH_4^+ . From the results, the changes in the current signal of 1-OHP containing different interferences were $< \pm 5\%$, which suggested that interferences had no significant effect on 1-OHP detection. Therefore, the poly(L-GA)/SPGE had good selectivity toward 1-OHP detection.

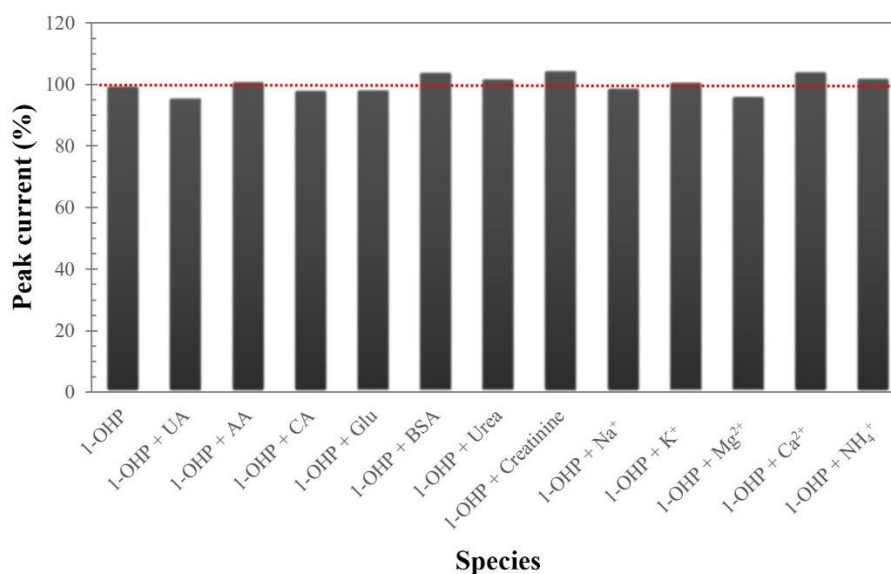


Figure 34 Effect of some interfering substances on the detection of 300 nM 1-OHP at the poly(L-GA)/SPGE by SWV under optimal conditions ($n = 3$).

4.2.9 Dilution and matrix effect

In the current study, a 100-fold dilution using Gly-NaOH (pH 9.4) was used to evade foreign interferences in urine samples before analysis. As presented in Figure 33b, the information obtained from two linear regression equations could be applied to

calculate the percentage of the matrix effect using the following equation (Moreno-González, Hamed, García-Campaña, & Gámiz-Gracia, 2017; Wan et al., 2018):

$$\text{Matrix effect} = [(S_M/S_S) - 1] \times 100$$

where S_M denotes the slope of calibration curve in matrix; and S_S denotes the slope of calibration curve in Gly-NaOH (pH 9.4). Based on the principle, the matrix effect was found to be $|7.57|\%$, suggesting that this value was $<|15|\%$, which confirmed that the proposed dilution was efficient to remove the interferences in urine.

4.2.10 Application in real urine samples

In a practical application, the determination of 1-OHP in six urine samples from healthy volunteers was executed for evaluation of the potential of the proposed method. As the results are summarized in Table 4, the percentage values of recovery and RSD acquired within the acceptable value ranges of 86.06%–119.08% and 2.57%–34.77%, respectively. These results suggested that the proposed method is accurate, precise, and reliable to determine the 1-OHP in real urine samples without any interference. Therefore, the poly(L-GA)/SPGE offered a powerful sensor for determining 1-OHP in urine samples.

Table 4 Results obtained from the determination of 1-OHP in healthy volunteer's urine using poly(L-GA)/SPGE (n = 3).

Real Samples	Spiked	Found	Recovery	RSD
	(nM)	(nM)	(%)	(%)
1 st volunteer	10	11.23	112.31	26.34
	500	577.96	115.59	2.57
2 nd volunteer	10	9.44	94.36	22.31
	500	526.60	105.32	7.14
3 rd volunteer	10	11.55	115.53	22.78
	500	456.68	91.34	12.68
4 th volunteer	10	11.18	111.75	11.81
	500	533.77	106.75	4.20
5 th volunteer	10	8.95	89.48	34.77
	500	430.28	86.06	11.38
6 th volunteer	10	11.91	119.08	7.26
	500	577.59	115.52	6.06

4.3 Highly efficient polymeric L-methionine-modified sensor: An application for the simultaneous determination of 5-aminosalicylic acid and sulfapyridine

The contents of this sub-project are in the process of writing the original research article.

4.3.1 Electrochemical behaviors of 5-ASA and SPD on poly(L-Met)/SPGE

For preliminary studies, the electrochemical behaviors of individual and simultaneous detection of 100 μM 5-ASA and SPD in a mixture of MeOH and 0.1 M PBS (pH 5.6) in a proportion of 20:80% v/v on SPGE and poly(L-Met)/SPGE were investigated by CV and SWV. Figure 35a and b illustrate cyclic voltammograms of the individual detection of 5-ASA and SPD on SPGE and poly(L-Met)/SPGE. At the unmodified SPGE (black dashed line), the anodic and cathodic peak potentials were noticed at around +0.11 and +0.02 V for 5-ASA, and +0.74 and -0.03 V for SPD. When modification of poly(L-Met) on SPGE was performed (red line), the peak potentials of the two compounds shifted to the negative direction, and the peak currents of the two compounds increased when compared to the unmodified SPGE. In addition, the appearance of the anodic and cathodic peak potentials indicated that the electrochemical reactions of these compounds were quasi-reversible processes. Subsequently, the simultaneous detection of 5-ASA and SPD on SPGE and poly(L-Met)/SPGE were studied by CV. The peak currents of the two compounds appeared at different peak potentials, which were consistent with the individual studies as evidenced in Figure 35c. Furthermore, SWV was used to confirm the performance of poly(L-Met)/SPGE. As shown in Figure 35d, square wave voltammograms of the simultaneous detection of 5-ASA and SPD on SPGE and poly(L-Met)/SPGE were compared. It suggested that the oxidation peaks of the two compounds were clearly separated at different peak potentials. Moreover, the anodic peak currents of these compounds were approximately 1.5 times larger than those of the unmodified SPGE. These results obtained from CV and SWV demonstrated that the modification of poly(L-Met) on SPGE exhibited the electrocatalytic properties of 5-ASA and SPD oxidation. Therefore, the developed poly(L-Met)/SPGE sensor was a powerful electrochemical sensor for the simultaneous analysis of 5-ASA and SPD.

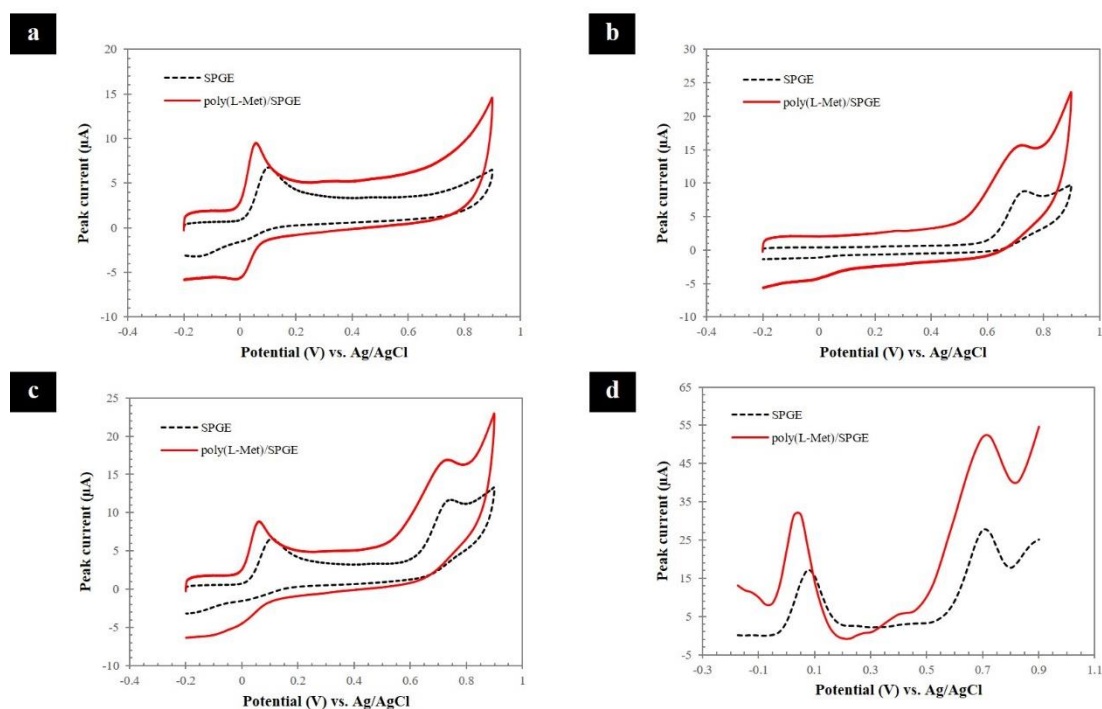


Figure 35 Cyclic voltammograms of individual 5-ASA (a) and SPD (b) detections; cyclic (c) and square wave voltammograms (d) of the simultaneous detection of 5-ASA and SPD in a mixture of MeOH and 0.1 M PBS (pH 5.6) in a proportion of 20:80% v/v on SPGE and poly(L-Met)/SPGE.

4.3.2 Effect of pH values and scan rates

Investigation of adjusting the pH values of the supporting electrolyte is very important to the electrochemical behavior and peak appearance of the analyte. Moreover, this investigation can provide information on the electron and proton numbers that participated in the electrochemical reaction of the analyte. In this work, the effect of pH values on the electrooxidation behavior of 5-ASA and SPD on poly(L-Met)/SPGE was carefully studied by adjusting the pH from 5.0 to 8.0 using SWV. Figure 36a presents the plot of peak current versus different pH values for the simultaneous detection of 100 μM 5-ASA and SPD in MeOH:PBS (20:80% v/v) on poly(L-Met)/SPGE via SWV. At low pH values, it provided a good electrochemical response to 5-ASA. Based on three acidity constants (pK_a) of the 5-ASA molecule, they have been reported for the carboxylic group ($-\text{COOH}$; $pK_a = 3$), amino group ($-\text{NH}_3^+$; $pK_a = 6$), and phenolic group ($-\text{OH}$; $pK_a = 13.9$)

(Nobilis et al., 2006) (Pastorini et al., 2008). From the information of pK_a , it was believed that the protonation of the amino group and phenolic group in the 5-ASA molecule at low pH values was easily oxidized at the poly(L-Met)/SPGE surface. Contrarily, the electrochemical response of SPD gradually increased from pH 5.0 to 5.6, then it was constant. According to the reported pK_a value of SPD = 8.4 (Białk-Bielińska et al., 2011), a pH value of 5.6 was adequate to convert the protonated SPD form, resulting in the effortless oxidation process at the poly(L-Met)/SPGE surface. Therefore, pH 5.6 was chosen compromisingly as the optimal pH value for the simultaneous detection of 5-ASA and SPD. Additionally, the plotting graphs between the peak potential (E_{pa}) and pH values for 5-ASA and SPD, respectively, were constructed as shown in Figure 36b. It was found that SPD provided one linear relationship, but 5-ASA offered two linear relationships. The phenomenon of 5-ASA might be caused by an intersection point at pH of about 6, which could be attributed to the amino group ($pK_a = 6$) of 5-ASA (Shahrokhian, Hosseini, & Kamalzadeh, 2013) (Torkashvand, Gholivand, & Taherkhani, 2015). The slope values of $-0.0542 \text{ V pH}^{-1}$ for SPD (red line) and $-0.0615 \text{ V pH}^{-1}$ of the first linear relationship for 5-ASA (green line) were close to the Nernstian theoretical value of -0.059 V pH^{-1} , signifying an equal number of protons and electrons participated in the electrochemical reaction as previously reported (Rajkumar, Choi, & Kim, 2021) (Sohouli, Karimi, Khosrowshahi, Rahimi-Nasrabadi, & Ahmadi, 2020) (Teradale, Lamani, Ganesh, Swamy, & Das, 2017) (Afshar, Zamani, & Karimi-Maleh, 2019).

The effect of scan rates is one of the important factors that can indicate whether the analyte's mass transfer process at the electrode surface is adsorption or diffusion controlled. In this work, the effect of scan rates on the simultaneous detection of $100 \mu\text{M}$ 5-ASA and SPD at the poly(L-Met)/SPGE was investigated in the range of $0.025\text{--}0.25 \text{ V s}^{-1}$ via CV (Figure 36c). The linear relationships between the peak current (I_{pa}) and the square root of the scan rate ($v^{1/2}$) for 5-ASA and SPD were revealed in Figure 36d, demonstrating the diffusion-controlled electrochemical process. Besides, when graphs were plotted between $\log I_{pa}$ and $\log v$ for 5-ASA and SPD, the slope values were close to

0.5, which confirmed that the electrochemical processes of the two analytes were controlled by the diffusion process (David K. Gosser, 1993).

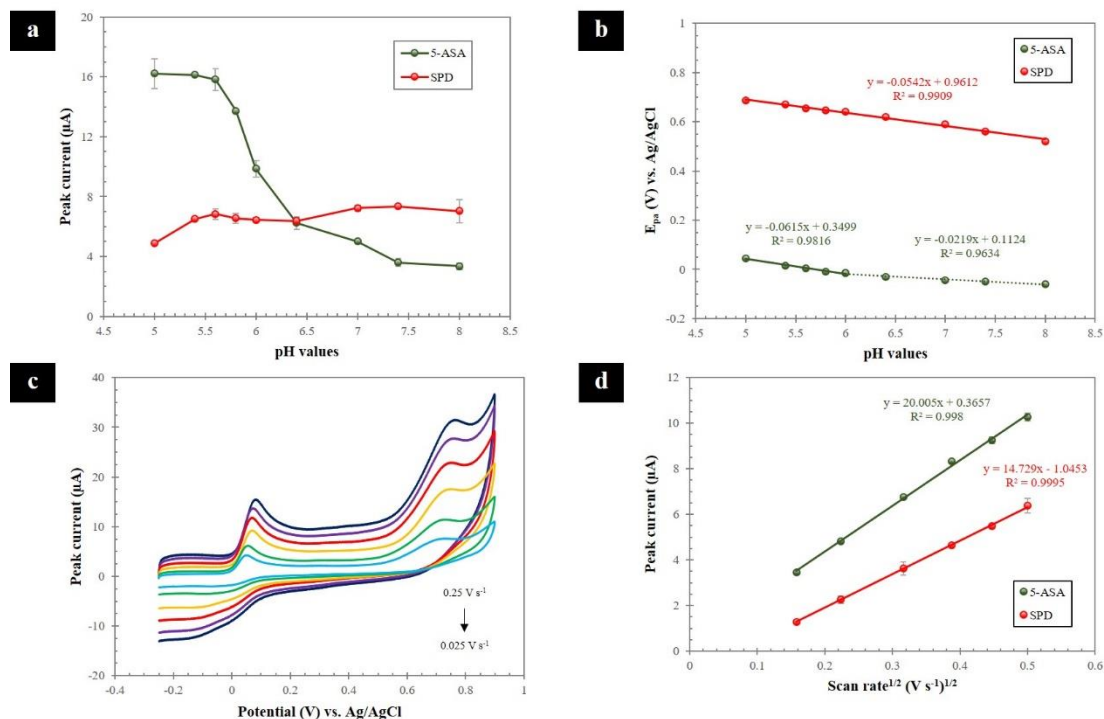


Figure 36 The plot of I_{pa} vs. pH values (a). and E_{pa} vs. pH values (b) for 5-ASA and SPD.

Cyclic voltammograms of the simultaneous detection of $100 \mu\text{M}$ 5-ASA and SPD in MeOH:PBS (20:80% v/v) at various scan rates (c) and the plot of I_{pa} vs. the square root of the scan rate (d). Error bars represent the standard deviation of the simultaneous detection of 5-ASA and SPD at various pH values and scan rates for three repetitive measurements ($n = 3$).

4.3.3 Optimization of electropolymerization for L-Met

The study of optimization parameters of the polymeric electropolymerization is significant to the formation of the film thickness on the electrode surface, resulting in the electrochemical response of the analyte. In this work, the concentration of L-Met solution, the number of scans for electropolymerization, and the scan rate for electropolymerization were studied. From the results in Figure 37, the optimal parameters for electropolymerization were the concentration of L-Met solution of 6 mM , the number of scans at 3 cycles, and the scan rate of 100 mV s^{-1} .

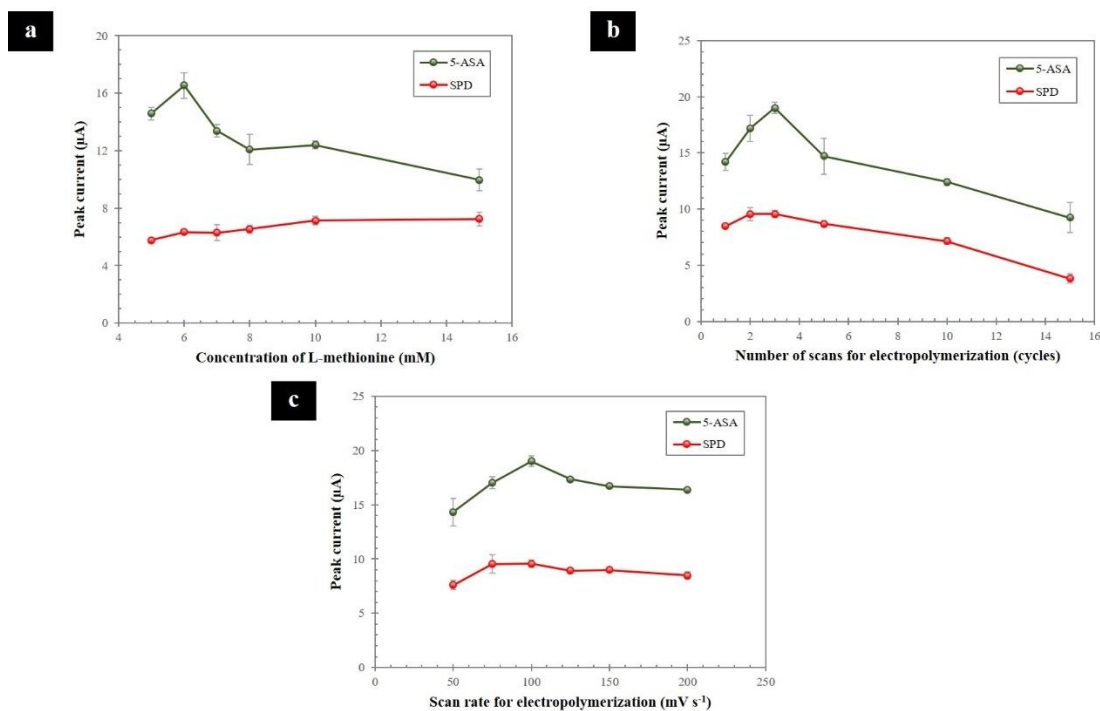


Figure 37 Influence of electropolymerization procedure, including concentration of L-methionine (a), number of scans (b), and scan rate (c). Error bars represent the standard deviation of the simultaneous detection of 5-ASA and SPD using SWV for three repetitive measurements ($n = 3$).

4.3.4 Influence of the proportion between MeOH and PBS

To obtain the high performance of the simultaneous 5-ASA and SPD detection, the proportion of a mixture between MeOH and 0.1 M PBS (pH 5.6) was investigated in the range of 5–40% v/v of MeOH using SWV. Figure 38a and b exhibit the results of the proportion studied of MeOH:PBS, which significantly impacted the electrochemical response of 5-ASA and SPD. Obviously, the proportion at 5% v/v of MeOH provided the highest peak currents of 5-ASA and SPD. In addition, the peak potentials of these analytes slightly shifted to the negative direction. These results might be associated with the good solubility of the analytes. However, at high proportions of MeOH, the poor peak currents of two analytes with a slight shift in the positive direction were observed. The decrease of the peak currents and the shift of the peak potentials were caused by the high solution resistance in the non-aqueous system, which might obstruct the electron transfer process

of the analytes at the electrode surface. Therefore, the proportion of the MeOH:PBS mixture at 5:95% v/v was selected as the best proportion for the simultaneous detection of 5-ASA and SPD.

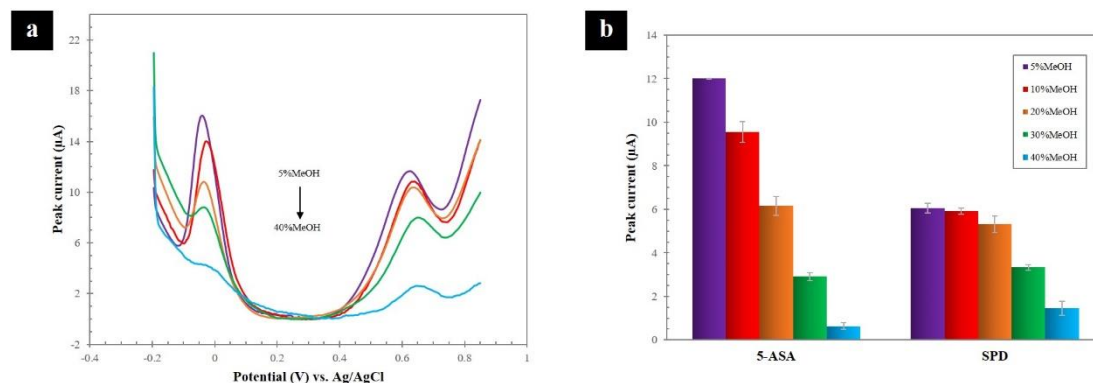


Figure 38 Square wave voltammograms (a) and a chart of the peak current (b) of the simultaneous detection of 5-ASA and SPD in a mixture of MeOH and PBS at different proportions.

4.3.5 Analytical performance

Under optimal conditions, the SWV technique was employed to verify the analytical performance of the proposed method for the simultaneous detection of 5-ASA and SPD at different concentrations, as depicted in Figure 39a. The linear dynamic ranges between the peak current and concentration of two metabolites were plotted in the range of 1–250 μM (Figure 39b). From the linear regression equations of two metabolites, the limits of detection (LODs) of each metabolite were found to be 0.60 and 0.57 μM for 5-ASA and SPD, respectively, which were calculated from $3\text{SD}/m$ (where SD denotes the standard deviation of the blank measurements ($n = 7$), m denotes the slope of the calibration curves). As compared to previously reported publications, especially in the field of electrochemical detection, this work is the first report on the application of a polymeric-modified screen-printed graphene electrode for the simultaneous detection of 5-ASA and SPD, indicating the therapeutic determinant of the action of SSZ. The sample application in urine is noninvasive, which has many advantages, such as expedient access, reduced pain or discomfort, no incisions, stitches, or scars, no hospital stays,

little downtime and recuperation, and cost savings. Furthermore, the developed sensor had various benefits, such as ease and rapidity of manufacture, inexpensiveness, and the need for a small sample volume. Since it has great efficiency, the proposed methodology could be an alternative to methods currently used to analyze 5-ASA and SPD simultaneously in biological fluid samples.

For simultaneous detection, it is necessary to investigate the reciprocal effect from both analytes. Therefore, only one standard solution of metabolites was studied by varying the concentration in the range of 1–50 μM while the concentration of other metabolites was fixed at 10 μM (Figure 39c–f). The peak currents exhibited good linearity without interfering with the others. From the results of the plotting graphs, the slopes of the two metabolites were consistent with the previous linearity study. These results confirmed that these metabolites had no influence on each other. Thus, the developed sensor offered a high potential for the simultaneous detection of 5-ASA and SPD in a real-world situation.

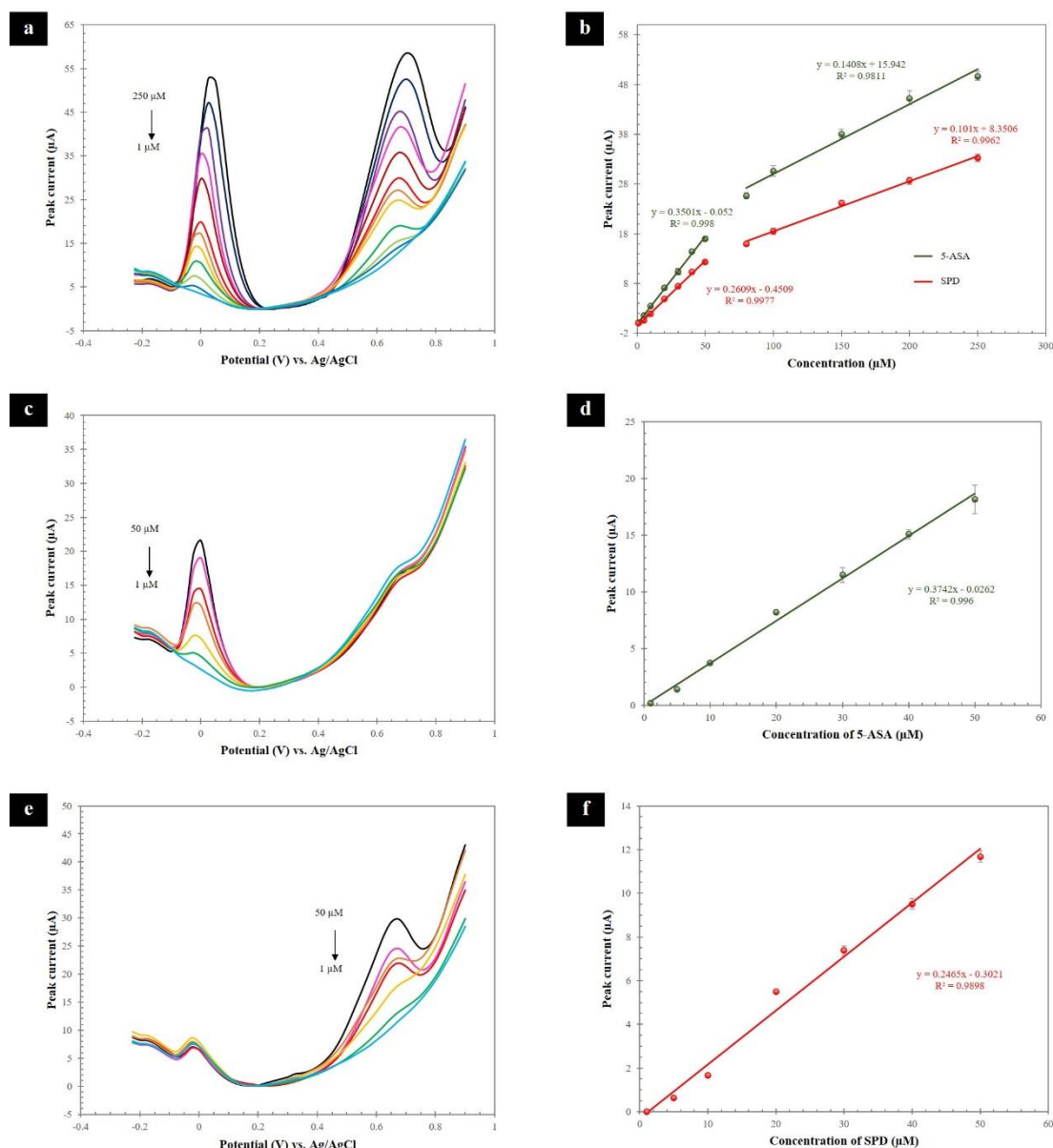


Figure 39 Square wave voltammograms for the simultaneous detection of 5-ASA and SPD (a) and the linear dynamic ranges between the peak current and concentration of 5-ASA and SPD (b). Square wave voltammograms (c) and the plotting graph (d) for the 5-ASA detection in the presence of 10 μM SPD. Square wave voltammograms (e) and the plotting graph (f) for the SPD detection in the presence of 10 μM 5-ASA.

4.3.6 Selectivity, reproducibility, and stability of the sensor

The SWV technique was used to estimate the selectivity of poly(L-Met)/SPGE for the simultaneous detection of 5-ASA and SPD in the presence of the common physiological interferences, including uric acid (UA), bovine serum albumin (BSA), ascorbic acid (AA), citric acid (CA), glucose (Glu), creatinine, and urea. Additionally, the effect of some substances, comprising NaCl, KCl, CaCl₂, MgCl₂, ZnSO₄, and (NH₄)₂S₂O₈, which could affect the simultaneous detection of 5-ASA and SPD. Figure 40 presents the percentages of the electrochemical responses of 20 μM 5-ASA and SPD detection in the presence of 40 μM UA, 20 μM BSA, 200 μM AA, 1 mM CA, 6 mM Glu, 100 μM creatinine, 8 mM urea, 20 mM NaCl, 20 mM KCl, 10 mM CaCl₂, 10 mM MgCl₂, 2 mM ZnSO₄, and 2 mM (NH₄)₂S₂O₈. From the results, the percentages of the electrochemical responses of two analytes in the presence of several interferences were <±5%, demonstrating that interferences had no significant effect on 5-ASA and SPD detection.

In terms of reproducibility, the SWV technique was also used for the simultaneous detection of 5-ASA and SPD at three concentrations (5, 20, and 50 μM). The relative standard deviation (RSD) values for seven repetitive measurements were <15%, which agreed with the AOAC recommendation (Latimer, 2016). For the long-term stability study of poly(L-Met)/SPGE, it was assessed using simultaneous detection of 5-ASA and SPD. The electrochemical response of two analytes could remain at 86.68% for 31 days, which suggests that this proposed sensor reveals good stability to simultaneously detect the 5-ASA and SPD.

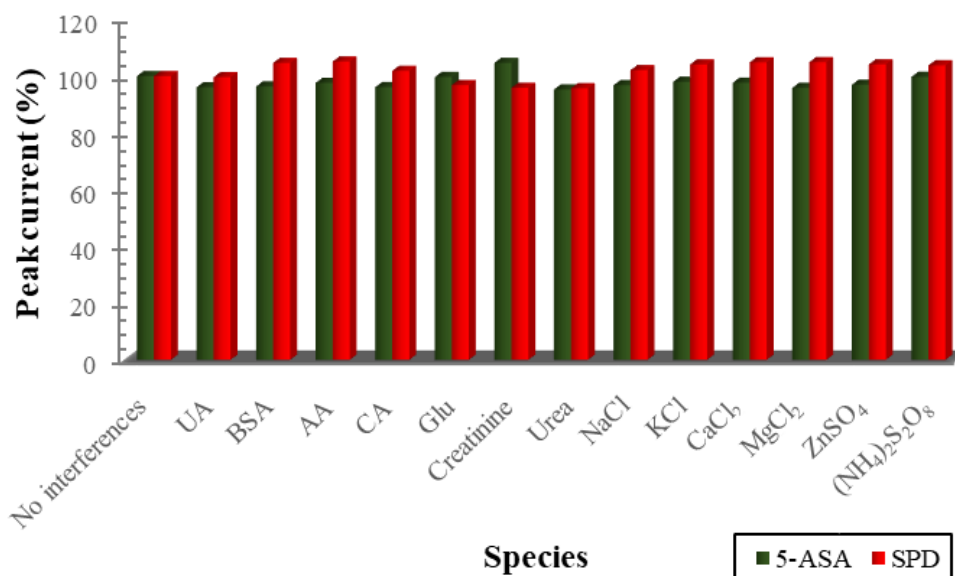


Figure 40 Influence of some interferences on the simultaneous detection of 5-ASA and SPD at the poly(L-Met)/SPGE.

4.3.7 Determination of 5-ASA and SPD in real samples

To ascertain the ability of the developed sensor and the feasibility of the proposed method, the simultaneous analysis of 5-ASA and SPD in practical applications was explored in real human urine samples using the standard addition method. Three human urine samples were diluted 600 times using a mixture between MeOH and 0.1 M PBS (pH 5.6) in a proportion of 5:95% v/v. Then, the known standard solutions of 5-ASA and SPD were spiked into the samples, and the accuracy and precision were evaluated. The results of this study are summarized in Table 5. The percentages of recovery and RSD values for intra-day and inter-day studies were obtained in the acceptable ranges by AOAC recommendation (Latimer, 2016), signifying the authenticated realization of the developed sensor and proposed method in real sample analysis. Therefore, the poly(L-Met)/SPGE had sufficient sensitivity, selectivity, reproducibility, and reliability to simultaneously monitor the 5-ASA and SPD in biological fluid samples.

Table 5 Practical applications of poly(L-Met)/SPGE for the simultaneous analysis of 5-ASA and SPD in real urine samples.

Urine Samples	Analytes	Spiked (μM)	Intra-day			Inter-day		
			Found concentration, mean \pm SD (μM)	Recovery (%)	RSD (%)	Found concentration, mean \pm SD (μM)	Recovery (%)	RSD (%)
1 st volunteer	5-ASA	10	9.52 \pm 1.26	95.17	13.29	9.92 \pm 0.40	99.19	4.01
		30	29.69 \pm 1.85	98.96	6.24	29.15 \pm 1.22	97.17	4.17
	SPD	10	9.10 \pm 0.84	91.03	9.19	9.42 \pm 0.37	94.16	3.91
		30	31.67 \pm 1.34	105.55	4.22	31.40 \pm 0.39	104.66	1.24
2 nd volunteer	5-ASA	10	8.23 \pm 0.83	82.26	10.12	9.06 \pm 0.86	90.62	9.52
		30	30.13 \pm 3.17	100.45	10.52	28.48 \pm 2.92	94.93	10.27
	SPD	10	8.60 \pm 0.83	85.96	9.64	8.13 \pm 0.56	81.29	6.95
		30	31.18 \pm 0.96	103.93	3.07	27.75 \pm 3.00	92.52	10.80
3 rd volunteer	5-ASA	10	9.31 \pm 1.25	93.15	13.43	9.46 \pm 0.15	94.58	1.56
		30	32.66 \pm 3.60	108.87	11.03	31.75 \pm 1.67	105.82	5.26
	SPD	10	8.20 \pm 0.25	82.02	3.06	8.50 \pm 0.63	84.94	7.41
		30	31.54 \pm 2.97	105.14	9.42	30.80 \pm 2.21	102.67	7.17

CHAPTER 5

CONCLUSIONS

The aims of this dissertation are to develop electrochemical sensors by searching for novel materials used in analytical sensing applications and to improve the performance of the developed sensors by integrating the excellent properties of the nanomaterials, polymers, or both for specific biomarker detection. The results obtained suggest that the developed sensors exhibit outstanding performance for monitoring the target analytes. Individual conclusions for each detection of important analytes were deduced as follows:

5.1 A new nanocomposite-based screen-printed graphene electrode for sensitive and selective detection of 8-hydroxy-2'-deoxyguanosine

An electrochemical sensing platform for 8-OHdG detection based on assembled layers of poly(L-methionine) and AuNPs-modified SPGE was successfully fabricated. The synergistic coupling effect of poly(L-methionine), AuNPs, and graphene can improve the specific surface area, enhance electrical conductivity, and promote the electrochemical activity of 8-OHdG. Under optimal conditions, the detection of 8-OHdG was achieved in the range of 1–50 μM with a limit of detection of 92 nM. Moreover, no enzymatic catalyst usability is needed to reduce interfering UA before analysis, leading to a savings in analysis costs. The main advantages of this developed sensor that are superior to those in previous reports are the simple steps for fabrication, the small size, disposability, portability, and the requirement of a small sample volume. As a benefit, the suggested method may be a viable alternative for screening the 8-OHdG level in the early stages of diagnosis and risk assessment of their levels in the human body.

5.2 A novel and easy-to-construct polymeric L-glutamic acid-modified sensor for urinary 1-hydroxypyrene detection: Human biomonitoring of polycyclic aromatic hydrocarbons exposure

An electrochemical analytical device using poly(L-GA) modified SPGE for the rapid, simple, sensitive, and selective determination of trace amounts of 1-OHP was successfully demonstrated. The developed sensing platform was easily fabricated by using only one modifier for the surface modification of SPGE via a single step of

electropolymerization. The poly(L-GA) thin film that adhered to the surface of SPGE demonstrated excellent electrocatalytic performance, increasing the specific surface area and promoting the electron-transfer rate, resulting in improved sensitivity and selectivity in 1-OHP detection. Under optimal conditions, the 1-OHP sensing provided a wide linear range with a low detection limit. Furthermore, no chromatographic sample preparation was required prior to analysis for removing interferences. This proposed methodology and developed sensor could be applied to successfully determine 1-OHP in human urine samples. This new platform provided the rapid and simple fabricating process, inexpensiveness, small size, disposability, need for a small sample volume, and suitability for portability. Therefore, this novel sensor might be employed as an alternative device for monitoring and analyzing trace 1-OHP concentrations in the environment and workplace that have a high possibility of illness risk linked to PAHs in the human body.

5.3 Highly efficient polymeric L-methionine-modified sensor: An application for the simultaneous determination of 5-aminosalicylic acid and sulfapyridine

In this present work, the success in the fabrication of an electrochemical sensor using poly(L-Met) as the sole modifier for modifying the SPGE surface via electropolymerization and the investigation of electroanalytical performance toward the simultaneous detection of 5-ASA and SPD were obtained. The developed electrochemical sensor had superior electrocatalytic performance to simultaneously detect two metabolites. Under optimal conditions, the poly(L-Met)/SPGE provided a wide linear dynamic range (1–250 μM), with detection limits of 0.60 and 0.57 μM for 5-ASA and SPD, respectively. In practical applications, this developed sensor and proposed methodology were successfully utilized for the simultaneous determination of 5-ASA and SPD in real human urine samples with high accuracy, precision, reproducibility, stability, and reliability. Therefore, the simultaneous detection of 5-ASA and SPD, metabolizing substances by SSZ, could provide the therapeutic determinant for SSZ's action and might be helpful for medical professionals in the treatment of rheumatoid arthritis and inflammatory bowel illnesses.

REFERENCES

- Afshar, S., Zamani, H. A., & Karimi-Maleh, H. (2019). Electrochemical Determination of Sulfapyridine using a New Approach of Modified Electrode based on Amplification with Room Temperature Ionic Liquid and ZnO Nanoparticle. *Anal. Bioanal. Electrochem.*, 11, 1781-1790.
- Arvind, A. S., & Farthing, M. J. G. (1988). Review: new aminosalicic acid derivatives for the treatment of inflammatory bowel disease. *Aliment. Pharmacol. Therap.*, 2(4), 281-289.
- Azizi, S. N., Ghasemi, S., & Amiripour, F. (2016). Nickel/P nanozeolite modified electrode: A new sensor for the detection of formaldehyde. *Sens. Actuators B: Chem.*, 227, 1-10.
- Bard, A. J., & Faulkner, L. R. (2001). *Electrochemical Methods: Fundamentals and Applications* (2nd ed.). New York: John Wiley & Sons, Inc.
- Beiranvand, M. (2021). A review of the biological and pharmacological activities of mesalazine or 5-aminosalicylic acid (5-ASA): an anti-ulcer and anti-oxidant drug. *Inflammopharmacology*, 29, 1279-1290.
- Benvidi, A., Dehghani-Firouzabadi, A., Mazloum-Ardakani, M., Mirjalili, B.-B. F., & Zare, R. (2015). Electrochemical deposition of gold nanoparticles on reduced graphene oxide modified glassy carbon electrode for simultaneous determination of levodopa, uric acid and folic acid. *Journal of Electroanalytical Chemistry*, 736, 22-29.
- Białk-Bielińska, A., Siedlewicz, G., Stepnowski, P., Pazdro, K., Fabiańska, A., & Kumirska, J. (2011). A very fast and simple method for the determination of sulfonamide residues in seawaters. *Anal. Methods*, 3, 1371-1378.
- Bonaccorso, F., Colombo, L., Yu, G., Stoller, M., Tozzini, V., Ferrari, A. C., . . . Pellegrini, V. (2015). Graphene, related two-dimensional crystals, and hybrid systems for energy conversion and storage. *Science*, 347(6217), 1246501.

- Cadet, J., Delatour, T., Douki, T., Gasparutto, D., Pouget, J.-P., Ravanat, J.-L., & Sauvaigo, S. (1999). Hydroxyl radicals and DNA base damage. *Mutation Research*, 424, 9-21.
- Cao, G., Wu, C., Tang, Y., & Wan, C. (2019). Ultrasmall HKUST-1 nanoparticles decorated graphite nanosheets for highly sensitive electrochemical sensing of DNA damage biomarker 8-hydroxy-2'-deoxyguanosine. *Anal. Chim. Acta*, 1058, 80-88.
- Chang, H., Wang, X., Shiu, K. K., Zhu, Y., Wang, J., Li, Q., . . . Jiang, H. (2013). Layer-by-layer assembly of graphene, Au and poly(toluidine blue O) films sensor for evaluation of oxidative stress of tumor cells elicited by hydrogen peroxide. *Biosens. Bioelectron.*, 41, 789-794.
- Charoenkitamorn, K., Chaiyo, S., Chailapakul, O., & Siangproh, W. (2018). Low-cost and disposable sensors for the simultaneous determination of coenzyme Q10 and α -lipoic acid using manganese (IV) oxide modified screen-printed graphene electrodes. *Analytica Chimica Acta*, 1004, 22-31.
- Cheemalapati, S., Devadas, B., & Chen, S. M. (2014). Highly sensitive and selective determination of pyrazinamide at poly-L-methionine/reduced graphene oxide modified electrode by differential pulse voltammetry in human blood plasma and urine samples. *Journal of Colloid and Interface Science*, 418, 132-139.
- Chen, B. H., & Chen, Y. C. (2001). Formation of Polycyclic Aromatic Hydrocarbons in the Smoke from Heated Model Lipids and Food Lipids. *J. Agric. Food Chem.*, 49(11), 5238-5243.
- Choudhary, D., Goykar, H., Kalyane, D., Sreeharsha, N., & Tekade, R. K. (2020). *Prodrug design for improving the biopharmaceutical properties of therapeutic drugs*. The Future of Pharmaceutical Product Development and Research.
- Cooke, M. S., Olinski, R., & Lof, S. (2008). Measurement and meaning of oxidatively modified DNA lesions in urine. *Cancer Epidemiology Biomarkers & Prevention*, 17(1).
- Cui, H., Cui, S., Tian, Q., Zhang, S., Wang, M., Zhang, P., . . . Li, X. (2021). Electrochemical Sensor for the Detection of 1-Hydroxypyrene Based on Composites of PAMAM-

- Regulated Chromium-Centered Metal-Organic Framework Nanoparticles and Graphene Oxide. *ACS Omega*, 6, 31184-31195.
- David K. Gosser, J. (1993). *Cyclic Voltammetry: Simulation and Analysis of Reaction Mechanisms* (1st). Wiley-VCH.
- Dhulkefi, A. J., Atacan, K., Bas, S. Z., & Ozmen, M. (2020). An Ag-TiO₂-reduced graphene oxide hybrid film for electrochemical detection of 8-hydroxy-2'-deoxyguanosine as an oxidative DNA damage biomarker. *Anal. Methods*, 12(4), 499-506.
- Essumang, D. K., Dodoo, D. K., & Adjei, J. K. (2013). Effect of smoke generation sources and smoke curing duration on the levels of polycyclic aromatic hydrocarbon (PAH) in different suites of fish. *Food Chem. Toxicol.*, 58, 86-94.
- France, N. (2022). Sulfasalazine. <https://www.drugs.com/sulfasalazine.html#dosage>
- Ganesh, P. S., & Swamy, B. E. K. (2015). Simultaneous electroanalysis of norepinephrine, ascorbic acid and uric acid using poly(glutamic acid) modified carbon paste electrode. *J. Electroanal. Chem.*, 752, 17-24.
- Ganesh, P. S., Swamy, B. E. K., & Harisha, K. V. (2017). Electropolymerisation of DL-methionine at carbon paste electrode and its application to the determination of catechol and hydroquinone. *Anal. Bioanal. Electrochem.*, 9, 47-64.
- Gao, L., Tang, Y.-Z., Hu, Y., Zhu, G., & Yang, X. (2015). Determination of Trace 1-Hydroxypyrene by Resin MN202 With Graphene Composite Modified Glassy Carbon Electrode. *IEEE Sens. J.*, 15(3), 1475-1481.
- Gomes, E. S., Leite, F. R. F., Ferraz, B. R. L., Mourao, H., & Malagutti, A. R. (2019). Voltammetric sensor based on cobalt-poly(methionine)-modified glassy carbon electrode for determination of estriol hormone in pharmaceuticals and urine. *Journal of Pharmaceutical Analysis*, 9(5), 347-357.
- Graille, M., Wild, P., Sauvain, J.-J., Hemmendinger, M., Canu, I. G., & Hopf, N. B. (2020). Urinary 8-OHdG as a Biomarker for Oxidative Stress: A Systematic Literature Review and Meta-Analysis. *International Journal of Molecular Sciences*, 21(11), 3743.

- Gugoasa, L. A. D., Pogacean, F., Kurbanoglu, S., Tudoran, L. B., Serban, A. B., Kacso, I., & Pruneanu, S. (2021). Graphene-Gold Nanoparticles Nanozyme-Based Electrochemical Sensor with Enhanced Laccase-Like Activity for Determination of Phenolic Substrates. *J. Electrochem. Soc.*, *168*, 067523.
- Guo, Z., Liu, X., Liu, Y., Wu, G., & Lu, X. (2016). Constructing a novel 8-hydroxy-2'-deoxyguanosine electrochemical sensor and application in evaluating the oxidative damages of DNA and guanine. *Biosens. Bioelectron.*, *86*, 671-676.
- Gutiérrez, A., Gutiérrez, S., García, G., Galicia, L., & Rivas, G. A. (2011). Determination of 8-Hydroxy 2'-Deoxyguanosine Using Electrodes Modified with a Dispersion of Carbon Nanotubes in Polyethylenimine. *Electroanalysis*, *23*(5), 1221-1228.
- Hao, J., Wu, K., Wan, C., & Tang, Y. (2018). Reduced graphene oxide-ZnO nanocomposite based electrochemical sensor for sensitive and selective monitoring of 8-hydroxy-2'-deoxyguanosine. *Talanta*, *185*, 550-556.
- He, J., Song, Z., Zhang, S., Wang, L., Zhang, Y., & Qiu, R. (2014). Methionine – Au Nanoparticle Modified Glassy Carbon Electrode: a Novel Platform for Electrochemical Detection of Hydroquinone. *Mater. Sci.*, *20*(4), 381-386.
- Henle, E. S., & Linn, S. (1997). Formation, Prevention, and Repair of DNA Damage by Iron/Hydrogen Peroxide. *The Journal of Biological Chemistry*, *272*(31), 19095-19098.
- Jeng, H. A., & Pan, C.-H. (2015). 1-Hydroxypyrene as a Biomarker for Environmental Health (pp. 595-612). *General Methods in Biomarker Research and their Applications*.
- Jia, L.-P., Liu, J.-F., & Wang, H.-S. (2015). Electrochemical performance and detection of 8-Hydroxy-2'-deoxyguanosine at single-stranded DNA functionalized graphene modified glassy carbon electrode. *Biosens. Bioelectron.*, *67*, 139-145.
- Kasai, H., Hayami, H., Yamaizumi, Z., Saito, H., & Nishimura, S. (1984). Detection and identification of mutagens and carcinogens as their adducts with guanosine derivatives. *Nucleic Acids Research*, *12*(4), 2127-2136.

- Katz, E., & Willner, I. (2003). Probing biomolecular interactions at conductive and semiconductive surfaces by impedance spectroscopy: Routes to impedimetric immunosensors, DNA-sensors, and enzyme biosensors. *Electroanalysis*, 15(11), 913-947.
- Khan, M. Z. H., Liu, X., Tang, Y., & Liu, X. (2018). Ultra-sensitive electrochemical detection of oxidative stress biomarker 8-hydroxy-2'-deoxyguanosine with poly (L-arginine)/graphene wrapped Au nanoparticles modified electrode. *Biosens. Bioelectron.*, 117, 508-514.
- Kim, D., Lee, S., & Piao, Y. (2017). Electrochemical determination of dopamine and acetaminophen using activated graphene-Nafion modified glassy carbon electrode. *Journal of Electroanalytical Chemistry*, 794, 221-228.
- Kim, K.-H., Jahan, S. A., Kabir, E., & Brown, R. J. C. (2013). A review of airborne polycyclic aromatic hydrocarbons (PAHs) and their human health effects. *Environ. Int.*, 60, 71-80.
- Kirsch, N., Honeychurch, K. C., Hart, J. P., & Whitcombe, M. J. (2005). Voltammetric Determination of Urinary 1-Hydroxypyrene Using Molecularly Imprinted Polymer-Modified Screen-Printed Carbon Electrodes. *Electroanalysis*, 17(7), 571-578.
- Klotz, U. (1985). Clinical Pharmacokinetics of Sulphasalazine, Its Metabolites and Other Prodrugs of 5-Aminosalicylic Acid. *Clin. Pharmacokinet.*, 10, 285-302.
- Kuila, T., Bose, S., Khanra, P., Mishra, A. K., Kim, N. H., & Lee, J. H. (2011). Recent advances in graphene-based biosensors. *Biosens. Bioelectron.*, 26(12), 4637-4648.
- Kumar, N., Rosy, & Goyal, R. N. (2017). A melamine based molecularly imprinted sensor for the determination of 8-hydroxydeoxyguanosine in human urine. *Talanta*, 166, 215-222.
- Kurbanoglu, S., Ozkan, S. A., & Merkoci, A. (2017). Nanomaterials-based enzyme electrochemical biosensors operating through inhibition for biosensing applications. *Biosens. Bioelectron.*, 89, 886-898.

- Lars Barregard, Møller, P., Henriksen, T., Mistry, V., Koppen, G., Pavel Rossner, J., . . .
Cooke, M. S. (2013). Human and Methodological Sources of Variability in the
Measurement of Urinary 8-oxo-7,8-dihydro-2'-deoxyguanosine. *Antioxidants &
Redox Signaling*, 18(18), 2377-2391.
- Latimer, G. W. (2016). *Official methods of analysis of AOAC international* (20th). AOAC
International.
- Li, J., & Zhang, X. (2012). Fabrication of Poly(Aspartic Acid)-Nanogold Modified Electrode
and Its Application for Simultaneous Determination of Dopamine, Ascorbic Acid,
and Uric Acid. *Am. J. Analyt. Chem.*, 3, 195-203.
- Li, M., Li, Y.-T., Li, D.-W., & Long, Y.-T. (2012). Recent developments and applications of
screen-printed electrodes in environmental assays—A review. *Anal. Chim. Acta*,
734, 31-44.
- Li, R., Jia, Z., & Trush, M. A. (2016). Defining ROS in Biology and Medicine. *HHS Public
Access*, 1(1), 9-21.
- Li, T. H., Jia, W. L., Wang, H. S., & Liu, R. M. (2007). Electrochemical performance of 8-
hydroxy-2'-deoxyguanosine and its detection at poly(3-methylthiophene) modified
glassy carbon electrode. *Biosens. Bioelectron.*, 22(7), 1245-1250.
- Li, Y., Li, Y., Du, C., Zhang, P., Cen, P., Liu, X., & Li, Y. (2021). Electrochemical Sensing of
1-hydroxypyrene on a Colloidal Gold Modified Zeolitic Imidazolate Frameworks-
67/Carbon Nanofiber Paste Electrode. *J. Electrochem. Soc.*, 168, 057509.
- Li, Y., Li, Y., Wang, Y., Ma, G., Liu, X., Lia, Y., & Soar, J. (2020). Application of zeolitic
imidazolate frameworks (ZIF-8)/ionic liquid composites modified nano-carbon
paste electrode as sensor for electroanalytical sensing of 1-hydroxypyrene.
Microchem. J., 159, 105433.
- Liu, X., Zhang, X.-Y., Wang, L.-L., & Wang, Y.-Y. (2014). A sensitive electrochemical sensor
for paracetamol based on a glassy carbon electrode modified with multiwalled
carbon nanotubes and dopamine nanospheres functionalized with gold
nanoparticles. *Microchimica Acta*, 181(11-12), 1439-1446.

- Łuczak, T. (2009). Comparison of electrochemical oxidation of epinephrine in the presence of interfering ascorbic and uric acids on gold electrodes modified with S-functionalized compounds and gold nanoparticles. *Electrochimica Acta*, 54(24), 5863-5870.
- Manavalan, S., Rajaji, U., Chen, S.-M., Steplin Paul Selvin, S., Govindasamy, M., Chen, T.-W., . . . Elshikh, M. S. (2018). Determination of 8-hydroxy-2'-deoxyguanosine oxidative stress biomarker using dysprosium oxide nanoparticles@reduced graphene oxide. *Inorg. Chem. Front.*, 5(11), 2885-2892.
- Martins, G. V., Marques, A. C., Fortunato, E., & Sales, M. G. F. (2016). 8-hydroxy-2'-deoxyguanosine (8-OHdG) biomarker detection down to picoMolar level on a plastic antibody film. *Biosens. Bioelectron.*, 86, 225-234.
- Martins, G. V., Tavares, A. P. M., Fortunato, E., & Sales, M. G. F. (2017). Paper-Based Sensing Device for Electrochemical Detection of Oxidative Stress Biomarker 8-Hydroxy-2'-deoxyguanosine (8-OHdG) in Point-of-Care. *Sci. Rep.*, 7(1), 14878-14889.
- Merkoçi, A. (2013). Nanoparticles Based Electroanalysis in Diagnostics Applications. *Electroanalysis*, 25(1), 15-27.
- Moreno-González, D., Hamed, A. M., García-Campaña, A. M., & Gámiz-Gracia, L. (2017). Evaluation of hydrophilic interaction liquid chromatography–tandem mass spectrometry and extraction with molecularly imprinted polymers for determination of aminoglycosides in milk and milk-based functional foods. *Talanta*, 171, 74-80.
- Nantaphol, S. (2016). *Electrochemical detection of organic and biological compounds with modified electrode*. (Doctoral dissertation). Chulalongkorn University, Bangkok.
- Nobilis, M., Vybíralová, Z., Sládková, K., Lísa, M., Holčápek, M., & Kvěťina, J. (2006). High-performance liquid-chromatographic determination of 5-aminosalicylic acid and its metabolites in blood plasma. *J. Chromatogr. A*, 1119, 299-308.

- Ojani, R., Raoof, J.-B., Maleki, A. A., & Safshekan, S. (2014). Simultaneous and sensitive detection of dopamine and uric acid using a poly(L-methionine)/gold nanoparticle-modified glassy carbon electrode. *Chinese J. Catal.*, 35(3), 423-429.
- Omidi, F., Khadem, M., Dehghani, F., Seyedsomeah, M., & Shahtaheri, S. J. (2020). Ultrasound-assisted dispersive micro-solid-phase extraction based on N-doped mesoporous carbon and high-performance liquid chromatographic determination of 1-hydroxypyrene in urine samples. *J. Sep. Sci.*, 43(13), 2602-2609.
- Pan, D., Zhou, Q., Rong, S., Zhang, G., Zhang, Y., Liu, F., . . . Pan, H. (2015). Electrochemical immunoassay for the biomarker 8-hydroxy-2'-deoxyguanosine using a glassy carbon electrode modified with chitosan and poly(indole-5-carboxylic acid). *Microchim. Acta*, 183(1), 361-368.
- Pang, Y., Huang, Y., Li, W., Feng, L., & Shen, X. (2019). Conjugated Polyelectrolyte/Graphene Multilayer Films for Simultaneous Electrochemical Sensing of Three Monohydroxylated Polycyclic Aromatic Hydrocarbons. *ACS Appl. Nano Mater.*, 12, 7785-7794.
- Pang, Y., Zhang, Y., Sun, X., Ding, H., Ma, T., & Shen, X. (2019). Synergistical accumulation for electrochemical sensing of 1-hydroxypyrene on electroreduced graphene oxide electrode. *Talanta*, 192, 387-394.
- Park, E.-M., Shigenaga, M. K., Degan, P., Korn, T. S., Kitzler, J. W., Wehr, C. M., . . . Ames, B. N. (1992). Assay of excised oxidative DNA lesions: Isolation of 8-oxoguanine and its nucleoside derivatives from biological fluids with a monoclonal antibody column. *Proceedings of the National Academy of Sciences*, 89(8), 3375-3379.
- Pastorini, E., Locatelli, M., Simoni, P., Roda, G., Roda, E., & Rod, A. (2008). Development and validation of a HPLC-ESI-MS/MS method for the determination of 5-aminosalicylic acid and its major metabolite N-acetyl-5-aminosalicylic acid in human plasma. *J. Chromatogr. B*, 872, 99-106.
- Peppercorn, M. A. (1984). Sulfasalazine: Pharmacology, clinical use, toxicity, and related new drug development. *Ann. Intern. Med.*, 101(3), 377-386.

- Piñón-Segundo, E., Mendoza-Muñoz, N., & Quintanar-Guerrero, D. (2013). Nanoparticles as Dental Drug-Delivery Systems *Nanobiomaterials in Clinical Dentistry* (pp. 475-495).
- Plosker, G. L., & Croom, K. F. (2005). Sulfasalazine: A review of its use in the management of rheumatoid arthritis. *Drugs*, 65(13), 1825-1849.
- Punjiya, M., Moon, C. H., Matharu, Z., Nejad, H. R., & Sonkusale, S. (2018). A three-dimensional electrochemical paper-based analytical device for low-cost diagnostics. *Analyst*, 143, 1059-1064.
- Pushpanjali, P. A., Manjunatha, J. G., & Srinivas, M. T. (2020). Highly sensitive platform utilizing poly(L-methionine) layered carbon nanotube paste sensor for the determination of voltaren. *FlatChem*, 24, 100207.
- Rajkumar, C., Choi, J.-H., & Kim, H. (2021). Mixture of carbon aerogel with Pd-WO₃ nanorods for amperometric determination of mesalazine. *Microchim. Acta*, 188, 135.
- Razmi, H., & Harasi, M. (2008). Voltammetric behavior and amperometric determination of ascorbic acid at cadmium pentacyanonitrosylferrate film modified GC electrode. *Int. J. Electrochem. Sci.*, 3, 82-95.
- Samori, P., Kinloch, I. A., Feng, X., & Palermo, V. (2015). Graphene-based nanocomposites for structural and functional applications: using 2-dimensional materials in a 3-dimensional world. *2D Materials*, 2(3), 030205.
- Schnekenburger, M., & Diederich, M. (2015). Nutritional Epigenetic Regulators in the Field of Cancer *Epigenetic Cancer Therapy* (pp. 393-425).
- Serrano, M., Bartolomé, M., Bravo, J. C., Paniagua, G., Gañan, J., Gallego-Picó, A., & Garcinuño, R. M. (2017). On-line flow injection molecularly imprinted solid phase extraction for the preconcentration and determination of 1-hydroxypyrene in urine samples. *Talanta*, 166, 375-382.
- Shah, A., Akhtar, M., Aftab, S., Shah, A. H., & Kraatz, H.-B. (2017). Gold copper alloy nanoparticles (Au-Cu NPs) modified electrode as an enhanced electrochemical

sensing platform for the detection of persistent toxic organic pollutants.

Electrochimica Acta, 241, 281-290.

- Shahrokhian, S., Hosseini, P., & Kamalzadeh, Z. (2013). Investigation of the Electrochemical Behavior of Mesalazine on the Surface of a Glassy Carbon Electrode Modified with CNT/PPY Doped by 1,5-Naphthalenedisulfonic Acid. *Electroanalysis*, 25, 2481-2491.
- Shang, T., Wang, P., Liu, X., Jiang, X., Hu, Z., & Lu, X. (2018). Facile synthesis of porous single-walled carbon nanotube for sensitive detection of 8-Hydroxy-2'-deoxyguanosine. *J. Electroanal. Chem.*, 808, 28-34.
- Shen, X., Cui, Y., Pang, Y., & Qian, H. (2012a). Graphene oxide nanoribbon and polyhedral oligomeric silsesquioxane assembled composite frameworks for pre-concentrating and electrochemical sensing of 1-hydroxypyrene. *Electrochim. Acta*, 59, 91-99.
- Shen, X., Cui, Y., Pang, Y., & Qian, H. (2012b). Pre-concentration and in situ electrochemical sensing of 1-hydroxypyrene on an electrodeposited poly(3-methylthiophene) film modified electrode. *J. Electroanal. Chem.*, 667, 1-6.
- Siangproh, W., Teshima, N., Sakai, T., Katoh, S., & Chailapakul, O. (2009). Alternative method for measurement of albumin/creatinine ratio using spectrophotometric sequential injection analysis. *Talanta*, 79(4), 1111-1117.
- Smith, A. D., Elgammal, K., Niklaus, F., Delin, A., Fischer, A. C., Vaziri, S., . . . Lemme, M. C. (2015). Resistive graphene humidity sensors with rapid and direct electrical readout. *Nanoscale*, 7(45), 19099-19109.
- Sohouli, E., Karimi, M. S., Khosrowshahi, E. M., Rahimi-Nasrabadi, M., & Ahmadi, F. (2020). Fabrication of an electrochemical mesalazine sensor based on ZIF-67. *Measurement*, 165, 108140.
- Tan, Y. Y., Jayawardena, K. D. G. I., Adikaari, A. A. D. T., Tan, L. W., Anguita, J. V., Henley, S. J., . . . Silva, S. R. P. (2012). Photo-thermal chemical vapor deposition growth of graphene. *Carbon*, 50(2), 668-673.

- Teradale, A. B., Lamani, S. D., Ganesh, P. S., Swamy, B. E. K., & Das, S. N. (2017). CTAB immobilized carbon paste electrode for the determination of mesalazine: A cyclic voltammetric method. *Sens. Bio-Sens. Res.*, *15*, 53-59.
- Thangphatthananarungruang, J., Chotsuwan, C., Jampasa, S., & Siangproh, W. (2022). A new nanocomposite-based screen-printed graphene electrode for sensitive and selective detection of 8-hydroxy-2'-deoxyguanosine. *FlatChem*, *32*, 100335.
- Thangphatthananarungruang, J., Chotsuwan, C., & Siangproh, W. (2023). A novel and easy-to-construct polymeric L-glutamic acid-modified sensor for urinary 1-hydroxypyrene detection: Human biomonitoring of polycyclic aromatic hydrocarbons exposure. *Talanta*, *253*, 123929.
- Thangphatthananarungruang, J., Lomae, A., Chailapakul, O., Chaiyo, S., & Siangproh, W. (2021). A low-cost paper-based diamond electrode for trace copper analysis at on-site environmental area. *Electroanalysis*, *33*, 226-232.
- Thangphatthananarungruang, J., Ngamaroonchote, A., Laocharoensuk, R., Chotsuwan, C., & Siangproh, W. (2018). A Novel Electrochemical Sensor for the Simultaneous Determination of Fat-Soluble Vitamins Using a Screen-Printed Graphene/Nafion Electrode. *Key Eng. Mater.*, *777*, 597-601.
- Thangphatthananarungruang, J., Yakoh, A., Laocharoensuk, R., Chotsuwan, C., Chailapakul, O., & Siangproh, W. (2020). High-efficient of graphene nanocomposite: Application to rapidly simultaneous identification and quantitation of fat-soluble vitamins in different matrix samples. *J. Electroanal. Chem.*, *873*, 114361.
- Torkashvand, M., Gholivand, M. B., & Taherkhani, F. (2015). Fabrication of an electrochemical sensor based on computationally designed molecularly imprinted polymer for the determination of mesalamine in real samples. *Mater. Sci. Eng. C*, *55*, 209-217.
- Valavanidis, A., Vlachogianni, T., & Fiotakis, C. (2009). 8-hydroxy-2'-deoxyguanosine (8-OHdG): A critical biomarker of oxidative stress and carcinogenesis. *Journal of Environmental Science and Health Part C*, *27*, 120-139.

- Varodi, C., Pogacean, F., Coros, M., Rosu, M.-C., Staden, R.-I. S.-v., Gal, E., . . . Mirel, S. (2019). Detection of 8-Hydroxy-2'-Deoxyguanosine Biomarker with a Screen-Printed Electrode Modified with Graphene. *Sensors*, *19*(19), 4297-4311.
- Wan, Y.-C., Liu, Y.-J., Liu, C., Ma, H.-T., Yu, H.-F., Kang, J.-W., . . . Lu, B. (2018). Rapid determination of neomycin in biological samples using fluorescent sensor based on quantum dots with doubly selective binding sites. *J. Pharm. Biomed. Anal.*, *30*(154), 75-85.
- Wang, J. (2006). *Analytical Electrochemistry* (3rd ed.). New Jersey: John Wiley & Sons, Inc.
- Wang, Y., Limon-Petersen, J. G., & Compton, R. G. (2011). Measurement of the diffusion coefficients of $[\text{Ru}(\text{NH}_3)_6]^{3+}$ and $[\text{Ru}(\text{NH}_3)_6]^{2+}$ in aqueous solution using microelectrode double potential step chronoamperometry. *J. Electroanal. Chem.*, *652*, 13-17.
- Wang, Y., Xie, J., Tao, L., Tian, H., Wang, S., & Ding, H. (2014). Simultaneous electrochemical determination of epirubicin and methotrexate in human blood using a disposable electrode modified with nano-Au/MWNTs-ZnO composites. *Sensors and Actuators B: Chemical*, *204*, 360-367.
- Wirasorn, K., Klarod, K., Hongsprabhas, P., & Boonsiri, P. (2014). Oxidative Stress, Antioxidant and Cancer. *Srinagarind Medical Journal*, *29*(2), 207-219.
- Wolf, J. M., & Lashner, B. A. (2002). Inflammatory bowel disease: Sorting out the treatment options. *Cleve. Clin. J. Med.*, *69*(8), 621-631.
- Wu, Y. (2011). Determination of 1-hydroxypyrene in human urine by a multi-wall carbon nanotubes-modified glassy carbon electrode. *Int. J. Environ. Anal. Chem.*, *91*(13), 1244-1255.
- Yang, H.-M., Wang, Y.-S., Li, J.-H., Li, G.-R., Wang, Y., Tan, X., . . . Kang, R.-H. (2009). Synchronous fluorescence determination of urinary 1-hydroxypyrene, beta-naphthol and 9-hydroxyphenanthrene based on the sensitizing effect of beta-cyclodextrin. *Anal. Chim. Acta*, *636*, 51-57.
- Yi, Z., Qiao, J., Wang, Y., Gao, K., Zhao, R., & Meng, X. (2019). Electrochemical Sensor Platform for 8-Hydroxy-2'-Deoxyguanosine Detection Based on Carboxyl-

Functionalized Carbon-Allotropic Nanomaterials Wrapped Gold Nanoparticles Modified Electrode. *Int. J. Electrochem. Sci.*, 14, 9098-9111.

- Yosypchuk, O., Barek, J., & Vyskočil, V. (2012). Voltammetric Determination of Carcinogenic Derivatives of Pyrene Using a Boron-Doped Diamond Film Electrode. *Anal. Lett.*, 45, 449-459.
- Zanolin, M. E., Girardi, P., Degan, P., Rava, M., Olivieri, M., Gennaro, G. D., . . . Marco, R. D. (2015). Measurement of a urinary marker (8-hydroxydeoxyguanosine, 8-OHdG) of DNA oxidative stress in epidemiological surveys: a pilot study. *The International journal of biological markers*, 30(3), 341-345.
- Zhang, H., Lu, H., Huang, H., Liu, J., Fang, X., Yuan, B.-F., . . . Chen, H. (2016). Quantification of 1-hydroxypyrene in undiluted human urine samples using magnetic solid-phase extraction coupled with internal extractive electrospray ionization mass spectrometry. *Anal. Chim. Acta*, 926, 72-78.
- Zhang, Q., Zhao, Q., Mingxuan Fu, Fan, X., Lu, H., Wang, H., . . . Wang, H. (2018). Carbon quantum dots encapsulated in super small platinum nanocrystals core-shell architecture/nitrogen doped graphene hybrid nanocomposite for electrochemical biosensing of DNA damage biomarker-8-hydroxy-20-deoxyguanosine. *Anal. Chim. Acta*, 1047, 9-20.
- Zhao, R.-N., Jia, L.-P., Feng, Z., Ma, R.-N., Zhang, W., Shang, L., . . . Wang, H.-S. (2019). Ultrasensitive electrochemiluminescence aptasensor for 8-hydroxy-2'-deoxyguanosine detection based on target-induced multi-DNA release and nicking enzyme amplification strategy. *Biosens. Bioelectron.*, 144, 111669.
- Zhu, Y., Murali, S., Stoller, M. D., Ganesh, K. J., Cai, W., Ferreira, P. J., . . . Ruoff, R. S. (2011). Carbon-based supercapacitors produced by activation of graphene. *Science*, 332(6037), 1537-1541.



Appendix

Appendix 1

FlatChem 32 (2022) 100335



Contents lists available at ScienceDirect

FlatChem

journal homepage: www.sciencedirect.com/journal/flatchem

A new nanocomposite-based screen-printed graphene electrode for sensitive and selective detection of 8-hydroxy-2'-deoxyguanosine

Jeerakit Thangphatthanarungruang^a, Chuleekorn Chotsuwan^b, Sakda Jampasa^c,
Weena Siangproh^{a,*}

^a Department of Chemistry, Faculty of Science, Srinakharinwirot University, Sukhumvit 23, Wattana, Bangkok 10110, Thailand

^b Nanohybrids for Industrial Solutions Research Team, National Nanotechnology Center, National Science and Technology Development Agency, Khlong Nueng, Khlong Luang, Pathumthani 12120, Thailand

^c Institute of Biotechnology and Genetic Engineering, Chulalongkorn University, Patumwan, Bangkok 10330, Thailand

ARTICLE INFO

Keywords:

8-Hydroxy 2'-deoxyguanosine
Oxidative DNA damage
Electrochemical sensor
Screen printed graphene electrode
Biological fluid samples

ABSTRACT

8-Hydroxy-2'-deoxyguanosine (8-OHdG) is a crucial marker used to appraise the degree of endogenous oxidative DNA damage in the human body. For routine clinical analysis, a simple, rapid, cost-effective, reliable, selective, sensitive, and portable approach is exceedingly required. In this work, we first reported on the fabrication of an electrochemical sensor based on poly(L-methionine) and gold nanoparticle-modified screen-printed graphene electrode (poly(L-Met)/AuNPs/SPGE) for the sensitive and selective detection of 8-OHdG in the presence of uric acid at a normal level in urine, which is the major interference when using square wave voltammetry. Sodium phosphate buffer solution containing sodium chloride and sodium dodecyl sulfate was used as the supporting electrolyte for specific detection of 8-OHdG. The oxidation peaks of 8-OHdG and uric acid can be obviously separated. Under optimal conditions, the linearity between the anodic peak current and the 8-OHdG concentration was obtained within the range of 1–50 μM , and the limit of detection (3SD/Slope) and limit of quantification (10SD/Slope) were found to be 92 and 306 nM, respectively. This fabricated sensor was successfully applied to determine the 8-OHdG concentration in biological fluid samples with good selectivity, sensitivity, reliability, reproducibility, accuracy, and precision. The promising results demonstrated that this proposed methodology could be useful for medical personnel in diagnosing the disease risk from 8-OHdG levels at an early stage.

Introduction

As we all know, reactive oxygen species (ROS) are a type of unstable molecules that can easily and highly react with other molecules in a cell. In the human body, ROS play a key role in physiology and pathology. These molecules can be used as intracellular signaling molecules demonstrating an imbalance between free radicals and antioxidants in the body's cells, leading to a situation known as oxidative stress [1,2]. Under the oxidative stress, various cellular biological structures, in particular DNA, can be harmed by an excessive ROS. Thus, the degree of DNA damage can be assessed from the concentration of ROS produced by body systems and is extremely significant and useful for medical applications.

8-Hydroxy-2'-deoxyguanosine (8-OHdG) is one of the most employed studied targets for oxidized metabolites and is used as a

specific marker for oxidative stress. 8-OHdG is a major product of guanine that is caused by the interaction of hydroxyl radical at the eighth carbon atom of the guanine DNA base. The amount of 8-OHdG can be used for risk assessment of the degree of endogenous oxidative DNA damage in the human body [3]. Normally, 8-OHdG can be found in several biological samples, e.g., urine, saliva, blood or serum, and tissue [4], and its corresponding concentration is further correlated with various diseases, such as cancers, aging, diabetes, and neurological disorders [5]. Note that the normal levels of 8-OHdG in healthy humans have been reported to be below 100 nM [6]. For this mentioned condition, development of the effective approach of sensitively and selectively detecting 8-OHdG in biological fluids is exceedingly required for disease risk assessment and early diagnosis.

In recent decades, various analytical methods have been reported on 8-OHdG detection, including post labeling methods [7,8], enzyme-

* Corresponding author.

E-mail address: wena@g.swu.ac.th (W. Siangproh).

<https://doi.org/10.1016/j.flat.2022.100335>

Received 7 November 2021; Received in revised form 4 January 2022; Accepted 6 January 2022

Available online 11 January 2022

2452-2627/© 2022 Elsevier B.V. All rights reserved.

linked immunosorbent assays [9,10], high-performance liquid chromatography [11,12], gas chromatography [13,14], capillary electrophoresis [15], and circular dichroism spectroscopy [16]. Although these methods provided high sensitivity and selectivity, unfortunately, there were still some limitations, such as sophisticated instruments, expensiveness, complexity of the pretreatment process, long analysis time, requirement of a large solvent/sample amount, and specialist skills for analysts. Moreover, these methods could not be able to reach the portability and were not suitable for routine clinical analysis. To overcome these inherent problems, the methodology for 8-OHdG detection offering a rapid, simple, portable, and sensitive assay is still in high demand.

Currently, electroanalytical methods have emerged as attractive alternative methods for biomarker detection owing to their simplicity, high sensitivity and accuracy, fast analysis time, low cost, portability, and compact setup. In addition, electrochemical devices have a small portable size in comparison with a conventional instrument; moreover, these devices require only a small sample volume for analysis. However, the electrochemical detection of 8-OHdG often suffers from the presence of interfering uric acid in biological fluids that can be oxidized near the oxidation peak potential of 8-OHdG. At present, the addition of uricase enzymes reduces the interference of uric acid [17–19]. Even though these proposed methods provided a good detection limit, there were still drawbacks, such as the limited lifetime and high cost of enzyme, the complicated procedure for enzyme preparation, and the long preparation time. Likewise, a commercial large-scale electrode—e.g., a glassy carbon electrode—was rarely suitable owing to its pretreatment, expensiveness, requirement of a large sample amount, and poor reproducibility. In addition, the modifiers used for electrode modification were sometimes inappropriate because they are expensive, have several steps for electrode modification, and are time-consuming. Thereby, the development of an electrochemical method to be used as an alternative choice is important to overcome the mentioned limitations.

Nowadays, owing to their desirable properties, screen-printed electrodes (SPEs), a kind of disposable electrochemical sensor based on screen-printing technology, have been substantially considered for the fabrication of portable, disposable, and cost-effective devices. In comparison with conventional electrodes, SPEs have many advantages, such as simple fabrication, small size, and requirement of a small sample volume [20,21]. To successfully accomplish the assay with high sensitivity and selectivity, surface modification of electrodes can be performed by using a type of nanomaterial. Graphene is a type of ink that is widely used for SPE fabrication owing to its high electrical conductivity, superior electron transportation, high mechanical and chemical stability, large surface area, and good biocompatibility, making it an incredibly attractive material from an electrochemical viewpoint for increasing the sensitivity of detection [22,23]. Furthermore, they can be conducted by employing a variety of modifiers to enhance the sensitivity and selectivity of electrochemical detection. Gold nanoparticles (AuNPs) are widely employed as metal nanoparticles for surface-modified electrodes. They have special physicochemical characteristics, e.g., large surface area, high conductivity, excellent electrocatalytic capability, and good biocompatibility [24]. Moreover, AuNPs can excellently react with organosulfur compounds at the electrode surface to form S–Au through covalent bonding, resulting in the enhancement of the stability of self-assembled monolayers [25,26]. In recent years, poly(amino acid)-modified electrodes have attracted great attention for determining various important biological samples and clinical species due to their simplicity, rapidity, and facility for fabrication. It can be used for the modification of the electrode surface via electropolymerization as it contains $-NH_2$ and $-COOH$ groups. Owing to the aforementioned benefits of AuNPs and poly(amino acids), several researchers have combined AuNPs and poly(amino acids) to increase the electroactive surface area and enhance the electrocatalytic performance of electrode, leading to high sensitivity and selectivity in detection.

Hence, we report for the first time on the development of a novel

electrochemical sensor based on AuNPs and poly(amino acid)-modified screen-printed graphene electrodes for specific 8-OHdG detection in various biological samples. To the best of our knowledge, there are no publications yet on the determination of 8-OHdG in the presence of interfering uric acid and chloride ions at normal levels, which directly affects interpretation of the results. To successfully fabricate the electrochemical sensor, a disposable screen-printed graphene electrode was used as an alternative device for 8-OHdG determination in biological fluid samples without using enzymatic catalysts.

Material and methods

Apparatuses, chemicals, and reagents

Electrochemical measurement was carried out using a model CHI660D electrochemical analyzer (CH Instrument, USA). All experiments were performed using a three-electrode system, including poly(L-methionine) and gold nanoparticles-modified screen-printed graphene working electrode, a graphene ink counter electrode, and a silver/silver chloride ink reference electrode, all were screen-printed onto the same transparent sheet. The screen-printed template blocks were generated by Chaiyaboon Co. Ltd. (Bangkok, Thailand).

Field emission scanning electron microscope and energy dispersive x-ray spectroscopy (FESEM-EDS) was performed with an electron microscope at 5 kV (JSM-7610F, JEOL, United Kingdom, England).

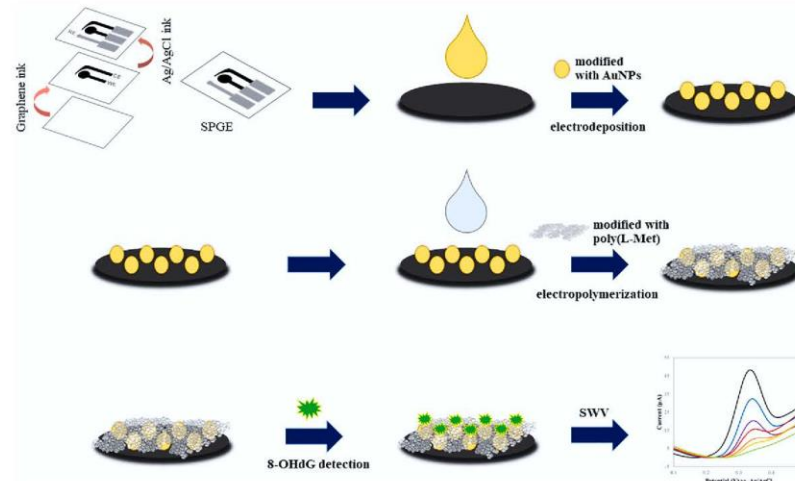
8-Hydroxy-2'-deoxyguanosine (8-OHdG) was acquired from Fujifilm Wako Pure Chemical Corporation (Osaka, Japan). Standard gold solution 1000 ppm (Product number: 08269, CAS: 7647-01-0), methionine, sodium dodecyl sulfate, uric acid, dopamine, ascorbic acid, bovine serum albumin, and citric acid were purchased from Sigma-Aldrich. Glucose, sodium chloride, potassium chloride, calcium chloride, magnesium chloride, methanol, sodium hydroxide, sodium dihydrogen orthophosphate ($NaH_2PO_4 \cdot 2H_2O$), di-sodium hydrogen orthophosphate ($Na_2HPO_4 \cdot 2H_2O$), and hydrochloric acid were obtained from Ajax Finechem Pty., Ltd. (New South Wales, Australia). Copper sulphate was received from Asia Pacific Specialty Chemicals Ltd. (New South Wales, Australia). Zinc sulphate was purchased from Merck (Darmstadt, Germany). Artificial urine was acquired from Carolina Biological Supply Company (Burlington, USA). Acetone was obtained from CaHC Co., Ltd. (Bangkok, Thailand). Graphene ink was received from Serve Science Co., Ltd. (Bangkok, Thailand). Silver/silver chloride (Ag/AgCl) ink was purchased from Sun chemical Ltd. (Slough, United Kingdom). All chemicals and reagents used in this work were of analytical grade and were used without any purification.

The stock standard solution of 8-OHdG was prepared in Milli-Q water and stored in the dark at 2–8 °C. The working solutions of 8-OHdG were prepared by dilution of the 1 mM solution of 8-OHdG with supporting electrolyte and mixed using a vortex mixer. Sodium phosphate buffer solution (Na-PBS) was prepared by mixing two stock solutions of NaH_2PO_4 and Na_2HPO_4 following the standard recipes. To obtain other pH values, 0.1 M Na-PBS was adjusted to the desired value by using 0.1 M hydrochloric acid or 0.1 M sodium hydroxide. All solutions were prepared in Milli-Q water from a Millipore water purification system ($R \geq 18.2 \text{ M}\Omega \text{ cm}$).

Human urine samples were collected from healthy human volunteers in our laboratory and immediately refrigerated at 4 °C. We informed all volunteers about what would happen to the human subjects in a trial. Human serum samples were taken from healthy patient and used without purification process.

Fabrication of the electrochemical sensor for 8-OHdG detection

The electrode pattern was designed by using Adobe Illustrator CS6. Screen-printed electrode (SPGE) was fabricated using an in-house screen-printing method on the transparent sheet substrate. For fabrication steps of SPGE, graphene ink was first screened onto the transparent



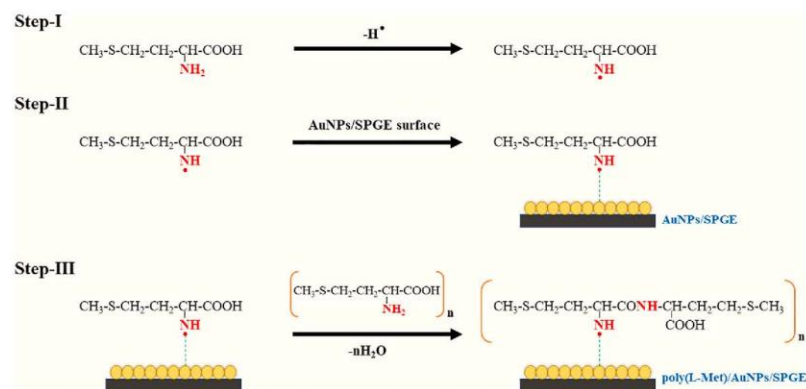
Scheme 1. Illustration of the fabrication of a new electrochemical sensor for 8-OHdG detection.

sheet as the first layer to obtain the working and counter electrode. Then, this screen-printed electrode was baked at 60 °C for 30 min to clear up the solvent from the electrode surface. The last step was the screening of Ag/AgCl ink as the reference electrode and conductive pads. Afterward, this screen-printed electrode was baked again at 60 °C for 30 min. Finally, the obtained screen-printed graphene electrode was kept in a dry place and ready to use for an experiment.

The sequential "layer-by-layer" film was fabricated on SPGE via cyclic voltammetry (CV). Initially, AuNPs-modified SPGE was prepared by dropping 50 μL of 1000 ppm standard gold solution in 5% hydrochloric acid onto the three-electrode surface of SPGE. Then, electrodeposition of gold atoms was performed in the potential range from -0.4 V to $+1.4\text{ V}$ with a scan rate of 150 mV s^{-1} for seven cycles. Subsequently, the electrode was rinsed with deionized water and air-dried. To prepare poly(L-Met)/AuNPs-modified SPGE, electropolymerization of L-methionine on the AuNPs/SPGE was performed by dropping 50 μL L-

methionine solution in 0.1 M sodium phosphate buffer solution at pH 7.0 onto the surface of AuNPs/SPGE and applying 10 cyclic voltammetric scans in the potential range from -0.6 V to $+2.0\text{ V}$ with a scan rate of 100 mV s^{-1} . Afterward, this electrode was then rinsed thoroughly with deionized water and air-dried once again. Finally, the poly(L-Met)/AuNPs-modified SPGE was obtained and stored in a dry place for analytical measurements. The preparation process of the fabricated electrochemical sensor for 8-OHdG detection is summarized in Scheme 1. To validate the performance of the proposed sensor, different sensors were also prepared using the same protocol without AuNPs and poly(L-Met).

CV was used as an efficient technique for the deposition of AuNPs and the polymeric thin-film layer of L-methionine on the surface of SPGE. The fabrication of layer-by-layer film on SPGE involves two steps: (1) electrodeposition of AuNPs on SPGE and (2) electropolymerization of L-methionine on AuNPs/SPGE. CV curves obtained from the



Scheme 2. Illustration of the possible structure of L-methionine film on AuNPs modified SPGE.

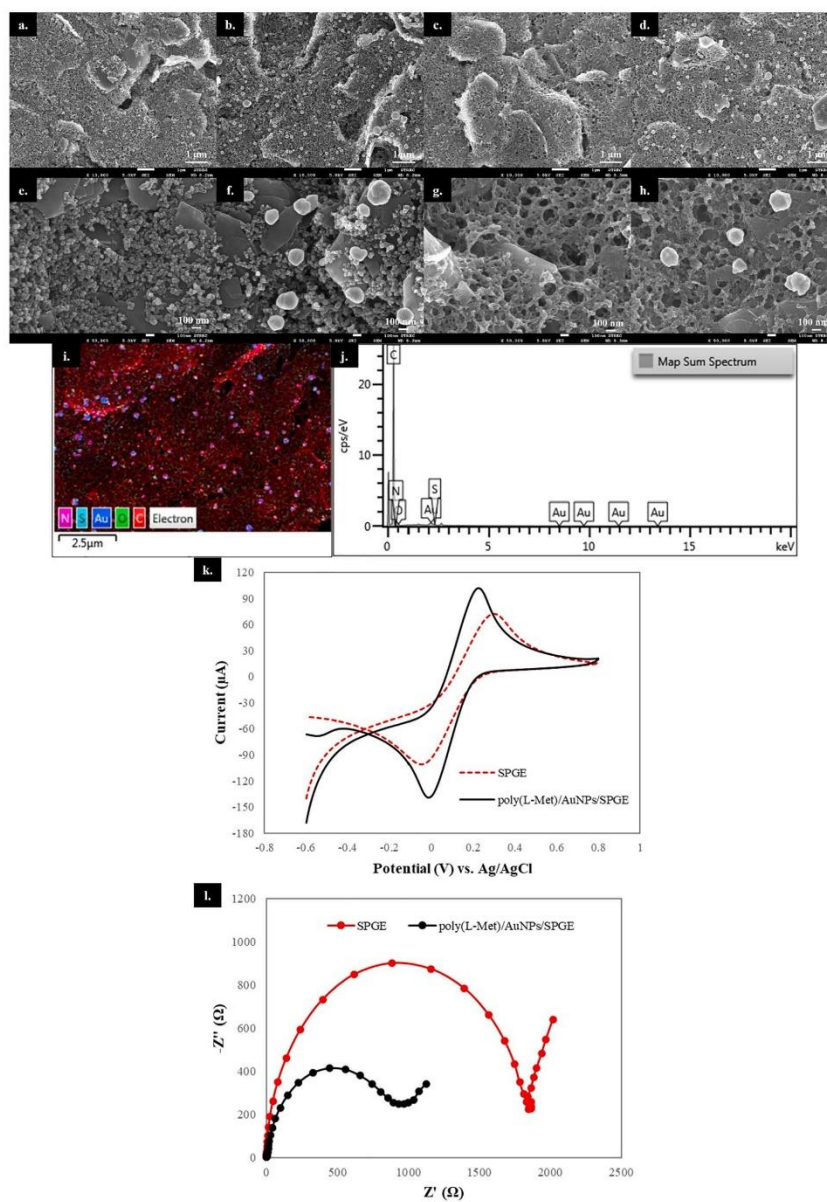


Fig. 1. SEM images of SPGE (a, e), AuNPs/SPGE (b, f), poly(L-Met)/SPGE (c, g), and poly(L-Met)/AuNPs/SPGE (d, h) at magnifications of 10,000 \times (a, b, c, d) and 50,000 \times (e, f, g, h). EDS mapping (i). Composition of poly(L-Met)/AuNPs/SPGE (j). Cyclic voltammograms of 5 mM $[\text{Fe}(\text{CN})_6]^{3-/4-}$ in 0.1 M KCl with a scan rate of 30 mV s^{-1} (k) and EIS Nyquist plots of 5 mM $[\text{Fe}(\text{CN})_6]^{3-/4-}$ in 0.1 M KCl (l) at the unmodified and modified SPGE.

electrodeposition of AuNPs at SPGE are presented in Fig. S1A. As can be seen from the figure, the resulting CV from AuNPs-modified SPGE appeared two peaks corresponding to the oxidation and reduction process of gold. Afterward, the poly(L-Met) on AuNPs/SPGE was prepared by placing L-methionine monomer, followed by electropolymerization. As presented in Fig. S1B, the oxidation peaks of L-methionine were observed around +1.7 V. For the first three cycles, the anodic peak currents gradually increased, indicating the formation and growth of the polymeric film on the electrode surface as seen previously [27]. After the fourth cycle, the increasing anodic peak current tended to be constant, suggesting that the poly(L-Met) film had increasingly grown and reached a saturation level [28]. A possible model illustrating the AuNPs electrodeposition and the electropolymerization onto the electrode surface is proposed in Scheme 2.

Electrochemical measurements

For the measurement process in this work, a 50 μ L aliquot of the standard or sample solution was dropped, covering the three-electrode area. CV was employed for the preliminary investigation of the electrochemical 8-OHDG behavior. The parameters were set in the potential range from 0.0 V to +0.3 V with a fixed scan rate of 100 mV s⁻¹. Contrarily, square wave voltammetry (SWV) was used for optimization and quantitative determination due to the benefits provided by the technique in terms of sensitivity. The affected SWV parameters were conducted in the potential range from +0.1 V to +0.5 V with a potential increment of 0.015 V, an amplitude of 0.05 V, and a frequency of 30 Hz. These SWV parameters were the optimal values that are ready to use as evidenced in Fig. S2. All experiments were conducted in triplicate at room temperature.

Electrochemical impedance spectroscopy (EIS) was performed using an Autolab electrochemical system with a potentiostat PGSTAT 204 (Utrecht, Netherlands). EIS measurements were performed in 5 mM K₃[Fe(CN)₆] containing 0.1 M KCl with a potential of 0.1 V, a frequency range from 0.1 Hz to 100 kHz, and an amplitude of 0.1 V.

Application of the proposed electrochemical sensor for the determination of 8-OHDG in real samples

Details of application in real samples are presented in material and method section of Supplementary Information (SI).

Results and discussion

Morphological characterization of the modified sensor

Surface morphologies of the unmodified and modified SPGE were characterized via scanning electron microscopy (SEM). Fig. 1 shows the SEM images of four different sensors at magnifications of 10,000 \times (a, b, c, and d) and 50,000 \times (e, f, g, and h). The unmodified SPGE (panels a and e) exhibits a rough, porous, and crumpled surface of graphene sheets. The spherical shape and size of AuNPs and their homogeneous distribution throughout the graphene sheets were observed on the SPGE surface (panels b and f) after electrodeposition of AuNPs on SPGE. Panels c and g, which exposes the surface of poly(L-Met)/SPGE following the electropolymerization sequence, shows that the surface of SPGE is covered by the polymeric thin-film layer of L-methionine caused by the formation of multiple uniformly aligned valleys of L-methionine. This morphological feature could improve the active surface area of the modified electrode [29]. Similarly, panels d and h display the surface morphology of poly(L-Met)/AuNPs-modified SPGE. It confirms that a homogeneous layer of graphene sheet is covered with well-dispersed L-methionine and AuNPs on the electrode surface.

Moreover, the surface composition was verified via energy-dispersive X-ray spectroscopy (EDS) (panels i and j). The EDS image and spectrum of the poly(L-Met)/AuNPs-modified SPGE showed the

presence of C, N, O, S, and Au atoms related to AuNPs, and the methionine molecular structure modified the electrode surface and the existence of graphene in the ink composition.

Electrochemical characterization of the poly(L-Met)/AuNPs-nanocomposite modified SPGE

To investigate the electrochemical behavior of the proposed sensor, the unmodified and modified SPGE were characterized via CV and EIS in 5 mM [Fe(CN)₆]^{3-/4-} in 0.1 M KCl. Fig. 1 in panel k presents a reversible redox peak corresponding to [Fe(CN)₆]^{3-/4-} at the unmodified and modified SPGE. At poly(L-Met)/AuNPs/SPGE, the peak potential separation (ΔE_p) decreased from +0.35 V to +0.23 V, whereas the current response increased compared with SPGE. We strongly believe that this phenomenon is a result of the synergistic effect of conductive graphene sheets, AuNPs, and a modified polymeric thin-film layer. Furthermore, the electroactive surface areas of sensors were increased from 0.096 cm² to 0.132 cm² for SPGE and poly(L-Met)/AuNPs/SPGE (Fig. S3).

EIS is a valuable and powerful method for investigating the impedance changes of the interface properties after modification of the electrode surface [30]. The EIS properties of the unmodified and modified SPGE were studied in the presence of a redox couple [Fe(CN)₆]^{3-/4-}. The semicircle diameter obtained from EIS refers to the charge transfer resistance (R_{ct}) at the electrode surface [31]. Fig. 1 in panel l illustrates Nyquist plots of 5 mM [Fe(CN)₆]^{3-/4-} containing 0.1 M KCl at SPGE and poly(L-Met)/AuNPs/SPGE. As evidenced, the diameter of the semicircle region of poly(L-Met)/AuNPs/SPGE was smaller than that of SPGE, which corresponds to the R_{ct} values (1846.4 Ω and 932.3 Ω for SPGE and poly(L-Met)/AuNPs/SPGE). These findings indicated that the composite film of poly(L-Met) and AuNPs was successfully modified on SPGE. Additionally, the electron-transfer apparent rate constant (k_{app}) of each sensor was calculated using the following equation [32]:

$$k_{app} = RT/n^2F^2AR_{ct}C$$

where R denotes the universal gas constant (8.31447 J K⁻¹ mol⁻¹); T , the absolute temperature (298 K); n , the number of electrons transferred during the redox reaction; F , Faraday's constant (96,485 C mol⁻¹); A , the surface area of the electrode (cm²); R_{ct} , the charge transfer resistance in Ω ; and C , the concentration of [Fe(CN)₆]^{3-/4-} (mol cm⁻³). The k_{app} values were found to be 3.003 $\times 10^{-4}$ cm s⁻¹ and 4.325 $\times 10^{-4}$ cm s⁻¹ for SPGE and poly(L-Met)/AuNPs/SPGE, respectively. The low R_{ct} and high k_{app} values of the modified electrode emphasized the formation of poly(L-Met)/AuNPs on SPGE that could provide excellent catalytic properties, leading to the enhancement of the electron-transfer process of redox [Fe(CN)₆]^{3-/4-}. In addition, the amount of incorporated L-methionine monomer to form the polymeric thin film was an approximate estimation by the total surface coverage of the electrode, which is calculated using the following equation [33,34]:

$$\Gamma = \frac{Q}{nFA}$$

where Γ (mol cm⁻²) denotes the surface coverage of the electrode; Q , the electric charge obtained via the integration of the oxidation peak in C; n , the number of electrons involved; F , Faraday's constant (96,485 C mol⁻¹); and A , the surface area of modified electrode in cm². By substituting the respective data in the equation, the Γ value of poly(L-Met)/AuNPs film adhering to the surface of SPGE was calculated to be 4.071 $\times 10^{-8}$ mol cm⁻². Therefore, poly(L-Met)/AuNPs/SPGE exhibited a superb property to be a good sensor on applications for the detection of target electroactive species.

Electrochemical behavior of 8-OHDG on poly(L-Met)/AuNPs/SPGE

To accomplish the utilization of the proposed sensor for 8-OHDG determination in clinical applications, the electrochemical behavior of

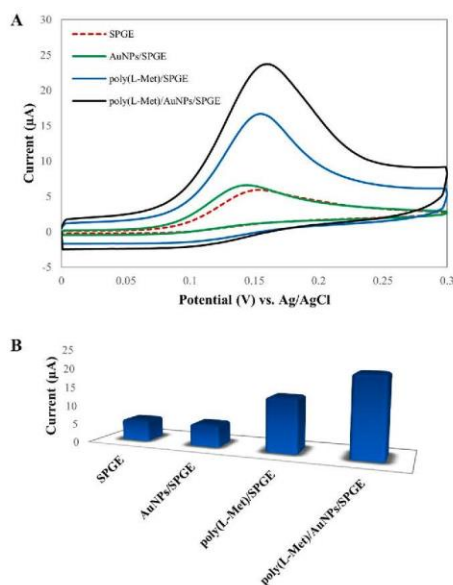


Fig. 2. Cyclic voltammograms (A) and a chart of the current intensity (B) of 100 μM 8-OHdG in 0.1 M Na-PBS (pH 7.0) at different sensors.

8-OHdG in 0.1 M Na-PBS (pH 7.0) at the unmodified and modified SPGE was investigated via CV. Fig. 2 displays cyclic voltammograms and a chart of the current intensity of 100 μM 8-OHdG compared between the use of unmodified SPGE and use of modified SPGE. On a bare SPGE (red dash line), a poor anodic peak current ($I_{pa} = 5.79 \mu\text{A}$) was observed around +0.15 V vs Ag/AgCl. The oxidation peak potential of 8-OHdG slightly shifted to the negative direction, and the anodic peak current of 8-OHdG still negligibly increased after the modification of AuNPs on SPGE (green line). This result may be concerned with the property of AuNPs, which could improve the electron-transfer kinetics of 8-OHdG at the electrode interface. Once poly(L-Met) was modified on SPGE (blue line), the anodic peak current of 8-OHdG considerably increased to 14.20 μA, which was 2.5 times higher than that obtained from bare SPGE. This suggested that the polymeric film of L-methionine could enhance the electrocatalytic capability of 8-OHdG oxidation. In addition, the anodic peak current of 8-OHdG dramatically increased in poly(L-Met)/AuNPs/SPGE (black line). The increased electrochemical signal of 8-OHdG was almost four times larger than that of the bare SPGE, resulting from the synergistic coupling effect between poly(L-Met) and AuNPs on SPGE. This combination provided a high specific surface area, enhanced electrical conductivity, and promoted electrochemical activity toward 8-OHdG detection. These results clearly indicated that poly(L-Met)/AuNPs/SPGE was an excellent electrochemical sensor for 8-OHdG detection.

Optimization of deposition for AuNPs and L-methionine

To achieve optimal conditions for 8-OHdG detection, the main parameters dealing with the formation of film on the electrode surface were investigated. The studied parameters included the concentration of standard gold and L-methionine solutions, the number of cycles for gold and L-methionine deposition, and the scan rate for gold and L-methionine deposition. These parameters are involved in the control of the AuNPs amount and film thickness on the electrode surface, which could

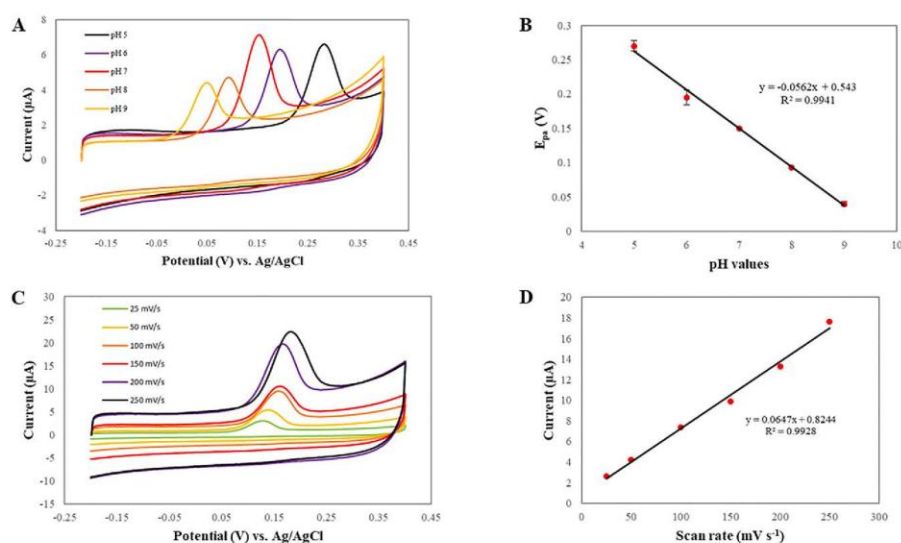


Fig. 3. Cyclic voltammograms of 10 μM 8-OHdG at the poly(L-Met)/AuNPs/SPGE using various pH values (A) and the plot of E_{pa} vs. pH values (B). Cyclic voltammograms of 10 μM 8-OHdG in 0.1 M Na-PBS (pH 7.0) at the poly(L-Met)/AuNPs/SPGE with different scan rates (C) and the plot of I_{pa} vs. scan rate (D).

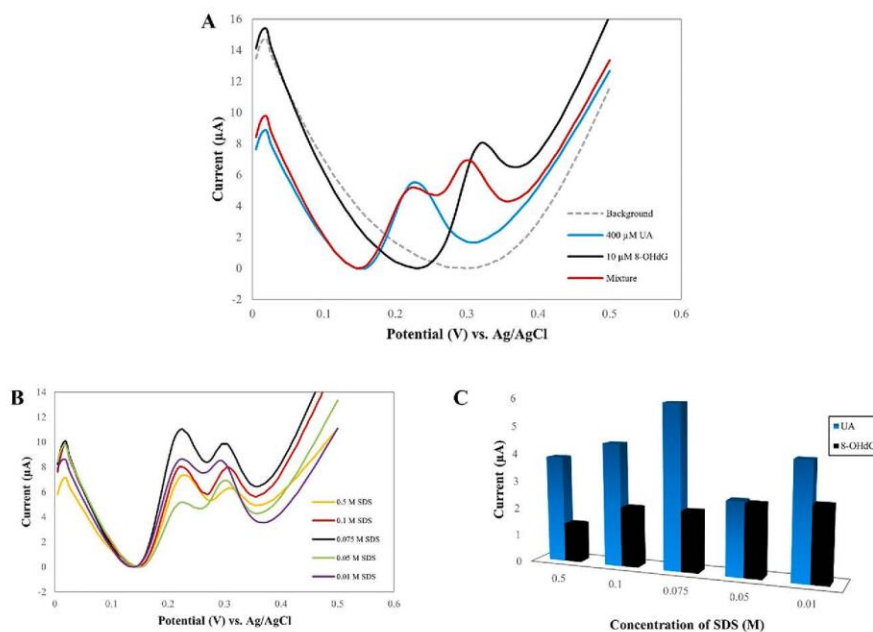


Fig. 4. Square wave voltammograms of 10 μM 8-OHdG and 400 μM UA in 0.05 M SDS containing 0.1 M NaCl in 0.1 M Na-PBS (pH 7.0) (A), the effect of the SDS concentration (B), and a chart of the current intensity of 8-OHdG and UA detection (C).

directly affect the transferred electrons at the electrode interface. From the results in Fig. S4, the optimal values are the concentration of standard gold solution of 1000 ppm, the number of cycles at 7 cycles, the scan rate of 150 mV s^{-1} , the concentration of L-methionine solution of 2 mM, the number of cycles at 10 cycles, and the scan rate of 100 mV s^{-1} .

Influence of pH values and scan rates

Adjustment of the pH values of supporting electrolyte significantly affects the oxidative behavior and peak appearance of 8-OHdG. Besides, it can provide information on the number of electrons and protons involved in the electrochemical process of 8-OHdG that occurred at the developed sensor. As shown in Fig. 3A, pH 7.0 was selected as the optimal for further experiments as it provided the highest current at a low oxidative potential. Also, as exhibited in Fig. 3B, the slope of $-0.0562 \text{ V pH}^{-1}$ was close to the Nernstian theoretical value of -0.059 V pH^{-1} [35]. Therefore, the number of protons and electrons in the electrochemical process of 8-OHdG was equal.

To clarify whether the mass transfer process of the analyte at the electrode surface is adsorption or diffusion controlled, the effect of the scan rate on the electrooxidation of 8-OHdG was studied by CV (Fig. 3C). From the linear regression equation between the anodic peak current (I_{pa}) and the scan rate (v) in Fig. 3D, it demonstrated that the mass transfer process at the electrode surface was controlled by adsorption-limited. In addition, a linear relationship between the log of current and the log of scan rate was plotted to confirm the result. From the linear regression equation, $y = -0.741 + 0.8121 \log v$ ($R^2 = 0.9929$), the slope value was close to 1, which is supposed to be surface adsorption [36].

To calculate the number of electrons (n), the linear regression equation between the anodic peak potential (E_{pa}) and the logarithm of

scan rate ($\ln v$) and Laviron's equation was used and found that the number of electrons (n) was calculated to be 2. Therefore, it could be concluded that the electrochemical mechanism of 8-OHdG on poly(L-Met)/AuNPs/SPGE involved two electrons and two protons, which is in agreement with previous reports [35,37,38].

Interference study

To estimate the selectivity of the newly proposed electrochemical platform, the effects of interference, comprising uric acid (UA), dopamine (DA), ascorbic acid (AA), citric acid (CA), bovine serum albumin (BSA), and glucose (Glu), which commonly coexist with 8-OHdG in biological fluids, were examined. In addition, the effects of some ions, including Na^+ , K^+ , Ca^{2+} , Mg^{2+} , Cu^{2+} , and Zn^{2+} , on 8-OHdG detection were investigated. Fig. S5 describes the current response of 10 μM 8-OHdG in the presence of 20 μM UA, 40 μM DA, 100 μM AA, 100 μM CA, 500 μM BSA, 500 μM Glu, 1 mM Na^+ , 1 mM K^+ , 1 mM Ca^{2+} , 1 mM Mg^{2+} , 1 mM Cu^{2+} , and 1 mM Zn^{2+} . From the results, it was found that there was no significant change in the current signal of 8-OHdG in the presence of interference.

However, the major limitation for the analysis of 8-OHdG in biological fluids, especially in urine, is the effect exerted by UA. Fig. S6 reveals the square wave voltammograms of 8-OHdG and UA detected by a developed sensor. As can be seen from Fig. S6A, an individual study of standard solution, UA and 8-OHdG appeared at +0.04 and +0.13 V, respectively. Surprisingly, when 20 μM UA was added to 10 μM 8-OHdG, a small shoulder peak appeared near the oxidation peak potential of 8-OHdG (Fig. S6B). Nonetheless, the physiological normal level of UA in human urine is 400 μM [39]. Therefore, the concentration of UA at 400 μM absolutely interfered with the detection of 8-OHdG. The effect of

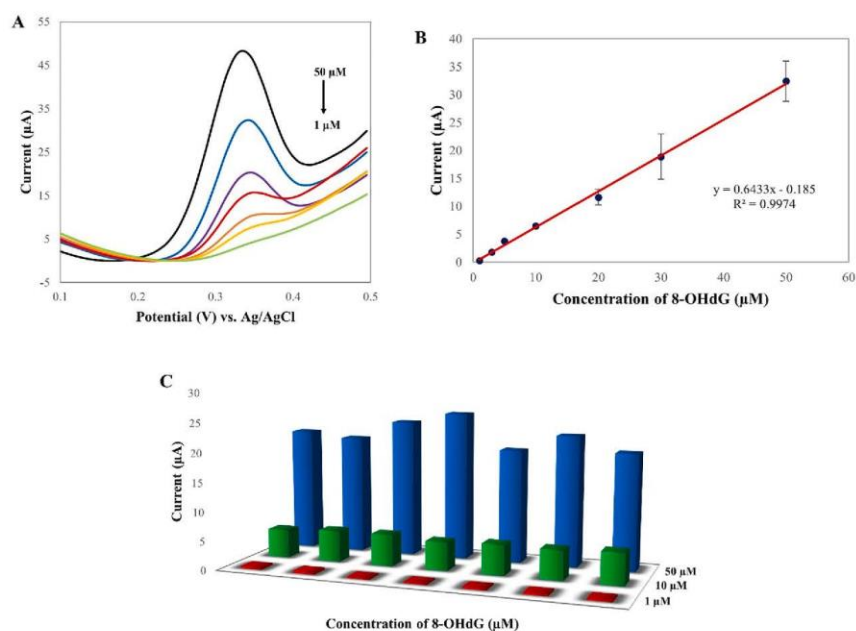


Fig. 5. Square wave voltammograms showing the electrochemical oxidation of 8-OHdG in 0.05 M SDS containing 0.1 M NaCl in 0.1 M Na-PBS (pH 7.0) at various concentrations on poly(L-Met)/AuNPs/SPGE (A). The calibration curve between the anodic peak current and the concentration of 8-OHdG (B). A chart of the current intensity of reproducibility studies at three concentrations (C).

chloride content in urine samples is also important. In a normal person's urine, the average concentration of chloride ions is 0.1 M [40]. Fig. S7 presents the square wave voltammograms of 8-OHdG containing various concentrations of NaCl in 0.1 M Na-PBS (pH 7.0). It demonstrated that there are no significant changes in the current signal of 8-OHdG. Nevertheless, the oxidation peak potentials of 8-OHdG shifted to the positive direction with increasing concentrations of chloride ions. This phenomenon could be concluded that the saturated solution of chloride affected the mass-transfer process at the electrode surface toward 8-OHdG detection. Hence, the determination of 8-OHdG containing the co-existence of UA and chloride ions in biological samples is a crucial concern that must be resolved.

Detection of a mixture of 8-OHdG and UA

To resolve the aforementioned problem, we aimed to use sodium dodecyl sulfate (SDS) containing 0.1 M NaCl in 0.1 M Na-PBS (pH 7.0) as the supporting electrolyte for 8-OHdG detection in the presence of UA at a high level. As evidenced in Fig. 4A, the oxidation peak potentials of individual 400 μM UA and 10 μM 8-OHdG were noticed at + 0.23 V (blue line) and + 0.32 V (black line). To confirm the expected result, a mixture of 400 μM UA and 10 μM 8-OHdG was added to the supporting electrolyte. As observed in the red line, the oxidation peaks of these compounds clearly separated at different peak potentials because SDS is an anionic surfactant that can block the diffusion rate of UA to the electrode surface, causing a difference in the rate of mass transfer from 8-OHdG. These results indicated that the use of saturated chloride in Na-PBS containing SDS as the supporting electrolyte greatly enhanced the selectivity of the proposed method and improved the possibility of 8-

OHDG determination in real biological fluid samples.

From the preliminary test, we strongly believe that the SDS concentration may affect the separation. Therefore, the effect of the SDS concentration was systematically studied for a mixture of 10 μM 8-OHdG and 400 μM UA. As evidenced in Fig. 4B and 4C, 0.05 M of SDS could obviously separate the oxidation peaks of 8-OHdG and UA and provide the highest current of 8-OHdG while strongly suppressing the response of UA. In addition, the resolution value between the oxidation peak potentials of 8-OHdG and UA was remarkably close to one. Thus, 0.05 M of the SDS concentration was selected as the suitable concentration for the preparation of the supporting electrolyte to detect 8-OHdG in real samples.

Analytical performance

To verify the analytical performance of the proposed method, the detection of 8-OHdG in various concentrations at poly(L-Met)/AuNPs/SPGE was evaluated via SWV. Under optimum conditions, the square wave voltammograms of the electrochemical oxidation of 8-OHdG at various concentrations are presented in Fig. 5A, and the linear regression equation obtained from the calibration curve is demonstrated in Fig. 5B. The limit of detection ($LOD = 3SD/Slope$) and limit of quantification ($LOQ = 10SD/Slope$) were found to be 92 and 306 nM, respectively. In addition, a comparison of the analytical performance between this proposed method and previous methods for 8-OHdG detection is summarized in Table S1. Although the analytical performance of some previous works offered a lower limit of detection compared with our method, there was no report on selectivity, particularly UA and chloride ions, at normal levels in humans, which affected

Table 1

Results obtained from the determination of 8-OHdG in artificial urine, healthy human urine, and human serum samples using poly(L-Met)/AuNPs/SPGE (n = 3).

Samples	Added (μM)	Found (μM)	Recovery (%)	RSD (%)
Artificial urine 1	5	4.79	95.73	3.85
	10	10.76	107.60	3.55
	50	49.08	98.16	9.29
Artificial urine 2	5	5.03	100.60	8.53
	10	9.53	95.27	3.11
	50	45.53	91.05	1.68
Artificial urine 3	5	4.51	90.19	14.36
	10	10.88	108.83	12.76
	50	46.67	93.33	6.40
Human urine 1	5	5.45	109.01	5.93
	10	10.61	106.12	7.01
	50	53.72	107.45	8.24
Human urine 2	5	4.76	95.16	3.80
	10	10.20	101.98	11.73
	50	51.05	102.10	0.51
Human urine 3	5	5.43	108.66	0.81
	10	10.22	102.20	7.00
	50	51.36	102.72	7.24
Human serum 1	5	4.83	96.50	2.30
	10	10.06	100.56	4.74
	50	48.09	96.17	8.99
Human serum 2	5	4.95	99.07	8.81
	10	10.97	109.73	0.59
	50	47.90	95.81	6.19
Human serum 3	5	5.43	108.59	6.36
	10	10.36	103.64	12.59
	50	50.07	100.15	2.20

the determination of 8-OHdG in real samples. Furthermore, we first proposed the use of poly(L-Met)/AuNPs/SPGE as a sensor for 8-OHdG detection without enzymatic catalysts to reduce the interference of UA in biological fluid samples. Our developed methodology not only provided high selectivity in the detection but also had sufficiently high potential for use in the determination of 8-OHdG in biological fluid samples.

The precision of the analytical performance by examining the relative standard deviation (RSD) for seven repetitive measurements of 8-OHdG solution was investigated. For the measurement, three concentrations (1, 10, and 50 μM) concerning the probable range in interesting samples were assessed for the reproducibility of the proposed sensor. As presented in Fig. 5C, the RSD values were lower than 18%, which could be acceptable by AOAC guidelines [41]. For stability test, poly(L-Met)/AuNPs/SPGE was stored at 4 $^{\circ}\text{C}$ for 20 days, and the anodic peak current of 10 μM 8-OHdG still remained at 80.32%, suggesting that this proposed sensor could be favorably employed for 8-OHdG analysis with excellent reproducibility and good stability.

Analytical application in real samples

To evaluate the applicability of this proposed method, quantitative determination of 8-OHdG was executed in artificial urine, healthy human urine, and human serum samples. For accuracy and precision, the percentages of recovery and RSD were estimated by spiking a known standard solution of 8-OHdG, and a standard addition method was used to prevent the matrix effect [42]. As shown in Table 1, the recovery and RSD values were found in the range of 90.19%–109.73% and 0.51%–14.36%, which could be acceptable by the AOAC guidelines [41]. These results indicated that this approach was acceptable and reliable for the determination of 8-OHdG in real samples. Thereby, poly(L-Met)/AuNPs/SPGE exhibited good accuracy and precision and could be used as an alternative choice for quantitative analysis of 8-OHdG in

biological fluid samples.

Conclusion

An electrochemical sensing platform for 8-OHdG detection based on assembled layers of poly(L-methionine) and AuNPs-modified SPGE was successfully fabricated. The synergistic coupling effect of poly(L-methionine), AuNPs, and graphene can improve the specific surface area, enhance electrical conductivity, and promote the electrochemical activity of 8-OHdG. Under optimal conditions, the detection of 8-OHdG was achieved in the range of 1–50 μM with the limit of detection of 92 nM. Moreover, no enzymatic catalyst usability is needed to reduce interfering UA before analysis, leading to saving analysis cost. The main advantages of this developed sensor that is superior to that in previous reports are the simple steps for fabrication, small size, disposability, portability, and requirement of a small sample volume. Hence, this proposed method could be suitable as an alternative method for screening 8-OHdG in early diagnosis for risk assessment of their level in the human body.

CRedit authorship contribution statement

Jeerakit Thangphathananarungruang: Conceptualization, Methodology, Validation, Investigation, Formal analysis, Writing – original draft, Visualization. **Chuleekom Chotsuwan:** Resources, Funding acquisition. **Sakda Jampasa:** Validation, Formal analysis, Writing – review & editing. **Weena Siangproh:** Conceptualization, Investigation, Resources, Writing – review & editing, Supervision, Project administration.

Declaration of Competing Interest

The authors declare that they have no known competing financial interest or personal relationship that could have appeared to influence the work reported in this paper.

Acknowledgments

JT would like to acknowledge the financial support from the Thailand Graduate Institute of Science and Technology (TGIST) (SCA-CO-2562-9695-TH). WS would like to acknowledge the financial support from the National Research Council of Thailand (NRCT) and Srinakharinwirot University through Research Grants for Talented Mid-Career Researchers (N41A640098). The authors would like to thank Enago (www.enago.com) for the English language review.

Appendix A. Supplementary data

Supplementary data to this article can be found online at <https://doi.org/10.1016/j.flatc.2022.100335>.

References

- [1] H. Chang, X. Wang, K.-K. Shin, Y. Zhu, J. Wang, Q. Li, B. Chen, H. Jiang, Layer-by-layer assembly of graphene, Au and poly(toluidine blue O) films sensor for evaluation of oxidative stress of tumor cells elicited by hydrogen peroxide, *Biosens. Bioelectron.* 41 (2013) 789–794.
- [2] S. Manavalan, U. Rajaji, S.-M. Chen, S. Steplán, P. Paul Selvin, M. Govindasamy, T.-W. Chen, M. Ajmal Ali, F.M.A. Al-Hemaid, M.S. Bshikh, Determination of 8-hydroxy-2'-deoxyguanosine oxidative stress biomarker using dysprosium oxide nanoparticles/reduced graphene oxide, *Inorg. Chem. Front.* 5 (11) (2018) 2885–2892.
- [3] P. Gupta, M. Oyama, R.H. Goyal, Electrochemical investigations of 8-hydroxy-deoxyguanosine and its determination at edge plane pyrolytic graphite electrode, *RSC Adv.* 6 (2016) 1722–1728.
- [4] G.V. Martins, A.C. Marques, E. Fortunato, M.G.F. Sales, 8-hydroxy-2'-deoxyguanosine (8-OHdG) biomarker detection down to picomolar level on a plastic antibody film, *Biosens. Bioelectron.* 86 (2016) 225–234.
- [5] R.-H. Zhao, L.-P. Jia, Z. Feng, R.-H. Ma, W. Zhang, L. Shang, Q.-W. Xue, H.-S. Wang, Ultrasensitive electrochemiluminescence aptasensor for 8-hydroxy-2'-

- deoxyguanosine detection based on target-induced multi-DNA release and nicking enzyme amplification strategy, *Biosens. Bioelectron.* 144 (2019) 111669.
- [6] L.-P. Jia, J.-F. Liu, H.-S. Wang, Electrochemical performance and detection of 8-Hydroxy-2'-deoxyguanosine at single-stranded DNA functionalized graphene modified glassy carbon electrode, *Biosens. Bioelectron.* 67 (2015) 139–145.
- [7] R.C. Gupta, J.M. Arif, An improved 32P-postlabelling assay for the sensitive detection of 8-oxodexyguanosine in tissue DNA, *Chem. Res. Toxicol.* 14 (8) (2001) 951–957.
- [8] I. Mamatouk, N. Bouaicha, M.J. Plessis, F. Périn, Detection by 32P-post labelling of 8-oxo-7,8-dihydro-2'-deoxyguanosine in DNA as biomarker of microcystin-LR- and nodularin-induced DNA damage in vitro in primary cultured rat hepatocytes and in vivo in rat liver, *Mutat. Res.* 564 (1) (2004) 9–20.
- [9] P. Rosner, V. Mistry, R. Singh, R.J. Sram, M.S. Cooke, Urinary 8-oxo-7,8-dihydro-2'-deoxyguanosine values determined by a modified ELISA improves agreement with HPLC-MS/MS, *Biochem. Biophys. Res. Commun.* 440 (4) (2013) 725–730.
- [10] C.-W. Hu, M.-T. Wu, M.-R. Chao, C.-H. Pan, C.-J. Wang, J.A. Swenberg, K.-Y. Wu, Comparison of analyses of urinary 8-hydroxy-2'-deoxyguanosine by isotopically dilution liquid chromatography with electrospray tandem mass spectrometry and by enzyme-linked immunosorbent assay, *Rapid Commun. Mass Spectrom.* 18 (4) (2004) 505–510.
- [11] S. Koide, Y. Kinoshita, H. Ito, J. Kimura, K. Yokoyama, I. Karube, Determination of human serum 8-hydroxy-2'-deoxyguanosine (8-OHdG) by HPLC-ED combined with solid phase extraction (SPE), *J. Chromatogr. B* 878 (23) (2010) 2163–2167.
- [12] G. Saravanabhavan, E. Bais, R. Vincent, P. Kamarathasan, A high performance liquid chromatography-electrochemical array method for the measurement of oxidative/nitrative changes in human urine, *J. Chromatogr. A* 1217 (19) (2010) 3269–3274.
- [13] S. Mei, G. Xu, J. Xing, C. Wu, Method for the analysis of 8-hydroxy-2'-deoxyguanosine in urine by gas chromatography, *Anal. Sci.* 17 (6) (2001) 779–781.
- [14] H.-S. Lin, A.M. Jenner, C.N. Ong, S.H. Huang, M. Whiteman, B. Halliwell, A high-throughput and sensitive methodology for the quantification of urinary 8-hydroxy-2'-deoxyguanosine: measurement with gas chromatography-mass spectrometry after single solid-phase extraction, *Biochem. J.* 380 (2004) 541–548.
- [15] X. Meng, Q. Liu, Y. Ding, Paper-based solid-phase microextraction for analysis of 8-hydroxy-2'-deoxyguanosine in urine sample by CE-LIF, *Electrophoresis* 38 (3–4) (2017) 494–500.
- [16] Y. Liu, M. Wei, L. Zhang, Y. Zhang, W. Wei, L. Yin, Y. Pu, S. Liu, Chitosanomic assemblies of gold nanoparticles for ultrasensitive detection of 8-hydroxy-2'-deoxyguanosine in human serum sample, *Anal. Chem.* 88 (12) (2016) 6509–6514.
- [17] J. Hao, K. Wu, C. Wan, Y. Tang, Reduced graphene oxide-ZnO nanocomposite based electrochemical sensor for sensitive and selective monitoring of 8-hydroxy-2'-deoxyguanosine, *Talanta* 185 (2018) 550–556.
- [18] Z. Yi, J. Qiao, Y. Wang, K. Gao, R. Zhao, X. Meng, Electrochemical sensor platform for 8-hydroxy-2'-deoxyguanosine detection based on carboxyl-functionalized carbon-allotrope nanomaterials wrapped gold nanoparticles modified electrode, *Int. J. Electrochem. Sci.* 14 (2019) 9098–9111.
- [19] G. Cao, C. Wu, Y. Tang, C. Wan, Ultrasmall HKUST-1 nanoparticles decorated graphite nanosheets for highly sensitive electrochemical sensing of DNA damage biomarker 8-hydroxy-2'-deoxyguanosine, *Anal. Chim. Acta* 1058 (2019) 80–88.
- [20] M. Li, Y.-T. Li, D.-W. Li, Y.-T. Long, Recent developments and applications of screen-printed electrodes in environmental assays—a review, *Anal. Chim. Acta* 734 (2012) 31–44.
- [21] J. Thangphathanarungruang, A. Ngamrueonchote, R. Laocharoenusk, C. Chotsuwan, W. Siangproh, A novel electrochemical sensor for the simultaneous determination of fat-soluble vitamins using a screen-printed graphene/nafion electrode, *Key Eng. Mater.* 777 (2018) 597–601.
- [22] J. Thangphathanarungruang, A. Yakoh, R. Laocharoenusk, C. Chotsuwan, O. Chailapakul, W. Siangproh, High-efficient of graphene nanocomposite application to rapidly simultaneous identification and quantitation of fat-soluble vitamins in different matrix samples, *J. Electroanal. Chem.* 873 (2020), 114361.
- [23] P. Nakthong, T. Kondo, O. Chailapakul, W. Siangproh, Development of an unmodified screen-printed graphene electrode for nonenzymatic histamine detection, *Anal. Methods* 12 (44) (2020) 5407–5414.
- [24] J. He, Z. Song, S. Zhang, L. Wang, Y. Zhang, R. Qiu, Methionine – Au nanoparticle modified glassy carbon electrode: a novel platform for electrochemical detection of hydroquinone, *Mater. Sci.* 20 (4) (2014) 381–386.
- [25] T. Lucezak, Comparison of electrochemical oxidation of epinephrine in the presence of interfering ascorbic and uric acids on gold electrodes modified with S-functionalized compounds and gold nanoparticles, *Electrochim. Acta* 54 (24) (2009) 5863–5870.
- [26] A. Bervili, A. Delghani-Frouzabadi, M. Mozroum-Ardakani, B. B. Mirjalili, R. Zare, Electrochemical deposition of gold nanoparticles on reduced graphene oxide modified glassy carbon electrode for simultaneous determination of levodopa, uric acid and folic acid, *J. Electroanal. Chem.* 736 (2015) 22–29.
- [27] P.S. Ganesh, B.E.K. Swamy, Simultaneous electroanalysis of norepinephrine, ascorbic acid and uric acid using poly(glutamic acid) modified carbon paste electrode, *J. Electroanal. Chem.* 752 (2015) 17–24.
- [28] J. Li, X. Zhang, Fabrication of poly(aspartic acid)/nanogold modified electrode and its application for simultaneous determination of dopamine, ascorbic acid, and uric acid, *Am. J. Anal. Chem.* 03 (03) (2012) 195–203.
- [29] P.S. Ganesh, B.E.K. Swamy, K.V. Harisha, Electropolymerisation of DL-methionine at carbon paste electrode and its application to the determination of catechol and hydroquinone, *Anal. Bioanal. Electrochem.* 9 (2017) 47–64.
- [30] E. Katz, I. Willner, Probing biomolecular interactions at conductive and semiconductive surfaces by impedance spectroscopy: routes to impedimetric immunosensors, DNA-sensors, and enzyme biosensors, *Electroanalysis* 15 (11) (2003) 913–947.
- [31] R. Ojani, J.-B. Raoof, A.A. Maleki, S. Safshekan, Simultaneous and sensitive detection of dopamine and uric acid using a poly(L-methionine)/gold nanoparticle-modified glassy carbon electrode, *Chinese J. Catal.* 35 (3) (2014) 423–429.
- [32] L.A.D. Guegous, F. Pogacean, S. Kurbanoglu, L.B. Tudoran, A.B. Serban, I. Kacsó, S. Pruneanu, Graphene-gold nanoparticles nanozyme-based electrochemical sensor with enhanced lacase-like activity for determination of phenolic substrates, *J. Electrochem. Soc.* 168 (2021), 067523.
- [33] P.A. Pushpanjali, J.G. Manjunatha, M.T. Scinivas, Highly sensitive platform utilizing poly(L-methionine) layered carbon nanotube paste sensor for the determination of voltaren, *FlatChem* 24 (2020), 100207.
- [34] H. Razmi, M. Haras, Voltammetric behavior and amperometric determination of ascorbic acid at cadmium pentacyanomethylferrate film modified GC electrode, *Int. J. Electrochem. Sci.* 3 (2008) 82–95.
- [35] Z. Guo, X. Liu, Y. Liu, G. Wu, X. Lu, Constructing a novel 8-hydroxy-2'-deoxyguanosine electrochemical sensor and application in evaluating the oxidative damages of DNA and guanine, *Biosens. Bioelectron.* 86 (2016) 671–676.
- [36] J. David, K. Gosser, *Cyclic Voltammetry: Simulation and Analysis of Reaction Mechanisms*, 1st ed., Wiley-VCH, 1993.
- [37] N. Kumar, Rosy, R.M. Goyal, A melamine based molecularly imprinted sensor for the determination of 8-hydroxydeoxyguanosine in human urine, *Talanta* 166 (2017) 215–222.
- [38] Tianyi Shang, Peilin Wang, Xinhui Liu, Xuechun Jiang, Zhongqi Hu, Xiaoquan Lu, Facile synthesis of porous single-walled carbon nanotube for sensitive detection of 8-Hydroxy-2'-deoxyguanosine, *J. Electroanal. Chem.* 808 (2018) 28–34.
- [39] M.Z.H. Khan, Xiaojiang Liu, Yunfei Tang, Xinhua Liu, Ultra-sensitive electrochemical detection of oxidative stress biomarker 8-hydroxy-2'-deoxyguanosine with poly(L-arginine)/graphene wrapped Au nanoparticles modified electrode, *Biosens. Bioelectron.* 117 (2018) 508–514.
- [40] Weena Siangproh, Norio Teshima, Tadao Sakai, Shuji Katoh, Orawon Chailapakul, Alternative method for measurement of albumin/creatinine ratio using spectrophotometric sequential injection analysis, *Talanta* 79 (4) (2009) 1111–1117.
- [41] G.W. Latimer, *Official methods of analysis of AOAC international*, 20th ed., AOAC International, 2016.
- [42] Jeerakit Thangphathanarungruang, Atchara Lomae, Orawon Chailapakul, Sudkate Chaiyo, Weena Siangproh, A low-cost paper-based diamond electrode for trace copper analysis at on-site environmental area, *Electroanalysis* 33 (1) (2021) 226–232.

Appendix 2

Talanta 253 (2023) 123929



Contents lists available at ScienceDirect

Talanta

journal homepage: www.elsevier.com/locate/talanta

A novel and easy-to-construct polymeric L-glutamic acid-modified sensor for urinary 1-hydroxypyrene detection: Human biomonitoring of polycyclic aromatic hydrocarbons exposure

Jeerakit Thangphatthanarungruang^a, Chuleekorn Chotsuwan^b, Weena Siangproh^{a,*}^a Department of Chemistry, Faculty of Science, Srinakharinwirot University, Sukhumvit 23, Wattana, Bangkok, 10110, Thailand^b Nanohybrids for Industrial Solutions Research Team, National Nanotechnology Center, National Science and Technology Development Agency, Khlong Nueng, Khlong Luang, Pathumthani, 12120, Thailand

ARTICLE INFO

Keywords:

Polycyclic aromatic hydrocarbons
1-Hydroxypyrene
Poly(L-glutamic acid)
Screen printed graphene electrode
Electrochemical sensor

ABSTRACT

1-Hydroxypyrene (1-OHP), a metabolite of polycyclic aromatic hydrocarbons (PAHs), is a frequently used biomarker for assessing human exposure to PAHs. Therefore, the technology that provides a quick, simple, cost-effective, portable, accurate, precise, and reliable test is still in great demand. To the best of our knowledge, the creation of an electrochemical device based on poly(L-glutamic acid)-modified a screen-printed graphene electrode (poly(L-GA)/SPGE) for 1-OHP detection was described for the first time. The developed sensor was simply and rapidly manufactured via only a single step of electropolymerization. All the concerned parameters and electroanalytical conditions were studied to obtain the best performance of the methodology. Under optimal conditions, the 1-OHP sensing provided a linear range of 1–1000 nM with the limits of detection and quantification of 0.95 and 3.16 nM, respectively. Moreover, this developed sensor was successfully utilized by determining 1-OHP in human urine samples. In comparison with conventional methods, this newly proposed electrochemical methodology might be tremendously valuable for 1-OHP evaluation in environmental and occupational applications, leading to the early detection of illness risk linked to PAHs in the human body.

1. Introduction

Polycyclic aromatic hydrocarbons (PAHs) are a class of organic chemical compounds that contain two or more fused benzene rings arranged in their structure [1]. PAHs are harmful environmental and dietary contaminants [2] that are typically formed during the incomplete combustion or pyrolysis of organic substances. The combustion of engines or various fuels in industrial plants, including coal and crude oil processing, petroleum refineries, gasoline stations, tire and rubber industries, and vehicle traffic, is the primary source of PAHs [3]. Moreover, they can be found in cooking processes. In our daily life, we are exposed to PAHs all the time through many routes, for example, inhalation, ingestion, and skin contact. However, there has been considerable concern about the toxicity of PAHs because they can damage or destroy proteins and DNA within a cell, leading to carcinogenic, teratogenic, and mutagenic effects [4], developing malformations, cardiovascular disease, deterioration of pulmonary function, obesity, and neurodevelopmental issues [5]. Therefore, monitoring PAH content in

the environment and workplace is becoming increasingly important for assessing the working population and environmental health risks.

Among various biomarkers for PAH assessing, 1-hydroxypyrene (1-OHP) is a well-studied target for PAH metabolites. Furthermore, 1-OHP is a useful biomarker and a trustworthy indicator to evaluate human PAH exposure in a variety of investigations, notably in environmental and occupational health. Generally, 1-OHP can be detected in urine because pyrene is absorbed through the gastrointestinal system, lungs, and/or skin and then converted to 1-OHP, which is eliminated in urine [6]. According to the American Conference of Governmental Industrial Hygienists, the biological monitoring benchmark for urinary 1-OHP is $1.0 \mu\text{g L}^{-1}$ [3]. Therefore, the invention of a simple, sensitive, and selective approach to monitor the amount of 1-OHP in urine is meaningful and of considerable significance.

Previously, several analytical methods using chromatographic and spectroscopic analysis were reported for determining 1-OHP in many applications [7–10]. Although these methods showed high accuracy and precision, regrettably, they still required tedious sample preparation,

* Corresponding author.

E-mail addresses: wecna@g.swu.ac.th, wecnasi@hotmail.com (W. Siangproh).<https://doi.org/10.1016/j.talanta.2022.123929>

Received 18 June 2022; Received in revised form 2 September 2022; Accepted 6 September 2022

Available online 9 September 2022

0039-9140/© 2022 Elsevier B.V. All rights reserved.

sophisticated and expensive instruments, time-consuming process, the need for a high solvent/sample volume, and analyst expertise. Consequently, these methods were restricted to routine, on-site, and real-time analysis. Alternatively, the electroanalytical method is a promising and attractive method to circumvent the aforementioned limitations due to its simplicity, short analysis time, inexpensive instruments, high accuracy and precision, and portability. In the past, various electrochemical methods were reported for 1-OHP quantitative determination (see Table S1). Nonetheless, there were still drawbacks with respect to the use of supporting electrolytes due to their inappropriate pH range for 1-OHP detection. Furthermore, the use of a glassy carbon electrode as the working electrode was seldom proper because of its early processing, high cost, and the need for a high solvent/sample volume. Additionally, the use of the modifiers to improve the sensitivity might be ineffective because certain works required multiple steps for electrode modification, the use of an expensive modifier, and a lengthy modification time. Therefore, the development of an electrochemical approach is still required to overcome the aforementioned constraints.

Currently, screen-printed electrodes (SPEs) can be easily and rapidly fabricated by the screen-printing method. For the material used in SPE fabrication, graphene ink is extensively used for electrochemical sensing applications because of its excellent electrical conductivity, large surface area, fast electron transport, good mechanical strength, and charge carriers with high mobility [11,12]. To achieve the best performance in terms of sensitivity and selectivity, modification of the electrode surface can be applied by using a variety of modifiers. Recently, amino acids are widely employed as polymer-modified electrodes due to their practical advantages, such as simplicity and rapidity of manufacturing, non-toxicity, inexpensiveness, high stability, and good biocompatibility [13,14]. Remarkably, they have various properties in electrochemical detection, for example, enhancing the electrocatalytic activity, promoting the electron-transfer rate, decreasing electrode surface fouling, providing reproducibility of the electrode response, and improving the electrode surface area [15,16]. In recent years, many publications have been reported for the modification of the electrode surface by employing various amino acids [17–20]. Poly(L-glutamic acid) (poly(L-GA)) is one of the amino acid polymers that can be easily synthesized via electropolymerization. The thin films of poly(L-GA) on the electrode surface directly generated by electrooxidation of their monomers are commonly used to facilitate the electron-transfer process at the electrode-solution interface for the determination of target analyte. Thus, a poly(L-GA) modified screen-printed graphene electrode (SPGE) could be employed as an electrochemical sensor to enhance the electrochemical capabilities for 1-OHP sensing.

Owing to the benefits of the materials mentioned, herein, we decided to develop an electrochemical sensor based on a poly(L-GA) modified SPGE for the detection of trace 1-OHP. Remarkably, the highlight of this work is the use of only one modifier for the surface modification of the electrode via only a single step of electropolymerization. Moreover, the types of supporting electrolytes were cautiously investigated to obtain a suitable and dependable pH range. All the concerned parameters were systematically studied as well. A disposable polymeric thin film modified SPGE could be applied to determine 1-OHP levels in biological fluid samples.

2. Materials and methods

2.1. Chemicals, materials, and apparatuses

Details of chemicals, materials, and apparatuses are revealed in the Supplementary Information (SI).

2.2. Fabrication of conductive polymer thin film modified SPGE

The design and manufacturing procedures of SPGE are explained in SI. The conductive polymer thin film layer modified SPGE was prepared

by electropolymerization of L-GA via CV. The procedure of SPGE modification was performed by dropping 100 μL of 30 mM L-GA solution in 0.1 M Na-PBS (pH 7.0) onto the surface of SPGE and scanning the potential range from -0.8 V to $+1.7$ V for 5 cycles at a scan rate of 100 mV s^{-1} . Then, the sensor was carefully cleaned with deionized water before being air-dried. Cyclic voltammograms for the electropolymerization of L-GA at SPGE are depicted in Fig. S1. A probable model demonstrating the electropolymerization of poly(L-GA) on the SPGE surface is presented in Scheme 1.

2.3. Electrochemical measurements

100 μL of 1-OHP standard solution was dropped onto the three-electrode system of poly(L-GA)/SPGE. CV was employed for characterization of the electrochemical properties of 1-OHP at the proposed electrode in the potential range from -0.6 V to $+0.8$ V at a scan rate of 100 mV s^{-1} . SWV was used for optimization and quantitative determination of 1-OHP with scanning the potential range from -0.4 V to $+0.3$ V. The optimal SWV parameters were a potential increment of 0.008 V, an amplitude of 0.1 V, a frequency of 40 Hz, and a quiet time of 180 s (Fig. S2).

EIS experiments were conducted in 5 mM $\text{K}_3[\text{Fe}(\text{CN})_6]$ in 0.1 M KCl with potential ranges ranging from 0.0 V to 0.1 V, frequency ranges ranging from 0.01 Hz to 50 kHz, and an amplitude of 0.1 V.

2.4. Sample preparation

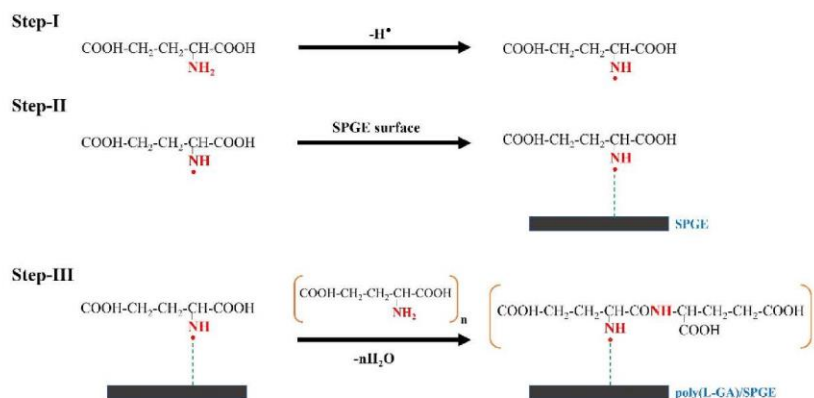
Details of sample preparation are described in SI.

3. Results and discussion

3.1. Surface composition and morphology studies

Surface morphologies of each sensor (SPGE and poly(L-GA)/SPGE) were investigated by scanning electron microscopy (SEM). Fig. 1a and b shows SEM images of SPGE and poly(L-GA)/SPGE at a magnification of $10,000\times$. The surface of the unmodified SPGE (Fig. 1a) was rugged, crumpled, and wrinkled. After the surface modification of L-GA onto SPGE via an electropolymerization procedure (Fig. 1b), its surface exhibited a smooth surface, which was covered by the formation of the poly(L-GA) on the SPGE surface. In addition, the surface composition of poly(L-GA) on the SPGE was approved via energy-dispersive X-ray spectroscopy (EDS). As displayed in Fig. 1c, the EDS mapping spectrum of poly(L-GA)/SPGE revealed the presence of C, N, and O atoms, relating to the structure of the glutamic acid molecular modified the electrode surface of SPGE.

To approve the deposition of the poly(L-GA) on SPGE, the surface composition was also characterized using X-ray photoelectron spectroscopy (XPS). XPS data of a bare SPGE (Fig. 1d) presents the C 1s core spectra; (C-C) appeared at 284.5 eV and (C=C) at 286.2 eV, corresponding to the presence of two carbon functionalities in the graphene structure. Fig. 1e describes the XPS core level spectra for C 1s, indicating the existence of four peaks at 284.8 , 285.7 , 286.6 , and 288.7 eV, corresponding to the (C-C), (C-O), (C-N), and (C=O) carbon bonding, respectively. We believed that these peaks occurred as a result of the structure of the polymerized L-GA monomer. Fig. 1f shows the O 1s XPS data and shows the existence of two different oxygen functionalities within the structure of the polymeric thin film; (O-C) appeared at 531.1 eV and (O=C) at 532.7 eV, which was attributed to the carboxylic groups of the L-GA structure. Additionally, the N 1s core spectra in Fig. 1g demonstrates a well-defined couple peak obtained at 399.7 and 400.8 eV, corresponding to the (N-C) and (^{15}N -C) amine groups in the L-GA structure. These findings obviously confirmed that the poly(L-GA) was successfully deposited on the SPGE surface.



Scheme 1. Mechanism of electropolymerization of L-GA on the SPGE surface.

3.2. Electrochemical characterization of the poly(L-GA)/SPGE

$\text{K}_3[\text{Fe}(\text{CN})_6]$ and $[\text{Ru}(\text{NH}_3)_6]\text{Cl}_3$ were selected as anionic and cationic redox probes to study the electrochemical behavior on poly(L-GA)/SPGE surface using CV. Fig. 2a shows CV voltammograms of two redox probes in 0.1 M KCl with a scan rate of 100 mV s^{-1} at the unmodified and modified SPGE. Certainly, the current signal of 5 mM $[\text{Fe}(\text{CN})_6]^{3-/4-}$ was greater than that of 5 mM $[\text{Ru}(\text{NH}_3)_6]^{3+/2+}$. When 5 mM $[\text{Fe}(\text{CN})_6]^{3-/4-}$ detection at the SPGE and poly(L-GA)/SPGE was compared (red dashed line and blue line), the peak potential separation (ΔE_p) at the poly(L-GA)/SPGE was reduced to +0.27 V, but the current signal was increased. This means that it is caused by the electrostatic interaction of the anionic redox probe and the positive charge of amine groups on poly(L-GA)/SPGE surface. Therefore, the poly(L-GA) thin film could enhance the electron-transfer process of $[\text{Fe}(\text{CN})_6]^{3-/4-}$, an anionic redox probe. Moreover, the electroactive surface area values of SPGE and poly(L-GA)/SPGE were estimated using the Randles-Sevcik equation as follows:

$$I_p = (2.69 \times 10^5) n^{3/2} A D_0^{1/2} \nu^{1/2} C_0^*$$

where I_p denotes the peak current; n denotes the number of electrons; A denotes the electroactive surface area; D_0 denotes the diffusion coefficient of redox probe species; ν denotes the scan rate (0.1 V s^{-1}); and C_0^* denotes the concentration of redox probe species ($5.0 \times 10^{-6} \text{ mol cm}^{-3}$). Based on known parameters for the $[\text{Fe}(\text{CN})_6]^{3-/4-}$ ($n = 1$ and $D_0 = 7.6 \times 10^{-6} \text{ cm}^2 \text{ s}^{-1}$) [21] and the $[\text{Ru}(\text{NH}_3)_6]^{3+/2+}$ ($n = 1$ and $D_0 = 8.43 \times 10^{-6} \text{ cm}^2 \text{ s}^{-1}$) [22], the electroactive surface area values of SPGE and poly(L-GA)/SPGE were calculated to be 0.120 and 0.150 cm^2 for $[\text{Fe}(\text{CN})_6]^{3-/4-}$ and 0.115 and 0.113 cm^2 for $[\text{Ru}(\text{NH}_3)_6]^{3+/2+}$.

Subsequently, $[\text{Fe}(\text{CN})_6]^{3-/4-}$ was selected as an anionic electroactive species to study the electron-transfer process to get a better understanding. As exhibited in Fig. 2b, the semicircle diameter of $[\text{Fe}(\text{CN})_6]^{3-/4-}$ at the poly(L-GA)/SPGE was smaller than that of SPGE, corresponding to the R_{ct} values (1.171 and $5.462 \text{ k}\Omega$ for poly(L-GA)/SPGE and SPGE, respectively). In addition, the electron-transfer apparent rate constant (k_{app}) was estimated using the equation as below [17,23]:

$$k_{app} = \frac{RT}{n^2 F^2 A R_{ct} C}$$

where R denotes the universal gas constant ($8.31447 \text{ J K}^{-1} \text{ mol}^{-1}$); T

denotes the absolute temperature (298 K); n denotes the number of electrons transferred during the redox reaction; F denotes the Faraday's constant ($96,485 \text{ C mol}^{-1}$); A denotes the surface area of the electrode (cm^2); R_{ct} denotes the charge transfer resistance with the potential range of 0–0.1 V in Ω ; and C denotes the concentration of $[\text{Fe}(\text{CN})_6]^{3-/4-}$ ($5.0 \times 10^{-6} \text{ mol cm}^{-3}$). The k_{app} values were calculated to be 8.121×10^{-5} and $3.031 \times 10^{-4} \text{ cm s}^{-1}$ for SPGE and poly(L-GA)/SPGE, respectively. The increased k_{app} value in the modified SPGE demonstrated that the modified poly(L-GA) on SPGE improved the electron-transfer process of redox $[\text{Fe}(\text{CN})_6]^{3-/4-}$. The total surface coverage (Γ) of the poly(L-GA)/SPGE was also estimated using the equation as provided in SI, which was found to be $16.62 \text{ nmol cm}^{-2}$. As a result of the electrochemical characterization study, it suggested that poly(L-GA) modified SPGE could be employed as an excellent sensor for the target electroactive species detection.

3.3. Effect of different types of supporting electrolytes on the electrochemical detection of 1-OHP at the poly(L-GA)/SPGE

To acquire the high sensitivity in the detection and the correctness, suitability, and reliability of the supporting electrolyte type, the influence of the supporting electrolyte type toward 1-OHP electrochemical detection on poly(L-GA)/SPGE was initially studied. For preliminary studies, 0.1 M Na-PBS at three pH values (5.6, 7.4, and 10.25) was used as the supporting electrolyte for investigating 1-OHP electrochemical behavior via SWV. From the results in Fig. 3a, when pH values were increased, the electrochemical signal of 1-OHP obviously increased. Nevertheless, at $\text{pH} \geq 10.25$, it was influenced by the effect of ionic strength due to the suitable and dependable pH range for Na-PBS of 5.0–8.0. Therefore, Na-PBS at high pH levels was ineffective to be used as the supporting electrolyte for 1-OHP detection. Subsequently, 0.05 M $\text{Na}_2\text{HPO}_4\text{-NaOH}$ (pH 10.5, 11.0, and 12.0) was chosen as the supporting electrolyte for the study owing to its pH range of 10.5–12.0. Fig. 3b shows that the highest current signal of 1-OHP was achieved at a low pH value (pH 10.5). However, to achieve the high sensitivity in detection, we found that in addition to these buffer solutions, Gly-NaOH buffer solution could be used as the supporting electrolyte due to its pH range of 8.5–10.5. Therefore, 0.05 M Gly-NaOH buffer solution at three pH values (8.4, 9.4, and 10.5) was immediately conducted. As observed in Fig. 3c, the highest current signal of 1-OHP was obtained at pH 9.4. Interestingly, square wave voltammograms (Fig. 3d) of 1-OHP detection using each supporting electrolyte type were compared. It was found that

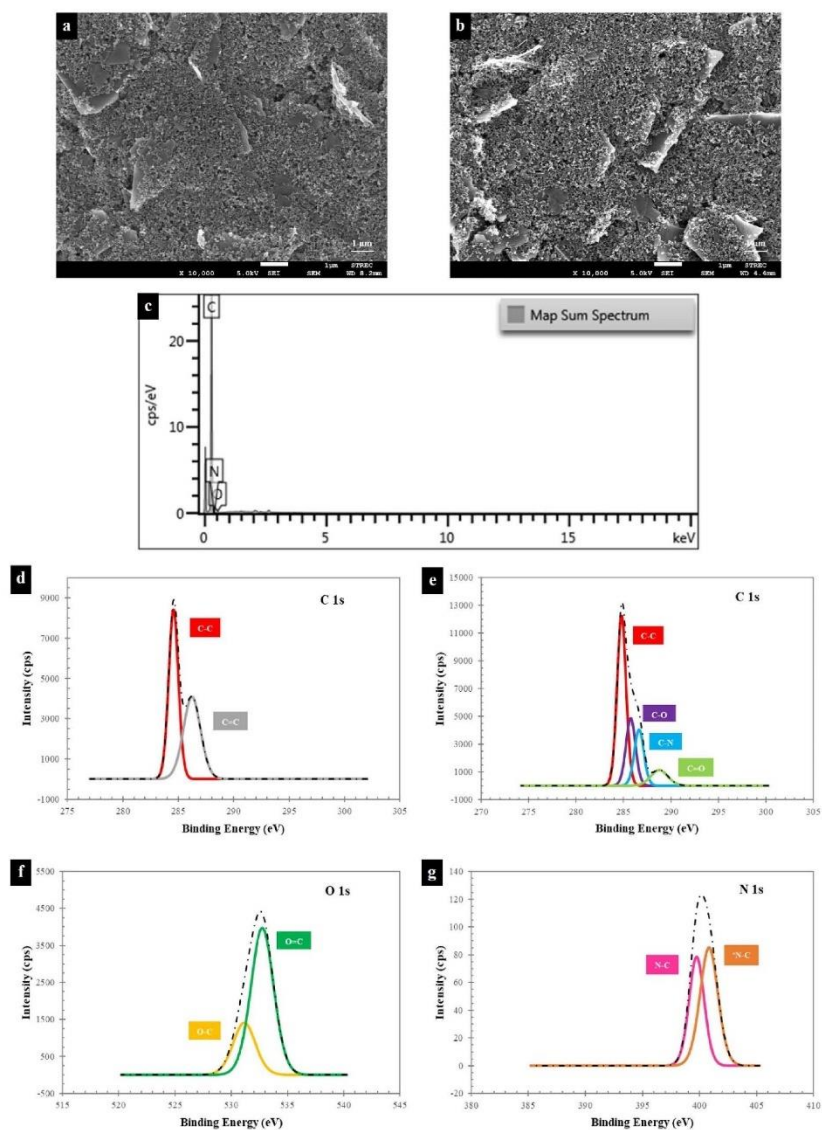


Fig. 1. SEM images of SPGE (a) and poly(L-GA)/SPGE (b) at a magnification of $10,000\times$. EDS mapping for the composition of poly(L-GA)/SPGE (c). XPS data of a bare SPGE (d) and the composite polymer fabricated on SPGE demonstrates the core level spectra for C 1s (e), O 1s (f), and N 1s (g).

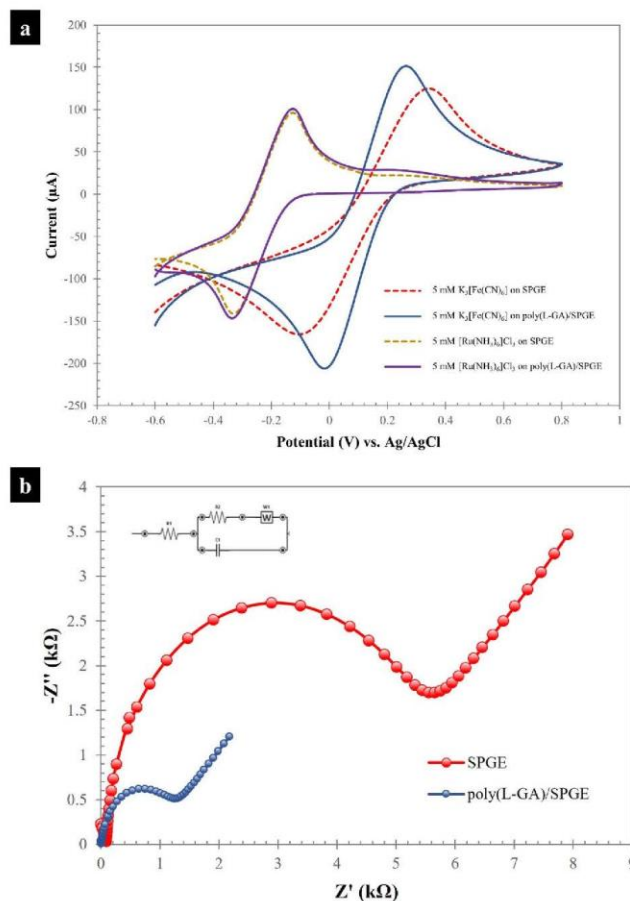


Fig. 2. Cyclic voltammograms of 5 mM $[Fe(CN)_6]^{3-/4-}$ and $[Ru(NH_3)_6]^{2+}$ in 0.1 M KCl with a scan rate of 100 mV s^{-1} at the SPGE and poly(L-GA)/SPGE (a). EIS Nyquist plots of 5 mM $[Fe(CN)_6]^{3-/4-}$ in 0.1 M KCl with the potential range of 0–0.1 V at the SPGE and poly(L-GA)/SPGE (b).

Gly-NaOH buffer solution not only gave the best electrochemical response for 1-OHP detection but also offered the oxidation peak potential of 1-OHP close to 0, resulting in improved selectivity of the proposed approach because most interferences can be easily oxidized at the positive potential. These findings suggested that Gly-NaOH played an important role in the electrooxidation of 1-OHP using the developed sensor. Thus, Gly-NaOH buffer solution was selected as an appropriate supporting electrolyte for this work.

3.4. Effect of pH values and scan rates

The study of different pH values on the oxidative behavior of 1-OHP in Gly-NaOH buffer solution was performed in the pH range of 8.4–10.5 using SWV. As depicted in Fig. 4a, the anodic peak currents of 1-OHP gradually increased with increasing pH values. However, at pH values

> 9.4, anodic peak currents were reduced. We believed that a pH value of 9.4 was sufficient to completely convert 1-OHP to the deprotonated form, which was easily oxidized at the electrode surface of poly(L-GA)/SPGE and electrostatically entirely interacted with the amine groups on the polymer backbone (pK_a value of 1-OHP = 7.44 [10]). Therefore, pH 9.4 was selected for further experiments. Also, as seen in the equation (Fig. 4b), the slope value of $-0.0527 \text{ V pH}^{-1}$ was close to the Nernstian theoretical value of -0.059 V pH^{-1} , demonstrating two-protons-transfer coupled with two-electrons-transfer reaction as previously reported [24–26].

The effect of scan rates on 1-OHP electrochemical oxidation on the poly(L-GA)/SPGE was studied in the range of $25\text{--}250 \text{ mV s}^{-1}$ via CV (Fig. 4c). A linear dependence (Fig. 4d) was gained between the current response of 1-OHP (I_{pa}) and the scan rate (v), indicating the adsorption-controlled process at the electrode surface. Furthermore, an adsorption

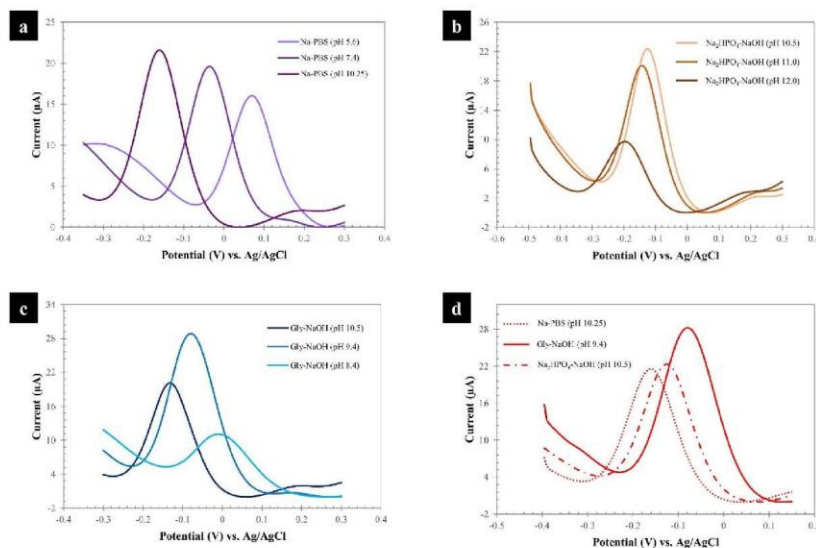


Fig. 3. Square wave voltammograms of 1-OHP detection using Na-PBS (a), $\text{Na}_2\text{HPO}_4\text{-NaOH}$ (b), and Gly-NaOH (c) as the supporting electrolyte. Square wave voltammograms for a comparison of each supporting electrolyte type in 1-OHP detection (d).

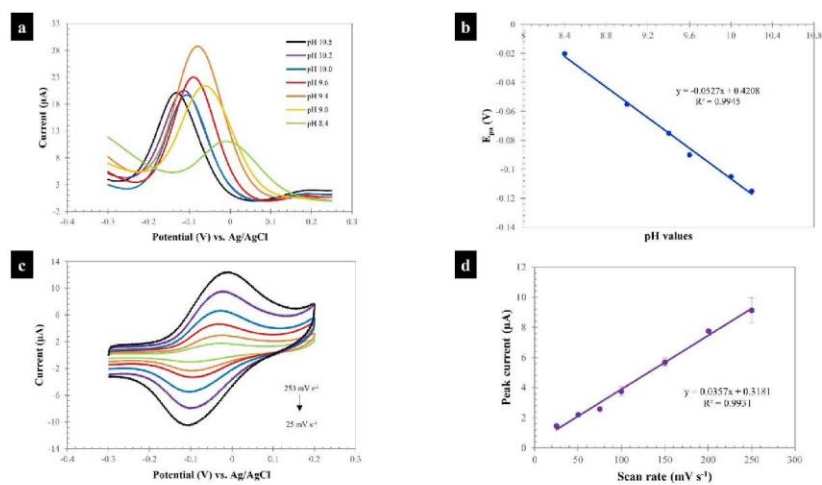


Fig. 4. Square wave voltammograms of 10 μM 1-OHP at the poly(L-GA)/SPGE with different pH values (a) and the plot of E_{pa} vs. pH values (b). Cyclic voltammograms of 50 μM 1-OHP in Gly-NaOH (pH 9.4) at the poly(L-GA)/SPGE at various scan rates (c) and the plot of I_{pa} vs. scan rate (d). Error bars represent the standard deviation of 1-OHP detection at different pH values and scan rates for three repetitive measurements ($n = 3$).

or diffusion controlled electrochemical process can be predicted from the slope of 1.0 or 0.5 by plotting $\log I_{pa}$ and $\log v$ [27,28]. From the linear regression equation, $\log I_{pa} = -1.057 + 0.8306 \log v$ ($R^2 = 0.9732$) (Fig. S3), it was found that the slope value was close to 1.0,

confirming the adsorption-controlled process.

3.5. Optimization of electropolymerization for L-GA

The optimization studies of electropolymerization for L-GA are presented in SI and Fig. S4.

3.6. Electrochemical behavior of 1-OHP on poly(L-GA)/SPGE

The electrochemical behavior of 1-OHP in Gly-NaOH (pH 9.4) on SPGE and poly(L-GA)/SPGE was subsequently studied by SWV. Fig. 5 shows the performance for the detection of 10 μM 1-OHP in Gly-NaOH (pH 9.4) on SPGE and poly(L-GA)/SPGE. The anodic peak current of 1-OHP ($i_{pa} = 9.27 \mu\text{A}$) was obtained at around -0.08 V on SPGE (red line). However, when the background signal of Gly-NaOH (pH 9.4) (red dashed line) at the unmodified SPGE was thoroughly magnified to be Fig. S5, the ghost peak appeared at around -0.10 V . We believed that this phenomenon might be caused by impurities from the graphene ink, which could not determine the 1-OHP at very low concentrations. Therefore, to resolve this issue, we aimed to use L-GA for the surface modification of SPGE. The ghost peak of the background current of Gly-NaOH (pH 9.4) did not occur after the surface modification (blue dashed line). Remarkably, the enlarged current signal of 1-OHP on poly(L-GA)/SPGE (blue line) was three times larger than that of the SPGE. These results suggested that the modified poly(L-GA) on SPGE revealed the electrocatalytic property of 1-OHP oxidation. Therefore, poly(L-GA)/SPGE could be employed as an excellent electrochemical sensor for 1-OHP analysis.

3.7. Analytical performance

Under optimal conditions, the analytical performance of this methodology was verified by detecting 1-OHP in different concentration via SWV. The anodic peak currents increased with increasing concentrations of 1-OHP (Fig. 6a, inset). The linear dynamic range (LDR) was relative in the range of 1–1000 nM (Fig. 6a). The limits of detection (LOD) and quantification (LOQ) were evaluated to be 0.95 (3SD/Slope) and 3.16 (10SD/Slope) nM, respectively. Furthermore, the analytical performance of this work was compared with that of previous works, as revealed in Table S1. Although this proposed method did not provide the lowest detection limit, however, the developed sensor had several advantages over the mentioned methods, such as the ease and rapidity of fabrication, the need for only one modifier for a single step of surface modification, and cost-effectiveness. This proposed sensor could also be applied for 1-OHP analysis in real samples. Moreover, the supporting electrolyte used in this work was within the suitable and dependable range of pH. Therefore, this assay had the perfect ability to be an

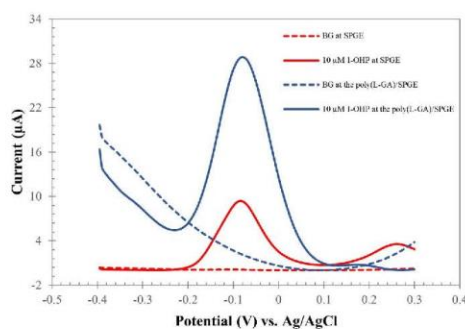


Fig. 5. Square wave voltammograms of 10 μM 1-OHP in Gly-NaOH (pH 9.4) at the unmodified and modified SPGE.

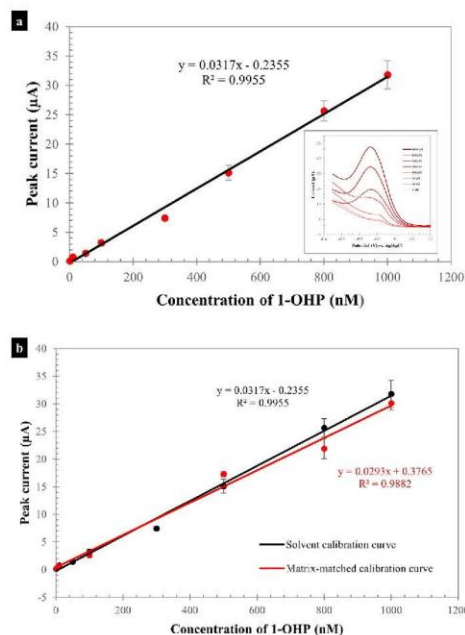


Fig. 6. The calibration curve between the anodic peak current and the concentration of 1-OHP in the range of 1–1000 nM (a) and corresponding square wave voltammograms of 1-OHP (inset). A comparison of the plotting graphs between a solvent calibration curve and a matrix-matched calibration curve (b). Error bars represent the standard deviation of 1-OHP detection at different concentrations for three repetitive measurements ($n = 3$).

alternative choice for the detection of 1-OHP in real-world applications.

In terms of reproducibility, three concentrations (10, 500, and 1000 nM) concerning the probable range in interesting samples were assessed. The relative standard deviation (RSD) values were $<32\%$, which was accepted by the AOAC recommendation [29]. For the stability study of poly(L-GA)/SPGE, the current signal of 10 μM 1-OHP remained at 98.55% for 21 days, indicating that this newly developed sensor provided good stability for 1-OHP detection.

3.8. Interference study

The effect of interferences, such as uric acid (UA), ascorbic acid (AA), citric acid (CA), glucose (Glu), bovine serum albumin (BSA), urea, and creatinine, along with the effect of some ions, comprising Na^+ , K^+ , Mg^{2+} , Ca^{2+} , and NH_4^+ , which might affect 1-OHP detection, was investigated. Fig. 7 describes the percentage of the current signal of 300 nM 1-OHP detection in the presence of 3 μM UA, 9 μM AA, 1500 nM CA, 300 nM Glu, 300 nM BSA, 3 μM urea, 300 nM creatinine, 30 μM Na^+ , 30 μM K^+ , 30 μM Mg^{2+} , 30 μM Ca^{2+} , and 30 μM NH_4^+ . From the results, the changes in the current signal of 1-OHP containing different interferences were $\leq \pm 5\%$, which suggested that interferences had no significant effect on 1-OHP detection. Therefore, the poly(L-GA)/SPGE had good selectivity toward 1-OHP detection.

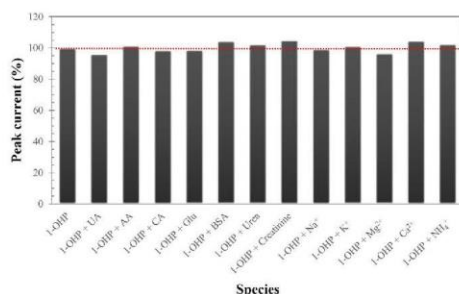


Fig. 7. Effect of some interfering substances on the detection of 300 nM 1-OHP at the poly(L-GA)/SPGE by SWV under optimal conditions ($n = 3$).

3.9. Dilution and matrix effect

In the current study, a 100-fold dilution using Gly-NaOH (pH 9.4) was used to evade foreign interferences in urine samples before analysis. As presented in Fig. 6b, the information obtained from two linear regression equations could be applied to calculate the percentage of the matrix effect using the following equation [30,31]:

$$\text{Matrix effect} = \left[\left(\frac{S_M}{S_S} \right) - 1 \right] \times 100$$

where S_M denotes the slope of calibration curve in matrix; and S_S denotes the slope of calibration curve in Gly-NaOH (pH 9.4). Based on the principle, the matrix effect was found to be 7.57%, suggesting that this value was < 15%, which confirmed that the proposed dilution was efficient to remove the interferences in urine. Additional details of the dilution and matrix effect are explained in SI and Table S2.

3.10. Application in real urine samples

In a practical application, the determination of 1-OHP in six urine samples from healthy volunteers was executed for evaluation of the potential of the proposed method. As the results are summarized in Table 1, the percentage values of recovery and RSD acquired within the acceptable value ranges of 86.06%–119.08% and 2.57%–34.77%, respectively. These results suggested that the proposed method is accurate, precise, and reliable to determine the 1-OHP in real urine samples without any interference. Therefore, the poly(L-GA)/SPGE offered a powerful sensor for determining 1-OHP in urine samples.

4. Conclusions

An electrochemical analytical device using poly(L-GA) modified SPGE for the rapid, simple, sensitive, and selective determination of trace 1-OHP was successfully demonstrated. The developed sensing platform was easily fabricated by using only one modifier for the surface modification of SPGE via a single step of electropolymerization. The poly(L-GA) thin film that adhered to the surface of SPGE demonstrated excellent electrocatalytic performance, increasing the specific surface area and promoting the electron-transfer rate, resulting in improved sensitivity and selectivity in 1-OHP detection. Under optimal conditions, the 1-OHP sensing supplied a wide linear range with a low detection limit. Furthermore, no chromatographic sample preparation was required prior to analysis for removing interferences. This proposed methodology and developed sensor could be applied to successfully determine 1-OHP in human urine samples. This new platform provided the rapid and simple fabricating process, inexpensiveness, small size,

Table 1

Results obtained from the determination of 1-OHP in healthy volunteer's urine using poly(L-GA)/SPGE ($n = 3$).

Real Samples	Spiked (nM)	Found (nM)	Recovery (%)	RSD (%)
1st volunteer	10	11.23	112.31	26.34
	500	577.96	115.59	2.57
2nd volunteer	10	9.44	94.36	22.31
	500	526.60	105.32	7.14
3rd volunteer	10	11.55	115.53	22.78
	500	456.68	91.34	12.68
4th volunteer	10	11.18	111.75	11.81
	500	533.77	106.75	4.20
5th volunteer	10	8.95	89.48	34.77
	500	430.28	86.06	11.38
6th volunteer	10	11.91	119.08	7.26
	500	577.59	115.52	6.06

disposability, need for a small sample volume, and suitability for portability. Therefore, this novel sensor might be used as an alternative device for monitoring and analyzing trace 1-OHP concentrations in the environment and workplace that have a high possibility of illness risk linked to PAHs in the human body.

Credit author statement

Jeerakit Thangphatthanarungruang: Conceptualization, Methodology, Validation, Investigation, Formal analysis, Writing – original draft, Visualization. Chuleekorn Chotsuwan: Resources, Funding acquisition. Weena Siangproh: Conceptualization, Investigation, Resources, Writing – review & editing, Supervision, Project administration

Declaration of competing interest

The authors declare that they have no known competing financial interests or personal relationships that could have appeared to influence the work reported in this paper.

Data availability

I have shared the link to my data/code at the Attach File step

Acknowledgments

JT would like to acknowledge the financial support from the Thailand Graduate Institute of Science and Technology (TGIST) (SCA-CO-2562-9695-TH). WS would like to acknowledge the financial support from the National Research Council of Thailand (NRCT) and Srinakharinwirot University through Research Grants for Talented Mid-Career Researchers (N41A640098). Special thanks to the National Nanotechnology Center (NANOTEC) Platform (Grant No. P1750196) and the National Science and Technology Development Agency (NSTDA) for supporting the facilities that enabled this work to be conducted. We would like to thank Enago (www.enago.com) for the English language review.

Appendix A. Supplementary data

Supplementary data to this article can be found online at <https://doi.org/10.1016/j.talanta.2022.123929>.

References

- [1] K.-H. Kim, S.A. Jahan, E. Kabir, R.J.C. Brown, A review of airborne polycyclic aromatic hydrocarbons (PAHs) and their human health effects, *Environ. Int.* 60 (2013) 71–80.
- [2] M. Serrano, M. Bartolomé, J.C. Bravo, G. Paniagua, J. Gañan, A. Gallego-Picó, R. M. Garcinuño, On-line flow injection molecularly imprinted solid phase extraction


- for the preconcentration and determination of 1-hydroxypyrene in urine samples, *Talanta* 166 (2017) 375–382.
- [3] F. Omidi, M. Khadem, F. Dehghani, M. Seyedsomeah, S.J. Shahtaheri, Ultrasound-assisted dispersive micro-solid-phase extraction based on N-doped mesoporous carbon and high-performance liquid chromatographic determination of 1-hydroxypyrene in urine samples, *J. Separ. Sci.* 43 (13) (2020) 2602–2609.
- [4] H. Zhang, H. Lu, H. Huang, J. Liu, X. Fang, B.-F. Yuan, Y.-Q. Feng, H. Chen, Quantification of 1-hydroxypyrene in undiluted human urine samples using magnetic solid-phase extraction coupled with internal extractive electrospray ionization mass spectrometry, *Anal. Chim. Acta* 926 (2016) 72–78.
- [5] Y. Pang, Y. Huang, W. Li, L. Feng, X. Shen, Conjugated poly(ethylene)/graphene multilayer films for simultaneous electrochemical sensing of three monohydroxylated polycyclic aromatic hydrocarbons, *ACS Appl. Nano Mater.* 12 (2019) 7785–7794.
- [6] H.A. Jeng, C.-H. Pan, 1-Hydroxypyrene as a Biomarker for Environmental Health, *General Methods in Biomarker Research and their Applications*, 2015, pp. 595–612.
- [7] O. Yosyphak, J. Berek, V. Vyskočil, Determination of 1-hydroxypyrene in human urine by HPLC with electrochemical detection at a boron-doped diamond film electrode, *Anal. Bioanal. Chem.* 404 (2012) 693–699.
- [8] A. Holm, P. Molander, E. Landanes, S. Øvrebo, T. Greibrokk, Fast and sensitive determination of urinary 1-hydroxypyrene by packed capillary column switching liquid chromatography coupled to micro-electrospray time-of-flight mass spectrometry, *J. Chromatogr. B* 794 (2003) 175–183.
- [9] H.-H. Lim, H.-S. Shin, Simultaneous determination of 2-naphthol and 1-hydroxypyrene in fish and shell fish contaminated with crude oil by gas chromatography-mass spectrometry, *Food Chem.* 138 (2013) 791–796.
- [10] H.-M. Yang, Y.-S. Wang, J.-H. Li, G.-R. Li, Y. Wang, X. Tan, J.-H. Xue, X.-L. Xiao, R.-H. Kang, Synchronous fluorescence determination of urinary 1-hydroxypyrene, beta-naphthol and 9-hydroxyphenanthrene based on the sensitizing effect of beta-cyclodextrin, *Anal. Chim. Acta* 636 (2009) 51–57.
- [11] J. Thangphatthanarungruang, A. Ngamaroonehote, R. Laocharoensuk, C. Chotsuwan, W. Siangproh, A novel electrochemical sensor for the simultaneous determination of fat-soluble vitamins using a screen-printed graphene/nafion electrode, *Key Eng. Mater.* 777 (2018) 597–601.
- [12] J. Thangphatthanarungruang, A. Yakoh, R. Laocharoensuk, C. Chotsuwan, O. Chaiapakul, W. Siangproh, High-efficient of graphene nanocomposite application to rapidly simultaneous identification and quantitation of fat-soluble vitamins in different matrix samples, *J. Electroanal. Chem.* 873 (2020), 114361.
- [13] W. Khancharoen, C.S. Henry, W. Siangproh, A novel L-cysteine sensor using in-situ electropolymerization of L-cysteine: potential to simple and selective detection, *Talanta* 237 (2022), 122983.
- [14] K. Kaewjua, W. Siangproh, A novel tyramine sensing-based polymeric L-histidine film-coated screen-printed graphene electrode: capability for practical applications, *Electrochim. Acta* 419 (2022), 140388.
- [15] P.S. Ganesh, B.E.K. Swamy, Simultaneous electroanalysis of norepinephrine, ascorbic acid and uric acid using poly(glytamic acid) modified carbon paste electrode, *J. Electroanal. Chem.* 752 (2015) 17–24.
- [16] P.T. Pinar, Y. Yurdum, Z. Şenitürk, Electrochemical oxidation of ranitidine at poly(dopamine) modified carbon paste electrode: its voltammetric determination in pharmaceutical and biological samples based on the enhancement effect of anionic surfactant, *Sens. Actuators. B Chem.* 273 (2018) 1463–1473.
- [17] J. Thangphatthanarungruang, C. Chotsuwan, S. Jampasa, W. Siangproh, A new nanocomposite-based screen-printed graphene electrode for sensitive and selective detection of 8-hydroxy-2'-deoxyguanosine, *HatChem* 32 (2022), 100335.
- [18] K.V. Harisha, B.E.K. Swamy, P.S. Ganesh, H. Jayadevappa, Electrochemical oxidation of haematoxylin at poly(alanine) modified carbon paste electrode: a cyclic voltammetric study, *J. Electroanal. Chem.* 832 (2019) 486–492.
- [19] S. He, P. He, X. Zhang, X. Zhang, K. Liu, L. Jia, F. Dong, Poly(glycine)/graphene oxide modified glassy carbon electrode: preparation, characterization and simultaneous electrochemical determination of dopamine, uric acid, guanaine and adenine, *Anal. Chim. Acta* 1031 (2018) 75–82.
- [20] B.R.L. Ferraz, F.R.F. Leite, A.R. Malagutti, Simultaneous determination of ethionamide and pyrazinamide using poly(L-leucine) film-modified glassy carbon electrode, *Talanta* 154 (2016) 197–207.
- [21] M. Punjija, C.H. Moon, Z. Matharu, H.R. Hejazi, S. Sonkusale, A three-dimensional electrochemical paper-based analytical device for low-cost diagnostics, *Analyst* 143 (2018) 1059–1064.
- [22] Y. Wang, J.G. Limon-Petersen, R.G. Compton, Measurement of the diffusion coefficients of [Ru(NH₃)₆]³⁺ and [Ru(NH₃)₆]²⁺ in aqueous solution using microelectrode double potential step chronoamperometry, *J. Electroanal. Chem.* 652 (2011) 13–17.
- [23] L.A.D. Gugous, F. Pogacean, S. Kurbanoğlu, L.B. Tudoran, A.B. Serban, I. Karso, S. Pruneanu, Graphene-gold nanoparticles nanozyme-based electrochemical sensor with enhanced lacase like activity for determination of phenolic substrates, *J. Electrochem. Soc.* 168 (2021), 067523.
- [24] X. Shen, Y. Cai, Y. Pang, H. Qian, Graphene oxide nanoribbon and poly(hedral oligomeric silsesquioxane assembled composite frameworks for pre-concentrating and electrochemical sensing of 1-hydroxypyrene, *Electrochim. Acta* 59 (2012) 91–99.
- [25] X. Shen, Y. Cai, Y. Pang, H. Qian, Pre-concentration and in situ electrochemical sensing of 1-hydroxypyrene on an electrodeposited poly(3-methylthiophene) film modified electrode, *J. Electroanal. Chem.* 667 (2012) 1–6.
- [26] Y. Pang, Y. Zhang, X. Sun, H. Ding, T. Ma, X. Shen, Synergistical accumulation for electrochemical sensing of 1-hydroxypyrene on electroreduced graphene oxide electrode, *Talanta* 192 (2019) 387–394.
- [27] J. David K. Gosser, *Cyclic Voltammetry: Simulation and Analysis of Reaction Mechanisms*, first ed., Wiley-VCH, 1993.
- [28] S.H. Azizi, S. Ghasemi, F. Amiripour, Nickel/P nanozelite modified electrode: a new sensor for the detection of formaldehyde, *Sens. Actuators. B Chem.* 227 (2016) 1–10.
- [29] G.W. Latimer, *Official Methods of Analysis of AOAC International*, twentieth ed., AOAC International, 2016.
- [30] D. Moreno-González, A.M. Hamed, A.M. García-Campaña, L. Gámiz-Gracia, Evaluation of hydrophilic interaction liquid chromatography-tandem mass spectrometry and extraction with molecularly imprinted polymers for determination of aminoglycosides in milk and milk-based functional foods, *Talanta* 171 (2017) 74–80.
- [31] Y.-C. Wan, Y.-J. Liu, C. Liu, H.-T. Ma, H.-F. Yu, J.-W. Kang, C.-L. Gao, Z.-Q. Wu, D. Zheng, B. Lu, Rapid determination of neomycin in biological samples using fluorescent sensor based on quantum dots with doubly selective binding sites, *J. Pharm. Biomed. Anal.* 30 (154) (2018) 75–85.

Appendix 3

วันที่สร้างเอกสาร 4 สิงหาคม 2564

ยื่นผ่านระบบอิเล็กทรอนิกส์
เลขที่คำขอ 2103002153

แบบ สป/สพ/อสป/001-ก
หน้า 1 ของจำนวน 3 หน้า

 คำขอรับสิทธิบัตร/อนุสิทธิบัตร <input type="checkbox"/> การประดิษฐ์ <input type="checkbox"/> การออกแบบผลิตภัณฑ์ <input checked="" type="checkbox"/> อนุสิทธิบัตร ข้าพเจ้าผู้ลงลายมือชื่อในคำขอรับสิทธิบัตร/อนุสิทธิบัตรมี ขอรับสิทธิบัตร/อนุสิทธิบัตร ตามพระราชบัญญัติสิทธิบัตร พ.ศ.2522 แก้ไขเพิ่มเติมโดยพระราชบัญญัติสิทธิบัตร(ฉบับที่ 2) พ.ศ.2535 และพระราชบัญญัติสิทธิบัตร (ฉบับที่ 3) พ.ศ.2542	สำหรับเจ้าหน้าที่	
	วันที่รับคำขอ 04/08/2564	เลขที่คำขอ
	วันที่ยื่นคำขอ 04/08/2564	
	สัญลักษณ์จำแนกการประดิษฐ์ระหว่างประเภท	
	ใช้กับแบบผลิตภัณฑ์ ประเภทผลิตภัณฑ์	
วันประกาศโฆษณา	เลขที่ประกาศโฆษณา	
วันออกสิทธิบัตร/อนุสิทธิบัตร	เลขที่สิทธิบัตร/อนุสิทธิบัตร	
ลายมือชื่อเจ้าหน้าที่		
1. ชื่อที่แสดงถึงการประดิษฐ์/การออกแบบผลิตภัณฑ์ อุปกรณ์เคมีไฟฟ้าสำหรับการตรวจวัดสารเรโซโตรอกซ์ไดออกไซด์ออกซิเจนในชั้นและวิธีการตรวจวัดสารเรโซโตรอกซ์ไดออกไซด์ออกซิเจนในตัวอย่างทางชีวภาพด้วยอุปกรณ์เคมีไฟฟ้าดังกล่าว		
2. คำขอรับสิทธิบัตรการออกแบบผลิตภัณฑ์นี้เป็นคำขอสำหรับผลิตภัณฑ์อย่างเดียวกันและเป็นคำขอลำดับที่ ในจำนวน _____ คำขอ ที่ยื่นในคราวเดียวกัน		
3. ผู้ขอรับสิทธิบัตร/อนุสิทธิบัตร <input type="checkbox"/> บุคคลธรรมดา <input type="checkbox"/> นิติบุคคล <input checked="" type="checkbox"/> หน่วยงานรัฐ <input type="checkbox"/> มูลนิธิ <input type="checkbox"/> อื่นๆ _____ ชื่อ มหาวิทยาลัยศรีนครินทรวิโรฒ ที่อยู่ 114 สถาบันวิทยาศาสตร์ทางปัญญาและวิจัย ซอย สุขุมวิท 23 ถนน สุขุมวิท 23 ตำบล/แขวง คลองเตยเหนือ อำเภอ/เขต วัฒนา จังหวัด กรุงเทพมหานคร รหัสไปรษณีย์ 10110 ประเทศ ไทย อีเมล jprwoffice@gmail.com <input type="checkbox"/> เลขประจำตัวประชาชน <input type="checkbox"/> เลขทะเบียนนิติบุคคล <input checked="" type="checkbox"/> เลขประจำตัวผู้เสียภาษีอากร 0 9 9 4 0 0 0 1 5 8 1 8 1 <input type="checkbox"/> เพิ่มเติม (ตั้งแบบ) ในกรณีที่มีการทำ สำเนาไว้ที่อื่น ท่านสะดวกใช้ทาง <input checked="" type="checkbox"/> อีเมล <input type="checkbox"/> อีเมลตัวแทน		3.1 สัญชาติ ไทย 3.2 โทรศัพท์ 0816327591 3.3 โทรสาร
4. สิทธิบัตรในการขอรับสิทธิบัตร/อนุสิทธิบัตร <input type="checkbox"/> ผู้ประดิษฐ์/ผู้ออกแบบ <input checked="" type="checkbox"/> ผู้รับโอน <input type="checkbox"/> ผู้ขอรับสิทธิโดยเหตุอื่น		
5. ตัวแทน (ถ้ามี) ชื่อ นางสาว นิศา รุ่งเรืองผล ที่อยู่ 114 มหาวิทยาลัยศรีนครินทรวิโรฒ ซอยสุขุมวิท 23 ถนนสุขุมวิท ตำบล/แขวง คลองเตยเหนือ อำเภอ/เขต วัฒนา จังหวัด กรุงเทพมหานคร รหัสไปรษณีย์ 10110 ประเทศ อีเมล _____ เลขประจำตัวประชาชน 3 2 2 0 1 0 0 2 9 0 9 1 7 <input type="checkbox"/> เพิ่มเติม (ตั้งแบบ)		5.1 ตัวแทนเลขที่ 2454 5.2 โทรศัพท์ 081-6327591 5.3 โทรสาร
6. ผู้ประดิษฐ์/ผู้ออกแบบผลิตภัณฑ์ <input type="checkbox"/> ชื่อและที่อยู่ผู้ยื่นคำขอ ชื่อ นางสาว วิภา เลียงเพราะ ที่อยู่ 335 หมู่ที่ 8 ตำบล/แขวง ทาเคอย อำเภอ/เขต ทายาง จังหวัด เพชรบุรี รหัสไปรษณีย์ 76130 ประเทศ ไทย อีเมล _____ เลขประจำตัวประชาชน 3 7 6 0 5 0 0 4 0 8 2 4 4 <input checked="" type="checkbox"/> เพิ่มเติม (ตั้งแบบ)		
7. คำขอรับสิทธิบัตร/อนุสิทธิบัตรนี้แยกจากหรือเกี่ยวข้องกับคำขอเดิม ผู้ขอรับสิทธิบัตร/อนุสิทธิบัตร ขอให้อธิบายได้ว่าคำขอรับสิทธิบัตร/อนุสิทธิบัตรนี้ ในวันเดียวกับคำขอรับสิทธิบัตร เลขที่ _____ วันยื่น _____ เพราะคำขอรับสิทธิบัตร/อนุสิทธิบัตรนี้แยกจากหรือเกี่ยวข้องกับคำขอเดิมเพราะ <input type="checkbox"/> คำขอเดิมมีการประดิษฐ์หลายอย่าง <input type="checkbox"/> ถูกคัดค้านเนื่องจากผู้ขอไม่มีสิทธิ <input type="checkbox"/> ขอเปลี่ยนแปลงประเภทของสิทธิ หมายเหตุ ในกรณีที่ไม่วางระบุละเอียดได้ครบถ้วน ให้จัดทำเป็นเอกสารแนบท้ายแบบพิมพ์นี้โดยระบุหมายเลขกำกับและหัวข้อที่แสดงรายละเอียด		
สำหรับเจ้าหน้าที่		
จำแนกประเภทสิทธิบัตร/อนุสิทธิบัตร <input type="checkbox"/> กลุ่มวิศวกรรม <input type="checkbox"/> กลุ่มเคมี <input type="checkbox"/> สิทธิบัตรการออกแบบ <input type="checkbox"/> อนุสิทธิบัตร สิทธิบัตรการประดิษฐ์ (วิศวกรรม) <input type="checkbox"/> สิทธิบัตรการประดิษฐ์ (เคมีเทคนิค) <input type="checkbox"/> สิทธิบัตรการออกแบบ (ออกแบบผลิตภัณฑ์ 1) <input type="checkbox"/> อนุสิทธิบัตร (วิศวกรรม) สิทธิบัตรการประดิษฐ์ (ไฟฟ้า) <input type="checkbox"/> สิทธิบัตรการประดิษฐ์ (ปิโตรเคมี) <input type="checkbox"/> สิทธิบัตรการออกแบบ (ออกแบบผลิตภัณฑ์ 2) <input type="checkbox"/> อนุสิทธิบัตร (เคมี) สิทธิบัตรการประดิษฐ์ (ฟิสิกส์) <input type="checkbox"/> สิทธิบัตรการประดิษฐ์ (เทคโนโลยีชีวภาพ) <input type="checkbox"/> สิทธิบัตรการออกแบบ (ออกแบบผลิตภัณฑ์ 3) สิทธิบัตรการประดิษฐ์ (เภสัชภัณฑ์)		

วันที่สร้างเอกสาร 4 สิงหาคม 2564

แบบ สป/คพ/อสป/001-ก
หน้า 2 ของจำนวน 3 หน้า

8. การยื่นคำขออนุญาตนำเข้า <input type="checkbox"/> PCT <input type="checkbox"/> เพิ่มเติม (ตั้งแนบ)				
วันที่ยื่นคำขอ	เลขที่คำขอ	ประเทศ	สัญลักษณ์จำแนกการประดิษฐ์ระหว่างประเทศ	สถานะคำขอ
8.1				
8.2				
8.3				
8.4 <input type="checkbox"/> ผู้ขอรับสิทธิบัตร/อนุสิทธิบัตรขอสิทธิให้ถือว่าได้ยื่นคำขอในวันที่ได้ยื่นคำขอรับสิทธิบัตร/อนุสิทธิบัตรในต่างประเทศเป็นครั้งแรกโดย <input type="checkbox"/> ได้ยื่นเอกสารหลักฐานพร้อมคำขอ <input type="checkbox"/> ขอยื่นเอกสารหลักฐานหลังจากวันยื่นคำขอ				
9. การแสดงการประดิษฐ์หรือการออกแบบผลิตภัณฑ์ของผู้ขอรับสิทธิบัตร/อนุสิทธิบัตรได้แสดงการประดิษฐ์ที่หน่วยงานของรัฐเป็นผู้จัด วันแสดง _____ วันปิดงานแสดง _____ ผู้จัด _____				
10. การประดิษฐ์เกี่ยวกับจุลชีพ				
10.1 เลขทะเบียนฝากเก็บ		10.2 วันที่ฝากเก็บ	10.3 สถาบันฝากเก็บ/ประเทศ	
11. ผู้ขอรับสิทธิบัตร/อนุสิทธิบัตร ขอยื่นเอกสารภาษาต่างประเทศก่อนในวันยื่นคำขอนี้ และจะจัดยื่นคำขอรับสิทธิบัตร/อนุสิทธิบัตรนี้ให้จัดทำเป็นภาษาไทยภายใน 90 วัน นับจากวันยื่นคำขอนี้ โดยขอเป็นภาษาไทย <input type="checkbox"/> อังกฤษ <input type="checkbox"/> ฝรั่งเศส <input type="checkbox"/> เยอรมัน <input type="checkbox"/> ญี่ปุ่น <input type="checkbox"/> อื่นๆ _____				
12. ผู้ขอรับสิทธิบัตร/อนุสิทธิบัตรขอให้อธิบดีประกาศโฆษณาคำขอรับสิทธิบัตรหรือรับจดทะเบียนและประกาศโฆษณาสิทธิบัตรนี้ หลังจากวันที่ _____ <input type="checkbox"/> ผู้ขอรับสิทธิบัตร/อนุสิทธิบัตรขอให้ใช้รูปเขียนหมายเลข _____ ในการประกาศโฆษณา				
3. คำขอรับสิทธิบัตร/อนุสิทธิบัตรนี้ประกอบด้วย			14. เอกสารประกอบคำขอ	
ก. แบบพิมพ์คำขอ _____ 3 หน้า			<input checked="" type="checkbox"/> เอกสารแสดงสิทธิในการขอรับสิทธิบัตร/อนุสิทธิบัตร	
ข. รายละเอียดการประดิษฐ์ หรือคำพรรณนาแบบผลิตภัณฑ์ _____ 6 หน้า			<input type="checkbox"/> หนังสือรับรองการแสดงการประดิษฐ์/การออกแบบผลิตภัณฑ์	
ค. ข้อต่อสิทธิ _____ 2 หน้า			<input checked="" type="checkbox"/> หนังสือมอบอำนาจ	
ง. รูปเขียน _____ 2 รูป _____ 1 หน้า			<input type="checkbox"/> เอกสารรายละเอียดเกี่ยวกับจุลชีพ	
จ. ภาพแสดงแบบผลิตภัณฑ์ <input type="checkbox"/> รูปเขียน _____ รูป _____ หน้า			<input type="checkbox"/> เอกสารการอนันต์วันยื่นคำขอในต่างประเทศเป็นวันยื่นคำขอในประเทศไทย	
<input type="checkbox"/> รูปถ่าย _____ รูป _____ หน้า			<input type="checkbox"/> เอกสารขอเปลี่ยนแปลงประเภทของสิทธิ	
ฉ. บทสรุปการประดิษฐ์ _____ 1 หน้า			<input checked="" type="checkbox"/> เอกสารอื่นๆ	
15. ข้าพเจ้าขอรับรองว่า <input checked="" type="checkbox"/> การประดิษฐ์นี้ไม่เคยยื่นขอรับสิทธิบัตร/อนุสิทธิบัตรมาก่อน <input type="checkbox"/> การประดิษฐ์นี้ได้พัฒนาปรับปรุงมาจาก _____				
16. ลายมือชื่อ <input type="checkbox"/> ผู้ขอรับสิทธิบัตร/อนุสิทธิบัตร <input checked="" type="checkbox"/> ตัวแทน			SN=3220100290917 (นางสาว นิตยา รุ่งเรืองผล)	

หมายเหตุ บุคคลใดยื่นขอรับสิทธิบัตรการประดิษฐ์หรือการออกแบบผลิตภัณฑ์ หรืออนุสิทธิบัตร โดยการแสดงข้อความอันเป็นเท็จแก่พนักงานเจ้าหน้าที่ เพื่อให้ได้ไปซึ่งสิทธิบัตรหรืออนุสิทธิบัตร ต้องระวางโทษจำคุกไม่เกินหกเดือน หรือปรับไม่เกินห้าพันบาท หรือทั้งจำทั้งปรับ

วันที่สร้างเอกสาร 4 สิงหาคม 2564

แบบ สป/สพ/อสป/012-ก

หน้า 3 ของจำนวน 3 หน้า

6. ผู้ประดิษฐ์/ผู้ออกแบบผลิตภัณฑ์ (ต่อ)

6.2 ชื่อ นาย จีระกิตต์ ตั้งพัฒน์มารุ่งเรือง สัญชาติ ไทย

บ้านเลขที่ 134/36 หมู่ที่ 10 ตำบล/แขวง ปากแพรก อำเภอ/เขต เมืองกาญจนบุรี จังหวัด กาญจนบุรี รหัสไปรษณีย์ 71000 ประเทศไทย

Signed by DIP-CA

วันที่สร้างเอกสาร 4 สิงหาคม 2564

หน้า 1 ของจำนวน 6 หน้า

รายละเอียดการประดิษฐ์

ชื่อที่แสดงถึงการประดิษฐ์

อุปกรณ์เคมีไฟฟ้าสำหรับการตรวจวัดสารเอทไฮดรอกซีทูต็อกซีกัวโนซีนและวิธีการตรวจวัดสารเอทไฮดรอกซีทูต็อกซีกัวโนซีนในตัวอย่างทางชีวภาพด้วยอุปกรณ์เคมีไฟฟ้างกล่าว

5 สาขาวิทยาการที่เกี่ยวข้องกับการประดิษฐ์

สาขาเคมีวิเคราะห์ที่เกี่ยวข้องกับการพัฒนาอุปกรณ์เคมีไฟฟ้าสำหรับการตรวจวัดสารเอทไฮดรอกซีทูต็อกซีกัวโนซีน

ภูมิหลังของศิลปะหรือวิทยาการที่เกี่ยวข้อง

- อนุมูลอิสระออกซิเจน (Reactive oxygen species, ROS) เป็นโมเลกุลที่ไม่เสถียร มีความว่องไวต่อการเกิดปฏิกิริยาทางเคมีและสามารถทำปฏิกิริยากับโมเลกุลต่าง ๆ ภายในเซลล์ของร่างกาย โดยอนุมูลอิสระออกซิเจนมีบทบาทสำคัญทางสรีรวิทยาและพยาธิวิทยา ปริมาณของโมเลกุลเหล่านี้ถูกใช้เป็นตัวบ่งชี้ถึงความไม่สมดุลระหว่างสารอนุมูลอิสระ (Oxidants) และสารต้านอนุมูลอิสระ (Antioxidants) ภายในเซลล์ของร่างกาย
- 10 ปรากฏการณ์ที่เกิดขึ้นนี้เรียกว่า ภาวะความไม่สมดุลของการเกิดอนุมูลอิสระ (Oxidative stress) หากร่างกายมีอนุมูลอิสระออกซิเจนมากเกินไปจะสามารถทำลายโครงสร้างต่างๆ ภายในเซลล์ได้ เช่น โปรตีน ไขมัน
- 15 น้ำตาล เยื่อหุ้มเซลล์ และดีเอ็นเอ โดยอนุมูลอิสระออกซิเจนมีความสัมพันธ์โดยตรงกับภาวะความไม่สมดุลของการเกิดอนุมูลอิสระและการก่อมะเร็งเนื่องจากการจำลองของดีเอ็นเอภายในเซลล์ได้รับความเสียหาย ดังนั้นการประเมินระดับความเสียหายของดีเอ็นเอภายในเซลล์จากปริมาณอนุมูลอิสระออกซิเจนที่มีต่อสุขภาพของมนุษย์จึงมีความสำคัญอย่างยิ่ง

- เอทไฮดรอกซีทูต็อกซีกัวโนซีน (8-Hydroxy-2'-deoxyguanosine, 8-OHdG) เป็นหนึ่งในโมเลกุลเป้าหมายที่มีการศึกษามากที่สุดและเป็นตัวบ่งชี้ที่จำเพาะ (Specific marker) สำหรับภาวะความไม่สมดุลของการเกิดอนุมูลอิสระ โมเลกุลเอทไฮดรอกซีทูต็อกซีกัวโนซีนเป็นผลิตภัณฑ์หลักของกัวนีน (Guanine) ที่เกิดจากอันตรกิริยาของอนุมูลอิสระไฮดรอกซิล (Hydroxyl radical) ที่อะตอมของคาร์บอนตำแหน่งที่แปดของฐานดีเอ็นเอของกัวนีน โดยปกติแล้วโมเลกุลชีวภาพเอทไฮดรอกซีทูต็อกซีกัวโนซีนสามารถพบในตัวอย่างทางชีวภาพหลากหลาย เช่น ปัสสาวะ น้ำลาย เลือดหรือเซรัม และเนื้อเยื่อ ซึ่งระดับของเอทไฮดรอกซีทูต็อกซีกัว
- 20 โนซีนในของเหลวในร่างกายจะมีความสัมพันธ์กับโรคต่าง ๆ มากมาย เช่น มะเร็ง การชราภาพ เบาหวาน และ
- 25 ความผิดปกติของระบบประสาท นอกจากนี้ปริมาณของเอทไฮดรอกซีทูต็อกซีกัวโนซีนยังสามารถใช้ในการประเมินระดับความเสียหายของดีเอ็นเอที่เกิดจากปฏิกิริยาออกซิเดชันภายในร่างกายมนุษย์ โดยระดับปกติ

ของเอชไอทรอกซีทูต็อกซีกัวโนซีนในมนุษย์ที่มีสุขภาพดีจะมีค่าต่ำกว่า 100 นาโนโมลาร์ ดังนั้นการพัฒนาอุปกรณ์และวิธีการตรวจวัดสารเอชไอทรอกซีทูต็อกซีกัวโนซีนที่มีความไว (Sensitivity) และความจำเพาะ (Selectivity) จึงเป็นสิ่งสำคัญสำหรับการช่วยงานด้านการประเมินความเสี่ยงของโรคและการวินิจฉัยทางคลินิกเบื้องต้น

- 5 โดยที่ผ่านมาได้มีการพัฒนาวิธีการตรวจวัดปริมาณสารเอชไอทรอกซีทูต็อกซีกัวโนซีนด้วยวิธีการต่าง ๆ เช่น วิธีการทางสเปกโทรเมตรี (Spectrometry) และทางโครมาโทกราฟี (Chromatography) แม้ว่าวิธีการเหล่านี้จะให้การวิเคราะห์ที่มีความไวและความจำเพาะ อย่างไรก็ตามวิธีการเหล่านี้ต้องอาศัยเครื่องมือที่มีราคาสูง มีความซับซ้อน ใช้เวลาในการวิเคราะห์นาน มีขั้นตอนการเตรียมตัวอย่างหลายขั้นตอน มีการใช้ปริมาณของสารตัวอย่างและตัวทำละลายจำนวนมากและความต้องการผู้ที่มีความเชี่ยวชาญในการใช้เครื่องมือ
- 10 ระดับสูง นอกจากนี้เครื่องมือและอุปกรณ์ที่ใช้ในวิธีการเหล่านี้ไม่สามารถนำออกไปใช้ทดสอบนอกห้องปฏิบัติการและไม่เหมาะสำหรับการวิเคราะห์ทางคลินิก ณ จุดดูแลผู้ป่วย หรือสถานพยาบาลห่างไกล ดังนั้นการคิดค้นอุปกรณ์และวิธีการตรวจวัดปริมาณสารเอชไอทรอกซีทูต็อกซีกัวโนซีนในตัวอย่างทางชีวภาพที่สามารถแก้ไขข้อจำกัดต่าง ๆ ดังกล่าวจึงถือว่าเป็นที่ต้องการอย่างยิ่ง เพื่อให้ได้มาซึ่งวิธีการที่มีความเรียบง่าย สะดวก รวดเร็ว พกพาได้ ราคาถูก ความไวและความจำเพาะสูง และคงไว้ซึ่งความถูกต้อง ปัจจุบันวิธีการ
- 15 วิเคราะห์ทางเคมีไฟฟ้าเป็นอีกหนึ่งวิธีการที่ได้รับความนิยมอย่างมากสำหรับการตรวจวัดสารบ่งชี้ทางชีวภาพ (Biomarkers) เนื่องจากเทคนิคทางเคมีไฟฟ้ามีข้อดีเหนือเทคนิคอื่น ๆ เช่น เป็นเทคนิคที่ใช้งานง่าย สะดวก ให้ความไวและความจำเพาะในการวิเคราะห์ที่สูง มีความแม่นยำ ใช้เวลาในการวิเคราะห์ที่รวดเร็ว เครื่องมือไม่มีความซับซ้อน ราคาไม่แพง สามารถพกพาและนำออกไปใช้นอกห้องปฏิบัติการได้ นอกจากนี้อุปกรณ์การวิเคราะห์ทางเคมีไฟฟ้ายังใช้ปริมาณของสารตัวอย่างที่น้อยมากในระดับไมโครลิตรและมีการออกแบบอุปกรณ์
- 20 ได้หลากหลายรูปแบบให้เหมาะกับงานที่จะนำไปประยุกต์ใช้

- จากการศึกษาผลงานวิจัยที่ผ่านมาที่เกี่ยวข้องกับการตรวจวัดปริมาณสารเอชไอทรอกซีทูต็อกซีกัวโนซีนด้วยวิธีการทางเคมีไฟฟ้ายังพบข้อจำกัดบางประการ กล่าวคือ เมื่อทำการตรวจวัดสารเอชไอทรอกซีทูต็อกซีกัวโนซีนในตัวอย่างทางชีวภาพ พบว่า การมีอยู่ของกรดยูริก (Uric acid) ที่ระดับความเข้มข้นสูง ๆ ในตัวอย่างทางชีวภาพจะส่งผลกระทบต่อสารเอชไอทรอกซีทูต็อกซีกัวโนซีน เนื่องจากสารทั้งสอง
- 25 ตัวนี้ปรากฏสัญญาณที่ตำแหน่งใกล้เคียงกันมากเพื่อแก้ไขข้อจำกัดดังกล่าว จึงได้มีการพัฒนาวิธีการวิเคราะห์โดยใช้เอนไซม์ยูริเคส (Uricase enzyme) เพื่อลดการรบกวนของกรดยูริกที่มีต่อการตรวจวัดสารเอชไอทรอกซีทูต็อกซีกัวโนซีน ถึงแม้ว่าการพัฒนาวิธีการวิเคราะห์ดังกล่าวจะให้ผลการวิเคราะห์ที่มีความจำเพาะและให้ความสามารถในการตรวจวิเคราะห์สารได้ที่ระดับความเข้มข้นต่ำ อย่างไรก็ตามพบว่า มีข้อเสีย คือ อายุการใช้งานของเอนไซม์ที่สั้น มีราคาแพง มีขั้นตอนการเตรียมเอนไซม์ที่ยุ่งยาก ซับซ้อน และใช้เวลานาน นอกจากนี้

ขั้วไฟฟ้าใช้งานที่จำหน่ายเชิงพาณิชย์ เช่น ขั้วไฟฟ้ากลาสคาร์บอน (Glassy carbon electrode, GCE) ที่ต้องใช้งานร่วมกับตัวดัดแปรผิวหน้าขั้วไฟฟ้า (Modifiers) เพื่อการตรวจวัดสารเอทไฮดรอกซีทูต็อกซีกัวโนซีนนั้นจะต้องมีการปรับสภาพ (Pretreatment) ผิวหน้าขั้วไฟฟ้าก่อนการใช้งาน มีราคาแพง ใช้ปริมาตรสารตัวอย่างที่มาก มีขั้นตอนการดัดแปรผิวหน้าขั้วไฟฟ้าหลายขั้นตอน นำมาซึ่งความยุ่งยาก ซับซ้อน และใช้เวลานาน อีกทั้งบางวัสดุที่นำมาใช้นั้นมีราคาสูง ดังนั้นจึงนำมาสู่การประดิษฐ์อุปกรณ์ขั้วไฟฟ้าแบบใหม่และวิธีการตรวจวัดสารเอทไฮดรอกซีทูต็อกซีกัวโนซีนด้วยขั้วไฟฟ้าแบบพิมพ์สกรีนกราฟีนที่มีการดัดแปรผิวหน้าขั้วไฟฟ้าด้วยอนุภาคทองและพอลิแอลเมไธโอนีน (poly(L-methionine) and gold nanoparticles modified screen-printed graphene electrode, poly(L-met)/AuNPs/SPGE) บนฐานแผ่นใสที่สามารถตรวจวัดสารเอทไฮดรอกซีทูต็อกซีกัวโนซีนในสภาวะที่มีกรดยูริกได้โดยไม่ใช้เอนไซม์เป็นตัวกลางรบกวนของกรดยูริก ซึ่งจากการสืบค้นข้อมูลเชิงวิทยาศาสตร์ยังไม่มีงานนำขั้วไฟฟ้าและวิธีการวิเคราะห์ดังกล่าวมาใช้สำหรับการตรวจวัดสารเอทไฮดรอกซีทูต็อกซีกัวโนซีนในตัวอย่างทางชีวภาพมาก่อน ทำให้ได้รับการตรวจวัดสารเอทไฮดรอกซีทูต็อกซีกัวโนซีนที่ง่าย สะดวกและรวดเร็ว มีความไวและความจำเพาะสูง ให้ความถูกต้องแม่นยำ และมีความน่าเชื่อถือ นอกจากนี้อุปกรณ์ขั้วไฟฟ้าง่ายๆ ดังกล่าวยังมีขนาดเล็กและราคาถูก อีกทั้งสามารถพกพาไปทดสอบในเชิงภาคสนามและเหมาะสำหรับการประยุกต์ใช้ในเชิงการวิเคราะห์ทางคลินิกได้อีกด้วย

15 ลักษณะและความมุ่งหมายของการประดิษฐ์

การประดิษฐ์นี้เกี่ยวกับการพัฒนาอุปกรณ์ขั้วไฟฟ้าด้วยการพิมพ์สกรีนขั้วไฟฟ้าลงบนฐานแผ่นใส ซึ่งจะประกอบไปด้วยขั้วไฟฟ้า 3 ขั้ว ได้แก่ 1. ขั้วไฟฟ้าใช้งาน (Working electrode) ที่มีองค์ประกอบเป็นกราฟีน 2. ขั้วไฟฟ้าช่วย (Counter electrode) ที่มีองค์ประกอบเป็นกราฟีน และ 3. ขั้วไฟฟ้าอ้างอิง (Reference electrode) ที่มีองค์ประกอบเป็นซิลเวอร์/ซิลเวอร์คลอไรด์ (Ag/AgCl) โดยบริเวณขั้วไฟฟ้าใช้งานจะมีการดัดแปรผิวหน้าขั้วไฟฟ้าด้วยอนุภาคทอง (Gold nanoparticles, AuNPs) และพอลิแอลเมไธโอนีน (poly(L-methionine), poly(L-met)) และวิธีการตรวจวัดสารเอทไฮดรอกซีทูต็อกซีกัวโนซีน

วัตถุประสงค์ของการประดิษฐ์นี้คือ เพื่อพัฒนาอุปกรณ์ขั้วไฟฟ้าโดยการดัดแปรผิวหน้าขั้วไฟฟ้าด้วยอนุภาคทองและพอลิแอลเมไธโอนีนและวิธีการตรวจวัดสารเอทไฮดรอกซีทูต็อกซีกัวโนซีนในตัวอย่างทางชีวภาพ เช่น ปัสสาวะ และ/หรือเซรัม ซึ่งอุปกรณ์ขั้วไฟฟ้าง่ายๆ ดังกล่าวสามารถประดิษฐ์ขึ้นได้ง่าย สะดวก รวดเร็ว มีขนาดเล็ก ราคาถูก อีกทั้งยังสามารถพกพาไปทดสอบในเชิงภาคสนามและเหมาะสำหรับการประยุกต์ใช้ในเชิงการวิเคราะห์ทางคลินิก นอกจากนี้วิธีการที่พัฒนาขึ้นให้ผลการวิเคราะห์ที่มีความไวและความจำเพาะสูงต่อการตรวจวัดสารเอทไฮดรอกซีทูต็อกซีกัวโนซีน โดยไม่จำเป็นต้องใช้เอนไซม์เป็นตัวกลางรบกวนจากกรดยูริก ซึ่งมีความเหมาะสมอย่างยิ่งต่อการนำไปใช้ประโยชน์สำหรับบุคลากรทางการแพทย์ในการวินิจฉัยความ

เสียงของโรคที่สัมพันธ์กับระดับสารเอชไอทรอกซีทูต็อกซีกัวโนซีนในตัวอย่างทางชีวภาพ เช่น ปัสสาวะ และ/หรือเซรัม

การเปิดเผยการประดิษฐ์โดยสมบูรณ์

- การประดิษฐ์นี้เกี่ยวข้องกับการสร้างอุปกรณ์เคมีไฟฟ้าแบบใหม่และการพัฒนาวิธีการตรวจวัดสาร
- 5 เอชไอทรอกซีทูต็อกซีกัวโนซีนในตัวอย่างทางชีวภาพ เช่น ปัสสาวะ และ/หรือเซรัม โดยใช้ชีวไฟฟ้าแบบพิมพ์
- สกรีนกราฟีนที่มีการตัดแปรมีวหน้าชีวไฟฟ้าด้วยอนุภาคทองและพอลิแอลเมไธโอนีน (poly(L-methionine) and gold nanoparticles modified screen-printed graphene electrode, poly(L-met)/AuNPs/SPGE) บนฐานแผ่นใส เพื่อนำไปประยุกต์ใช้ในเชิงการวิเคราะห์และการวินิจฉัยทางคลินิกได้
- ลำดับต่อไปจะกล่าวถึงรายละเอียดและขั้นตอนการพัฒนาอุปกรณ์เคมีไฟฟ้า รวมถึงวิธีการนำ
- 10 อุปกรณ์เคมีไฟฟ้าดังกล่าวไปใช้ในการวิเคราะห์สารเอชไอทรอกซีทูต็อกซีกัวโนซีน โดยแสดงดังต่อไปนี้
1. การสร้างชีวไฟฟ้าแบบพิมพ์สกรีนกราฟีนบนฐานแผ่นใส

โดยขั้นตอนการสร้างชีวไฟฟ้าแบบพิมพ์สกรีนกราฟีนบนฐานแผ่นใส ดังแสดงตามรูปที่ 1 ซึ่งมีรายละเอียดดังต่อไปนี้

 - 1.1 ทำการออกแบบชีวไฟฟ้าแบบพิมพ์สกรีน ซึ่งใช้เป็นอุปกรณ์ตรวจวัดสารเอชไอทรอกซีทูต็อกซี
 - 15 ซีกัวโนซีน โดยทำการออกแบบให้มียอดประกอบของชีวไฟฟ้า 3 ชั้น ได้แก่ ชีวไฟฟ้าใช้งาน ชีวไฟฟ้าช่วย และชีวไฟฟ้าอ้างอิง ที่มีขนาดที่เล็กและพกพาได้สะดวก
 - 1.2 ทำการสกรีนชีวไฟฟ้า 2 ชั้น ด้วยหมึกกราฟีนลงบนฐานแผ่นใส เพื่อใช้เป็นชีวไฟฟ้าใช้งานและชีวไฟฟ้าช่วย จากนั้นนำไปเข้าตู้อบที่อุณหภูมิ 60 องศาเซลเซียส เป็นเวลา 30-60 นาที
 - 1.3 ทำการสกรีนชีวไฟฟ้าอีก 1 ชั้น ด้วยหมึกซิลเวอร์/ซิลเวอร์คลอไรด์ลงบนฐานแผ่นใสที่ได้จาก
 - 20 ข้อ 1.2 เพื่อใช้เป็นชีวไฟฟ้าอ้างอิง จากนั้นนำไปเข้าตู้อบที่อุณหภูมิ 60 องศาเซลเซียส เป็นเวลา 30 นาที แล้วจะได้ชีวไฟฟ้าแบบพิมพ์สกรีนกราฟีนสำหรับการตัดแปรมีวหน้าด้วยอนุภาคทองและพอลิแอลเมไธโอนีน
 2. วิธีการตัดแปรมีวหน้าชีวไฟฟ้าแบบพิมพ์สกรีนกราฟีนด้วยอนุภาคทองและพอลิแอลเมไธโอนีน

โดยขั้นตอนการตัดแปรมีวหน้าชีวไฟฟ้าแบบพิมพ์สกรีนกราฟีนด้วยอนุภาคทองและพอลิแอล

 - 25 เมไธโอนีน ดังแสดงตามรูปที่ 2 ซึ่งมีรายละเอียดดังต่อไปนี้
 - 2.1 ทำการตัดแปรมีวหน้าชีวไฟฟ้าแบบพิมพ์สกรีนกราฟีนด้วยอนุภาคทองด้วยวิธีอิเล็กโทรเดโพสิชัน (Electrodeposition) โดยการเตรียมสารละลายมาตรฐานทองที่ช่วงความเข้มข้น 400-1000

ไมโครกรัมต่อมิลลิลิตร ในสารละลายฟอสเฟตบัฟเฟอร์ จากนั้นหยดสารละลายมาตรฐานของลงบนขั้วไฟฟ้าแบบพิมพ์สกรีนกราฟีนด้วยปริมาตร 50 ไมโครลิตร แล้วทำการให้ศักย์ไฟฟ้าโดยใช้เทคนิคไซคลิกโวลแทมเมตรี (Cyclic voltammetry, CV) ระหว่างศักย์ไฟฟ้า -0.4 ถึง +1.4 โวลต์ อัตราการสแกน 50-200 มิลลิโวลต์ต่อวินาที จำนวนรอบการสแกน 5-15 รอบ จากนั้นทำการล้างผิวหน้าขั้วไฟฟ้าใช้งานด้วยน้ำปราศจากไอออนแล้วทิ้งไว้ให้แห้งที่อุณหภูมิห้อง

2.2 ทำการดัดแปรผิวหน้าขั้วไฟฟ้าด้วยพอลิแอลเมไธโอนีนด้วยวิธีอิเล็กโทรพอลิเมอไรเซชัน (Electro-polymerization) โดยการเตรียมสารละลายมอนอเมอร์แอลเมไธโอนีน (L-methionine) ที่ช่วงความเข้มข้น 1-7 มิลลิโมลาร์ ในสารละลายฟอสเฟตบัฟเฟอร์ จากนั้นหยดสารละลายมอนอเมอร์แอลเมไธโอนีนลงบนขั้วไฟฟ้าแบบพิมพ์สกรีนกราฟีนที่ผ่านการดัดแปรผิวหน้าขั้วไฟฟ้าด้วยอนุภาคทองที่ได้จากข้อ 2.1 ด้วยปริมาตร 50 ไมโครลิตร แล้วทำการให้ศักย์ไฟฟ้าระหว่าง -0.6 ถึง +2.0 โวลต์ ด้วยเทคนิคไซคลิกโวลแทมเมตรี อัตราการสแกน 50-250 มิลลิโวลต์ต่อวินาที จำนวนรอบการสแกน 5-15 รอบ จากนั้นทำการล้างผิวหน้าขั้วไฟฟ้าใช้งานด้วยน้ำปราศจากไอออน แล้วทิ้งไว้ให้แห้งที่อุณหภูมิห้อง จะได้ขั้วไฟฟ้าใช้งานแบบพิมพ์สกรีนกราฟีนที่มีการดัดแปรผิวหน้าขั้วไฟฟ้าด้วยอนุภาคทองและพอลิแอลเมไธโอนีนสำหรับการตรวจวัดสารเอทไฮดรอกซีทูต็อกซีกัวโนซีน

3. วิธีการตรวจวัดสารเอทไฮดรอกซีทูต็อกซีกัวโนซีน

โดยขั้นตอนการตรวจวัดสารเอทไฮดรอกซีทูต็อกซีกัวโนซีนจะมีรายละเอียดดังต่อไปนี้

3.1 ทำการเตรียมสารละลายมาตรฐานเอทไฮดรอกซีทูต็อกซีกัวโนซีนในสารละลายผสมของสารละลายโซเดียมโดเดซิลซัลเฟต (Sodium dodecyl sulfate, SDS) สารละลายโซเดียมคลอไรด์ (Sodium chloride, NaCl) และสารละลายฟอสเฟตบัฟเฟอร์ ซึ่งทำหน้าที่เป็นสารละลายอิเล็กโทรไลต์ (Supporting electrolyte)

3.2 ทำการหยดสารละลายมาตรฐานเอทไฮดรอกซีทูต็อกซีกัวโนซีนหรือสารตัวอย่างลงบนอุปกรณ์เคมีไฟฟ้าที่มีการดัดแปรผิวหน้าขั้วไฟฟ้าด้วยอนุภาคทองและพอลิแอลเมไธโอนีนด้วยปริมาตร 50 ไมโครลิตร โดยใช้เทคนิคสแควร์เวฟโวลแทมเมตรี (Square wave voltammetry, SWV) ซึ่งอุปกรณ์เคมีไฟฟ้าดังกล่าวจะถูกเชื่อมต่อกับเครื่องโพเทนชิโอสแตท (Potentiostat) จากนั้นทำการสแกนศักย์ไฟฟ้าตั้งแต่ +0.1 ถึง +0.5 โวลต์ โดยใช้ค่าการเพิ่มขึ้นของศักย์ไฟฟ้า (Potential increment) เท่ากับ 0.015 โวลต์ ค่าแอมพลิจูด (Amplitude) เท่ากับ 0.05 โวลต์ และค่าความถี่ (Frequency) เท่ากับ 30 เฮิรตซ์

3.3 ทำการสร้างกราฟมาตรฐานจากสารละลายมาตรฐานเอทไฮดรอกซีทูต็อกซีกัวโนซีน เพื่อหาปริมาณวิเคราะห์ของสารเอทไฮดรอกซีทูต็อกซีกัวโนซีน ซึ่งสามารถทำได้จากการตรวจวัดสัญญาณการ

วันที่สร้างเอกสาร 4 สิงหาคม 2564

หน้า 6 ของจำนวน 6 หน้า

ตอบสนองทางเคมีไฟฟ้าของสารละลายมาตรฐานเอทไฮดรอกซีทูต็อกซีกัวโนซีนในรูปของกระแสไฟฟ้า จากนั้นนำไปสร้างกราฟความสัมพันธ์ระหว่างค่าสัญญาณที่ตรวจวัดได้ในรูปของกระแสไฟฟ้าในหน่วยไมโครแอมแปร์ (μA) เป็นแกน y และค่าความเข้มข้นของสารละลายมาตรฐานเอทไฮดรอกซีทูต็อกซีกัวโนซีนในหน่วยไมโครโมลาร์ (μM) เป็นแกน x พบว่า กราฟมาตรฐานสำหรับการตรวจวัดปริมาณสารเอทไฮดรอกซีทูต็อกซีกัวโนซีนอยู่ในช่วงความเข้มข้น 1 ถึง 50 ไมโครโมลาร์

คำอธิบายรูปเขียนโดยย่อ

รูปที่ 1 ขั้นตอนการสร้างขั้วไฟฟ้าแบบพิมพ์สกรีนกราฟีนบนฐานแผ่นใส

รูปที่ 2 ขั้นตอนการตัดแปรมีวหน้าขั้วไฟฟ้าแบบพิมพ์สกรีนกราฟีนด้วยอนุภาคทองและพอลิแอลเมไธโอนีน

วิธีการในการประดิษฐ์ที่ดีที่สุด

10 ดึงที่กล่าวมาแล้วในหัวข้อการเปิดเผยการประดิษฐ์โดยสมบูรณ์

ข้อถ้อยสัญญา

1. วิธีการตัดแปรมีวหน้าขั้วไฟฟ้าแบบพิมพ์สกรีนกราฟีนด้วยอนุภาคทองและพอลิแอลเมไธโอนีน โดยมีขั้นตอนดังต่อไปนี้

- ขั้นตอนที่ 1 ทำการตัดแปรมีวหน้าขั้วไฟฟ้าแบบพิมพ์สกรีนกราฟีนด้วยอนุภาคทองด้วยวิธีอิเล็กโตรเดโพสิชัน (Electrodeposition) โดยการเตรียมสารละลายมาตรฐานทองที่ช่วงความเข้มข้น 400-1000 ไมโครกรัมต่อมิลลิลิตร ในสารละลายฟอสเฟตบัฟเฟอร์ จากนั้นหยดสารละลายมาตรฐานทองลงบนขั้วไฟฟ้าแบบพิมพ์สกรีนกราฟีนด้วยปริมาตร 50 ไมโครลิตร แล้วทำการให้ศักย์ไฟฟ้าโดยใช้เทคนิคไซคลิกโวลแทมเมตรี (Cyclic voltammetry, CV) ระหว่างค่าศักย์ไฟฟ้า -0.4 ถึง +1.4 โวลต์ อัตราการสแกน 50-200 มิลลิโวลต์ต่อวินาที จำนวนรอบการสแกน 5-15 รอบ จากนั้นทำการล้างมีวหน้าขั้วไฟฟ้าใช้งานด้วยน้ำปราศจากไอออนแล้วทิ้งไว้ให้แห้งที่อุณหภูมิห้อง

- ขั้นตอนที่ 2 ทำการตัดแปรมีวหน้าขั้วไฟฟ้าด้วยพอลิแอลเมไธโอนีนด้วยวิธีอิเล็กโตรพอลิเมอไรเซชัน (Electro-polymerization) โดยการเตรียมสารละลายมอนอเมอร์แอลเมไธโอนีน (L-methionine) ที่ช่วงความเข้มข้น 1-7 มิลลิโมลาร์ ในสารละลายฟอสเฟตบัฟเฟอร์ จากนั้นหยดสารละลายมอนอเมอร์แอลเมไธโอนีนลงบนขั้วไฟฟ้าแบบพิมพ์สกรีนกราฟีนจากขั้นตอนที่ 1 ด้วยปริมาตร 50 ไมโครลิตร แล้วทำการให้ศักย์ไฟฟ้าระหว่าง -0.6 ถึง +2.0 โวลต์ ด้วยเทคนิคไซคลิกโวลแทมเมตรี อัตราการสแกน 50-250 มิลลิโวลต์ต่อวินาที จำนวนรอบการสแกน 5-15 รอบ จากนั้นทำการล้างมีวหน้าขั้วไฟฟ้าใช้งานด้วยน้ำปราศจากไอออนแล้วทิ้งไว้ให้แห้งที่อุณหภูมิห้อง จะได้ขั้วไฟฟ้าใช้งานแบบพิมพ์สกรีนกราฟีนที่ตัดแปรมีวหน้าขั้วไฟฟ้าด้วยอนุภาคทองและพอลิแอลเมไธโอนีนสำหรับการตรวจวัดสารเอทไฮดรอกซีทูตออกซีกัวโนซีน

2. วิธีการตรวจวัดสารเอทไฮดรอกซีทูตออกซีกัวโนซีนด้วยวิธีการทางเคมีไฟฟ้าโดยใช้อุปกรณ์เคมีไฟฟ้าที่ผ่านวิธีการตัดแปรมีวหน้าขั้วไฟฟ้าตามข้อถ้อยสัญญาที่ 1 โดยมีขั้นตอนดังต่อไปนี้

- ขั้นตอนที่ 1 ทำการเตรียมสารละลายมาตรฐานเอทไฮดรอกซีทูตออกซีกัวโนซีนในสารละลายผสมระหว่างสารละลายโซเดียมโดเดซิลซัลเฟต (Sodium dodecyl sulfate, SDS) สารละลายโซเดียมคลอไรด์ (Sodium chloride, NaCl) และสารละลายฟอสเฟตบัฟเฟอร์ ซึ่งทำหน้าที่เป็นสารละลายอิเล็กโทรไลต์ (Supporting electrolyte)

- ขั้นตอนที่ 2 ทำการหยดสารละลายมาตรฐานเอทไฮดรอกซีทูตออกซีกัวโนซีนหรือสารตัวอย่างลงบนอุปกรณ์เคมีไฟฟ้าที่มีการตัดแปรมีวหน้าขั้วไฟฟ้าด้วยอนุภาคทองและพอลิแอลเมไธโอนีนด้วยปริมาตร 50 ไมโครลิตร โดยใช้เทคนิคสแควร์เวฟโวลแทมเมตรี (Square wave voltammetry, SWV) ซึ่งอุปกรณ์เคมีไฟฟ้าดังกล่าวจะเชื่อมต่อกับเครื่องโพเทนชิโอสแตต (Potentiostat) จากนั้นทำการสแกนศักย์ไฟฟ้าตั้งแต่ +0.1 ถึง

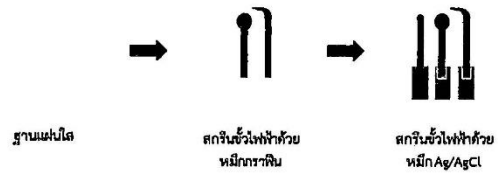
+0.5 โวลต์ โดยใช้ค่าการเพิ่มขึ้นของศักย์ไฟฟ้า (Potential increment) เท่ากับ 0.015 โวลต์ ค่าแอมพลิจูด (Amplitude) เท่ากับ 0.05 โวลต์ และค่าความถี่ (Frequency) เท่ากับ 30 เฮิร์ตซ์

- ขั้นตอนที่ 3 ทำการสร้างกราฟมาตรฐานจากสารละลายมาตรฐานเอทไฮดรอกซีฟลูออโรออกซีกัวโนซีน เพื่อหาปริมาณวิเคราะห์ของสารเอทไฮดรอกซีฟลูออโรออกซีกัวโนซีน ซึ่งสามารถทำได้จากการตรวจวัดสัญญาณการตอบสนองทางเคมีไฟฟ้าของสารละลายมาตรฐานเอทไฮดรอกซีฟลูออโรออกซีกัวโนซีนที่ความเข้มข้นต่าง ๆ ในรูปของกระแสไฟฟ้า จากนั้นนำไปสร้างกราฟความสัมพันธ์ระหว่างค่าสัญญาณที่ตรวจวัดได้ในรูปของกระแสไฟฟ้า ในหน่วยไมโครแอมแปร์ (μA) เป็นแกน y และค่าความเข้มข้นของสารละลายมาตรฐานเอทไฮดรอกซีฟลูออโรออกซีกัวโนซีนในหน่วยไมโครโมลาร์ (μM) เป็นแกน x พบว่ากราฟมาตรฐานสำหรับการตรวจวัดปริมาณสารเอทไฮดรอกซีฟลูออโรออกซีกัวโนซีนอยู่ในช่วงความเข้มข้น 1 ถึง 50 ไมโครโมลาร์

วันที่สร้างเอกสาร 4 สิงหาคม 2564

หน้า 1 ของจำนวน 1 หน้า

รูปเขียน



รูปที่ 1



รูปที่ 2

วันที่สร้างเอกสาร 4 สิงหาคม 2564

หน้า 1 ของจำนวน 1 หน้า


บทสรุปการประดิษฐ์

การประดิษฐ์นี้เป็นการพัฒนาอุปกรณ์เคมีไฟฟ้าและวิธีการตรวจวัดสารเอทไฮดรอกซีทูต็อกซีกัวโนซีนในตัวอย่างทางชีวภาพ โดยใช้ชีวไฟฟ้าแบบพิมพ์สกรีนกราฟีนที่มีการตัดแปรมิวหน้าชีวไฟฟ้าด้วยอนุภาคทองและพอลิแอลไมโธโธเนียน ซึ่งประกอบไปด้วย 2 ขั้นตอน ได้แก่ 1. ขั้นตอนการตัดแปรมิวหน้าชีวไฟฟ้าแบบพิมพ์สกรีนกราฟีนด้วยอนุภาคทองด้วยวิธีอิเล็กโตรเคปโตะซิชั่น 2. ขั้นตอนการตัดแปรมิวหน้าชีวไฟฟ้าด้วยพอลิแอลไมโธโธเนียนด้วยวิธีอิเล็กโตรพอลิเมอไรเซชัน จากนั้นทำการตรวจวัดสารเอทไฮดรอกซีทูต็อกซีกัวโนซีนโดยใช้อุปกรณ์เคมีไฟฟ้าที่ผ่านวิธีการตัดแปรมิวหน้าชีวไฟฟ้าในสองขั้นตอนดังกล่าวด้วยวิธีทางเคมีไฟฟ้า ซึ่งจะทำให้การวัดค่ากระแสไฟฟ้าด้วยเทคนิคสแควร์เวฟโวลแทมเมตรี โดยทำการสแกนศักย์ไฟฟ้าตั้งแต่ +0.1 ถึง +0.5 โวลต์ ใช้ค่าการเพิ่มขึ้นของศักย์ไฟฟ้าเท่ากับ 0.015 โวลต์ ค่าแอมพลิจูด เท่ากับ 0.05 โวลต์ และค่าความถี่เท่ากับ 30 เฮิร์ตซ์ พบว่า อุปกรณ์เคมีไฟฟ้าและวิธีการที่พัฒนาขึ้นมาสามารถตรวจวัดปริมาณสารเอทไฮดรอกซีทูต็อกซีกัวโนซีนในช่วงความเข้มข้น 1 ถึง 50 ไมโครโมลาร์ อีกทั้งสามารถนำไปประยุกต์ใช้สำหรับการตรวจวัดปริมาณสารเอทไฮดรอกซีทูต็อกซีกัวโนซีนในตัวอย่างทางชีวภาพ เช่น ปัสสาวะ และ/หรือเซรัม ซึ่งมีตัวรบกวนหลากหลายชนิด โดยไม่ใช่เอนไซม์เป็นตัวลดการรบกวน นอกจากนี้ยังสามารถให้ผลการตรวจวัดที่รวดเร็ว มีความไวและความจำเพาะสูง ให้ความถูกต้อง แม่นยำ และมีความน่าเชื่อถือ อีกทั้งสามารถพกพานำออกไปใช้ทดสอบนอกห้องปฏิบัติการและเหมาะสำหรับการประยุกต์ใช้ในเชิงการวิเคราะห์ทางคลินิก ดังนั้นการประดิษฐ์นี้จึงมีศักยภาพที่เหมาะสมและเป็นประโยชน์อย่างมากต่อบุคลากรทางการแพทย์สำหรับการวินิจฉัยความเสี่ยงของโรคต่อระดับสารเอทไฮดรอกซีทูต็อกซีกัวโนซีนในตัวอย่างทางชีวภาพ เช่น ปัสสาวะ และ/หรือเซรัม

Appendix 4

วันที่ส่งเอกสาร 18 พฤษภาคม 2565

แบบ สป/สผ/อสน/001-ก
หน้า 1 ของจำนวน 3 หน้า

 คำขอรับสิทธิบัตร/อนุสิทธิบัตร <input type="checkbox"/> การประดิษฐ์ <input type="checkbox"/> การออกแบบผลิตภัณฑ์ <input checked="" type="checkbox"/> อนุสิทธิบัตร ข้าพเจ้าผู้ลงลายมือชื่อในคำขอรับสิทธิบัตร/อนุสิทธิบัตรนี้ ขอรับสิทธิบัตร/อนุสิทธิบัตร ตามพระราชบัญญัติสิทธิบัตร พ.ศ.2522 แก้ไขเพิ่มเติมโดยพระราชบัญญัติสิทธิบัตร(ฉบับที่ 2) พ.ศ.2535 และพระราชบัญญัติสิทธิบัตร (ฉบับที่ 3) พ.ศ.2542	สำหรับเจ้าหน้าที่	
	วันที่รับคำขอ 18/05/2565	เลขที่คำขอ
	วันที่ยื่นคำขอ 18/05/2565	2203001218
	สัญลักษณ์จำแนกการประดิษฐ์ระหว่างประเทศ	
	ใช้กับแบบผลิตภัณฑ์ประเภทผลิตภัณฑ์	
วันประกาศโฆษณา	เลขที่ประกาศโฆษณา	
วันออกสิทธิบัตร/อนุสิทธิบัตร	เลขที่สิทธิบัตร/อนุสิทธิบัตร	
ลายมือชื่อเจ้าหน้าที่		
1. ชื่อที่แสดงถึงการประดิษฐ์/การออกแบบผลิตภัณฑ์ อุปกรณ์เคมีไฟฟ้าสำหรับการตรวจวัดสารเมตาโบไลต์ในโครมาโทกราฟีและวิธีการตรวจวัดสารเมตาโบไลต์ในโครมาโทกราฟีในตัวอย่างปัสสาวะด้วยอุปกรณ์ดังกล่าว		
2. คำขอรับสิทธิบัตรการออกแบบผลิตภัณฑ์นี้เป็นคำขอสำหรับผลิตภัณฑ์อย่างเดียวกันและเป็นคำขอลำดับที่ ในจำนวน คำขอ ที่ยื่นในคราวเดียวกัน		
3. ผู้ขอรับสิทธิบัตร/อนุสิทธิบัตร <input type="checkbox"/> บุคคลธรรมดา <input type="checkbox"/> นิติบุคคล <input checked="" type="checkbox"/> หน่วยงานรัฐ <input type="checkbox"/> บุคคล <input type="checkbox"/> อื่นๆ		3.1 สัญชาติ ไทย 3.2 โทรศัพท์ 0816327591 3.3 โทรสาร
ชื่อ มหาวิทยาลัยศรีนครินทรวิโรฒ ที่อยู่ 114 สถาบันพุทธศาสตร์ทางปัญญาและวิจัย ซอย สุขุมวิท 23 ถนน สุขุมวิท 23 ตำบล/แขวง คลองเตยเหนือ อำเภอ/เขต วัฒนา จังหวัด กรุงเทพมหานคร รหัสไปรษณีย์ 10110 ประเทศไทย อีเมล ipswnoffice@gmail.com		
<input type="checkbox"/> เลขประจำตัวประชาชน <input type="checkbox"/> เลขทะเบียนนิติบุคคล <input checked="" type="checkbox"/> เลขประจำตัวผู้เสียภาษีอากร 0 9 9 4 0 0 0 1 5 8 1 8 1 <input type="checkbox"/> เพิ่มเติม (ตั้งแบบ) ในกรณีที่มีการนำ ชื่อสารกับท่าน ท่านสะดวกใช้ทาง <input checked="" type="checkbox"/> อีเมลผู้ขอ <input type="checkbox"/> อีเมลตัวแทน		
4. สิทธิบัตรในการขอรับสิทธิบัตร/อนุสิทธิบัตร <input type="checkbox"/> ผู้ประดิษฐ์/ผู้ออกแบบ <input checked="" type="checkbox"/> ผู้รับโอน <input type="checkbox"/> ผู้ขอรับสิทธิโดยเหตุอื่น		
5. ตัวแทน (ถ้ามี) ชื่อ นางสาว นิตยา รุ่งเรืองผล ที่อยู่ 114 มหาวิทยาลัยศรีนครินทรวิโรฒ ซอยสุขุมวิท 23 ถนนสุขุมวิท ตำบล/แขวง คลองเตยเหนือ อำเภอ/เขต วัฒนา จังหวัด กรุงเทพมหานคร รหัสไปรษณีย์ 10110 ประเทศไทย อีเมล เลขประจำตัวประชาชน 3 2 2 0 1 0 0 2 9 0 9 1 7 <input type="checkbox"/> เพิ่มเติม (ตั้งแบบ)		5.1 ตัวแทนเลขที่ 2454 5.2 โทรศัพท์ 081-6327591 5.3 โทรสาร
6. ผู้ประดิษฐ์/ผู้ออกแบบผลิตภัณฑ์ <input type="checkbox"/> ชื่อและที่อยู่เดียวกันกับผู้ขอ ชื่อ นางสาว วิภา เสี่ยงเพราะ ที่อยู่ 114 มหาวิทยาลัยศรีนครินทรวิโรฒ คณะวิทยาศาสตร์ ภาควิชาเคมี ซอย สุขุมวิท 23 ตำบล/แขวง คลองเตยเหนือ อำเภอ/เขต วัฒนา จังหวัด กรุงเทพมหานคร รหัสไปรษณีย์ 10110 ประเทศไทย อีเมล เลขประจำตัวประชาชน 3 7 6 0 5 0 0 4 0 8 2 4 4 <input checked="" type="checkbox"/> เพิ่มเติม (ตั้งแบบ)		
7. คำขอรับสิทธิบัตร/อนุสิทธิบัตรนี้แยกจากหรือเกี่ยวข้องกับคำขอเดิม ผู้ขอรับสิทธิบัตร/อนุสิทธิบัตร ขอให้ถือว่าได้ยื่นคำขอรับสิทธิบัตร/อนุสิทธิบัตรนี้ ในวันเดียวกับคำขอรับสิทธิบัตร เลขที่ _____ วันยื่น _____ เพราะคำขอรับสิทธิบัตร/อนุสิทธิบัตรนี้แยกจากหรือเกี่ยวข้องกับคำขอเดิมเพราะ <input type="checkbox"/> คำขอเดิมมีการประดิษฐ์หลายอย่าง <input type="checkbox"/> ถูกคัดค้านเนื่องจากผู้ขอไม่มีสิทธิ <input type="checkbox"/> ขอเปลี่ยนแปลงประเภทของสิทธิ หมายเหตุ ในกรณีที่ไม่อาจระบุรายละเอียดได้ครบถ้วน ให้จัดทำเป็นเอกสารแนบท้ายแบบพิมพ์นี้โดยระบุหมายเลขกำกับชื่อและหัวข้อที่แสดงรายละเอียด		
สำหรับเจ้าหน้าที่		
จำแนกประเภทสิทธิบัตร/อนุสิทธิบัตร <input type="checkbox"/> กลุ่มวิศวกรรม <input type="checkbox"/> กลุ่มเคมี <input type="checkbox"/> สิทธิบัตรการออกแบบ <input type="checkbox"/> อนุสิทธิบัตร สิทธิบัตรการประดิษฐ์ (วิศวกรรม) <input type="checkbox"/> สิทธิบัตรการประดิษฐ์ (เคมีเทคนิค) <input type="checkbox"/> สิทธิบัตรการออกแบบ (ออกแบบผลิตภัณฑ์ 1) <input type="checkbox"/> อนุสิทธิบัตร (วิศวกรรม) สิทธิบัตรการประดิษฐ์ (ไฟฟ้า) <input type="checkbox"/> สิทธิบัตรการประดิษฐ์ (ชีวเคมี) <input type="checkbox"/> สิทธิบัตรการออกแบบ (ออกแบบผลิตภัณฑ์ 2) <input type="checkbox"/> อนุสิทธิบัตร (เคมี) สิทธิบัตรการประดิษฐ์ (ฟิสิกส์) <input type="checkbox"/> สิทธิบัตรการประดิษฐ์ (เทคโนโลยีชีวภาพ) <input type="checkbox"/> สิทธิบัตรการออกแบบ (ออกแบบผลิตภัณฑ์ 3)		

Signed by DIP-CA

8. การยื่นคำขออนุญาตออกอากาศ <input type="checkbox"/> PCT <input type="checkbox"/> เพิ่มเติม (ดังแนบ)				
วันยื่นคำขอ	เลขที่คำขอ	ประเทศ	สัญลักษณ์จำแนกการประดิษฐ์ระหว่างประเทศ	สถานะคำขอ
8.1				
8.2				
8.3				
8.4 <input type="checkbox"/> ผู้ขอรับสิทธิบัตร/อนุสิทธิบัตรขอสิทธิให้ถือว่าได้ยื่นคำขอนี้ในวันที่ได้ยื่นคำขอรับสิทธิบัตร/อนุสิทธิบัตรในต่างประเทศเป็นครั้งแรกโดย <input type="checkbox"/> ได้ยื่นเอกสารหลักฐานพร้อมคำขอนี้ <input type="checkbox"/> ขอยื่นเอกสารหลักฐานหลังจากวันยื่นคำขอนี้				
9. การแสดงการประดิษฐ์หรือการออกแบบผลิตภัณฑ์ผู้ขอรับสิทธิบัตร/อนุสิทธิบัตรได้แสดงการประดิษฐ์ที่หน่วยงานของรัฐเป็นผู้จัด วันแสดง วันเปิดงานแสดง ผู้จัด				
10. การประดิษฐ์เกี่ยวกับจุลชีพ				
10.1 เลขทะเบียนฝากเก็บ		10.2 วันที่ฝากเก็บ		10.3 สถาบันฝากเก็บ/ประเทศ
11. ผู้ขอรับสิทธิบัตร/อนุสิทธิบัตร ขอยื่นเอกสารภาษาต่างประเทศก่อนในวันยื่นคำขอนี้ และจะจัดยื่นคำขอรับสิทธิบัตร/อนุสิทธิบัตรที่จัดทำเป็นภาษาไทยภายใน 90 วัน นับจากวันยื่นคำขอนี้ โดยขอเป็นภาษา <input type="checkbox"/> อังกฤษ <input type="checkbox"/> ฝรั่งเศส <input type="checkbox"/> เยอรมัน <input type="checkbox"/> ญี่ปุ่น <input type="checkbox"/> อื่นๆ				
12. ผู้ขอรับสิทธิบัตร/อนุสิทธิบัตร ขอให้อธิบายประเภทโฆษณาคำขอรับสิทธิบัตร หรือรับจดทะเบียน และประกาศโฆษณาอนุสิทธิบัตรนี้ หลังจากวันที่ <input type="checkbox"/> ผู้ขอรับสิทธิบัตร/อนุสิทธิบัตรขอให้ใช้รูปเขียนหมายเลข <input type="checkbox"/> ในการประกาศโฆษณา				
13. คำขอรับสิทธิบัตร/อนุสิทธิบัตรนี้ประกอบด้วย			14. เอกสารประกอบคำขอ	
ก. แบบพิมพ์คำขอ	2	หน้า	<input type="checkbox"/> เอกสารแสดงสิทธิในการขอรับสิทธิบัตร/อนุสิทธิบัตร	
ข. รายละเอียดการประดิษฐ์ หรือคำพรรณนาแบบผลิตภัณฑ์	5	หน้า	<input type="checkbox"/> หนังสือรับรองการแสดงผลการประดิษฐ์/การออกแบบผลิตภัณฑ์	
ค. ข้อถ้อยสิทธิ	2	หน้า	<input checked="" type="checkbox"/> หนังสือมอบอำนาจ	
ง. รูปเขียน	2	รูป	1	หน้า
จ. ภาพแสดงแบบผลิตภัณฑ์ <input type="checkbox"/> รูปเขียน		รูป		หน้า
<input type="checkbox"/> ภาพถ่าย		รูป		หน้า
ฉ. บทสรุปการประดิษฐ์			1	หน้า
14. เอกสารประกอบคำขอ <input type="checkbox"/> เอกสารรายละเอียดเกี่ยวกับจุลชีพ <input type="checkbox"/> เอกสารการขอนับวันยื่นคำขอในต่างประเทศเป็นวันยื่นคำขอในประเทศไทย <input type="checkbox"/> เอกสารขอเปลี่ยนแปลงประเภทของสิทธิ <input checked="" type="checkbox"/> เอกสารอื่นๆ				
15. ข้าพเจ้าขอรับรองว่า <input checked="" type="checkbox"/> การประดิษฐ์นี้ไม่เคยยื่นขอรับสิทธิบัตร/อนุสิทธิบัตรมาก่อน <input type="checkbox"/> การประดิษฐ์นี้ได้พัฒนาปรับปรุงมาจาก				
16. ลายมือชื่อ <input type="checkbox"/> ผู้ขอรับสิทธิบัตร/อนุสิทธิบัตร <input checked="" type="checkbox"/> ตัวแทน (นางสาวนิยดา ทุ่งเรืองผล)				

หมายเหตุ บุคคลใดยื่นขอรับสิทธิบัตรการประดิษฐ์หรือการออกแบบผลิตภัณฑ์ หรืออนุสิทธิบัตร โดยการแสดงข้อความอันเป็นเท็จแก่พนักงานเจ้าหน้าที่ เพื่อให้ได้ไปซึ่งสิทธิบัตรหรืออนุสิทธิบัตร ต้องระวางโทษ จำคุกไม่เกินหกเดือน หรือปรับไม่เกินห้าพันบาท หรือทั้งจำทั้งปรับ

เพิ่มเติมข้อ 6. ผู้ประดิษฐ์/ผู้ออกแบบผลิตภัณฑ์ ชื่อและที่อยู่เดียวกับผู้ขอ

ชื่อ นายจิรกิตติ ตั้งพัฒนางรุ่งเรือง

ที่อยู่ ศูนย์วิจัยกสิกรรม 32/19-20 หมู่ 6

ถนน พหลโยธิน ตำบล คลองหนึ่ง อำเภอ คลองหลวง จังหวัด ปทุมธานี รหัสไปรษณีย์ 12120 ประเทศไทย

อีเมล jeerakit.thangphat@gmail.com

เลขประจำตัวประชาชน

1	7	1	9	9	0	0	2	7	4	1	0	7
---	---	---	---	---	---	---	---	---	---	---	---	---

หน้า 1 ของจำนวน 5 หน้า

รายละเอียดการประดิษฐ์

ชื่อที่แสดงถึงการประดิษฐ์

อุปกรณ์เคมีไฟฟ้าสำหรับการตรวจวัดสารเมทาโบไลต์วันไฮดรอกซีไพรีนและวิธีการตรวจวัดสารเมทาโบไลต์วันไฮดรอกซีไพรีนในตัวอย่างปัสสาวะด้วยอุปกรณ์ดังกล่าว

5

สาขาวิทยาการที่เกี่ยวข้องกับการประดิษฐ์

สาขาเคมีวิเคราะห์ที่เกี่ยวข้องกับการพัฒนาอุปกรณ์เคมีไฟฟ้าสำหรับการตรวจวัดสารเมทาโบไลต์วันไฮดรอกซีไพรีน

10 **ภูมิหลังของศิลปะหรือวิทยาการที่เกี่ยวข้อง**

โพลีไซคลิกอะโรมาติกไฮโดรคาร์บอน (Polycyclic Aromatic Hydrocarbons, PAHs) เป็นกลุ่มสารเคมีที่เป็นสารประกอบไฮโดรคาร์บอนที่ปนเปื้อนอยู่ในสิ่งแวดล้อม ซึ่งจะมีโครงสร้างทางเคมีเป็นวงเบนซีนตั้งแต่ 2 วงขึ้นไปจัดเรียงตัวเป็นเส้นตรง เป็นมุม หรือเป็นกลุ่ม โดยโพลีไซคลิกอะโรมาติกไฮโดรคาร์บอนเกิดจากการเผาไหม้ไม่สมบูรณ์ (Incomplete combustion) หรือกระบวนการไพโรไลซิส (Pyrolysis) ของสารอินทรีย์ ซึ่งส่วนใหญ่มาจากการเผาไหม้ของเครื่องยนต์หรือเชื้อเพลิงต่าง ๆ ในโรงงานอุตสาหกรรม เช่น ถ่านหิน น้ำมันดิบ และแก๊สโซลีน เป็นต้น นอกจากนี้สารประกอบกลุ่มโพลีไซคลิกอะโรมาติกไฮโดรคาร์บอนยังสามารถเกิดได้จากการปรุงอาหาร เช่น การปิ้งย่าง หรือทอดโดยใช้ไขมันที่อุณหภูมิสูง ๆ ซึ่งปกติแล้วในชีวิตประจำวันมนุษย์เราสัมผัสกับสารประกอบกลุ่มโพลีไซคลิกอะโรมาติกไฮโดรคาร์บอนอยู่ตลอดเวลา โดยการหายใจเข้าสู่ร่างกายผ่านทางอากาศ ได้แก่ ฝุ่น คาร์บอนจากรถยนต์ บุหรี่ หรือไฟฟ้า สารพิษของยางมะตอยที่ทำถนน ตลอดจนการรับประทานอาหารประเภทปิ้งย่าง เมื่อสารประกอบกลุ่มโพลีไซคลิกอะโรมาติกไฮโดรคาร์บอนเข้าสู่ร่างกายสามารถก่อความเสียหายหรือทำลายโปรตีนหรือดีเอ็นเอภายในเซลล์ได้จึงนำไปสู่การกลายพันธุ์ต่อร่างกายมนุษย์ (Mutagenic to human body) การพัฒนาการที่ผิดปกติ (Developmental malformations) ผลกระทบที่ทำให้ทารกอวัยวะพิการ (Teratogenic effects) เนื้องอก (Tumors) และมะเร็ง (Cancers) ดังนั้นการประเมินระดับความเสียหายของโปรตีนหรือดีเอ็นเอภายในเซลล์จากสารประกอบกลุ่มโพลีไซคลิกอะโรมาติกไฮโดรคาร์บอนที่เป็นสารก่อมลพิษทางสิ่งแวดล้อมที่มีผลต่อสุขภาพของมนุษย์จึงมีความสำคัญอย่างยิ่ง

วันไฮดรอกซีไพรีน (1-Hydroxypyrene, 1-OHP) เป็นสารเมทาโบไลต์ของโพลีไซคลิกอะโรมาติกไฮโดรคาร์บอนที่มักเกิดขึ้นและมีมากในสารผสมของสารประกอบกลุ่มโพลีไซคลิกอะโรมาติกไฮโดรคาร์บอน ซึ่งเป็นสารบ่งชี้ทางชีวภาพ (Biomarkers) ที่สำคัญและตัวบ่งชี้ที่เชื่อถือได้ (Reliable indicator) สำหรับการ

หน้า 2 ของจำนวน 5 หน้า

ประเมินการสัมผัสกับสารประกอบกลุ่มโพลีไซคลิกอะโรมาติกไฮโดรคาร์บอนเข้าสู่ร่างกายของมนุษย์ ซึ่งสามารถใช้เป็นการเตือนภัยถึงระดับความเสี่ยงต่อสุขภาพและการประเมินความปลอดภัยในการทำงานได้ โดยเฉพาะอย่างยิ่งในกลุ่มแรงงานที่มีอาชีพในการสัมผัสสารประกอบกลุ่มนี้สูง โดยปกติแล้วสารเมทาโบไลต์วันไฮดรอกซีไพรีนสามารถตรวจพบได้ในปัสสาวะ ซึ่งการตรวจวัดสารเมทาโบไลต์วันไฮดรอกซีไพรีนในปัสสาวะ

5 นั้นไม่เป็นอันตราย ทำได้ง่ายและเข้าถึงได้ง่าย โดยค่าเกณฑ์มาตรฐานการเฝ้าติดตามทางชีวภาพสำหรับสารเมทาโบไลต์วันไฮดรอกซีไพรีนในปัสสาวะ คือ 1 ไมโครกรัม/ลิตรหรือ 4.582 นาโนโมลาร์ ดังนั้นการพัฒนาอุปกรณ์และวิธีการตรวจวัดสารเมทาโบไลต์วันไฮดรอกซีไพรีนที่ง่าย มีความไว (Sensitivity) และความจำเพาะ (Selectivity) จึงเป็นสิ่งสำคัญสำหรับการเฝ้าติดตามและประเมินความปลอดภัยของสุขภาพที่จะนำไปสู่ความเสี่ยงของโลก

10 โดยที่ผ่านมามีการพัฒนาวิธีการตรวจวัดปริมาณสารเมทาโบไลต์วันไฮดรอกซีไพรีนด้วยวิธีการต่างๆ เช่น วิธีการทางสเปกโทรเมตรี (Spectrometry) และทางโครมาโทกราฟี (Chromatography) แม้ว่าวิธีการเหล่านี้จะให้การวิเคราะห์ที่มีความไวและความจำเพาะ อย่างไรก็ตามวิธีการเหล่านี้ต้องอาศัยเครื่องมือที่มีราคาสูง มีความซับซ้อน ใช้เวลาในการวิเคราะห์นาน มีขั้นตอนการเตรียมตัวอย่างหลายขั้นตอน มีการใช้ปริมาตรของสารตัวอย่างและตัวทำละลายจำนวนมากและมีความต้องการผู้ที่มีความเชี่ยวชาญในการใช้เครื่องมือ

15 ระดับสูง นอกจากนี้เครื่องมือและอุปกรณ์ที่ใช้ในวิธีการเหล่านี้ไม่สามารถนำออกไปใช้ทดสอบนอกห้องปฏิบัติการและไม่เหมาะสำหรับการวิเคราะห์ในการเฝ้าติดตามและประเมินความปลอดภัยของสุขภาพ ดังนั้นการคิดค้นอุปกรณ์และวิธีการตรวจวัดปริมาณสารเมทาโบไลต์วันไฮดรอกซีไพรีนในตัวอย่างปัสสาวะที่สามารถแก้ไขข้อจำกัดต่าง ๆ ดังกล่าวจึงถือว่าเป็นที่ต้องการอย่างยิ่ง เพื่อให้ได้มาซึ่งวิธีการที่มีความง่าย สะดวก รวดเร็ว พกพาได้ ราคาถูก ความไวและความจำเพาะสูง และคงไว้ซึ่งความถูกต้อง ปัจจุบันวิธีการ

20 วิเคราะห์ทางเคมีไฟฟ้าเป็นอีกหนึ่งวิธีการที่ได้รับความนิยมอย่างมากสำหรับการตรวจวัดสารบ่งชี้ทางชีวภาพ เนื่องจากเทคนิคทางเคมีไฟฟ้ามีข้อดีเหนือเทคนิคอื่น ๆ เช่น เป็นเทคนิคที่ใช้งานง่าย สะดวก ให้ความไวและความจำเพาะในการวิเคราะห์ที่สูง มีความแม่นยำ ใช้เวลาในการวิเคราะห์ที่รวดเร็ว เครื่องมือไม่มีความซับซ้อน ราคาไม่แพง สามารถพกพาและนำออกไปใช้ในนอกห้องปฏิบัติการได้ นอกจากนี้อุปกรณ์การวิเคราะห์ทางเคมีไฟฟ้ายังใช้ปริมาตรของสารตัวอย่างที่น้อยมากในระดับไมโครลิตรและมีการออกแบบอุปกรณ์ได้

25 หลากหลายรูปแบบให้เหมาะกับงานที่จะนำไปประยุกต์ใช้

จากการศึกษาผลงานวิจัยที่ผ่านมาที่เกี่ยวข้องกับการตรวจวัดปริมาณสารเมทาโบไลต์วันไฮดรอกซีไพรีนด้วยวิธีการทางเคมีไฟฟ้ายังพบข้อจำกัดบางประการ กล่าวคือ เมื่อทำการตรวจวัดสารเมทาโบไลต์วันไฮดรอกซีไพรีนด้วยขั้วไฟฟ้าชนิดต่าง ๆ เช่น ขั้วไฟฟ้ากลาสคาร์บอน (Glassy carbon electrode, GCE) ขั้วไฟฟ้าคาร์บอนเพสต์ (Carbon paste electrode, CPE) และขั้วไฟฟ้าฟิล์มบางโพรบอนโดปโดมอนด์

หน้า 3 ของจำนวน 5 หน้า

- (Boron-doped diamond electrode, BDDE) เป็นต้น ต้องใช้งานร่วมกับตัวดัดแปรผิวหน้าขั้วไฟฟ้า (Modifiers) เพื่อการตรวจวัดสารเมทาโบไลต์วันไฮดรอกซีไพรีนนั้นจะต้องมีขั้นตอนการดัดแปรผิวหน้าขั้วไฟฟ้าหลายขั้นตอน ใช้ตัวดัดแปรผิวหน้าขั้วไฟฟ้าหลายตัว นำมาซึ่งความยุ่งยาก ซับซ้อน และใช้เวลานาน อีกทั้งบางวัสดุที่นำมาใช้นั้นมีราคาสูง ดังนั้นจึงนำมาสู่การประดิษฐ์อุปกรณ์เคมีไฟฟ้าแบบใหม่และวิธีการ
- 5 ตรวจวัดสารเมทาโบไลต์วันไฮดรอกซีไพรีนด้วยขั้วไฟฟ้าแบบพิมพ์สกรีนกราฟีนที่มีการดัดแปรผิวหน้าขั้วไฟฟ้าด้วยพอลิ แอลกลูตามิก (poly(L-Glutamic acid) modified screen-printed graphene electrode, poly(L-GA)/SPGE) บนฐานแผ่นใส ซึ่งจากการสืบค้นข้อมูลเชิงวิทยาศาสตร์ยังไม่มีกรรมวิธีนำขั้วไฟฟ้าและวิธีการวิเคราะห์ดังกล่าวมาใช้สำหรับการตรวจวัดสารเมทาโบไลต์วันไฮดรอกซีไพรีนในตัวอย่างปัสสาวะมาก่อน อีกทั้งวิธีการที่พัฒนาขึ้นมานี้มีขั้นตอนการดัดแปรผิวหน้าขั้วไฟฟ้าใช้งานกราฟีนเพียงขั้นตอนเดียว ซึ่งทำให้การ
- 10 ตรวจวัดสารเมทาโบไลต์วันไฮดรอกซีไพรีนมีความง่าย สะดวก และรวดเร็ว นอกจากนี้อุปกรณ์เคมีไฟฟ้าดังกล่าวยังมีขนาดเล็กและวัสดุที่ใช้ในการดัดแปรผิวหน้าขั้วไฟฟ้านั้นราคาถูก อีกทั้งสามารถพกพาไปทดสอบในภาคสนามและเหมาะสำหรับการประยุกต์ใช้ในการเฝ้าติดตามและประเมินความปลอดภัยของสุขภาพได้อีกด้วย
- 15 **ลักษณะและความมุ่งหมายของการประดิษฐ์**
 การประดิษฐ์นี้เกี่ยวกับการพัฒนาอุปกรณ์เคมีไฟฟ้าด้วยการพิมพ์สกรีนขั้วไฟฟ้าลงบนฐานแผ่นใส ซึ่งจะประกอบไปด้วยขั้วไฟฟ้า 3 ขั้ว ได้แก่ 1. ขั้วไฟฟ้าใช้งาน (Working electrode) ที่มีองค์ประกอบเป็นกราฟีน 2. ขั้วไฟฟ้าช่วย (Counter electrode) ที่มีองค์ประกอบเป็นกราฟีน และ 3. ขั้วไฟฟ้าอ้างอิง (Reference electrode) ที่มีองค์ประกอบเป็นซิลเวอร์/ซิลเวอร์คลอไรด์ (Ag/AgCl) โดยบริเวณขั้วไฟฟ้าใช้งานจะมีการดัด
- 20 แปรผิวหน้าขั้วไฟฟ้าด้วยพอลิแอลกลูตามิก (poly(L-Glutamic acid), poly(L-GA)) และวิธีการตรวจวัดสารเมทาโบไลต์วันไฮดรอกซีไพรีน
 วัตถุประสงค์ของการประดิษฐ์นี้คือ เพื่อพัฒนาอุปกรณ์เคมีไฟฟ้าโดยการดัดแปรผิวหน้าขั้วไฟฟ้าด้วยพอลิแอลกลูตามิกและวิธีการตรวจวัดสารเมทาโบไลต์วันไฮดรอกซีไพรีนในตัวอย่างปัสสาวะ ซึ่งอุปกรณ์เคมีไฟฟ้าดังกล่าวสามารถประดิษฐ์ขึ้นได้ง่าย สะดวก รวดเร็ว มีขนาดเล็ก ราคาถูก อีกทั้งยังสามารถพกพาไป
- 25 ทดสอบในเชิงภาคสนามและเหมาะสำหรับการประยุกต์ใช้ในการเฝ้าติดตามและประเมินความปลอดภัยของสุขภาพ นอกจากนี้วิธีการที่พัฒนาขึ้นให้ผลการวิเคราะห์ที่มีความไวและความจำเพาะสูงต่อการตรวจวัดสารเมทาโบไลต์วันไฮดรอกซีไพรีน ซึ่งมีความเหมาะสมอย่างยิ่งต่อการนำไปใช้ประโยชน์สำหรับการเฝ้าติดตามและประเมินความปลอดภัยของสุขภาพที่นำไปสู่ความเสี่ยงของโรคที่สัมพันธ์กับสารประกอบกลุ่มโพลีไซคลิกอะโรมาติกไฮโดรคาร์บอนต่อร่างกายมนุษย์

หน้า 4 ของจำนวน 5 หน้า

การเปิดเผยการประดิษฐ์โดยสมบูรณ์

การประดิษฐ์นี้เกี่ยวข้องกับการสร้างอุปกรณ์เคมีไฟฟ้าและการพัฒนาวิธีการตรวจวัดสารเมทาโบไลต์
วันไฮดรอกซีไพรีนในตัวอย่างปัสสาวะ โดยใช้ขั้วไฟฟ้าแบบพิมพ์สกรีนกราฟีนที่มีการดัดแปรผิวหน้าขั้วไฟฟ้า
5 ด้วยพอลิแอลกลูตามิก (poly(L-Glutamic acid) modified screen-printed graphene electrode,
poly(L-GA)/SPGE) บนฐานแผ่นใส เพื่อนำไปประยุกต์ใช้ในเชิงการวิเคราะห์สำหรับการเฝ้าติดตามและ
ประเมินความปลอดภัยของสุขภาพได้

ลำดับต่อไปจะกล่าวถึงรายละเอียดและขั้นตอนการพัฒนาอุปกรณ์เคมีไฟฟ้า รวมถึงวิธีการนำ
อุปกรณ์เคมีไฟฟ้าดังกล่าวไปใช้ในการวิเคราะห์สารเมทาโบไลต์วันไฮดรอกซีไพรีน โดยแสดงดังต่อไปนี้

10 1. การสร้างขั้วไฟฟ้าแบบพิมพ์สกรีนกราฟีนบนฐานแผ่นใส

โดยขั้นตอนการสร้างขั้วไฟฟ้าแบบพิมพ์สกรีนกราฟีนบนฐานแผ่นใส ดังแสดงตามรูปที่ 1 ซึ่งมี
รายละเอียดดังต่อไปนี้

1.1 ทำการออกแบบขั้วไฟฟ้าแบบพิมพ์สกรีน ซึ่งใช้เป็นอุปกรณ์ตรวจวัดสารเมทาโบไลต์วันไฮดร
15 ออกซีไพรีน โดยทำการออกแบบให้มีองค์ประกอบของขั้วไฟฟ้า 3 ขั้ว ได้แก่ ขั้วไฟฟ้าใช้งาน ขั้วไฟฟ้าช่วย และ
ขั้วไฟฟ้าอ้างอิง ที่มีขนาดเล็กและพกพาได้สะดวก

1.2 ทำการสกรีนขั้วไฟฟ้า 2 ขั้ว ด้วยหมึกกราฟีนลงบนฐานแผ่นใส เพื่อใช้เป็นขั้วไฟฟ้าใช้งานและ
ขั้วไฟฟ้าช่วย จากนั้นนำไปเข้าตู้อบที่อุณหภูมิ 60 องศาเซลเซียส เป็นเวลา 45-60 นาที

1.3 ทำการสกรีนขั้วไฟฟ้าอีก 1 ขั้ว ด้วยหมึกซิลเวอร์/ซิลเวอร์คลอไรด์ลงบนฐานแผ่นใสที่ได้จาก
ข้อ 1.2 เพื่อใช้เป็นขั้วไฟฟ้าอ้างอิง จากนั้นนำไปเข้าตู้อบที่อุณหภูมิ 60 องศาเซลเซียส เป็นเวลา 45-60 นาที
20 แล้วจะได้ขั้วไฟฟ้าแบบพิมพ์สกรีนกราฟีนสำหรับการดัดแปรผิวหน้าด้วยพอลิแอลกลูตามิก

2. วิธีการดัดแปรผิวหน้าขั้วไฟฟ้าแบบพิมพ์สกรีนกราฟีนด้วยพอลิกลูตามิก

การดัดแปรผิวหน้าขั้วไฟฟ้าแบบพิมพ์สกรีนกราฟีนด้วยพอลิกลูตามิกดังแสดงตามรูปที่ 2 ซึ่งทำ
ได้จากวิธีการอิเล็กโทรพอลิเมอไรเซชัน (Electropolymerization) โดยการเตรียมสารละลายมอนอเมอร์
แอลกลูตามิก (L-Glutamic acid) ที่ช่วงความเข้มข้น 10-50 มิลลิโมลาร์ ในสารละลายโซเดียมฟอสเฟต
25 บัฟเฟอร์ จากนั้นหยดสารละลายมอนอเมอร์แอลกลูตามิกดังกล่าวลงบนขั้วไฟฟ้าแบบพิมพ์สกรีนกราฟีน แล้ว
ทำการให้ศักย์ไฟฟ้าระหว่าง -0.8 ถึง +1.7 โวลต์ ด้วยเทคนิคไซคลิกโวลแทมเมตรี อัตราการสแกน 50-200
มิลลิโวลต์ต่อวินาที จำนวนรอบการสแกน 3-20 รอบ จากนั้นทำการล้างผิวหน้าขั้วไฟฟ้าใช้งานด้วยน้ำ
ปราศจากไอออน แล้วทิ้งไว้ให้แห้งที่อุณหภูมิห้อง จะได้ขั้วไฟฟ้าใช้งานแบบพิมพ์สกรีน กราฟีนที่มีการดัดแปร
ผิวหน้าขั้วไฟฟ้าด้วยพอลิแอลกลูตามิกสำหรับการตรวจวัดสารเมทาโบไลต์วันไฮดรอกซีไพรีน

หน้า 5 ของจำนวน 5 หน้า

3. วิธีการตรวจวัดสารเมทาโบไลต์วันไฮดรอกซีไพรีน

โดยขั้นตอนการตรวจวัดสารเมทาโบไลต์วันไฮดรอกซีไพรีนจะมีรายละเอียดดังต่อไปนี้

3.1 ทำการเตรียมสารละลายมาตรฐานวันไฮดรอกซีไพรีนในสารละลายบัฟเฟอร์ไกลซีนและโซเดียมไฮดรอกไซด์ (Glycine-NaOH Buffer) ซึ่งทำหน้าที่เป็นสารละลายอิเล็กโทรไลต์ (Supporting electrolyte)

3.2 ทำการหาค่ามาตรฐานจากสารละลายมาตรฐานวันไฮดรอกซีไพรีนหรือสารตัวอย่างลงบนอุปกรณ์เคมีไฟฟ้าที่มีการตัดแปรผิวหน้าขั้วไฟฟ้าด้วยพอลิแอลกลูตามิก โดยใช้เทคนิคสแควร์เวฟโวลแทมเมตรี (Square wave voltammetry, SWV) ซึ่งอุปกรณ์เคมีไฟฟ้าง่ายๆ จะถูกเชื่อมต่อกับเครื่องโพเทนชิโอสแตท (Potentiostat) จากนั้นทำการสแกนศักย์ไฟฟ้าตั้งแต่ -0.4 ถึง +0.3 โวลต์ โดยใช้ค่าการเพิ่มขึ้นของศักย์ไฟฟ้า (Potential increment) เท่ากับ 0.008 โวลต์ ค่าแอมพลิจูด (Amplitude) เท่ากับ 0.1 โวลต์ ค่าความถี่ (Frequency) เท่ากับ 40 เฮิร์ตซ์ และเวลาก่อนการวิเคราะห์ (Quiet time) เท่ากับ 180 วินาที

3.3 ทำการสร้างกราฟมาตรฐานจากสารละลายมาตรฐานวันไฮดรอกซีไพรีน เพื่อหาปริมาณวิเคราะห์ของสารเมทาโบไลต์วันไฮดรอกซีไพรีน ซึ่งสามารถทำได้จากการตรวจวัดสัญญาณการตอบสนองทางเคมีไฟฟ้าของสารละลายมาตรฐานวันไฮดรอกซีไพรีนที่ความเข้มข้นต่าง ๆ ในรูปของกระแสไฟฟ้า จากนั้นนำไปสร้างกราฟความสัมพันธ์ระหว่างค่าสัญญาณที่ตรวจวัดได้ในรูปของกระแสไฟฟ้าในหน่วยไมโครแอมแปร์ (μA) เป็นแกน y และค่าความเข้มข้นของสารละลายมาตรฐานวันไฮดรอกซีไพรีนในหน่วยนาโนโมลาร์ (nM) เป็นแกน x พบว่า กราฟมาตรฐานสำหรับการตรวจวัดปริมาณสารเมทาโบไลต์วันไฮดรอกซีไพรีนอยู่ในช่วงความเข้มข้น 1 ถึง 1000 นาโนโมลาร์

20 คำอธิบายรูปเขียนโดยย่อ

รูปที่ 1 ขั้นตอนการสร้างขั้วไฟฟ้าแบบพิมพ์สกรีนกราฟีนบนฐานแผ่นใส

รูปที่ 2 ขั้นตอนการตัดแปรผิวหน้าขั้วไฟฟ้าแบบพิมพ์สกรีนกราฟีนด้วยพอลิแอลกลูตามิก

วิธีการในการประดิษฐ์ที่ดีที่สุด

25 ดึงที่กล่าวมาแล้วในหัวข้อการเปิดเผยการประดิษฐ์โดยสมบูรณ์

หน้า 1 ของจำนวน 2 หน้า

ข้อถ้อยสัญญา

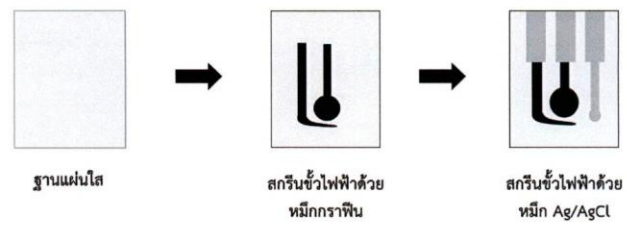
1. วิธีการตัดแปรผิวหน้าขั้วไฟฟ้าแบบพิมพ์สกรีนกราฟีนด้วยพอลิแอลกลูตามิก โดยมีขั้นตอนดังต่อไปนี้
 - ขั้นตอนที่ 1 ทำการตัดแปรผิวหน้าขั้วไฟฟ้าแบบพิมพ์สกรีนกราฟีนด้วยพอลิแอลกลูตามิกด้วยวิธีอิเล็กโทรพอลิเมอร์ไรเซชัน (Electropolymerization) โดยการเตรียมสารละลายมอนอเมอร์แอลกลูตามิก (L-Glutamic acid) ที่ช่วงความเข้มข้น 10-50 มิลลิโมลาร์ ในสารละลายโซเดียมฟอสเฟตบัฟเฟอร์
 - 5 ขั้นตอนที่ 2 ทำการหดยดสารละลายมอนอเมอร์แอลกลูตามิกดังกล่าวลงบนขั้วไฟฟ้าแบบพิมพ์สกรีนกราฟีน
 - ขั้นตอนที่ 3 ทำการให้ศักย์ไฟฟ้าระหว่าง -0.8 ถึง +1.7 โวลต์ ด้วยเทคนิคไซคลิกโวลแทมเมตรี อัตราการสแกน 50-200 มิลลิโวลต์ต่อวินาที จำนวนรอบการสแกน 3-20 รอบ
 - 10 ขั้นตอนที่ 4 ทำการล้างผิวหน้าขั้วไฟฟ้าใช้งานด้วยน้ำปราศจากไอออน แล้วทิ้งไว้ให้แห้งที่อุณหภูมิห้อง จะได้ขั้วไฟฟ้าใช้งานแบบพิมพ์สกรีนกราฟีนที่มีการตัดแปรผิวหน้าขั้วไฟฟ้าด้วยพอลิแอลกลูตามิก สำหรับการตรวจวัดสารเมทาโบไลต์วันไฮดรอกซีไพรีน
2. วิธีการตรวจวัดสารเมทาโบไลต์วันไฮดรอกซีไพรีนด้วยวิธีการทางเคมีไฟฟ้าโดยใช้อุปกรณ์เคมีไฟฟ้าที่ผ่าน
 - 15 วิธีการตัดแปรผิวหน้าขั้วไฟฟ้าตามข้อถ้อยสัญญาที่ 1 โดยมีขั้นตอนดังต่อไปนี้
 - ขั้นตอนที่ 1 ทำการเตรียมสารละลายมาตรฐานวันไฮดรอกซีไพรีนในสารละลายบัฟเฟอร์ไกลซีนและโซเดียมไฮดรอกไซด์ (Glycine-NaOH Buffer) ซึ่งทำหน้าที่เป็นสารละลายอิเล็กโทรไลต์ (Supporting electrolyte)
 - ขั้นตอนที่ 2 ทำการหดยดสารละลายมาตรฐานวันไฮดรอกซีไพรีนหรือสารตัวอย่างลงบนอุปกรณ์เคมีไฟฟ้าที่มีการตัดแปรผิวหน้าขั้วไฟฟ้าด้วยพอลิแอลกลูตามิก โดยใช้เทคนิค สแควร์เวฟโวลแทมเมตรี (Square wave voltammetry, SWV) ซึ่งอุปกรณ์เคมีไฟฟ้าดังกล่าวจะถูกเชื่อมต่อกับเครื่องโพเทนชิโอสแตท (Potentiostat) จากนั้นทำการสแกนศักย์ไฟฟ้าตั้งแต่ -0.4 ถึง +0.3 โวลต์ โดยใช้ค่าการเพิ่มขึ้นของศักย์ไฟฟ้า (Potential increment) เท่ากับ 0.008 โวลต์ ค่าแอมพลิจูด (Amplitude) เท่ากับ 0.1 โวลต์ ค่าความถี่ (Frequency) เท่ากับ 40 เฮิร์ตซ์ และเวลาก่อนการวิเคราะห์ (Quiet time) เท่ากับ 180 วินาที
 - 25 ขั้นตอนที่ 3 ทำการสร้างกราฟมาตรฐานจากสารละลายมาตรฐานวันไฮดรอกซีไพรีน เพื่อหาปริมาณวิเคราะห์ของสารเมทาโบไลต์วันไฮดรอกซีไพรีน ซึ่งสามารถทำได้จากการตรวจวัดสัญญาณการตอบสนองทางเคมีไฟฟ้าของสารละลายมาตรฐานวันไฮดรอกซีไพรีนที่ความเข้มข้นต่าง ๆ ในรูปของกระแสไฟฟ้า จากนั้นนำไปสร้างกราฟความสัมพันธ์ระหว่างค่าสัญญาณที่ตรวจวัดได้ในรูปของกระแสไฟฟ้าในหน่วยไมโครแอมแปร์ (μA) เป็นแกน y และค่าความเข้มข้นของสารละลายมาตรฐานวันไฮดรอกซีไพรีนในหน่วยนาโนโมลาร์

หน้า 2 ของจำนวน 2 หน้า

(กฟ) เป็นแกน x พบว่ากราฟมาตรฐานสำหรับการตรวจวัดปริมาณสารเมทาโบไลต์วินไฮดรอกซีไพรีนในช่วง
ความเข้มข้น 1 ถึง 1000 นาโนโมลาร์

หน้า 1 ของจำนวน 1 หน้า

รูปเขียน



รูปที่ 1

สารละลายมอนอเมอร์แอลกลูตามิก



ขี้ไฟฟ้าใช้งานแบบพิมพ์สกรีนกราฟีนที่มีการตัดแปรมีหน้าขี้ไฟฟ้าด้วยพอลิแอลกลูตามิก

รูปที่ 2

หน้า 1 ของจำนวน 1 หน้า

บทสรุปการประดิษฐ์

การประดิษฐ์นี้เป็นการพัฒนาอุปกรณ์เคมีไฟฟ้าและวิธีการตรวจวัดสารเมทาโบไลต์วันไฮดรอกซีไพรีนในตัวอย่างปัสสาวะ โดยใช้ขั้วไฟฟ้าแบบพิมพ์สกรีนกราฟีนที่มีการดัดแปรผิวหน้าขั้วไฟฟ้าด้วยพอลิแอลกลูตามิกด้วยวิธีอิเล็กโทรพอลิเมอไรเซชัน จากนั้นทำการตรวจวัดสารเมทาโบไลต์วันไฮดรอกซีไพรีนโดยใช้อุปกรณ์เคมีไฟฟ้าที่ผ่านวิธีการดัดแปรผิวหน้าขั้วไฟฟ้าง่ายด้วยวิธีทางเคมีไฟฟ้า ซึ่งจะทำการวัดค่ากระแสไฟฟ้าด้วยเทคนิคสแควร์เวฟโวลแทมเมตรี โดยทำการสแกนศักย์ไฟฟ้าตั้งแต่ -0.4 ถึง +0.3 โวลต์ ใช้ค่าการเพิ่มขึ้นของศักย์ไฟฟ้าเท่ากับ 0.008 โวลต์ ค่าแอมพลิจูด เท่ากับ 0.1 โวลต์ ค่าความถี่ เท่ากับ 40 เฮิรตซ์ และเวลาก่อนการวิเคราะห์ เท่ากับ 180 วินาที พบว่า อุปกรณ์เคมีไฟฟ้าและวิธีการที่พัฒนาขึ้นมาสามารถตรวจวัดปริมาณสารเมทาโบไลต์วันไฮดรอกซีไพรีนในช่วงความเข้มข้น 1 ถึง 1000 นาโนโมลาร์ อีกทั้งสามารถนำไปประยุกต์ใช้สำหรับการตรวจวัดปริมาณสารเมทาโบไลต์วันไฮดรอกซีไพรีนในตัวอย่างปัสสาวะ ซึ่งให้ผลการตรวจวัดที่รวดเร็ว มีความไวและความจำเพาะสูง ให้ความถูกต้อง แม่นยำ และมีความน่าเชื่อถือ นอกจากนี้ยังสามารถพกพานำออกไปใช้ทดสอบนอกห้องปฏิบัติการและเหมาะสำหรับการประยุกต์ใช้ในการเฝ้าติดตามและประเมินความปลอดภัยของสุขภาพ ดังนั้นการประดิษฐ์นี้จึงมีศักยภาพที่เหมาะสมและเป็นประโยชน์อย่างมากต่อการนำไปใช้ประโยชน์สำหรับการเฝ้าติดตามและประเมินความปลอดภัยของสุขภาพที่นำไปสู่ความเสี่ยงของโรคที่สัมพันธ์กับสารประกอบกลุ่มโพลีไซคลิกอะโรมาติกไฮโดรคาร์บอนต่อร่างกายมนุษย์

VITA

